uOttawa

L'Université canadienne
Canada's university

FACULTÉ DES ÉTUDES SUPÉRIEURES ET POSTOCTORALES

uOttawa

L'Université canadienne
Canada's university

FACULTY OF GRADUATE AND POSDOCTORAL STUDIES

Jun Wu

AUTEUR DE LA THÈSE / AUTHOR OF THESIS

M.A.Sc. (Civil Engineering)

GRADE / DEGREE

Department of Civil Engineering

FACULTÉ, ÉCOLE, DÉPARTEMENT / FACULTY, SCHOOL, DEPARTMENT

Development of a Peel Test Procedure for Adhesive Applied Roof Systems

TITRE DE LA THÈSE / TITLE OF THESIS

Dr. H. Tanaka

DIRECTEUR (DIRECTRICE) DE LA THÈSE / THESIS SUPERVISOR

Dr. Bas Baskarean

CO-DIRECTEUR (CO-DIRECTRICE) DE LA THÈSE / THESIS CO-SUPERVISOR

EXAMINATEURS (EXAMINATRICES) DE LA THÈSE / THESIS EXAMINERS

Dr. B. Martin-Perez

Dr. D. T. Lau

Gary W. Slater

Le Doyen de la Faculté des études supérieures et postdoctorales / Dean of the Faculty of Graduate and Postdoctoral Studies

Development of a Peel Test Procedure for Adhesive Applied Roof Systems

By

Jun Wu

A thesis presented to the University of Ottawa in partial fulfillment of the requirements for

The Degree of Master of Applied Science
in Civil Engineering

The M.A.Sc. program in Civil Engineering is a joint program with Carleton University administered by the Ottawa-Carleton Institute for Civil Engineering

Department of Civil Engineering
University of Ottawa
Ottawa, Canada
2008

Your file Votre référence
ISBN: 978-0-494-50940-1
Our file Notre référence
ISBN: 978-0-494-50940-1

This thesis is dedicated to my husband and my lovely sons,

for their support and patience during my studies at the university.

This thesis is dedicated to the memory of my grandparents.

Acknowledgments

The present research was carried out as a part of the collaborative research project between the National Research Council Canada (NRC) and the University of Ottawa, titled "Development of wind uplift standard for adhesive applied low slope roof systems", under the support of NSERC CRD grant (CRDPJ 3065819-04). This research is also sponsored by four Canadian roofing industry partners, namely IKO Industries Ltd.; Soprema Inc. Canada; Tremco Inc. Canada and Bakor Inc., as well as Roofing Contractors Association of British Columbia, Canada (RCABC). Their support and commitments are greatly appreciated.

First of all, I thank my supervisors, **Dr. Bas Baskaran & Dr. Hiroshi Tanaka**, for their excellent supervision. Dr. Bas not only exemplified excellence in research and scientific communication, but also gave me lots of generous financial support. I learned tremendous roofing knowledge from his rich experiences in the field. During the final stages of my thesis writing, his valuable guidance and criticisms have served as a momentum that constantly pushes the thesis towards perfection. I appreciate the enormous input from Dr. Tanaka, his strong motivation and timely encouragement. Throughout my thesis-writing period, he offered very useful suggestion and spent huge amount of time reviewing the thesis. It was a wonderful learning experience and a great pleasure working with him.

It has always been my great pleasure to be acquainted with other colleagues at IRC/NRC and graduate students at University of Ottawa and Carleton University. Every one of them will leave a long-lasting memory in my mind. **Dr. Ralph Paroli**, Director of the Building Envelope & Structure of NRC, allowed me to carry out my research work at NRC. **Jayson Current** and **Bona Murty**, my labmates, have been always available for help, listening to my complaints and giving me suggestions. I wish all the best for their future endeavors! Other colleagues,

especially **Steven Ko, Helen Yew, Amor Duric, Kevin Deeljur, Sebastian Evoniak, Sudhakar Molleti** and **Lan Lin** provided various support and kind assistance during my thesis research and writing.

I am grateful to a number of people for their generous support of my Master's study. Here is a list of some of them: **Mr. Dave Miller, Mr. Peter Saunders, Mr. Marcel Lemieux, Mr. Paul Hastings, Mr. Paul Neville and Mr. Mike Bisson.** Thank you all for your time and assistance in the preparation of the experimental samples. In addition, **John K. Perrins** and **Doug Tatlor**, at the workshop of University of Ottawa helped in the fabrication of several components of my experimental apparatus.

My special appreciation goes to my sons, **Randy** and **Ranger**, for tolerating my absence for the study. Finally, my biggest thanks of all go to my husband, **Shihuan**, for his consistent encouragement and patient support.

Abstract

Roofing systems are an important component of the building envelope. Though the Adhesive Applied Roof Systems (AARS) are gaining popularity in North America, systematic review of the existing national and international standards revealed that there is no proper testing procedure established to quantify the peel resistance of AARS. The objective of the present study is to develop a peel testing procedure based on systematic laboratory investigations.

Specimens (6 in. x 6 in. or 152 mm x 152 mm) composed of insulation and cover board were adhered together by applying cold adhesives. To represent the realistic conditions of the field construction, specimens were prepared using components from four industrial sources. Specimens were then subjected to a peeling force at two different locations with various peel angles ranging from 7.5° to 45° to simulate the blister shape, that can occur on AARS under several wind action. Additional specimen sizes were also tested for selected combinations to evaluate the size effect. A total of 378 specimens with various physical parameters were constructed, cured for 28 days and tested using an Instron machine at a constant loading speed. For all cases, the failure load as well as the failure mode was recorded.

Data analysis indicates that the failure load decreases as the peel angle increases, though it increases with the sample size. Generalized curves reflecting the peel resistance versus peel angle and the sample size are presented. Failure mode analysis identified the weakest link of the AARS samples under simulated wind induced peeling force. Based on the experimental investigation, a standard peel test method was drafted. This standard has an essential importance for the evaluation of AARS performance under wind-induced peel forces, which will be applicable to the new roofing assemblies as well as the existing roofing assembly to be replaced or recovered.

Table of Contents

List of Tables

List of Figures

Glossary

Symbols:

a	width of the specimen
b	the length subjected to the peeling stress
F	peel force
H	the vertical distance between the top of specimen to the inside edge of the free roller as defined in p.48
L	the horizontal distance between the middle point of the gripper to the inside edge of the free roller as defined in p.48
P	probability
θ, θ_1, θ_2	peel initial angle

Abbreviations:

AARS	Adhesive Applied Roof Systems
ACB	Asphalt Core Cover Board
Adh	Adhesive Failure
AF	Acrylic Facer Insulation
ASTM	American Society for Testing and Materials
BS	British Standard
BUR	the built-up roof
CB	Cover Board
CB/B	Cover Board Brittle
CB/Se	Cover Board Separation
CB/Sp	Cover Board Splitting
CEN	Comité Européen de Normalization
CMHC	Canada Mortgage and Housing Corporation

C-P	Corner Position
DIN	Deutsches Institut für Normung
EN	the European Standard
E-P	Edge Position
Facer/D	Insulation Facer Delamination
Facer/R	Insulation Facer Rupture
Facer/T	Insulation Facer Tearing
FB	Fiber Cover Board
FOV	Failure Occurrence Value as defined in p.92
ISO	the International Organization for Standardization
MARS	Mechanically Attached Roofing Systems
PF	Paper facer Insulation
SD	Standard Deviation

Chapter 1 Introduction

1.1 Roofing Systems

A roof is the top enclosure of a building and is comprised of the roofing – the actual covering – and frames that support the whole roofing system. The roofing system is an integral component of the building envelope. It is designed to protect the occupants from harsh outdoor environmental conditions such as wind load, precipitation, ultraviolet light and temperature.

One of the most salient differences between residential roofing systems (Figure 1.1) and commercial roofing systems (Figure 1.2) is the roof slope (Baker, 1980). Residential roofs generally have steeper slopes. However, the commercial roofs, such as those found in industrial buildings, factories and warehouses, are mostly low-sloped (Borujerdi, 2004, Molleti, 2006).

In Canada, the most traditional commercial roofing system is the built-up roof (BUR). A BUR system consists of successive layers of roofing felts, laminated together with bitumen or asphalt (Figure 1.3 (a)). BUR systems are installed using a hot-mopped technique, where hot asphalt is mopped over the roof as an adhesive (Figure 1.3 (b)). There are distinct disadvantages associated with BUR. The hot-mopped application method generates toxic gases. Hot mopping is also a labour intensive-process which drives up the cost to install the roof.

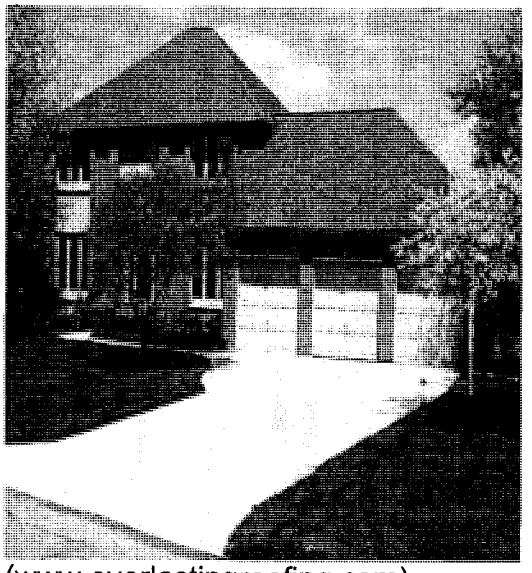

(www.everlastingroofing.com)

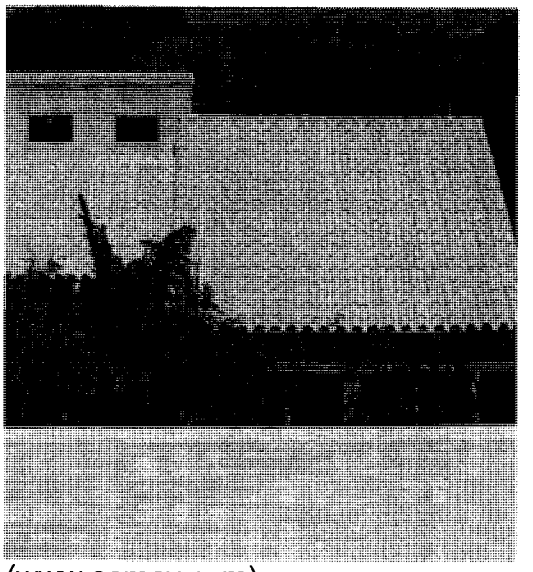

(www.somay.com)

Figure 1.1 Photographs of typical steep slope roofing

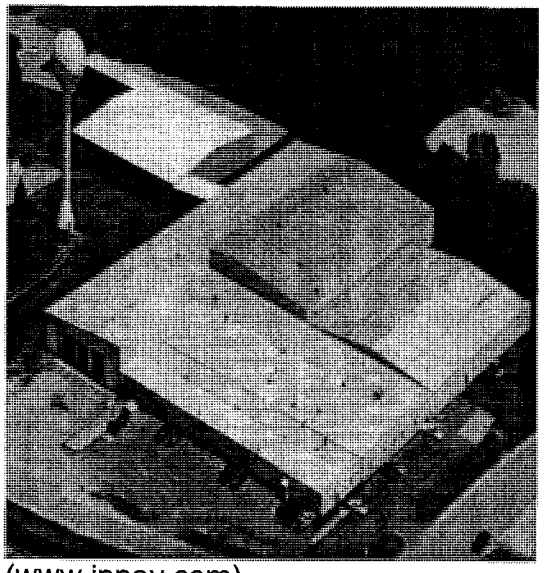

(www.innov.com)

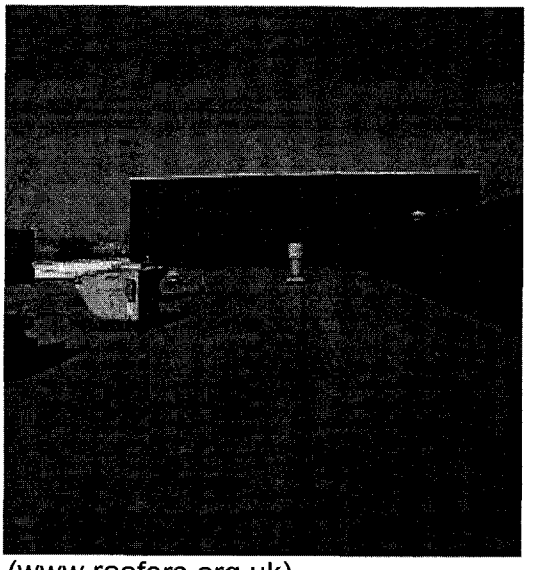

(www.roofers.org.uk)

Figure 1.2 Photographs of typical low slope roofing

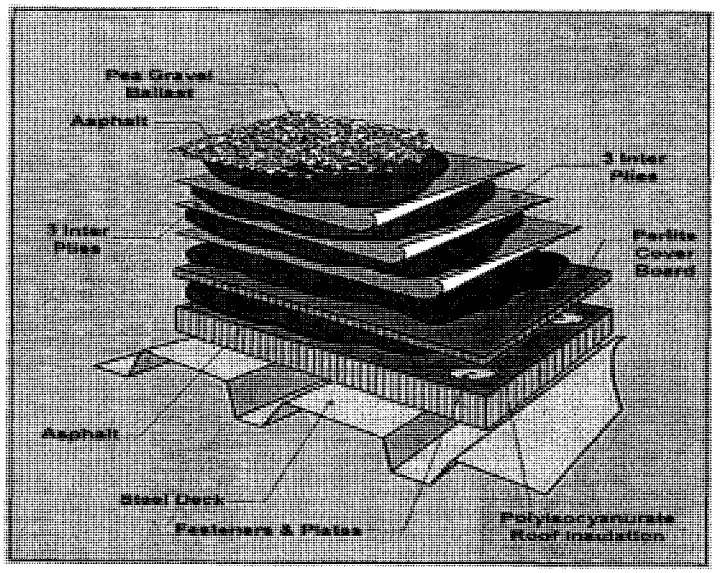

(a) Schematic and layout of BUR

(www.rooftopics.com)

(www.randpc.com)

(b) Field installation process of BUR

Figure 1.3 Schematics and field installation of built-up roofing

1.2 Adhesive Applied Roofing System

Due to the aforementioned disadvantages of traditional BUR systems, alternatives to the use of hot asphalt or bitumen have been developed. The use of cold adhesives has gained popularity only recently. This trend has been driven partly by the sensitivity of some individuals to hot asphalt fumes, but mainly due to higher environmental and insurance regulations. In addition, the development of new materials and technology has also contributed to the increased use of cold adhesives.

Adhesive Applied Roofing System (AARS) is a new generation of BUR that uses cold adhesives to secure all components to form a compact roofing system. AARS consists of multiple components assembled together with specialized adhesives. AARS usually includes six layers as shown below (Figure 1.4):

- Structure deck;
- Vapor barrier;
- Insulation;
- Cover board;
- Base sheet; and
- Cap sheet.

The major function of roof deck is to support the structural multiple of roofing components and environmental loads, whereas the vapor barrier is designed to limit vapor diffusion and airflow into the roofing system. The insulation's function is thermal protection. It is also to resist degradation caused by moisture and to protect other components from corrosion, and the cover board protects insulation from physical and chemical damages. Finally the covering membranes, base sheet and cap sheet, provide water protection to the underlying roofing components.

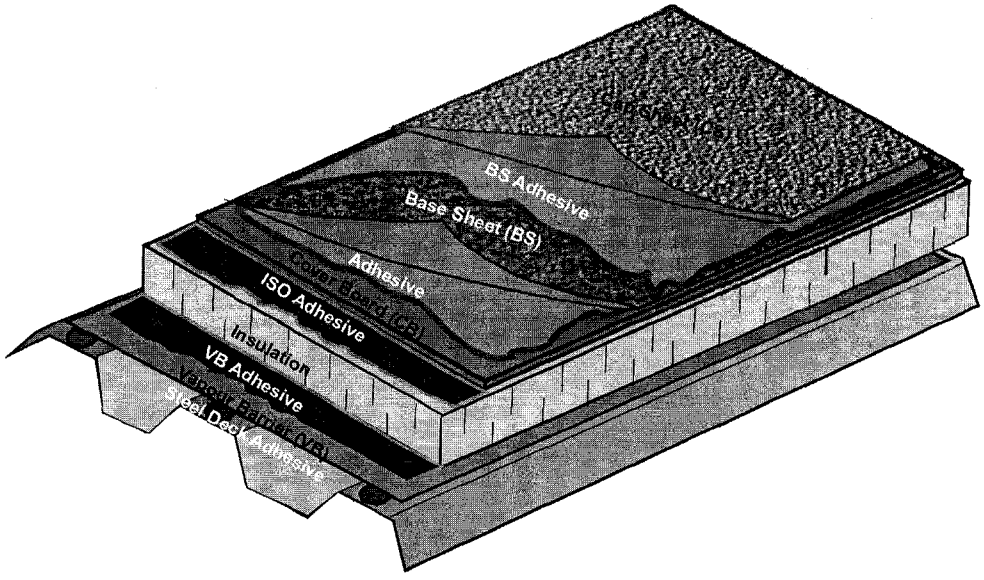

(a) Schematic

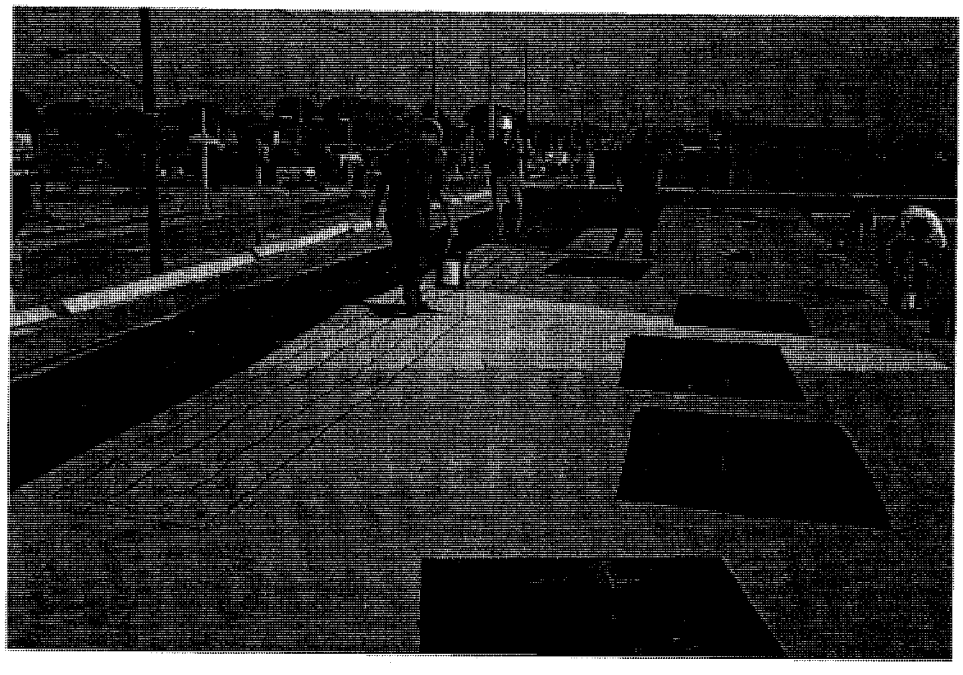

(b) Field installation (Courtesy of Bakor Inc.)

Figure 1.4 Schematic layout and field installation of an AARS assembly (Baskaran et al, 2007)

Table 1.1 A comparison of the various features of BUR and AARS

Build-Up Roofing System (BUR)	Adhesive Applied Roofing System (AARS)
Fastener corrosion and penetration problems	No fastener corrosion and penetration problems
Thermal birding	Excellent thermal performance
Kettle and flame required	No kettle and flame required
Hot-mopped adhesive	Cold adhesive
Danger of fire	No danger of fire
Strong odour fumes and air pollution	Environmental friendly and reduced odour

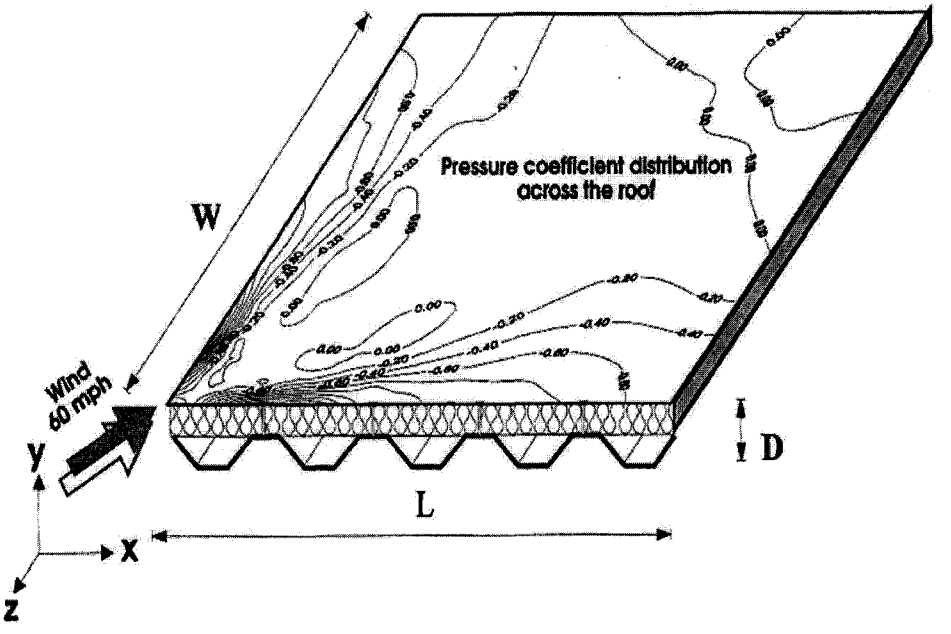

Figure 1.5 Pressure variations on a building roof under wind (Baskaran and Kashef, 1995).

Table 1.1 compares the advantages and disadvantages of BUR and AARS systems. AARS hold several advantages over conventional BUR systems. The fasteners in the BUR act as thermal bridges and allow more heat to escape from the building envelope. These same fasteners also create holes in the building envelope which leads to a travel path for the ingress of moisture. Moisture inside the building envelope can lead to poorer roofing performance in two specific areas. Moisture can lead to the growth of mould - this results in poorer insulation performance. Moisture can also cause the fasteners to begin to rust. This impairs the fastener's ability to hold loads. In addition, BUR systems also have the disadvantage of environmental pollution due to the fumes associated with the hot-mopped adhesive procedure. In contrast, the primary advantages of AARS systems are their proven performance due to less moisture seepage, decreased thermal bridging, and ease of use. These advantages make them a more suitable application in new roofing constructions.

1.3 Problem Definition

Wind is a significant factor in causing damage to roofing systems. Previous studies have shown that most wind damage to buildings occur on the roof cladding (Uematsu et al 1999, Baskaran et al, 2007). Wind causes stress on the roofing system (Tanaka, et al, 1999). Figure 1.5 illustrates an example of an intensive wind-induced pressure pattern on a flat roof, caused due to exposure to wind blowing diagonally to its corner (Baskaran and Kashef, 1995). In this figure, it is clear that particularly high uplifting forces take place near the corner and perimeter of the roof. The pressure decreases as wind blows across the roof. AARS systems, subjected to these wind pressures, may experience membrane lifting which leads to blister peeling failures. Figures 1.6 & 1.7 show some photographs of blister development in roof assemblies. Figure 1.6 shows membrane lifting and peeling failures caused by the hurricane Katrina (Baskaran, et al, 2007). Figure 1.7 shows several blisters in roof assemblies. However, the roof is still fulfilling in purpose. Blister failure is the single most common premature failure of AARS, and it leads to the loss of watertight

integrity of AARS membrane (Thomas, 1993). When a blister occurs, as shown in Figure 1.7, the peeling force acts normal to the membrane and the angle defined as θ is in the range of $0^{\circ} \leq \theta \leq 45^{\circ}$ as shown in Figure 1.8.

Little is known about the resistance of AARS against wind uplift. Currently, there are no standards that can be used to evaluate the wind uplift resistance of AARS. Although several studies have been undertaken to examine the effects of moisture inside residential buildings (i.e. CMHC 1987), and the mechanics and material characteristics of the fully adhered systems (Burnette,1987 & Burch,1991), little is known on the subject regarding commercial buildings' roofing systems - particularly regarding the wind uplift performance of AARS. As a result, the knowledge acquired in the past is of little use in predicting the problems that the new generation of roof systems may experience due to wind action.

1.4 Project Overall and Thesis Objectives

Although AARS have become popular in the Canadian roofing market, there is a lack of standard procedures and approved testing methods for this system, particularly regarding wind loading. To develop wind uplift standards for AARS, a collaborative research project was initiated. The project entitled "Development of wind uplift standard for adhesive applied low slope roof systems" is carried out by the National Research Council Canada, University of Ottawa and four Canadian roofing industry partners, supported by a NSERC (Natural Sciences and Engineering Research Council of Canada) CRD (Collaborative Research and Development) grant (CRDPJ 3065819-04). Overall, this joint project includes the following five tasks (Current, Murty, Wu, Baskaran and Tanaka, 2008):

- Task I: Pullout testing
- Task II: Peel testing
- Task III: Wind uplift testing
- Task IV: Numerical modeling
- Task V: Development of design guidelines

(a) Membrane lift up and sag

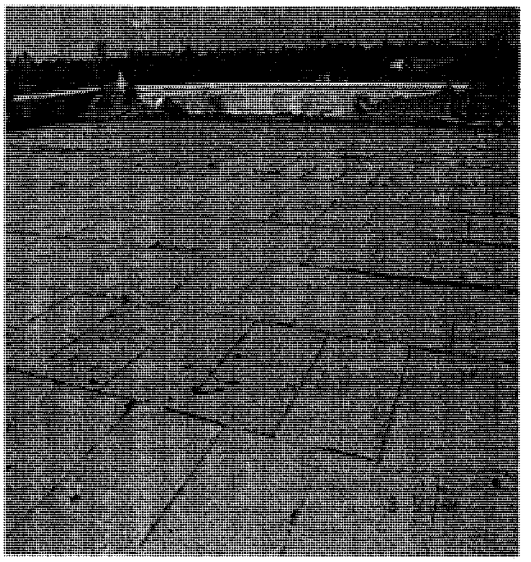

(b) Complete peel of membrane from fiberboard

(c) Peeled roof

Figure 1.6 Examples of blistering failure after hurricane "Katrina" (Baskaran, et al, 2007)

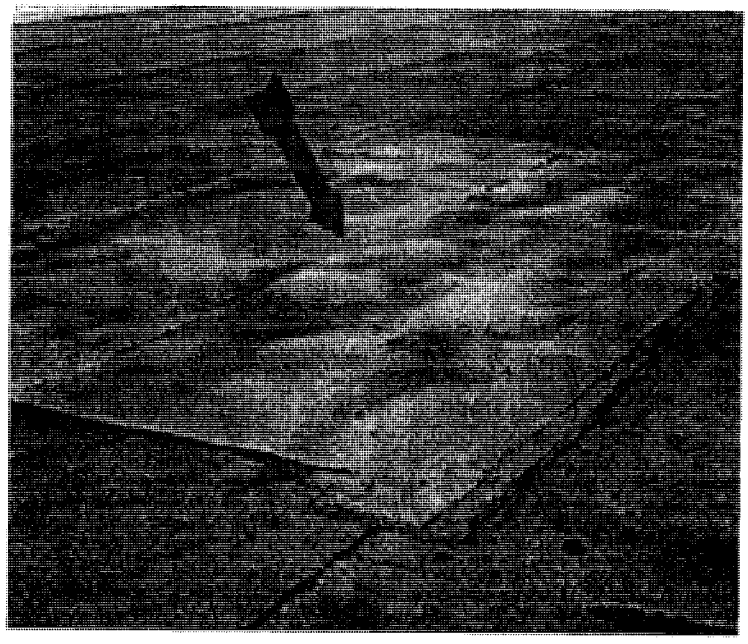

Figure 1.7 Development of blisters on roof assemblies (www.waynesroofing.com)

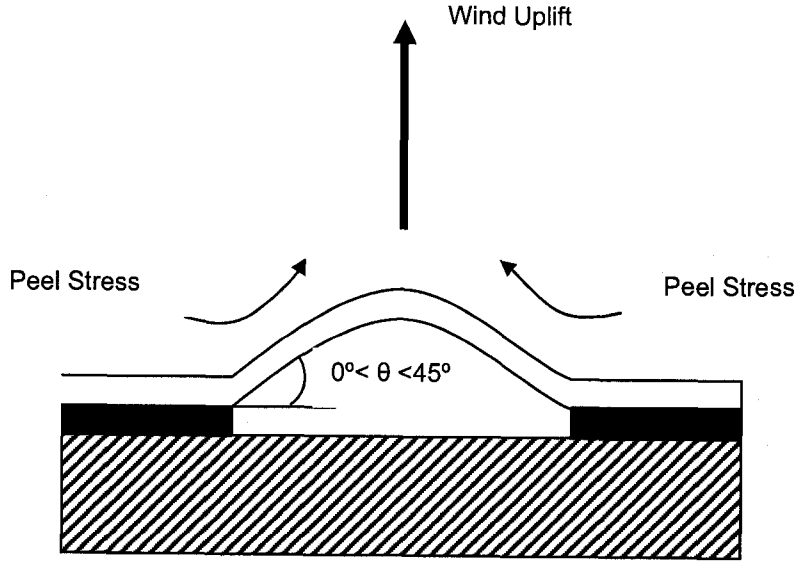

Figure 1.8 Peel stresses and angle of blister caused by wind uplift

This thesis comprises one part of the aforementioned research project and addresses Task II – peel testing. The deliverable of this thesis project is *"to develop a standardized test method for determining the peel resistance of AARS systems"*. This has been achieved by the following objectives:

1) Objective 1: Review the existing standards, including North American and European standards.

2) Objective 2: Experimentally investigate surface-to-surface contact of different material configurations that play a key role in the performance of the AARS.

3) Objective 3: Systematically analyze the failure modes and quantify the failure occurrence value of different components.

At present, no evaluation standards are available for the Canadian roofing community to quantify the wind peel resistance of the AARS. Therefore, developing a standard to quantify the peel resistance of AARS will facilitate the technology transfer of the proposed research. It is anticipated that these results will benefit not only the manufacturers but also the entire roofing industry, including applicators, consultants and designers.

1.5 Thesis Outline

In addition to the current Chapter, the thesis is comprised of the following chapters:

Chapter 2 reviews the existing peel test standards, which are relevant to the present study. These standards are currently in practice in both North America and Europe and are used to govern the peel tests of different materials. These standards are compared by selecting key parameters to identify their commonalities.

Chapter 3 is dedicated to the explanations of experimental setups and procedures developed in this study. First, the different experiments used to examine the effect of specimen size, peel position and peel angle on AARS samples are summarized. Then, the rationale of selecting cover board, insulation and adhesive materials and the experimental design of different material configurations on peel resistance are presented. Third, detailed steps of sample assembling process are illustrated. Finally, the experimental apparatus used for peel testing is introduced and the experimental procedures are listed.

Chapter 4 presents the results and discusses the influence of component configurations and effects of peel test parameters. This chapter presents the effects of different AARS components, namely two types of insulation, two types of cover board and the adhesive, on peel resistance. Then, the effects of peel position, peel angle and sample size on peel resistance are analyzed. Standard curves are generated to describe the generalized effects of these variables on the peel resistance.

Chapter 5 analyzes the various failure modes that were observed during the study. First, the failure modes observed in the study are defined. Next, a quantitative analytical method for comparing the frequencies of the occurrence of various failure modes is established and applied to quantify the failure frequency. Finally, a correlative analysis of failure modes and their corresponding peel resistance is presented.

Chapter 6 proposes a draft standard test method for peel resistance of AARS.

Chapter 7 summarizes the general conclusions of this study. It also identifies the future work that is needed to enhance the present findings.

Chapter 2 Literature Review

2.1 Introduction

As mentioned in Chapter 1, AARS are becoming popular in the Canadian roofing market. However, there is no standard to evaluate the wind uplift resistance of AARS. Wind uplift actions generate peeling forces that induce the separation of components and cause the premature failure of AARS. Therefore, the peel resistance is an important factor to be considered for the design and quality control of AARS. A peel test is an experimental approach that examines the peel resistance of bonded components through mechanical separation of bonded layers. A peel test standard provides regulatory guidelines that specify the scope and experimental conditions used to determine the peel resistance of specific samples. It will become an essential tool for the evaluation of AARS performance under wind actions and will benefit both roofing researchers and manufacturers.

As the first step of this thesis, a literature survey of the existing peel test standards is conducted in order to provide some background knowledge for the establishment of a standard peel test protocol for AARS. An extensive literature review of the various peel test standards reveals that some of the tests are intended for the determination of the resistance-to-peel strength of an adhesive used to bond a rigid component with a flexible component, while other peel tests are used to determine the relative peel resistance of adhesive bonds between two flexible components. Several of these peel test standards are currently practiced in North American and European countries. These existing standards include ASTM, ISO, and European standards such as BS-EN, DIN-EN.

2.1.1 Terminologies Often Used in the Peel Test Standards

In all of these different standards, an **adherend** refers to a material that is held to another material by means of an adhesive (ASTM D 907 – 06). A **flexible adherend**

refers to an adherend that has such dimensions and physical properties as to permit bending in any angle up to 90° without breaking or cracking (ASTM D 1876 -01). A **rigid adherend** is a hard or stiff adherend that is incapable of bending.

ISO – The International Organization for Standardization is a worldwide federation of national standards bodies, or the ISO member bodies. Its standards are developed by the ISO technical committees and subcommittees. ISO standards are developed based on three principles. One is consensus, in the sense that it takes into account the views of all interested parties, such as manufacturers, testing laboratories, governments, professional engineering groups, and so on. The second principle is industry wide, meaning that the standards are to satisfy industries and customers world wide. The third principle is voluntary, meaning the requirement for using ISO standards is market driven and voluntary. ISO standards are the result of agreements between ISO member bodies. Many ISO standards are implemented in different countries in the world (www.ISO.org).

ASTM International, originally known as the American Society for Testing and Materials, is one of the largest voluntary standards development organizations in the world. ASTM represents a trusted source for technical standards for materials, products, systems, and services. As such, ASTM standards are often practiced in Canada.

EN refers to European Standards that are issued by the European Committee for Standardization or Comité Européen de Normalisation (CEN). The EN standards are normally used by the 13 members of the CEN countries. Since any standards may have minor variations from one country to another, each European country may have its own modified EN standards. For example, BS-EN and DIN-EN represent modified EN standards for UK and Germany, respectively. British Standards (BS) is the UK's national standards organization that produces standards and information products. DIN stands for Deutsches Institut für Normung. In convention, each EN standard code number refers to only one standard, regardless of the country code

variation. For example, DIN-EN 12345 and BS-EN 12345 should refer to the German and British modified versions of the same standard.

2.2 Review of ISO Peel Test Standard

ISO has issued many standards for different peel test applications. For example, the ISO 8510-1:2006 is a standard entitled "Adhesives – Peel Test for a Flexible-Bonded-to-Rigid Test Specimen Assembly – Part 1: 90 Degree Peel". This standard specifies a 90° peel test for the determination, under specific conditions, of the peel resistance of a bonded assembly consisting of a flexible and a rigid adherend. Similarly, ISO 8510-2:2006 is a variation of the ISO 8510-1 and specifies the 180° peel test under identical conditions. In contrast, the ISO 11339:2003 standard entitled "Adhesives – T-Peel Test for Flexible-to-Flexible Bonded Assemblies" specifies a T-peel test for two flexible adherends. Here, the ISO 4578:1997 standard is chosen to be reviewed in this section.

ISO 4578 Standard: "Adhesives – determination of peel resistance of high-strength adhesive bonds – floating-roller method"

This standard defines the peel resistance testing method by using a floating-roller method. This floating roller is designed for free rolling in order to maintain the peel angle during the test. The apparatus includes a tensile testing machine and a peel test fixture that is used to support the test samples. The testing machine measures and records the maximum and minimum loads for each individual specimen. The machine also plots a chart of force versus crosshead movement or peeled distance during each test.

The specimens to be examined consist of two layers of adherend materials, **one rigid and one flexible**, bonded together (Figure 2.1). After the specimens are assembled, they are cured for a duration of at least 24 hours based on ISO standard 9142. The size of the rigid bottom specimen is (1 ± 0.02) in. or (25 ± 0.5) mm wide and (8 – 10) in. or (200 – 250) mm long. The flexible top adhered has the same

width, (1 ± 0.02) in. or (25 ± 0.5) mm, as the rigid bottom adhered, but it is 2 in. or 50 mm longer than rigid adhered. There is 1.6 in. or 40 mm of unbounded length between the overlap and the far end of the joint. This creates a lap joint as shown in Figure 2.1. The unbounded portion of the flexible adherend is then bent perpendicularly to the rigid adherend so that the specimen can be held by the jaws of the tensile testing machine. During the test, the machine peels a flexible adherend from a rigid one at a given angle defined by the peel test fixture and the floating roller. This peel angle roughly falls in the range of 60° to 120°. Each set of specimen tests are repeated no less than five times. The constant crosshead separation rate is (4 ± 0.02) in./min or (100 ± 5) mm/min.

2.3 Review of ASTM Standards for Peel Test

2.3.1 ASTM D 3167- 03a Standard: "Standard test method for floating roller peel resistance of adhesives"

This standard is similar to ISO 4578. It uses the same apparatus and a similar test method, with only two differences:

1. The first one is the specimen size. The specimen is 0.5 in. or 12.7 mm in width, 8 in. or 203.2 mm in length for bottom rigid membrane, and 10 in. or 254 mm long for top flexible membrane in the ASTM D 3167. The specimens have 2 in. or 50.8 mm outer edge at the end of the flexible membrane, but they do not have any unbounded length other than this edge.
2. The second difference is the crosshead rate. It is controlled at 6 in./min or 152 mm/min .

2.3.2 ASTM D 6862-04 Standard: "Standard test method for 90 degree peel resistance of adhesives"

This standard is also designated to test the peel resistance of a specimen where **a rigid and a flexible adherend** are bonded together, but the peeling angle is kept at approximately 90°. The apparatus consists of a testing machine and a test fixture. The fixture is a platform for supporting the test specimen. It can be smoothly driven

horizontally at the same crosshead speed. During the testing, the flexible adherend is kept at 90° angle with the fixed rigid adherent. The fixed rigid adherent is held by the platform (Figure 2.2 (a)). Force-extension curves are automatically generated by a computer that is connected to the testing machine. The crosshead speed is 10 in./min or 254 mm/min.

The recommended specimen size for this standard test is 4 in. x 12 in., or 102 mm x 305 mm as shown in Figure 2.2 (b). The unbounded end of the flexible adherend is bent perpendicular to the rigid adherend, and then clamped by the testing machine. Each sample set includes minimum of 4 specimens. The curing time of the specimens after assembly includes 4 hours, 24 hours, 7 days and 14 days.

2.3.3 ASTM D 1876-01 Standard: "Standard test method for peel resistance of adhesives (T-peel test)"

This standard is intended to test the peel resistance of the adhesive bonds of **two flexible adherends**. The test apparatus is a tensile testing machine. The machine has similar capabilities to the aforementioned test machines. Since the un-separated portion of the specimen and the two separated adherends resemble a T shape (180°) during the test, this type of standard test is also called T-peel test.

The specimen is comprised of two flexible adherends that are bonded together with adhesives. First, the test panels are cut into 6 in. x 12 in. or 152 mm x 305 mm pieces. The test panels are then bonded together, but an unbounded margin of approximately 3 in. or 76mm is left. These bonded panels are further cut into 1 in. or 25 mm wide and 12 in. or 305 mm long specimens (Figure 2.3). After that, the specimens are kept at a relative humidity of 50 ± 2% at 23 ± 1° C or 73.4 ± 1.8° F for 7 days before the test. Minimum ten specimens are tested in each sample set. During the test, the 3 in. or 76 mm unbounded ends of each sample are bent apart to 180° and both ends are inserted into the clamps of the testing machine to allow the jaws to clamp the specimen. The load is applied at a constant crosshead speed

of 10 in./min or 254 mm/min . The machine automatically records the curves of load versus head movement or load versus distance peeled.

2.4 Review of an EN Standard for Peel Test

European committee also issued a few standards for different peel test applications. For examples, BS-EN 12316 (DIN-EN 12316) standard includes two parts. Part 1 (12316-1:200) is focused on peel resistance of "bitumen sheets" and Part 2 (12316-2:200) is focused on "plastic and rubber sheets" and is reviewed below.

BS-EN 12316-2:2000 (DIN-EN 12361-2) Standard: "Flexible sheets for waterproofing-determination of peel resistance of joints" Part 2: "plastic and rubber sheets for roof waterproofing"

The purpose of BE-EN 12316-2:2000 (DIN-EN 12361-2) Standard is to specify a method to test the peeling resistance of joints between two identical adjacent roof waterproofing sheets of plastic or rubber. This standard is similar to the ASTM D 1876 T-peel standard. The test apparatus uses a tensile testing machine and it is used to perform the force and extension tests. Figure 2.4 shows the preparation of the specimen from specially made side and end laps. Five specimens are prepared for each sample set.

- The width of specimen is (2 ± 0.04) in. or (50 ± 1) mm; and
- The length of specimen is (width of joint + 4) in. or (width of joint + 100) mm.

Specimens are kept at 23 ± 2°C and 50 ± 5% relative humidity conditions for 2 hours before test. During the test, the specimen is firmly held in the clamps of the tensile testing machine, and the distance between the clamps is controlled at (4 ± 0.2) in. or (100 ± 5) mm. The grip separation speed is (4 ± 0.4) in./min or (100 ± 10) mm/min . The machine automatically records the applied force and extension until the test specimen separates.

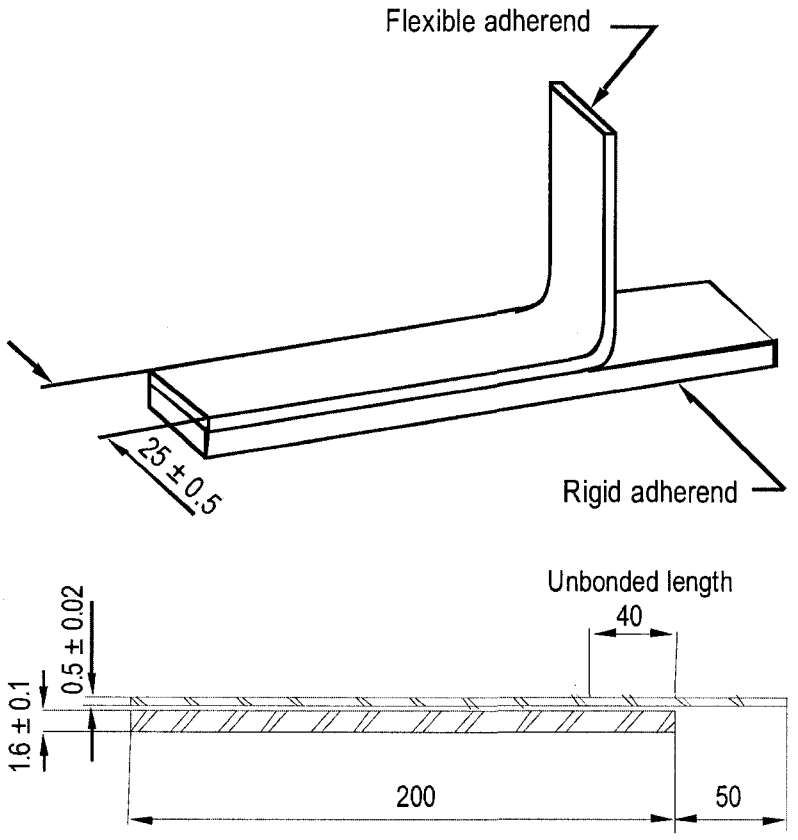

Figure 2.1 A flexible-rigid adherend specimen under floating-roller peel test (ISO 4578: 1997)

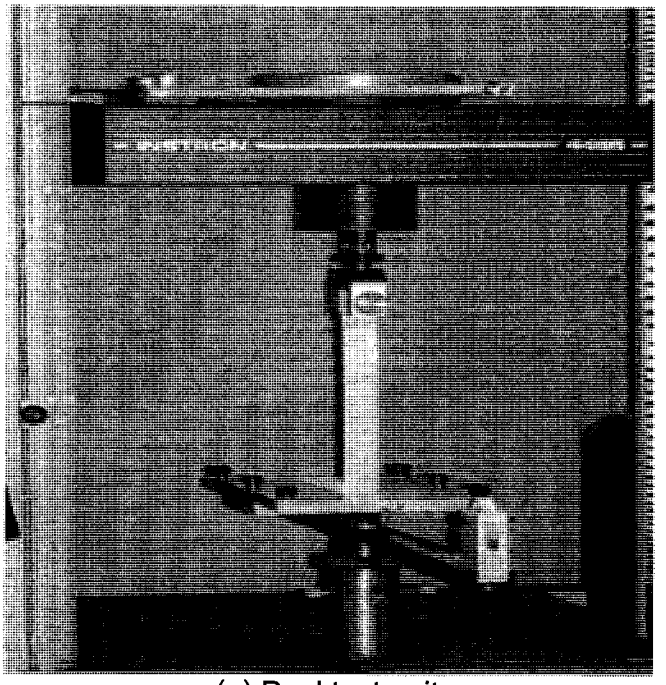

(a) Peel test unit

Sample size is 102 mm by 305 mm (approximately 4" by 12"). Exact size of samples to be determined by manufacturer and consumer.

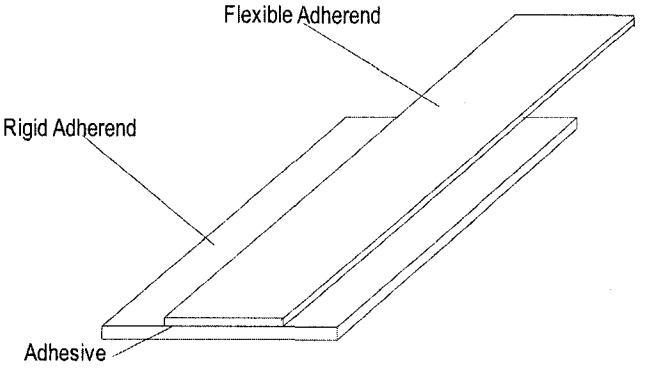

(b) Top View

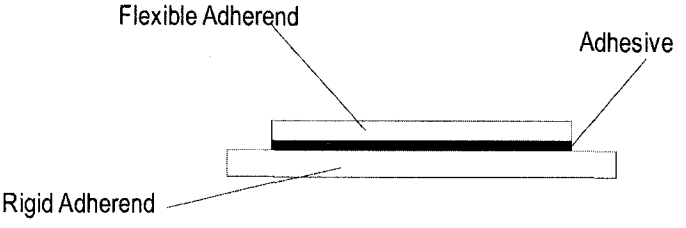

(c) End View

Figure 2.2 A flexible-rigid adherend specimen under 90 degree peel test (ASTM D 6862-04)

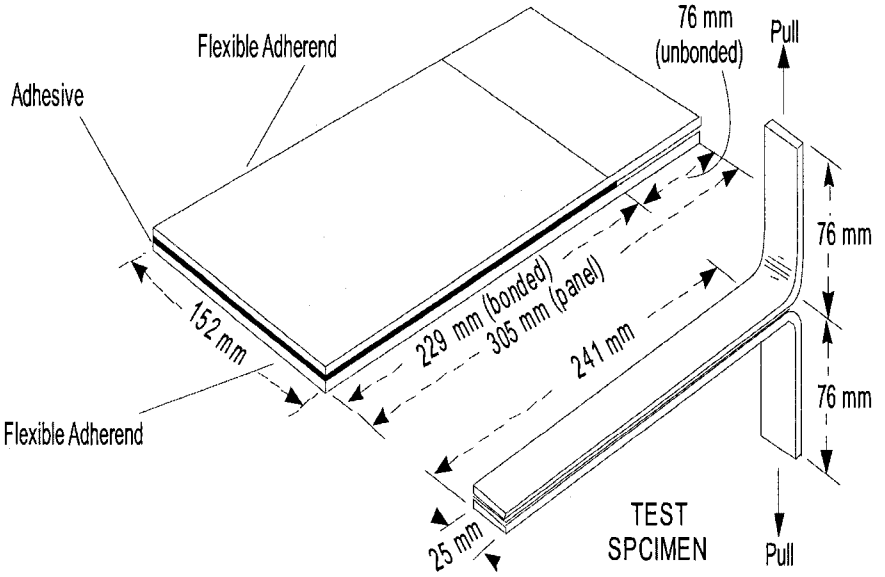

Figure 2.3 A flexible-flexible adherend test panel and test specimen under T-peel test (ASTM D 1876 - 01)

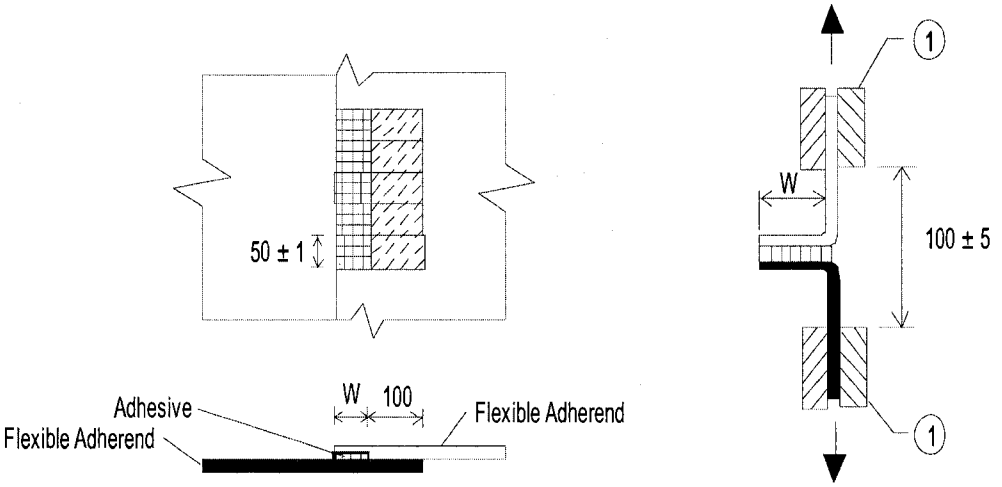

Key:
w: Width of joint, dimensions in millimeters
1: Grip

Figure 2.4 A flexible-flexible adherend test panel and test specimen under T-peel test (BS-EN 12316-2:2000)

2.5 A Summary of the Existing Peel Test Standards

Based on above literature review, Tables 2.1 to 2.3 summarize and compare several test parameters. From these tables, main similarities and differences of the existing standards are highlighted as follows:

- Scope: Limited to evaluate the relative peel resistance of adhesive bonds between either rigid and flexible adherends or between flexible and flexible adherends
- Specimen size (Length x Width);
  - ✓ Rigid-flexible adherends (ISO):
    - o Rigid adherend: (8-10) in. x 1 in. or (200 -250) mm x 25 mm
    - o Flexible adherend: (10-12) in. x 1 in. or (250 -300) mm x 25 mm
  - ✓ Rigid-flexible adherends under floating roller test (ASTM):
    - o Rigid adherends: 8 in. x 0.5 in. or 203.3 mm x 12.7 mm
    - o Flexible adherend: 10 in. x 0.5 in. or 254 mm x 12.7 mm
  - ✓ Rigid-flexible adherends under 90 degree test (ASTM):
    - o Both adherends: 4 in. x 12 in. or 102 mm x 305 mm
  - ✓ Flexible-flexible adherends under T-peel test (ASTM):
    - o Both flexible adherends: 12 in. x 1 in. or 305 mm x 25 mm
  - ✓ Flexible-flexible adherend (BS EN):
    - o Both flexible adherends: 6 in. x 2 in. or 150 mm x 50 mm
- Number of Specimens: 2 to 10 specimens for each test
- Curing time: 2 hours to 14 days
- Curing Condition:
  - o Humidity: 50 ± 2%
  - o Temperature: 23 ± 2 °C or 73.4 ± 3.6 °F
- Unbounded length: 1.6 in. to 4 in. or 40 mm to 100 mm
- Loading speed: 4 in./min or 100 mm/min to 10 in./min or 254 mm/min
- Peel angle: 0 to 180 degree
- Calculation: The average resistance-to-peel load

2.6 Concluding Remarks

This chapter presented a survey of various existing standards for peel resistance tests of adhesive joints. From these existing standards, it is evident that all of them have been developed for testing adherend assemblies in which either a rigid and a flexible components are bonded together or two flexible components are bonded together. However, in reality, most of roofing assemblies, particularly AARS systems, are composed of rigid layers that are bonded together with adhesive. It is imperative, therefore, that a standard procedure should be established to evaluate the peeling performance of two bonded rigid roofing components.

Table 2.1 Standard parameters of ISO 4578 peel test standard

Standard Designation	ISO 4578
Standard Name	Adhesives-Determination of peel resistance of high-strength adhesive bonds-floating -roller method
Scope	Determine the relative peel resistance of adhesive bonds between **a rigid** adherend and **a flexible** adherend under specified conditions of preparation and testing
Test Specimens Preparation	1.May be prepared individually or cut from bonded panels 2. Shall consist of two adherends properly prepared and bonded together
Specimen Size	a). (25 ± 0.5) mm or (1± 0.02) in. width b). (200 – 250) mm or (8 – 10) in. length for rigid adherend; (250 – 300) mm or (10 – 12) in. length for flexible adherend
Specimen Number	Not less than five or specified in the material specification
Curing Time	Select ageing conditions given in ISO 9142 1. For (3±1)h in the case of specimens exposed at a relative humidity higher than 50%, 2. For at least 24 h for all other specimens
Thickness of Adherend	The thickness of the flexible adherend shall be (0.5 ± 0.02) mm; the thickness of the rigid adherend shall be (1.6 ± 0.1)mm
Unbounded Length	40 mm or 1.6 in.
Conditioning and Testing Atmosphere	Given in ISO 291 or agreed between the adhesive user and the adhesive manufacturer
Rate of Speed	(100 ± 5) mm/min or (4 ± 0.2) in./min
Expression of Results	1. Autographic curve: a) by using a planimeter; b) a gravimetric method; c) by drawing the best straight line through the peeling curve, using a straight edge; and d) by any other method, such as the used of a computer 2. Record the maximum and minimum forces for each individual specimen
Calculation	N/A

Table 2.2 Standard parameters of ASTM peel test standards

Standard Designation	ASTM D3167-03a	ASTM D6862-04	ASTM D1876-01
Standard Name	Standard Test Method for floating Roller Peel Resistance of Ahesives	Standard Test Method for 90 Degree Peel Resistance of Adhesives	Standard Test Method for Peel Resistance of Adhesives (T-Peel Test)
Scope	Determine the relative peel resistance of adhesive bonds between **a rigid** adherend and **a flexible** adherend under specified conditions of perparation and testing	Determine the resistance-to-peel strength of an adhesive bond between **one rigid** adherend and **one flexible** adherend when tested at an angle of appromimately **90 degrees** under specified conditions of perparation and testing.	Determine the relative peel resistance of adhesive bonds between **two flexible** adherends by means of a **T-type** specimen
Test Specimens Preparation	1. Laminated test panels consist of two adherends properly prepared and bonded togher (254mm x 76.2mm or 10in. x 3in.), cut the bonded panels into 12.7 mm or 0.5 in. wide test specimens 2. Cut the bonded panels into specimen size	Laminated test panels consist of two adherends properly prepared and bonded together	1. Laminated test panels consist of two flexible adherends properly prepared and bonded together (152mm or 6 in. wide by 305mm or12 in. long), but bonded only over aproximate 241 mm or 9 in. of their length. 2. Cut the bonded panels into specimen size
Specimen Size	a). 12.7mm or 0.5in. in width b). 254mm or 10in. in length for flexible member, 203.2 mm or 8 in. in length for rigid member	102 mm x 305 mm or 4 in. x 12 in. Exact size of samples to be determined by manufacturer and consumer	25 mm x 305 mm or 1 in. x 12 in.
Specimen Number	2 specimens/each temperature tested /each of three bonded panels	4 specimens /per aging conditon	10 specimens/each adhesive
Curing Time	N/A	4h, 24h, 7days, 14days after assembly	7 days
Thickness of Adherend	1. Shall be specified in the material specification or 2. Flexible adherend shall be 0.63mm or 0.025in. thick and rigid adherend shall be 1.63 mm or 0.064 in. thick	1. Shall be specified in the material specification 2. Flexible adherend shall be 0.63mm or 0.025in. thick and rigid adherend shall be 1.63 mm or 0.064 in. thick	N/A
Unbounded Length	50.8mm or 2 in.	N/A	76 mm or 3 in.
Conditioning and Testing Atmosphere	N/A	N/A	Shall be capable of maintaining a relative humidity of 50± 2% at 23 ± 1° C or 73.4 ± 1.8° F
Rate of Speed	152 mm/min or 6 in./min	254 mm/min or 10 in./min	254 mm/min or 10 in./min.
Expression of Results	1. Autographic curve of load versus head movement or load versus distance peeled 2. Record the load over at least a 7.6 mm or 3 in. length of the bond line	1. Autographic curve the force-extension curve 2. Record the load over at least a 7.6 cm or 3 in. separation length of the lond line or as agree to by the adhesive manufacturer and the end user	1. Autographic curve of load versus head movement or load versus distance peeled 2. Record the peel resistance over at least a 127 mm or 5 in. length of the bond line after the initial peak
Calculation	The average peeling load in pounds-force per inch or kilomewtons per metre of the specimen width required to separate the adherends	The average resistance-to-peel strength in kilonewtons per meter or pounds-force per inch of the specimen width required to separate the adherends	Determine from the autographic curve for the first 127 mm or 5 in. of peeling after the initial peak the average peeling load in pounds per inch of the specimen width required to separate the adherends

Table 2.3 Standard paramaters of EN 12316 peel test standard

Standard Designation	BS EN 12316-2:2000 (DIN EN 12316-2)
Standard Name	Flexible sheets for waterproofing-- determination of peel resistance of joints Part 2: plastic and rubber sheets for roof waterproofing
Scope	This European Standards specifies a method for determining the resistance to peeling of joints between two adjacent sheets of the same plastic or rubber sheet for roof waterproofing.
Test Specimens Preparation	1. Before jointing, test pieces should be previously conditioned for at least 20 h at (23± 2)°C and at a relative humidity between 30% and 70 %. 2. After jointing, the test piece shall be conditioned for a minimum of 2 h at (23± 2) °C and at (50± 5)% RH before testing. 3. From each of these joint test pieces, five rectangular test specimens (50 ± 1) mm or (2 ± 0.04) in. wide shall be cut, perpendicular to the joint.
Specimen Size	(50 ± 1) mm or (2 ± 0.04) in. wide, (width of joint + 100) mm or (width of joint + 4) in. length
Specimen Number	Five per set
Curing Time	Before jointing, 20 h; After jointing, minimum 2 h before testing
Thickness of Adherend	N/A
Unbounded Length	100mm or 4 in.
Conditioning and Testing Atmosphere	Temperature shall be at (23± 2)°C
Rate of Speed	(100 ± 10) mm/min. or (4 ± 0.4) in./min
Expression of Results	1. Jointing information. 2. Evaluation: a) Maximum peel resistance; and b) Average peel resistance.
Calculation	Calculate peel resistance as the mean (using the maximum or average peel force as occurs for each specimen) expressed in N/50 mm. State the peel resistance to the nearest Newton with the corresponding standard deviation.

CHAPTER 3 Experimental Set Up

3.1 Introduction

In Adhesive Applied Roofing Systems (AARS), the properties of materials play a key role in the system performance. One main objective of this study is to experimentally quantify the peel resistance of representative AARS samples using various peel test regimes. Peel resistance is defined as the tensile force required to completely separate two bonded components. The principle of this method is to pull one adherend component away from another adherend component until it breaks off or separates into two discrete layers.

This chapter presents the experimental setups for peel tests that are carried out in two phases:

- Phase I investigated the effects of insulation and cover board material combinations and peel positions on the peel resistance of various AARS specimens.
- Phase II evaluated the effects of peeling angle and the size of the specimen of selected material combinations on the peel resistance.

First, the experimental apparatus used for the peel tests is described (Section 3.2). The central component of the apparatus is an Instron 5566 machine that generates and measures peel forces during the peel tests. The functions of several other key components of the experimental apparatus, including the fixer, gripper and angle controller, are also introduced in Section 3.2.

Next, in Section 3.3, the various insulation and cover board materials commonly used in AARS are described, and the rationale of examining two different types of insulation and two different types of cover board is presented.

The experimental variables or parameters used for peel tests are reported in Section 3.4, with a comprehensive table summarizing all the samples and variables examined in this study. These variables include peel angles, peel positions and sample sizes. Six different peel angles, two different peel positions and four different sample sizes are examined in this study.

Finally, the procedures of setting up the peel test experiments are described in Section 3.5. Particularly, the sample mounting and angle control setting are explained in detail since these procedures involve novel designs in this study and are critical to the accuracy of experimental results. At the end of this section, a step-by-step protocol of the peel test is explained.

3.2 Experimental Apparatus

The peel test apparatus has four main components that are as follows:

- Instron 5566
- Fixer
- Gripper
- Angle controller

3.2.1 Instron 5566

The equipment utilized in the peel test is an Instron 5566 machine shown in Figure 3.1. The Instron test system performs mechanical (including tensile, compressive, shear, peel and flex) tests on a wide variety of materials. A mechanical test typically involves subjecting a specimen of known materials to varying forces. The forces used to determine the mechanical characteristics of the specimen can be compressive, tensile, flexural, or tensional. The resulting characteristics are used for specific purposes, such as material characterization, selection, quality assurance and failure analysis.

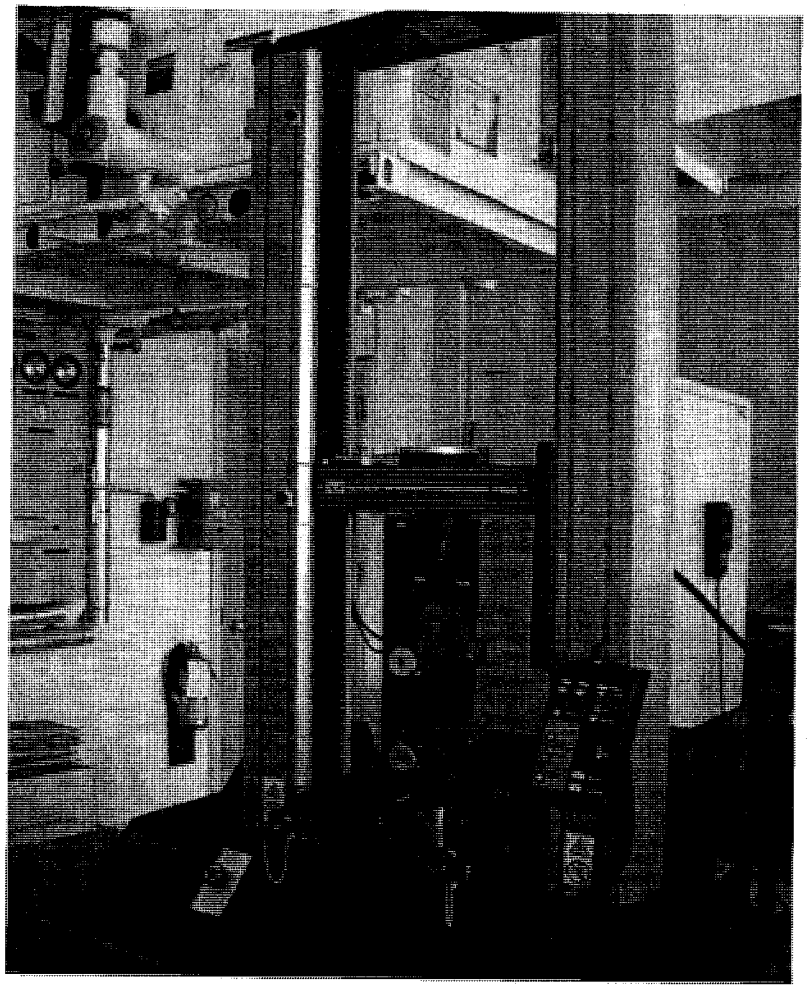

Figure 3.1 A front view of the Instron 5566

The main components of the Instron system include testing frames that are designed for generating tension, compression and reverse stress with high precision, accuracy, safety, and reliability. In addition, the machine has a self-aligning jaw that is connected to the test specimen with a steel wire. The self-alignment function ensures that the applied force would act upon the centerline of the specimen assembly when a peel force is applied.

This system is computer-controlled and uses software called Bluehill2 to control and monitor the test, collect data and generate reports required by the user. The user can use Bluehill2 software to create his/her own report and graphic templates, test results, customized layouts and styles. Bluehill2 software includes a few test types, such as tension, compression and peel. The Bluehill2 software supports three different types of peel tests; 90° peel, 180° peel and T-peel. In the present study, all specimens were tested using the 90° peel test feature of the Instron 5566 system. The 90° peeling test allows for peel angles ranging from 0 - 90°.

3.2.2 Fixer

The fixer is fabricated with an aluminum or steel plate. It is used to hold the specimen stable during the peel test. The fixer is mounted on a supporting table. Figure 3.2 (a) & (b) shows a sketch and a photograph of the fixer. The fixer's size is 16 in. or 406 mm long, 14 in. or 356 mm wide and 4 in. or 102mm deep. For specimens less than 4 in. or 102 mm thick, plywood dummies are inserted beneath the specimen so the total height is equal to 4 in. or 102 mm. Steel plates are used on three sides of the fixer to keep the specimen in position during the experiment (Figure 3.2). A movable vertical steel plate is used to clamp the specimen tightly in place. This 6 in. or 153 mm high movable steel plate is connected to three steel threaded rods: one at the bottom, the other two at the top. Together they are used to adjust the specimen's position. Specifically, the bottom steel rod can move the steel plate forward or backward until it reaches the required specimen size; then the top rod is adjusted to hold the specimen tightly. The specimen is further secured with a row of small screws.

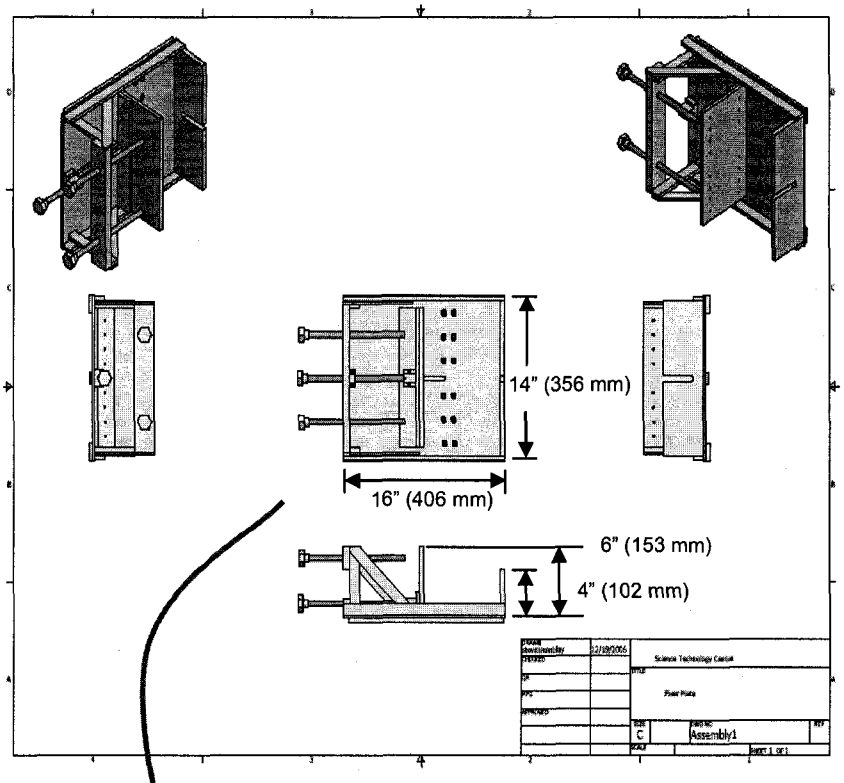

(a) Sketches of the fixer

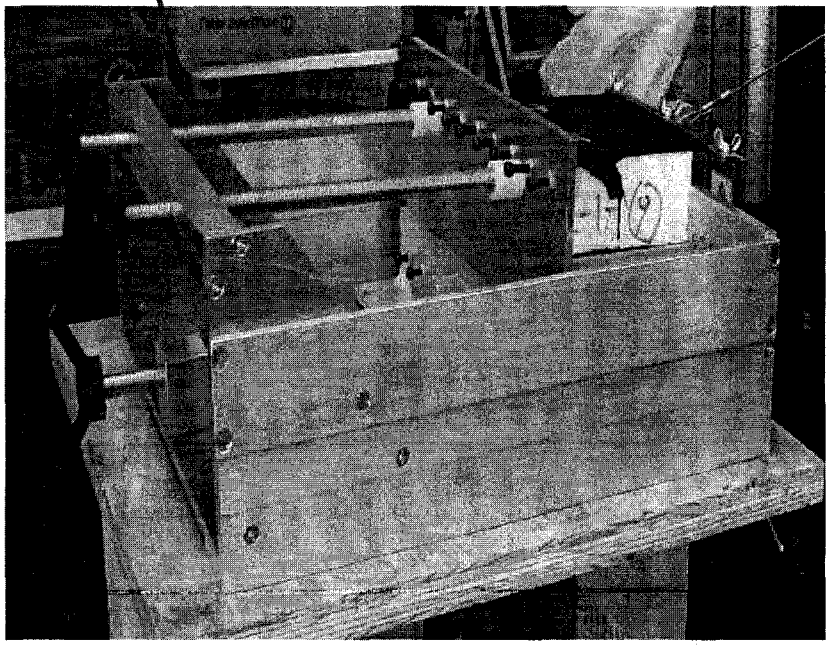

(b) A photograph of the fixer

Figure 3.2 Schematics and a photograph of the fixer for mounting the test specimen

3.2.3 Grippers

Grippers are a link connecting the specimen to the Instron machine. Two types of grippers are used in this study; one designed for edge positioned (E-P) specimens, where specimens are peeled along an edge that is devoid of adhesive (details explained in 3.4.2); the other designed for corner position (C-P) specimens, where specimens are peeled at a corner devoid of adhesive.

The main component of the E-P gripper consists of two pieces of parallel steel plates (Figure 3.3 (a)) that firmly grip the 0.5 in. or 18 mm overhang of the top rigid adherend. The length of these steel plates ranges from 8 in. or 203 mm to 12 in. or 305 mm to accommodate different sized specimens. The gripper is connected to the Instron machine by a steel wire with the diameter of 1/8 in. (3 mm) or 1/16 in. (1.5 mm) depending on the peel force applied. The steel wire is threaded through the centerline of the specimen assembly.

The grippers for C-P specimens are composed of a pair of steel claws that clamp onto the corner of a specimen (Figure 3.4 (a)). The bottom claw is sharpened so that it can be easily inserted into the unbound corner space between the two layers of adherends.

The grippers are tightened onto the top adherend layer by screws. When the thickness of the top adherend is more than 1/2 in. or 18 mm in thickness, springs are installed into the gripper in order to balance this thickness and achieve the maximum grip force (Figure 3.3 (b) & 3.4 (b)). Otherwise the gripper may slip during the test. When a thinner top adherend, which is thinner than 1/2 in. or 18mm thick, is tested, no springs are required.

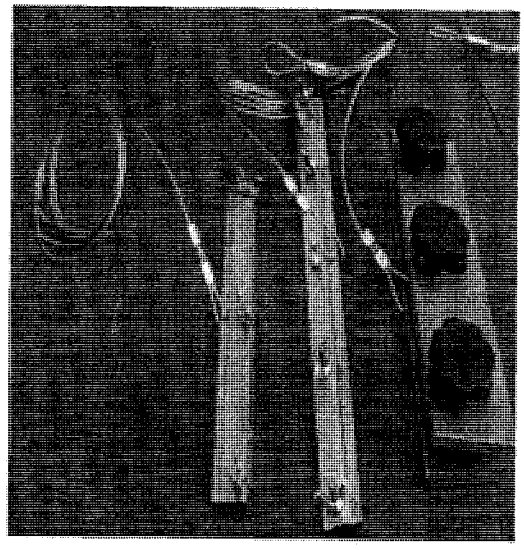

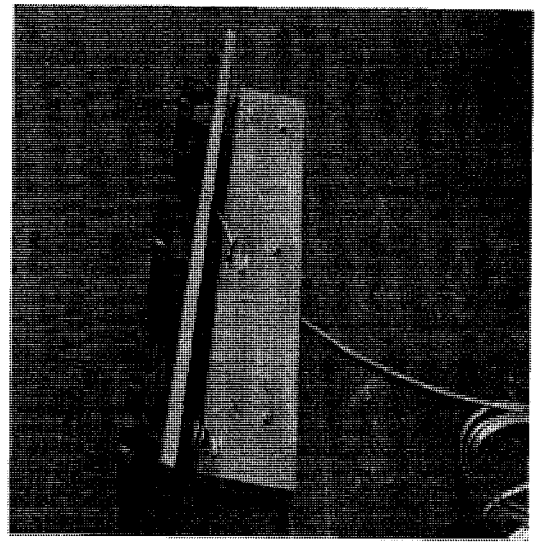

(a) Three typical grippers (b) A close view of a gripper

Figure 3.3 Photographs of grippers used for edge position peel test

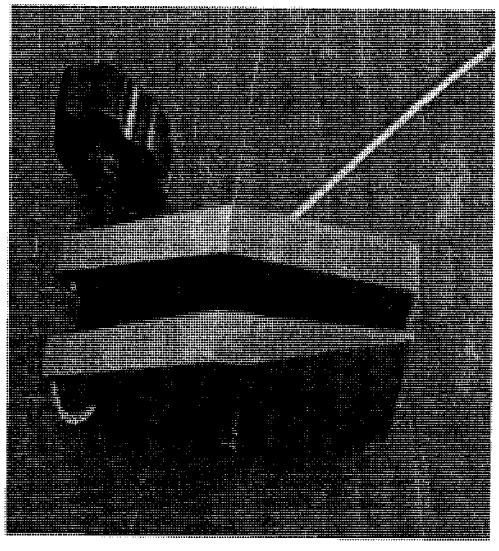

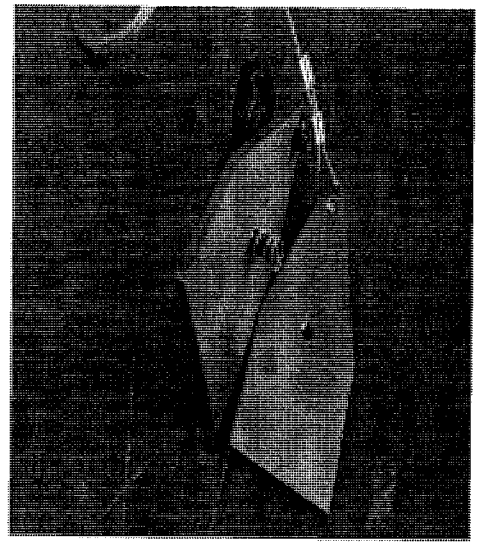

(a) A typical gripper (b) A close view of a gripper

Figure 3.4 Photographs of grippers used for corner position peel test

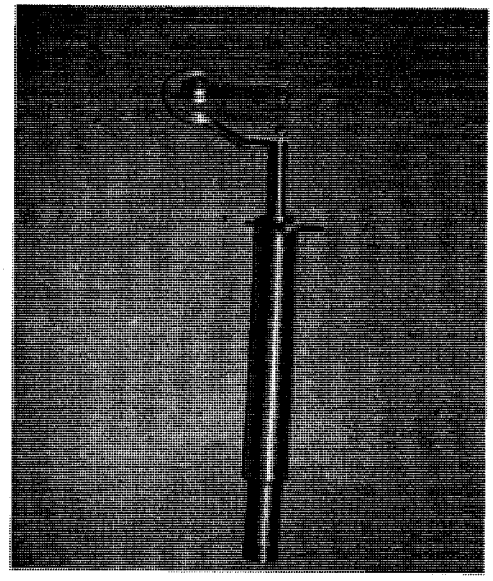

(a) A full view

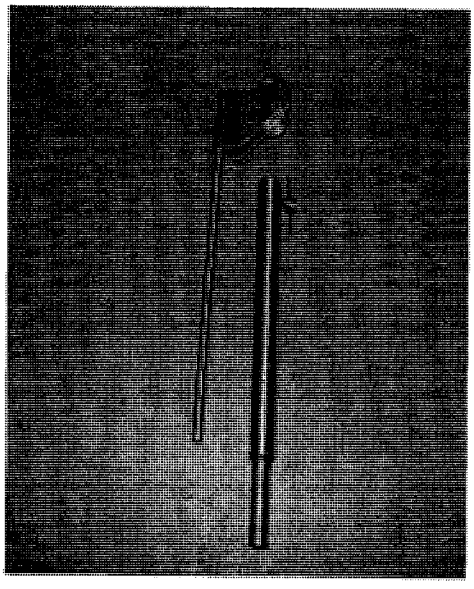

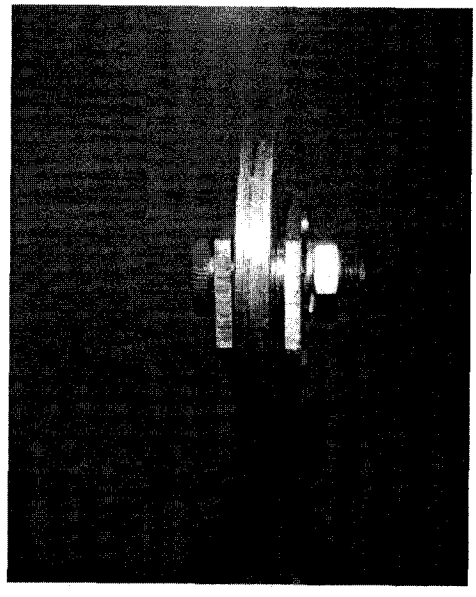

(b) Pulley detached from the steel tubes (c) A close view of the roller on the pulley

Figure 3.5 Photographs of the angle controller

3.2.4 Angle Controller

The angle controller (Figure 3.5 (a)) serves to control the initial peel angel. The Instron machine includes two self-aligning jaws. Before commencing, the bottom jaw is removed from the Instron machine and replaced with a shaft. The function of this shaft is to hold the angle controller. The angle controller has two parts; a pulley and a steel holder (Figure 3.5 (b)). The holder consists of an inner solid steel bar, which is 8 in. or 203 mm long, 3/8 in. or 10 mm in diameter, and an outer steel tube, which is 8 in. or 203 mm long, 7/8 in. or 22 mm in diameter. The length of the holder can be adjusted by sliding the inner steel bar along the outer tube. The inner steel bar is scaled by 1/4 in. or 6 mm increments for fine-tuning the peel angle. The initial peel angle, which is determined by the roller height, is adjusted by sliding the inner steel bar into the holder. During experiments, the steel wire of the gripper goes though the pulley of the angle controller (Figure 3.5 (c)), and connects to the Instron's upper jaw. The pulley is used to keep the steel wire moving freely during the peel test with minimum friction.

3.3 Sample Components Selection

In general, AARS can have many material components layered together by the application of adhesives. Typical components are: 1) deck, 2) vapour barrier, 3) insulation, 4) cover board and 5) layers of membrane. This study examined only the insulation and cover board, because these two components are the most unstable under wind-induced peeling forces. This study tests specimens composed of insulation and cover board that have been adhered together using cold-applied adhesives. Figure 3.6 is a flow chart showing the detailed material components and configurations of specimens examined in this study.

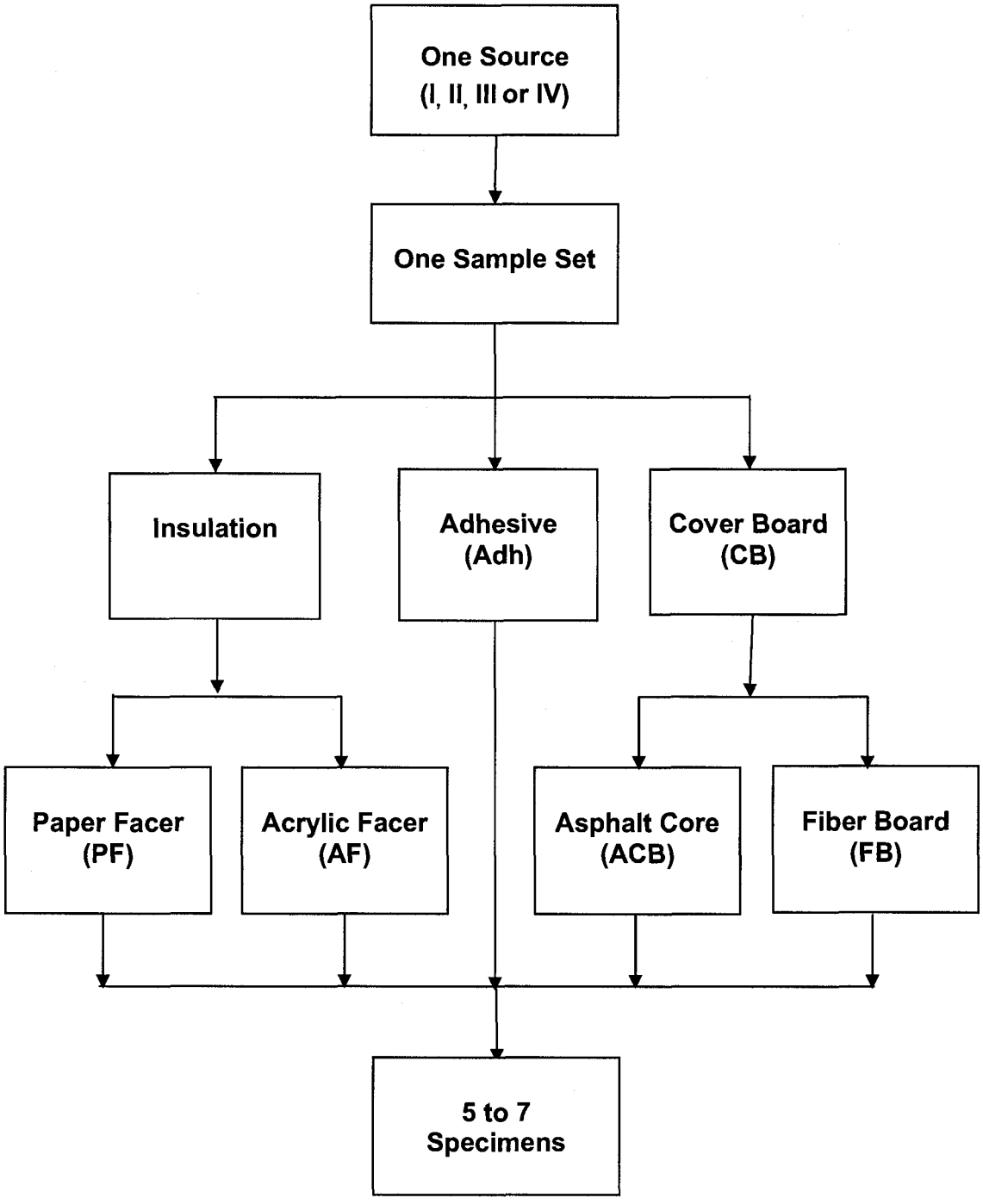

Figure 3.6 A matrix showing the material components of specimens examined in this study

3.3.1 Selection of Insulation Materials

The insulation is placed over the vapour barrier of the AARS assembly. The insulation is designed to resist degradation caused by moisture and to protect the steel deck from corrosion. In modern building construction, many types of insulation are commonly used. These include acoustical, radiant, reflective and thermal insulations.

This study focuses its attention on thermal insulation, which is the most popular insulation material in North America. Most thermal insulations consist of a central polyicocyanurate foam layer sandwiched between two layers of facing materials. In this study, two commonly available commercial thermal insulation products are examined. These two types of insulation differ in their facer materials: one is Paper Facer (PF) and the other is Acrylic Facer (AF). PF is a type of organic glass reinforced facer and AF is a non-organic reinforced facer.

The insulation specimens examined in this study are cut from commercial thermal insulation products (48 in. x 48 in. x 2 in. or 1219 mm x 1219 mm x 51 mm; width x length x thickness). The thickness of the insulation used in this study was chosen to be 2 in. or 50 mm, because previously published studies indicate that the median thickness of insulation in the roofing systems of North America is (1.6 ± 0.4) in. or (41 ± 10) mm within a range from 1 in. to 4 in. or 25 mm to 100 mm (Dechow and Epstein,1997).

3.3.2 Selection of Cover Board Materials

Cover board (CB) is placed on top of the insulation to protect it from physical and chemical damages, such as mechanical impact due to heavy loads, overheating during the application of torch (melting), and possible corrosion by erosive chemicals. There are several types of cover board commonly used in commercial roofing: asphalt, wood fibre, perlite, gypsum, and cement boards.

This study investigates the properties of two types of cover board; the asphalt core cover board (ACB), and the fibre board cover board (FB). The ACB consists of a high-melting-point asphalt core and mineral fillers of non-moven glass fibre mats. It is a rigid, flat sheet that is fire-resistant, non-warping, non-shrinking and non-curling at thicknesses ranging from 1/8 in. or 3 mm to 1 in. or 24 mm. Normal width is 36 in. or 914 mm, 48 in. or 1219 mm and 60 in. or 1524 mm, and nominal lengths extend up to 72 in. or 1829 mm. The dimensions of ACB sheets used in this study are 48 in. x 60 in. or 1219 mm x 1524 mm with a thickness of 1/8 in. or 3 mm.

The main components of FB are wood fibers and recycled paper. FB is highly moisture resistant and promotes membrane adhesion. Unfortunately, it has a propensity to absorb water and may quickly degrade into an unstable mixture of cellulous fibers under humid conditions. Therefore, FB is commonly used in low heat or unheated manufacturing plants. Commonly available thicknesses of FB are 7/16 in. or 11 mm and 1/2 in. or 12.5 mm. The dimensions of FB sheets used in this study are 48 in. x 24 in. or 1219 mm x 610 mm with a thickness of 1/2 in. or 12.5 mm.

3.3.3 Selection of Cold Adhesives

Cold adhesives (Adh) are designed to be used for all aspects of adhering roofing components, including the adherent of insulation and cover boards. Cold applied adhesives are characterized by their ability to be applied at ambient temperatures, generally above 4°C or 40°F, without the need for primary heating (A guide for the wind design of adhesive applied roofing systems, 2007). Cold applied adhesives are formulated and designed for specific uses such as function, exposure, material compatibility and/or desired rate of cure.

In AARS, the method of adhesive application can be either ribbon format, or full coat coverage format. In ribbon format, the adhesive is applied in lines like ribbons, with 8 in. or 203 mm to 10 in. or 254 mm spaces between each ribbon. In full coat coverage format, the adhesive is uniformly spread over the top surface of one

component, and the second component is placed on top. Although the ribbon format is more widely used in the construction industry, in this study the adhesives for all specimens were applied in full coat coverage format, due to the small size of the specimens examined.

This study was carried out in collaboration with four Canadian roofing industrial partners. Both of the insulation types, PF & AF, came from one particular partner, but the CB, both ACB and FB types, and cold adhesives came from all four partners, who prepared their own specimens independently. Each industrial partner constructed its specimens using insulation from a common source, but the CB and adhesives used varied in chemical and physical properties.

3.4 Test Parameters

3.4.1 Specimen Size

Four different specimen sizes are examined in this study. These are:

- 4 in. x 4 in. or 102 mm x 102 mm;
- 6 in. x 6 in. or 152 mm x 152 mm;
- 8 in. x 8 in. or 203 mm x 203 mm; and
- 10 in. x 10 in. or 254 mm x 254 mm.

The 6 in. x 6 in. or 152 mm x 152 mm size is called the "standard size" in this study. This is the specimen size used for examining other variables, such as different peel position, peel angles, and different CB and insulation materials.

All specimens examined in Phase I are 6 in. x 6 in. or 152 mm x 152 mm "standard size", but with different cover board, insulation configurations and peel positions (details explained in 3.4.2). The "standard size" specimens in Phase II were assembled with only one type of CB (ACB) and two types of insulation (PF or AF). The additional specimens of different sizes were assembled with ACB type of CB, and PF type of insulation.

3.4.2 Peel Position

Two different peel positions are examined in Phase I of this study: one is the edge position (E-P) (Figure 3.7 (a)); another is the corner position (C-P) (Figure 3.7 (b)). In Phase I, specimens tested in edge position (E-P) were assembled with two types of CB, ACB or FB, and two types of insulation, PF or AF. Specimens tested in the corner position (C-P) were assembled with one type of CB, ACB, and two types of insulation, PF or AF. Typically, all specimens were tested for E-P tests in Phase II.

Figure 3.8 (a) shows a sketch of an E-P specimen. When the cover boards were intended to prepare specimens for edge peel (E-P) experiments, they were cut into pieces that were 0.5 in. or 13 mm longer than the insulation, so that a 0.5 in. or 13 mm overhang devoid of adhesive is available for gripping during the peel test. For example, 6 in. x 6 in. or 152 mm x152 mm specimens' CB size is 6 in. x 6.5 in. or 152 mm x 165 mm. Then the CB and the insulation were bonded together by applying adhesives in full coverage format. The A-A cross-section in Figure 3.8(b) shows that the CB had a 0.5 in. or 13 mm long overhang on one side of the specimen when CB is fully adhered to the insulation. Figure 3.9 shows a picture of the E-P specimen's preparation process.

For C-P experiments, the CB and insulation sheets were cut into uniform sizes, such as 6 in. x 6 in. or 152 mm x 152 mm, for the assembly of corner peeling (C-P) specimens. A line was drawn across one corner to form an isosceles triangle. Then the adhesive was uniformly applied over the whole surface except for the triangle corner. Finally the insulation was bonded with the CB (Figure 3.10). The function of this un-bonded corner is similar to the overhang of the E-P specimen. It is left for the insertion of the gripper.

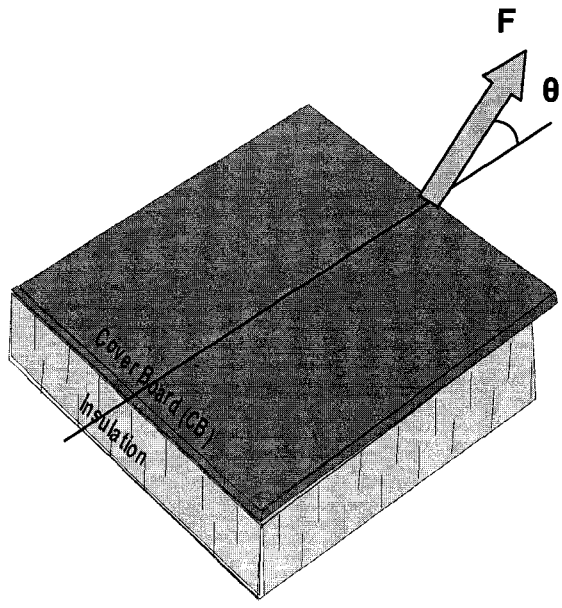

(a) A specimen tested in E-Position

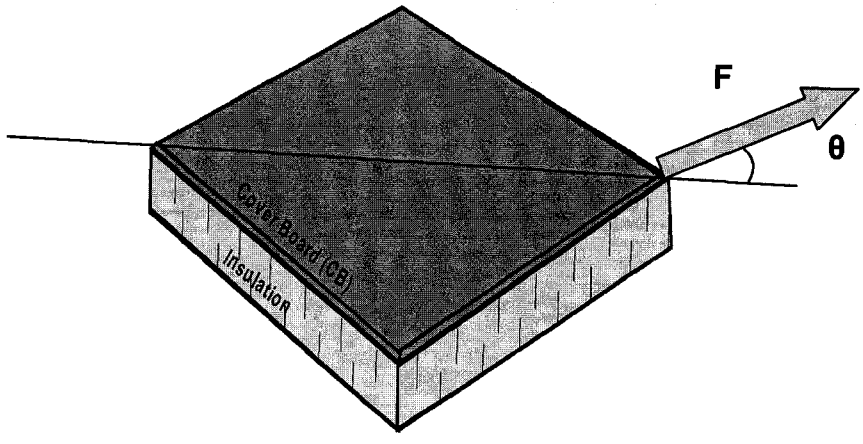

(b) A specimen tested in C-Position

Figure 3.7 Schematic diagraphs of specimens used for different peel positions

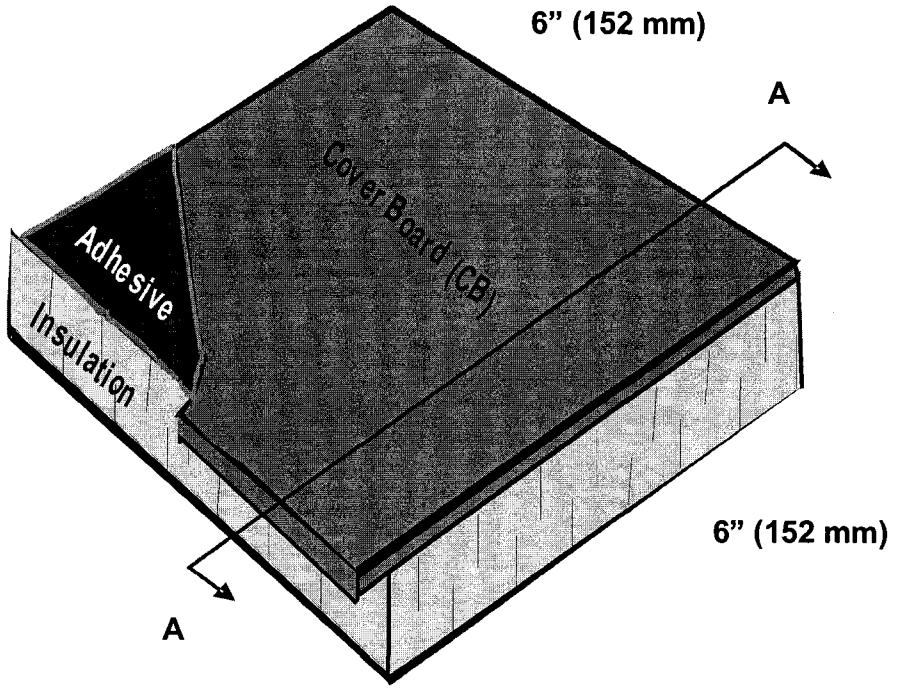

(a) A 3-dimensional view

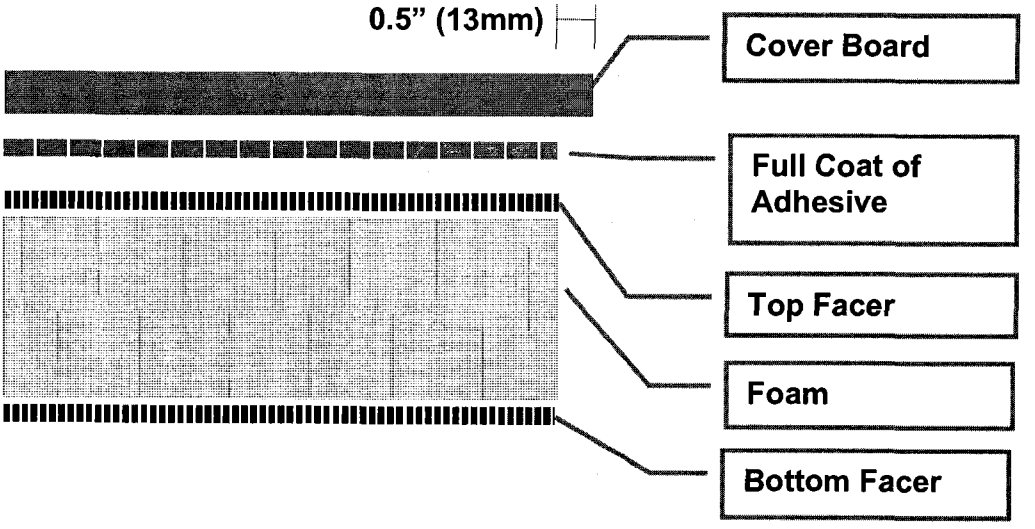

(b) A-A cross-section view

Figure 3.8 Schematic diagraphs of a typical E-P specimen

Figure 3.9 Adhesive appliances for E-Position specimen preparation

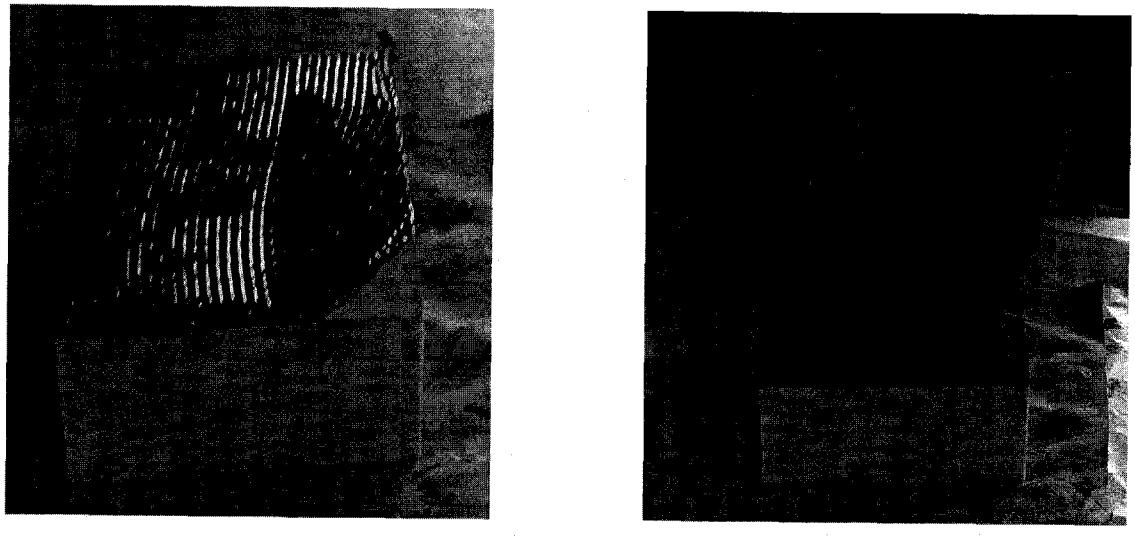

Figure 3.10 Adhesive appliances for C-Position specimen preparation

3.4.3 Peel Angle

In all Phase I and some Phase II experiments that are designed to examine the effects of cover board and insulation configurations, sample sizes, and peel positions, the specimens were peeled at a 15° angle. In order to investigate the effects of different peel angles on peel resistance, 6 different peel angles were examined in Phase II. They range from 7.5° to 45° with 7.5° intervals.

3.4.4 Test Matrix

In order to provide realistic representation of AARS used in the field construction, different specimens using from four different industrial sources were prepared. Although all the insulation materials were from a common source, the cover boards and adhesives were from four different industrial sources and fabricated independently by the four partners. The construction process accounts for the variations in the field application process. For example, some industrial sources used a roller to construct the bonding between cover board and insulation, whereas others didn't use any special methods to stabilize the adhesion between cover board and insulation. The adhesive application methods were also somewhat different among the sources. For example, some industrial sources completely mixed the cold adhesive using electric mixer before applying to specimens, whereas others directly spread the cold adhesive to the insulation surface. In this thesis, the thickness and application protocol of the adherends are completely determined by the industrial partners, in order to best simulate the field application protocols. Therefore, the test results were expected to be influenced by this diversity of fabrication and material combination. The variations in the application method from one industrial source to another may also affect the wind uplift performance of the AARS in the field.

In Phase I, each industrial partner constructed 6 sets of small-scale assembly that were numbered *-1 to *-6, where * is the ID number to indicate the industrial sources: I, II, III or IV. Each sample set has seven specimens. A total of 168 specimens (6 sets x 7 specimens per set, from 4 industrial sources) were fabricated for peel tests in the Phase I study.

In Phase II, based on the material availability and the results of the Phase I experiments, materials from two industrial partners representing distinct peel resistance (a "good" performance and a "bad" performance), were chosen for further examination. Hence, in this phase of study, the specimens were labeled as "S*" or "S'*", where S indicates PF/ACB specimens, S' indicates AF/ACB specimens, and * indicates the industrial source ID number. Each industrial partner constructed 12 sets of "standard size" samples and 3 sets of additional size samples. Each set of sample contains seven specimens, similar to those in Phase I study. Therefore, a total of 210 specimens (15 sets x 7 specimens x 2 industrial sources) were fabricated for the Phase II tests. Altogether, 378 samples were constructed for the present study. Table 3.1 shows the detailed description of all specimens examined in the small scale peel tests.

In each phase, after all specimens were prepared by individual industry partners, the industry source ID number was marked on the top face of the specimen. The specimens were then moved to a storage room and laid on shelves. The specimens were cured for 28 days, or sometimes longer. The curing rate of cold adhesives can vary according to their chemical formulation, application (type and adhesive coverage rate), and environmental conditions (temperature and humidity). For AARS, the performance of cold adhesives is normally stable after 28 days.

Table 3.1 A summary of all samples examined in this study

Phase	Source ID	Specimen Size (in.)	Test Angle (°)	Peel Position	Insulation Type	CB Type	Sample ID	Number of Specimens
I	I, II, III, IV	6 x 6	15	E-P	PF	ACB	*-1	168
						FB	*-2	
					AF	ACB	*-3	
						FB	*-4	
				C-P	PF	ACB	*-5	
					AF		*-6	
II	II, IV	6 x 6	7.5	E-P	PF	ACB	(S')*-1	168
					AF		S*-1	
			15		PF		(S')*-2	
					AF		S*-2	
			22.5		PF		(S')*-3	
					AF		S*-3	
			30		PF		(S')*-4	
					AF		S*-4x4	
			37.5		PF		(S')*-5	
					AF		S*-5	
			45		PF		(S')*-6	
					AF		S*-6	
		4 x 4	15	E-P	PF	ACB	S*-4x4	14
		8 x 8					S*-8x8	14
		10 x 10					S*-10x10	14
Totall Specimens								378

* is the ID number to indicate the industrial sources

3.5 Step by Step Experimental Protocol

3.5.1 Specimen Mounting

During the edge position peel tests, the centre line of the fixer and the supporting table is aligned with the centre point of the shaft. Wooden dummies are placed under the specimen to align the specimen's top with the gripper. The specimen is then mounted at the central position of the fixer (Figure 3.11 (a)). During the corner position peel tests, the fixer is rotated 45 degrees so that one corner is aligned with the shaft centre point. Then, a specimen is mounted on that corner of the fixer so that the unbound corner is aligned with the centre line of the shaft (Figure 3.11 (b)). When mounting a specimen, the overhang or unbounded corner of the cover board is clamped by the gripper and connected to the upper jaw of the Instron machine through a steel wire, so that the specimen can be stretched at a constant extension rate of 1.0 in./min or 25.4 mm/min at a pre-defined angle.

3.5.2 Angle Control

Figure 3.12 displays how to set up the peel test angle. First, the horizontal distance (L in Figure 3.12 (a)) between the middle point of the gripper to the inside edge of the free roller is measured using a ruler and a carpenter's level. Next, the height of the roller (vertical distance H in Figure 3.12 (a)) is calculated based on the formula $\tan(\theta) = H/L$, where θ is the pre-defined peel test angle. Third, the height of the roller (H) is adjusted by sliding the inside steel bar of angle controller, as mentioned in section 3.3.4. Finally, the actual peel angle is confirmed using the angle locator (Figure 3.12 (b)).

3.5.3 Peel Test Protocol

The testing protocol includes the following steps:

- The Bluehill2 software is opened and the 90° peel method is chosen (keep in mind this is not the actual peel angle, which is set up as described above).
- An extension rate (1.0 in./min or 25.4 mm/min in this study) is defined by the user.

- A tabular display of the results and the related information is selected. In this study, the information chosen to be typed in the system and displayed includes specimen dimensions, temperature, humidity, and specimen label. In addition, at the maximum load, the load at the first peak, the average resistance-to-peel load values and the lasting time were selected to be displayed in a table after the peel test. The table can also show statistical analysis, such as the maximum and minimum readings of peak load, and the mean value of the whole sample set, as well as their standard deviation (SD).
- A graphic display of the test results is defined. In this study, a chart of the applied peel force versus time was plotted during each test.
- The specimen is then mounted in the fixer and the test angle is set up as described in the section 3.5.2.
- The Instron is calibrated by balancing the load channel after the specimen is properly set up in the system.
- Varying peel forces are generated by Instron and applied to the specimen at the constant peel rate of 1.0 in/min until the specimen fails. No slippage of more than 2mm at the connection between the steel wire of gripper and the Instron machine's upper jaw was observed throughout the tests.
- The failure mode is evaluated based on pre-defined criteria (see Chapter 5 for a list of the types of failures) and recorded as photograph manually.

(a) Edge position peel test

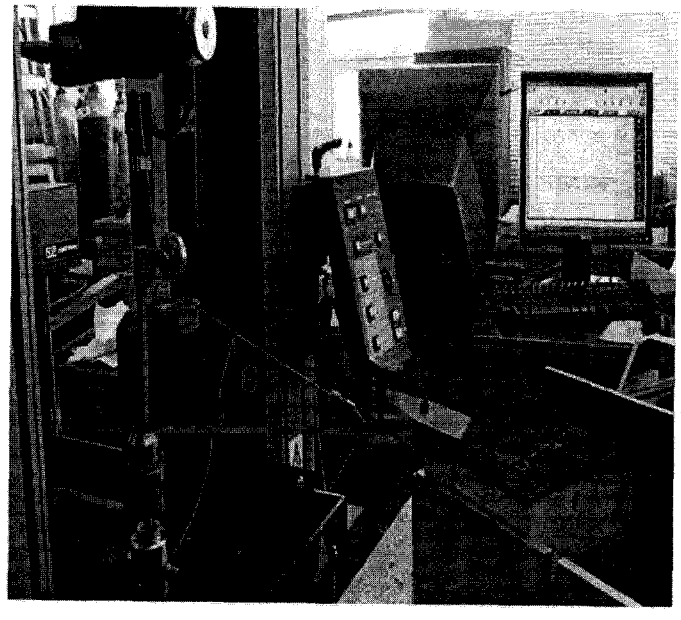

(b) Corner position peel test

Figure 3.11 Photo graphs of E-P and C-P experimental set-up

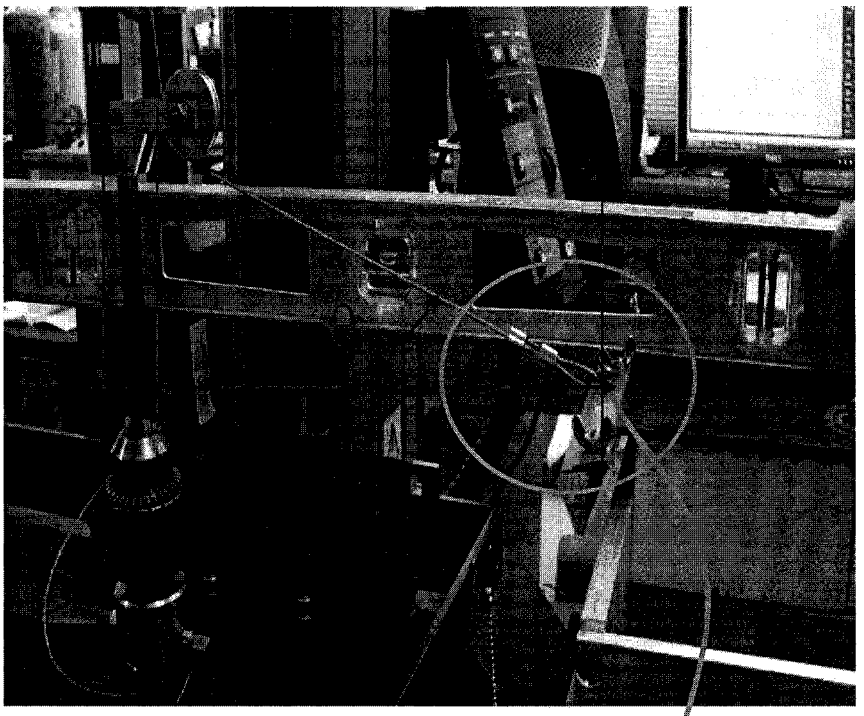

(a) A detailed view of angle set up

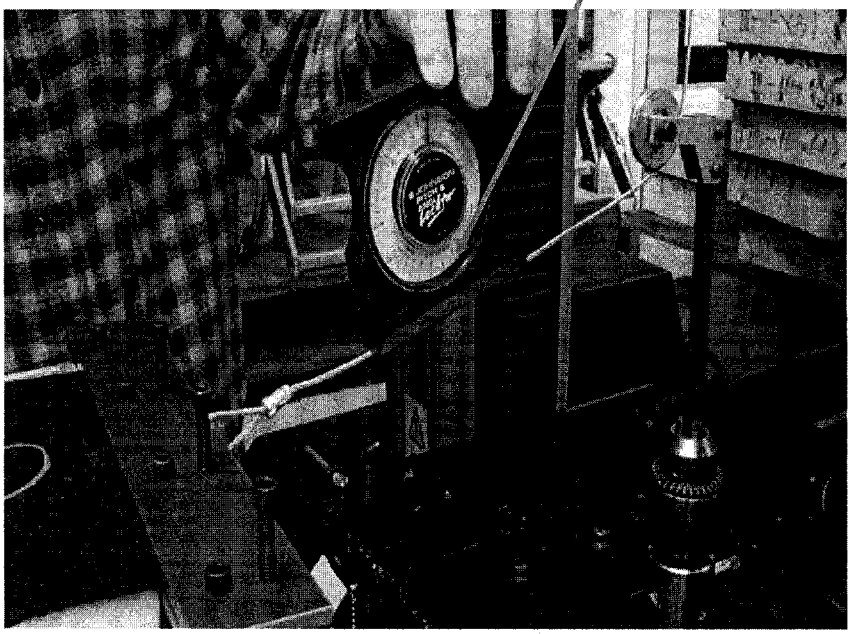

(b) Confirming angle by angle locator

Figure 3.12 Peel test angle set-up

Chapter 4 Results and Discussion

4.1 General Overview

This chapter presents the experimental results from the peel test investigations. For satisfactory system performance, each component of the AARS assembly should possess resistance higher than the wind-induced peeling force. These results are expected to make a significant contribution to the development of a regulatory standard for AARS.

A total of 378 experimental results from 54 different samples, that were provided by four industry sources as outlined in Table 3.1. These groups of samples were tested in two phases, Phases I and II. The experiments were carried out with different peeling parameters and sample components. The raw experimental data are found in Appendices 1 to 6. Each appendix presents four sets of information, which includes:

1) Summary tables of the mean peel resistance and failure mode of various samples from the same source;
2) Time history of the load;
3) A table of the measured maximum load and time;
4) Illustrations of typical failure modes.

These results comprise a database from which a relatively simple design criterion is to be developed.

Section 4.2 describes an analysis of the experimental results. First, the peak peel resistance of a given sample is derived from the time history curve. Next, the mean and standard deviation of the peel resistance are calculated from a set of samples. Finally the experimental repeatability was examined to ensure the reliability of the test results.

Section 4.3 reports the effects of various roofing components on the peel resistance. Specifically, different configurations of two types of insulation (AF and PF) and two types of cover board (FB and ACB) were examined. Also, the normalized peel resistance ratios were developed to provide a relative magnitude of the peel resistance as an indicator of wind resistance of different roofing assemblies.

Section 4.4 investigates how the peel resistance results might be affected by the mode of wind peeling, which is simulated through variations in experimental parameters. Specifically, the effects of peeling angle, peeling position, and sample size were examined. The results presented in this section are expected to become an essential component of a standard protocol for the evaluation of peel resistance of AARS. A draft test protocol is presented in Chapter 6.

4.2 Data Analysis

4.2.1 Time History of Loading

As mentioned in section 3.5.1, during the peel test the Instron machine 5566 applies a peel force at the speed of 1 in./min or 25.4 mm/min. Figure 4.1 shows time histories of applied peeling force obtained from a sample set of six specimens. Each curve illustrates how the peeling load applied on an AARS specimen changes as the specimen looses its peel resistance.

The peel test curve starts with an applied load of 0 at time 0, and stops when the specimen is completely peeled off. Each curve represents the performance of a specific specimen during its peeling process. The Y-axis shows the magnitude of peel force (in lbf) at the corresponding time given on X-axis. It should be noted that the maximum of Y-values vary from specimen to specimen because the performance, namely the pattern and location of failure, varies among different AARS specimens. The peel resistance and failure time of each specimen can be identified from the time history curve. The peak load on each curve is indicated by

an arrow, representing the "peel resistance" of the specimen. In this study, the peel resistance of different specimens is determined by following this procedure.

4.2.2 Analysis of the Test Results

As mentioned in Chapter 3, each sample set of experiments involves 5 to 7 specimens. The Instron 5566 generates a table that indicates the measured maximum load, or the peak load reading, for each specimen during the test. Table 4.1 depicts such a table containing the measured maximum loads for the set of 6 specimens shown in Figure 4.1. This table shows that the maximum loads of the 6 specimens range from 200 lbf to 275 lbf, or 890 N to 1223 N, and the failure time ranges from 50 sec. to 62 sec. For this sample set, the table also shows the mean and standard deviation of the peak loads for the whole sample set.

The original data for each sample set contains 5 to 7 specimens. However, in order to maintain consistency throughout this study, only 5 specimens from each sample set were selected for the calculation of the mean peel resistance. If there were only 5 specimens involved in a set, all 5 results were used for calculating the average. If there were 6 or 7 specimens involved in the same set, the 5 peel resistance readings with the minimum standard deviations were used for the analysis. For example, in Table 4.1, the extreme data points 200 lbf, or 890 N, was excluded following the criterion mentioned above. Then, the mean value, which is 263 lbf or 1170 N, and the standard deviation, which is 11 lbf or 49 N, was calculated from the remaining five peel resistance data samples.

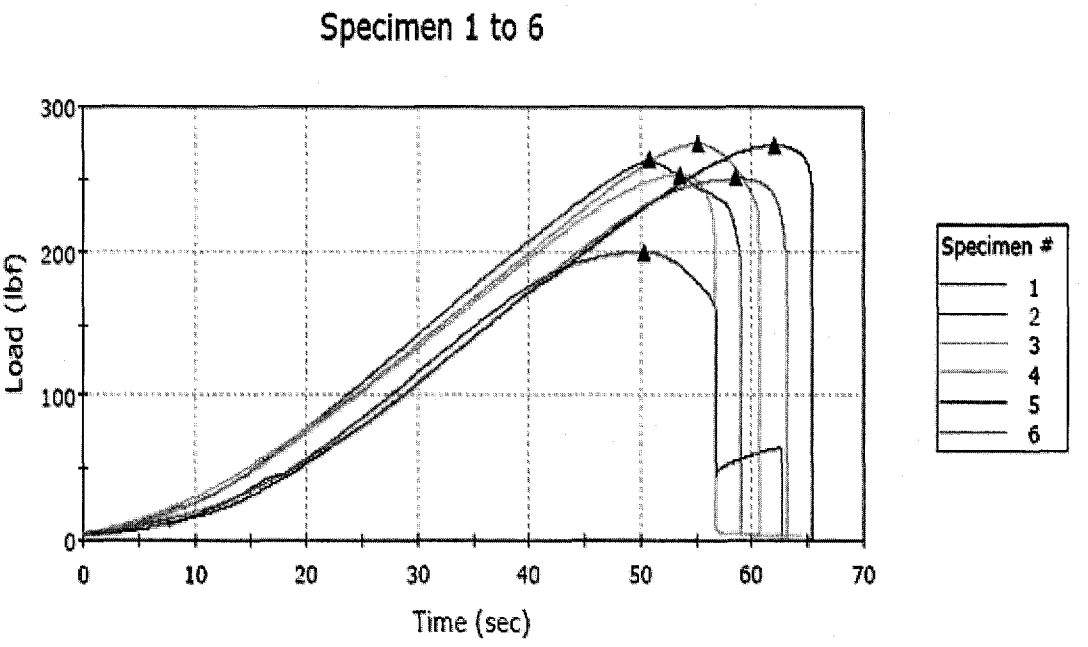

Figure 4.1 Typical time history curves of peel resistance [*PF-ACB-7.5°-E (S4'-1)*]

Table 4.1Measured load and time for source I *PF-ACB-7.5°-E (S4'-1)* sample set

	Maximum Load (lbf)	Time at Maximum Load (sec)	Load at First Peak (lbf)	Time at First Peak (sec)	Average Load at Average Value (All Peaks) (lbf)
1	263	51	263	51	263
X 2	200	50	200	50	200
3	254	54	254	54	254
4	275	55	275	55	275
5	273	62	273	62	273
6	251	59	251	59	251
Maximum	275	62	275	62	275
Mean	263	56	263	56	263
Minimum	251	51	251	51	251
Standard Deviation	11	4	11	4	11
Mean + 1 SD	274	60	274	60	274
Mean - 1 SD	252	52	252	52	252

4.2.3 Repeatability of the Peel Test Experiments

In order to validate the experimental data reported in this thesis, identical samples were examined in two independent experiments to make sure of the repeatability of the test results. During Phase I and II experiments, two groups of samples were prepared for this purpose. These specimens were subjected to an initial peel angle of 15° which the force applied at the edge position. The samples were identical in terms of their cover board and insulation configurations, and they were tested independently on different days. To investigate the repeatability of the test results, statistical analysis of the test results from these two sample sets were attempted.

Figure 4.2 shows the peel resistance of samples examined in two independent experiments (Phase I: PF/ACB sample ID# IV and Phase II: sample ID# S4'). In this figure, both the average and standard deviation of peel resistance are shown. It is evident that both experiments generated similar mean peel resistance values, which are (223 ± 33) lbf and (241 ± 22) lbf, or (992±147) N and (1072 ±98) N, respectively.

In order to statistically demonstrate that these two mean values are not significantly different from each other, the Student t-test was attempted. The Student t-test is often used to calculate the statistical significance of observed differences between the means of two samples. It is first assumed that the means of the two samples are not significantly different. This is called the null hypothesis. Then, the probability (p) of the hypothesis being true is calculated by using the formulae listed in Appendix 8. If the calculated p-value is less than 0.05, then the probability of the two mean values having no *statistically meaningful difference* is less than 5%. If the probability of the two values having no statistically meaningful difference is low, then probability of the values differing statistically is high, meaning the values must be *statistically different*. On the other hand, if the calculated p-value is more than 0.05, then the hypothesis is accepted and it is concluded that there is no significant difference between the two mean values.

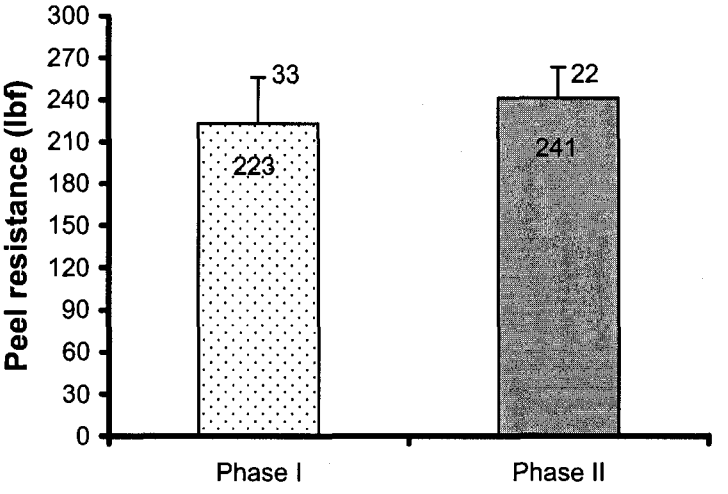

Figure 4.2 Peel test repeatability comparsion for sample set 1

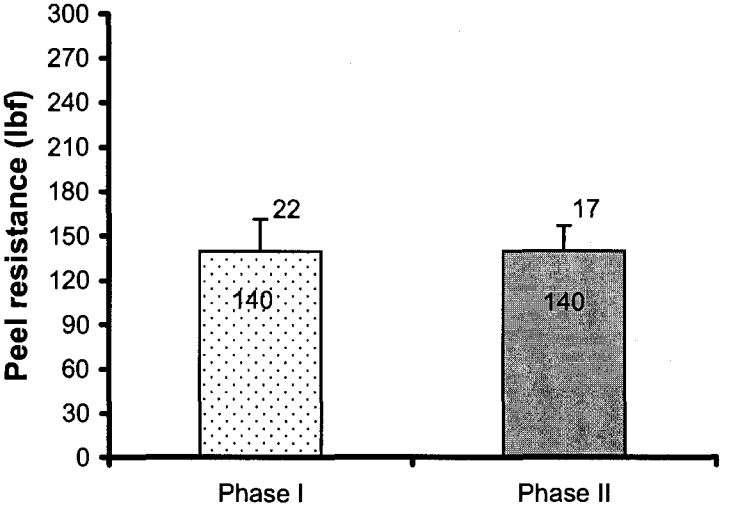

Figure 4.3 Peel test repeatability comparsion for sample set 2

In the above experimental data, the calculated p-value was 0.33 (>> 0.05), and thus the null hypothesis is accepted. Therefore, the statistical analysis by using the Student t-test indicates that there is no significant statistical difference between the results of these two experiments.

Similar results were observed for the second sample set. Figure 4.3 shows the peel resistance of two identical AF/ACB samples examined in two independent experiments (Phase I: IV set sample and Phase II: S4 set sample), which are shown in Figure 4.2. The figure shows that the mean peel resistances are the same for both experiments; only the standard deviation values are slightly different, which is (140±22) lbf, or (623±98) N, compared to (140±17) lbf, or (623±76) N. Statistical analysis by the Student t-test indicates that there is no significant statistical difference between the results of these two independent experiments ($p = 0.98 >> 0.05$).

The computation of p-values for Figure 4.2 and 4.3 adds substantial credibility to the test results regarding the repeatability of the experiment. For the purpose of engineering analysis, the experiments carried out in this study are repeatable and the experimental data are valid. Most importantly, these results indicate that the experimental paradigms described in this study can be applied to the establishment of a standard protocol for the evaluation of peel resistance of AARS.

4.2.4 Comparison of the Test Results

Having established the validity and repeatability of the peel test results, following the criteria in section 4.2.2, the mean peel resistances of various samples were calculated and compared. When making comparisons, it is essential that all experiments be carried out under the same testing conditions. Table 4.2 summarizes the peel resistance of various samples comprised of paper facer insulation and asphalt core cover board (shown as PF/ACB). These parallel samples were provided by four different industry partners, where each of industry partners is identified as a 'Source'. All the specimens were peeled at the edge position (E-P) at a 15° peel

angle. Nine similar tables are compiled for all other samples that are assembled with different configurations of cover board and insulation (Appendix 7).

Comparison of the data in Table 4.2 indicates that the measured peel resistance of individual specimens varies from 89 lbf to 259 lbf or 396 N to 1152 N. Although the sample configuration was identical (PF/ACB in this case), the components were constructed and provided by different industrial sources. Thus, the measured peel resistance varies significantly even under the same testing conditions. The circled numbers indicate the maximum (259 lbf or 1152 N) and minimum (89 lbf or 396 N) values of the peel resistance for all four industry sources. Figure 4.4 shows the time history curves of these two specimens. Since these two specimens are from two different sources (Source I and Source II) and each source has different ACB formula and fabrication protocol, the dramatic difference in their performance under peel pressure must be related to the difference in material properties. This means that even similar types of AARS may be quite different in peel resistance, depending on the materials that are used and how they are assembled. Given the variations between materials, a normalized "peel resistance ratio" was introduced in the present study for the quantitative comparison of the effects of material configurations on AARS peel resistance. The method for calculation of the peel resistant ratio is described in 4.3.1.

Table 4.2 Peel resistance comparison of PF-ACB-15°-E samples from four industrial sources (I - IV)

Test ID	I-1	II-1	III-1	IV-1
Specimen #	**PF/ACB**	**PF/ACB**	**PF/ACB**	**PF/ACB**
#1	243	121	196	192
#2	216	99	185	210
#3	228	104	209	258
#4	259	100	227	197
#5	215	89	190	258
Average Load	**232**	**102**	**202**	**223**
Standard Deviation	**19**	**12**	**17**	**33**

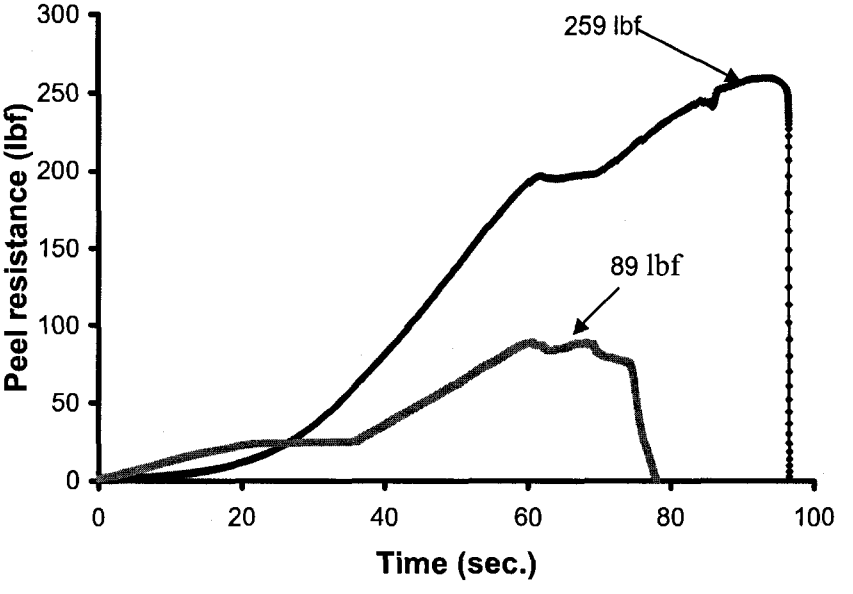

Figure 4.4 Time history curves of best and worst performed PF-ACB-15°-E specimens

4.3 Influence of Component Configurations

In order to evaluate the performance of AARS made of different combinations of insulation and cover board under wind peeling action, the effect of sample components on the peel resistance is investigated in this section. This knowledge is necessary for the development of a testing standard for AARS. The material component configurations, as previously indicated in Chapter 3, include two types of insulation and two types of cover board. This section is aimed at providing an overview of the AARS wind peel resistance performance for samples peeled at the edge positions and 15° peel angles. All the data in this section are from the Phase I experiments.

4.3.1 Influence of Cover Board

In this section, the influence of two cover boards (**ACB** and **FB**) on the peel resistance of roofing assemblies is investigated. To illustrate the impact of cover board, the peel resistance of samples containing the asphalt core cover board (**ACB**) is compared to that with the fiber cover board (**FB**). Both were assembled with the identical insulation (AF or PF).

Figure 4.5 compares the peel resistance of **ACB** specimens with that of **FB** specimens, when PF was used as the insulation. The Y-axis gives the peel resistance obtained from the two different CB configurations of parallel samples from four sources. The results indicate that although the peel resistance of similarly configured specimens varies with the source of materials, the **ACB** cover board consistently outperformed **FB** cover board.

The graphic presentation also shows that rank of performance by material sources was found to be S1>S4>S3>S2. This rank of performance presumaby reflects the different material properties and installation procedure used by different industrial sources. As mentioned in Chapter 3, each source used its own CB and adhesive to construct their specimens. For example, the chemical formulations used to make

similar cover board materials and adhesives differ from source to source. In addition to variations in materials, the fabrication protocol is also different because the field application method of each industrial source is different. Specimen fabrication can significantly affect its peel resistance. Variations involved in the fabrication include cleanness of the board surfaces, asphalt thickness and uniformity of adherent applications. For PF/**ACB** versus PF/**FB** samples shown in Figure 4.5, Source 1 has the maximum peel resistance of 232 lbf or 1032 N versus 117 lbf or 520 N (**ACB** vs. **FB**), while the minimum peel resistance with the same sample component resulted 102 lbf or 454 N (**ACB**) versus 44 lbf or 196 N (**FB**) in the case of the specimens from Source 2. These results suggest that the materials from Source 1 resist higher wind peel force than materials from any of the other sources.

Since one of the main objectives of this thesis is to develop a peel standard protocol that can be adopted in a future wind design guide for AARS, it is more reasonable to compare performance of AARS which different material combinations for example PF/**ACB** vs. PF/**FB**, without taking into account the effect of the difference of industrial sources. For this purpose, a normalized **peel resistance ratio** would be a good indicator of the relative performance. The normalized results should provide a straightforward and unbiased indication of performance regarding which kind of roofing components are more resistant to wind peeling, regardless of the quality of materials or manufacturers.

For example, this study developed a peel resistance ratio of **ACB against FB** for the quantitative comparison of the performance of these two cover boards. It normalizes the testing results of PF/**FB** sample assemblies from all four industry sources to 1. The ratio of samples from each source is then calculated as the peel resistance of **ACB** sample divided by that of **FB** sample. The **ACB against FB** peel resistance ratios of the peel resistance data in Figure 4.5 were calculated as shown below.

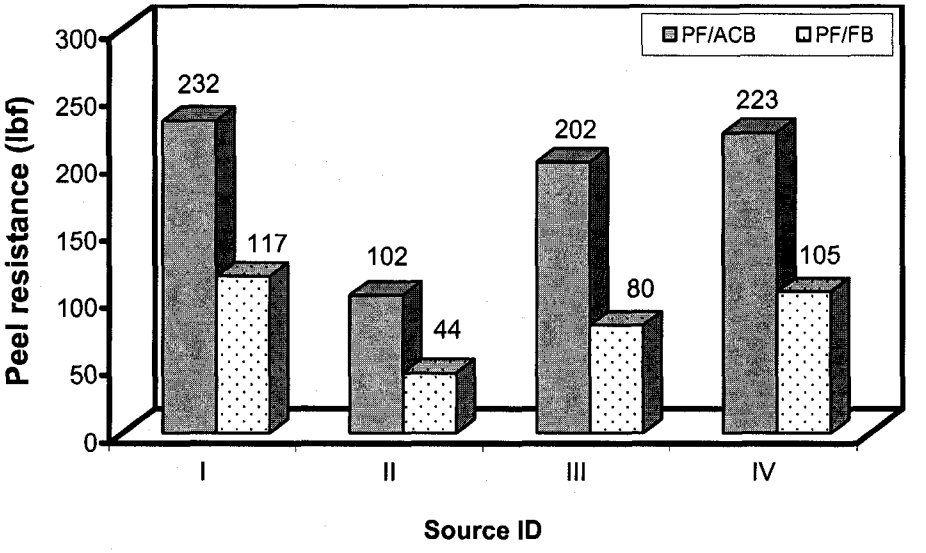

Figure 4.5 Influence of cover board on the peel resistance of PF samples under 15° and E-Position

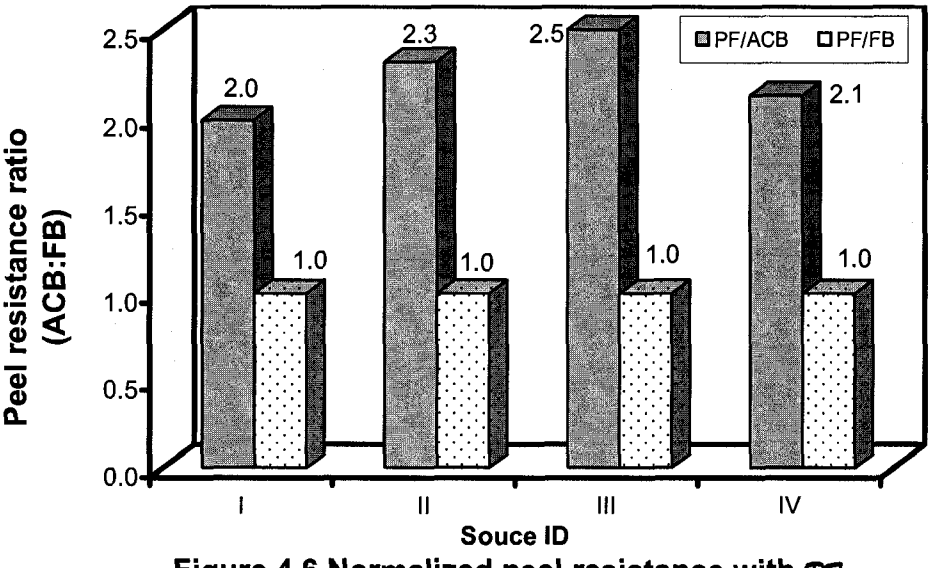

Figure 4.6 Normalized peel resistance with PF samples of different cover board under 15° and E-Position

- Source 1 **ACB: FB** Ratio: 232/117 ≈ 2.0
- Source 2 **ACB: FB** Ratio: 102/44 ≈2.3
- Source 3 **ACB: FB** Ratio: 202/80 ≈2.5
- Source 4 **ACB: FB** Ratio: 223/105 ≈2.1

These ratios are plotted in Figure 4.6, where Y-axis gives the peel resistance ratio of **ACB** against **FB,** where FB ratio is normalized to 1, when PF is used as the insulation material. It is evident from this figure that the specimens with **ACB** perform better than those with **FB**. The peel resistance ratio for this set of samples ranges from 2.1 to 2.5. These ratios show that the samples with ACB resist at least twice as much of the peel force than the samples with FB.

As mentioned in Chapter 3, **FB** is mainly composed of wood fibers and recycled paper whereas **ACB** is comprised of high melt asphalt core with glass fiber mineral filler. The wood fibers and recycled paper have higher moisture content, suggesting that **FB** has less stiffness. In contrast, the asphalt and glass fiber have higher ductility. Therefore, when the specimen is subjected to the peel force under the same test conditions, **FB** fails more easily than **ACB**. The reason is due to the lack of stiffness in **FB**, resulting in less than a half in peel resistance when compared to **ACB**.

Similar results were observed when AF was used as insulation in combination with different cover boards (**ACB** vs. **FB**). Figure 4.7 presents the peel resistance of specimens with **ACB** compared to those with **FB**. Similar to the results in Figure 4.5, specimens with **ACB** outperformed those with **FB**. Figure 4.8 shows the normalized peel resistance ratio. The **ACB against FB** ratio ranges from 1.4 to 2.2, again suggesting that **ACB** is more resistant to the peeling force than **FB**. The consistently better performance of **ACB** over **FB,** regardless of insulation configuration and material sources, further indicates that the peel test methods used in this study are applicable to various other materials and roofing configurations.

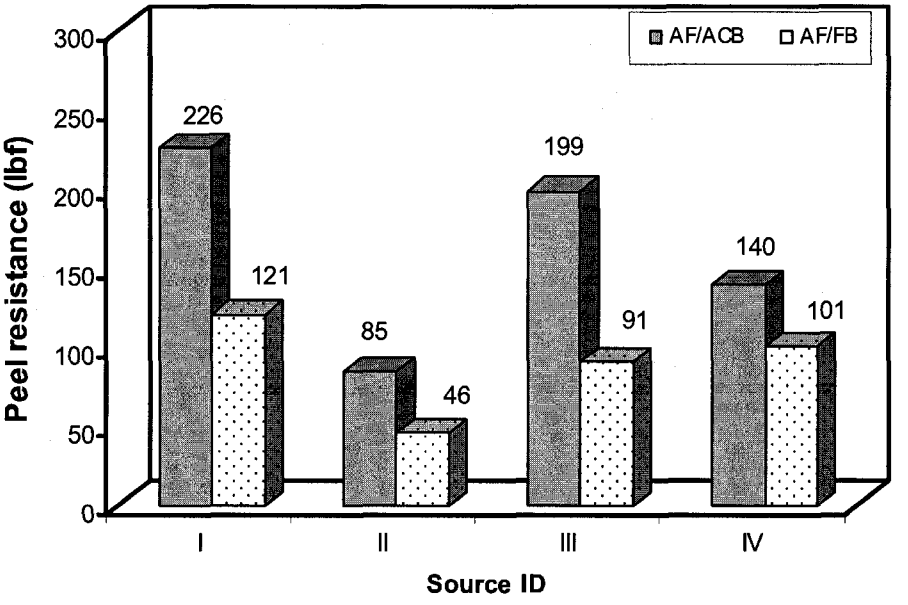

Figure 4.7 Influence of cover board on the peel resistance of AF samples under 15° and E-Position

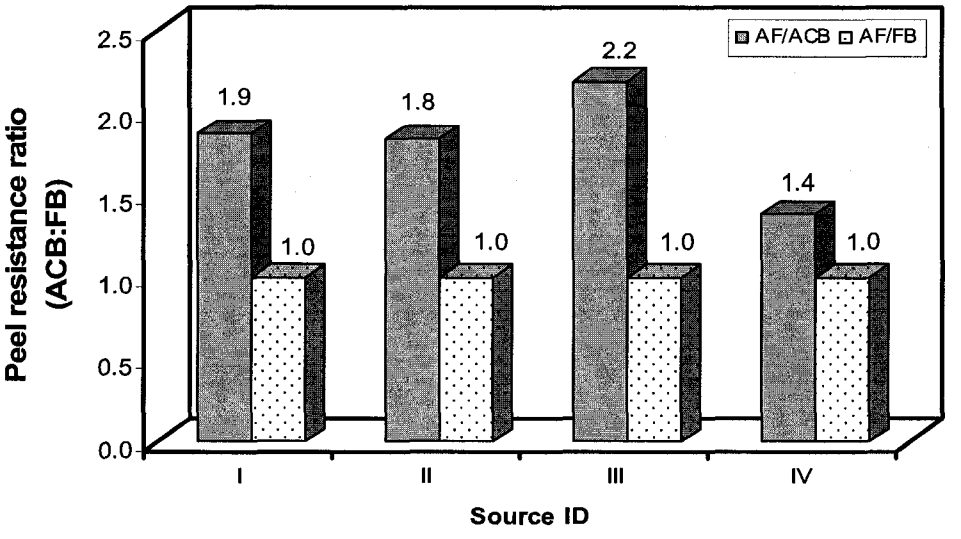

Figure 4.8 Normalized peel resistance with AF samples of different cover board under 15° and E-Position

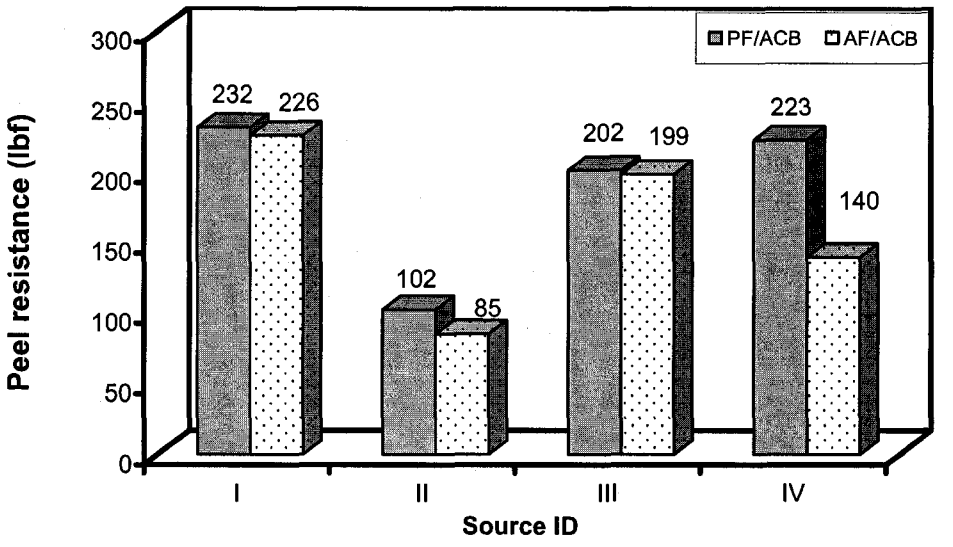

Figure 4.9 Influence of insulation on the peel resistance of *ACB* samples under 15° and E-Position

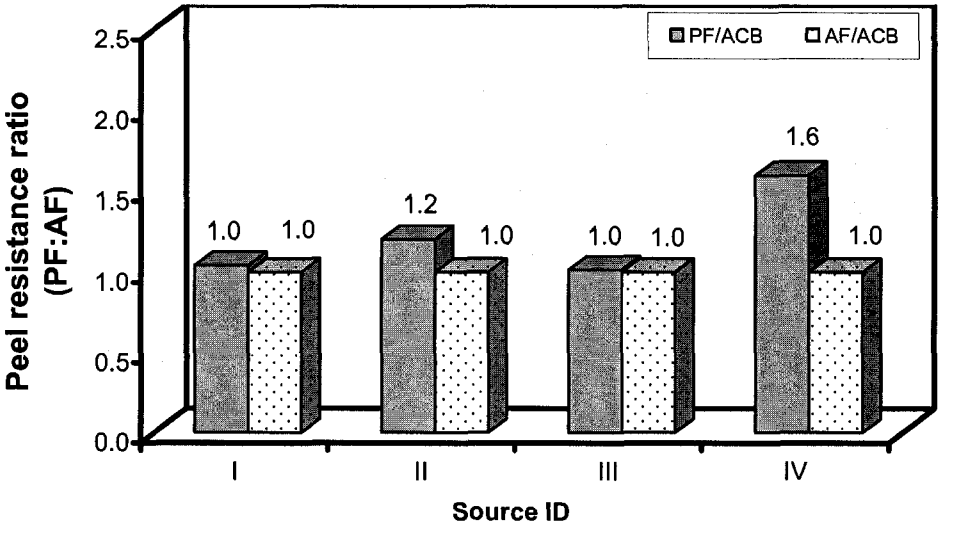

Figure 4.10 Normalized peel resistance with *ACB* samples of different insulation under 15° and E-Position

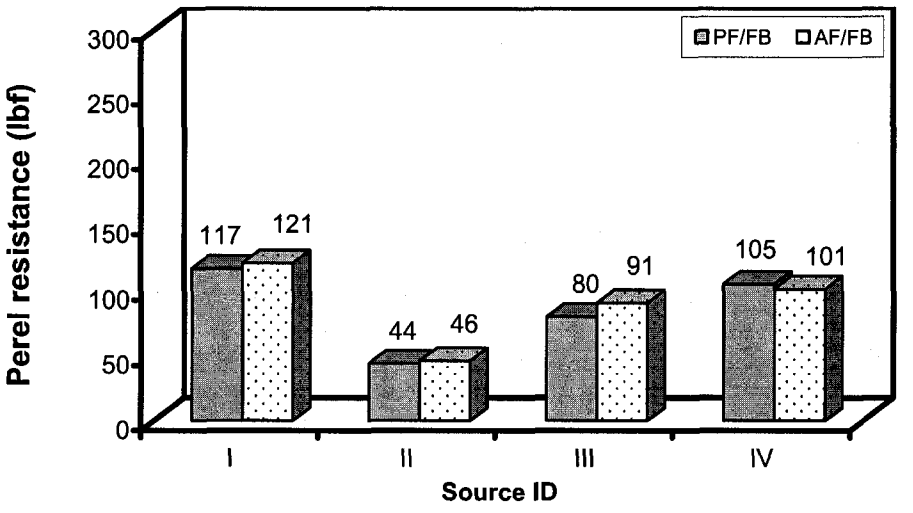

Figure 4.11 Influence of insulation on the peel resistance of FB samples under 15° and E-Position

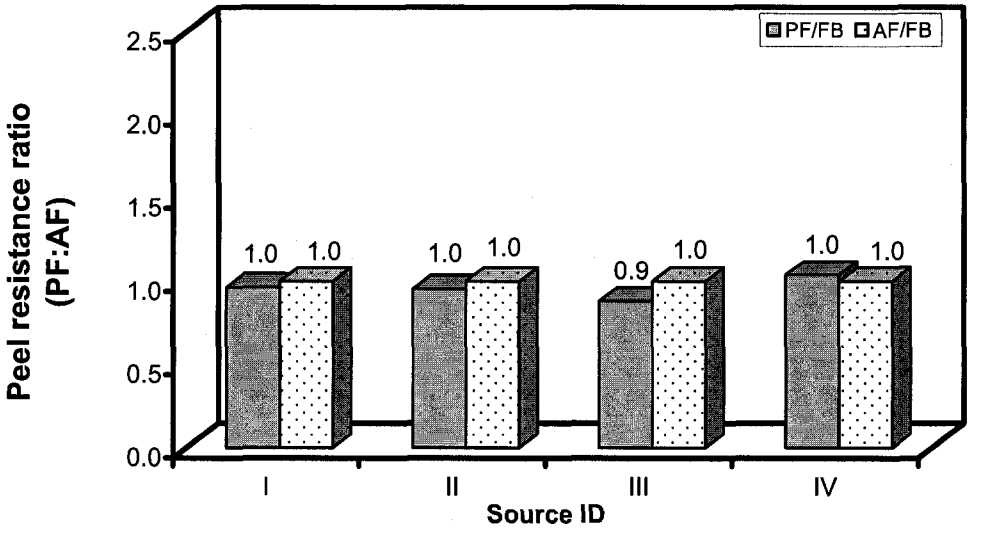

Figure 4.12 Normalized peel resistance with FB samples of different insulation under 15° and E-Position

4.3.2 Influence of Insulation

In this section, the influence of insulation materials on the peeling strength of roofing assembly is examined. To do this, the peel resistance of samples with the identical cover board (CB) materials, (Asphalt Core Cover Board or Fiber Cover Board), but with different insulation materials, (**Paper Facer** vs. **Acrylic Facer**) were compared.

Figure 4.9 shows the peel resistance of specimens composed of the Asphalt Core Cover Board (ACB) with two different types of thermal insulations, Paper Facer (**PF**) and Acrylic Facer (**AF**). The rank of absolute peel resistance by industry sources is S1>S4>S3>S2 (Figure 4.9), which is consistent with the previous rankings. When the peel resistance ratio of **PF against AF** is analyzed (Figure 4.10), it is obvious that specimen with PF performed marginally better than those with AF. This is true for three out of the four sources, with the peel resistance ratios ranging from 1.0 to 1.2. Only one source's sample showed a peel resistance ratio of 1.6.

At the time of writing this thesis, not all of the specifications for the insulation material are available. The only available specification is water vapor permeability as a guide for the wind design of adhesive applied roofing systems p.21. Information in this guide indicates that **PF** has higher water absorption than **AF**, suggesting that **AF** should have higher brittleness and lower extensibility than **PF**, whereas **PF** should be softer and more flexible than **AF**. In other words, it is reasonable to predict that **AF** insulation can suffer lower tensile strength than **PF** insulation. Indeed, the experimental results were consistent with this prediction; i.e., when the specimens were composed of the same ACB component, **PF** performed better than **AF** in peel resistance.

In a parallel experiment, the peel resistance of **PF** and **AF** insulations, when FB is used as the cover board, is also compared (Figure 4.11). The absolute peel resistance ranking of the specimens from the four industry sources agreed with the previous ranking, namely S1>S4>S3>S2. When the peel resistance ratio of **PF against AF** is examined, however, **PF** and **AF** performed similarly. As shown in

Figure 4.12, the ratio ranges from 0.9 to 1.0. This suggests that if the AARS uses FB as the roofing cover board, the insulation has no significant influence on the peel resistance. The reason for this is due to the lack of stiffness in FB, resulting in cover board failure regardless of which insulation was used. This interpretation is strongly supported by the results of 4.3.1 and also by the results from the failure mode analysis in Chapter 5. Based on these results, only ACB were used in Phase II tests as the cover board component in combination with different insulation materials.

From the comparison of these different types of roof assemblies, provided by different industrial sources, the results of the present study indicate that the significant differences exist in peel resistance performance. The differences depend on material combinations and application methodology used by the industrial sources.

4.4 Effect of Peel Test Parameters

In this section, the effects of different experimental parameters on the peel resistance are investigated. These test parameters include the peel positions, peel angles and size of the test samples.

4.4.1 Effect of Peel Positions

In Phase I, in addition to examining peel resistance at the edge position (**E-P**) for all samples, peel resistance when peeled at corner position was also examined in two groups of samples. These samples were subjected to peeling force at corner position (**C-P**) with 15° angle peeling line. The results from **E-P** and **C-P** tests on identical sample assemblies under the same conditions were then compared.

Figure 4.13 shows the analysis of unit peel force when specimens are subjected to **E-P** and **C-P** positions. In general, if a specimen is subjected to the same peel force, the peeling stress intensity for **C-P** is larger than that for **E-P** at the early stage of the test. In this figure, "a" is the specimen's width and "F" is the peel force acting on the

specimen. Hence, the length subjected to the peeling stress is always equal to "a" for **E-P** specimen. However, the length subjected to the peeling stress for **C-P** specimen, "b", is initially much smaller than "a" and continually increases until it reaches the diagonal length of the specimen, followed by continual decreases after that line (Figure 4.13). In this scenario, the peeling stress for **E-P** specimen (F/a) is smaller than that of **C-P** specimen (F/b) in the early stage of the test. This analysis leads to a conclusion that the specimens peeled at **C-P** would fail more easily than those peeled at **E-P** because **C-P** initially generates higher peeling stress than **E-P** cases.

Figure 4.14 is a time history curve for two identical specimens that are peeled at different positions (**E-P** vs. **C-P**). From this curve, it is clear that the peel force of **C-P** specimen increases faster than that of **E-P** specimen initially. Moreover, the **C-P** specimen fails in a shorter time and has a lower peel resistance than the **E-P** specimen.

Figure 4.15 shows the mean peel resistance of **AF**/ACB sample assemblies examined at two different peel positions. The results indicate that the peel resistance of **E-P** is higher than that of **C-P**, except for samples provided by Source II (discussed below). Following similar quantification strategies used in Section 4.3, normalized peel resistance ratio of **E-P against C-P** is calculated; where of the peel resistance of all C-P samples from each source is normalized to "1". Figure 4.16 shows the normalized peel resistance ratio. Again, all samples except those from Source II showed lower peel resistance at **C-P** positions than **E-P** positions. The **E-P: C-P** peel ratio ranges from 1.2 to 1.8 except for Source II, which is 0.6.

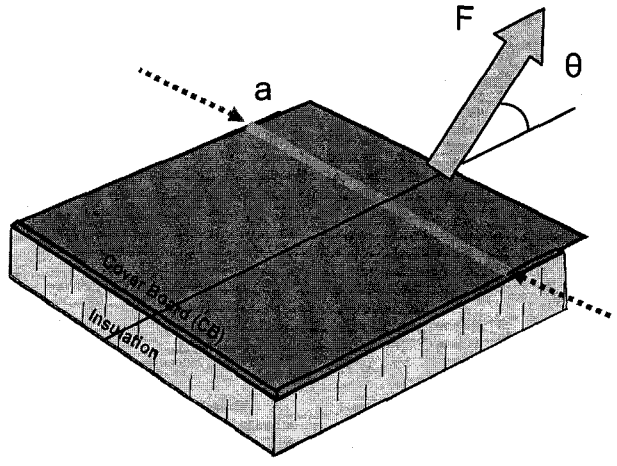

(a) Edge position

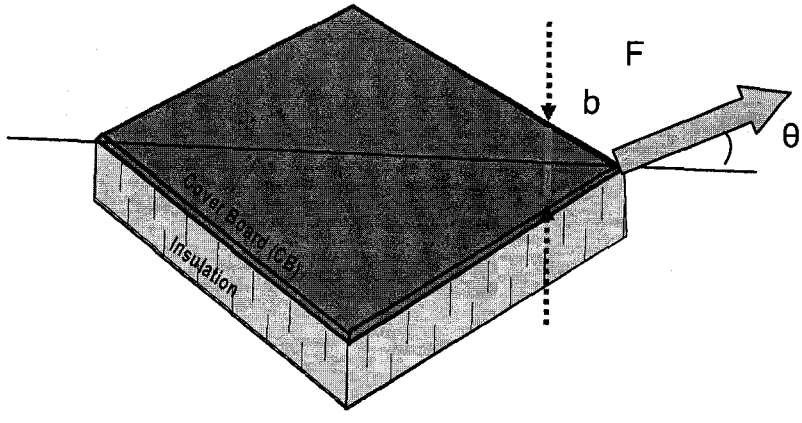

(b) Corner position

Figure 4.13 Peel force analysis at different peel positions

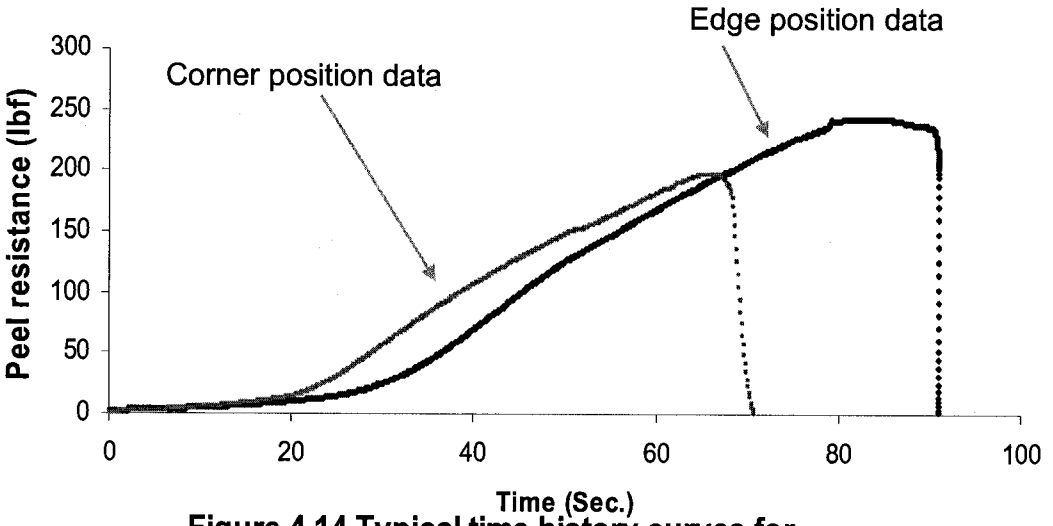

Figure 4.14 Typical time history curves for two different peel positions

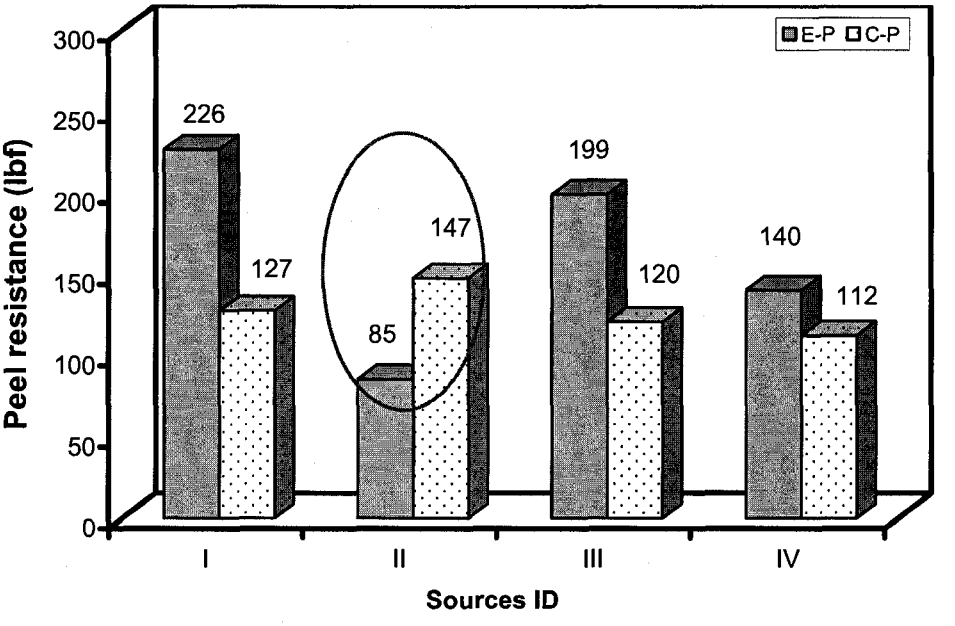

Figure 4.15 Effect of peel positions on the peel resistanfce of AJ/ACB sample under 15°

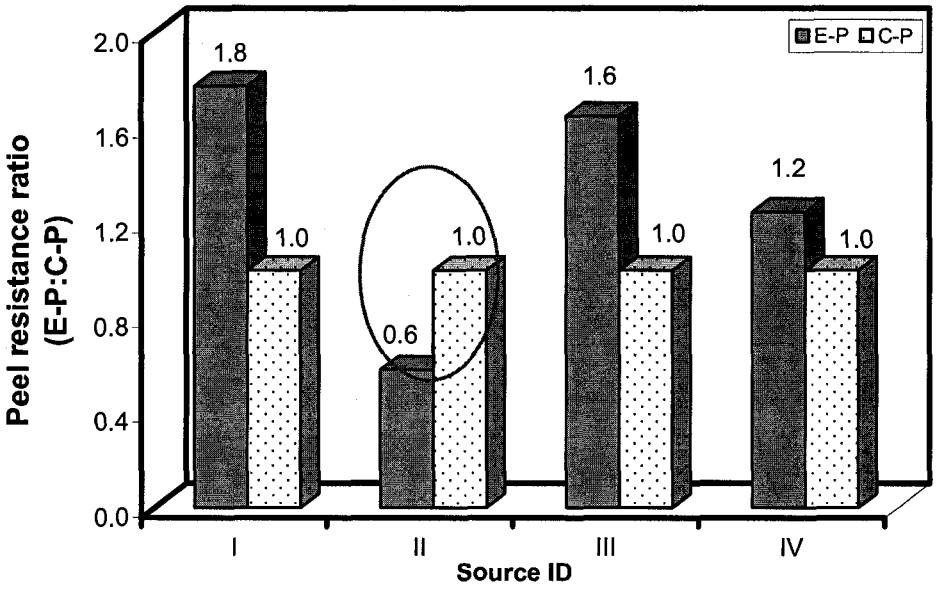

Figure 4.16 Normalized peel resistance at different peel positions with AJ/ACB samples under 15°

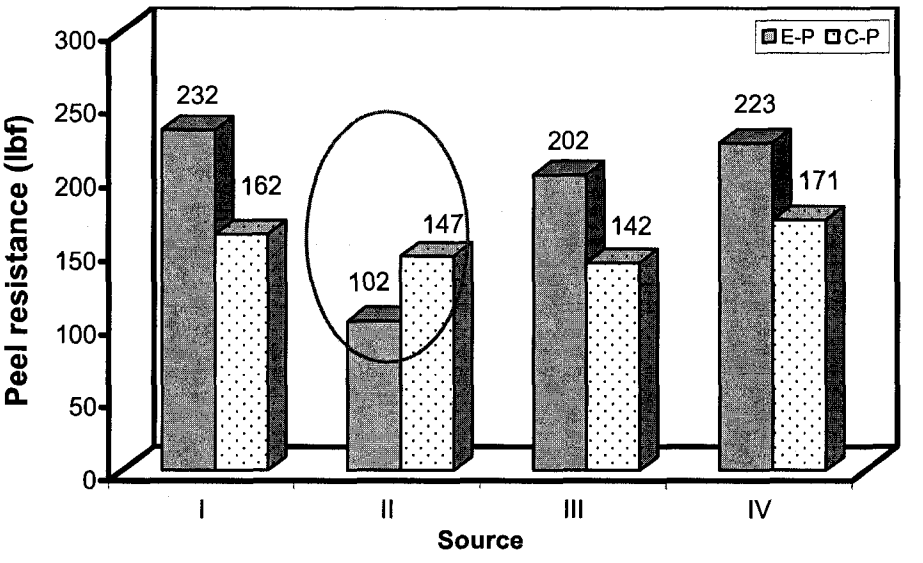

Figure 4.17 Effect of peel positions on the peel resistanfce of *PJ/ACB* sample under 15°

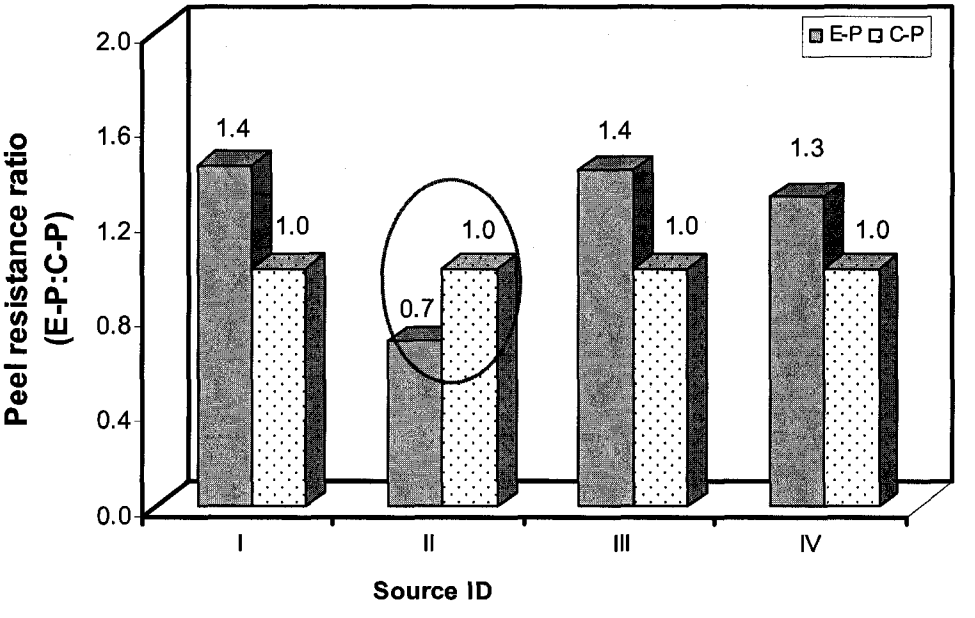

Figure 4.18 Normalized peel resistance at different peel positions with *PJ/ACB* samples under 15°

Likewise, comparison of **E-P** versus **C-P** peel resistance of **PF**/ACB specimens indicates that lower peel resistance occurs at C-P than E-P positions in all samples, except for those from Source II (Figure 4.17). The **E-P against C-P** peel ratio ranges from 1.3 to 1.4 except for Source II samples, for which the ratio is 0.7 (Figure 4.18). The majority of the results, with one exception discussed below, are consistent with the earlier prediction that the peeling stress for **C-P** is larger than that for **E-P** at the test beginning period, resulting in faster failure and lower peel resistance of **C-P** samples than that of **E-P** samples.

Interestingly, samples from Source II showed unexpected results; i.e., the peel resistance was found higher with C-P than of E-P. The **E-P against C-P** peel resistance ratio is 0.6 for the **AF**/ACB sample set and 0.7 for the **PF**/ACB sample set. Based on the aforementioned peel force analysis at **C-P** and **E-P** positions, one would predict that if the peel failure occurs at a later, where "b" is larger than "a", then the peeling stress of **C-P** would be smaller than **E-P** ($F/b < F/a$). Indeed, the C-P failure records indicate that, unlike samples from other three sources where all failure occurs at a "b" value smaller than "a", the Source II samples fail at a position where the "b" value is larger than "a" (Appendix 1 – 4: each sample 5 & 6 photographs). Therefore, the peel resistance of **C-P** was higher than that of **E-P**. The failure mode analysis for both peel positions strongly supports this prediction (Chapter 5). The reason for this different mode of failure is not immediately clear, though the way the adhesive was applied to the test specimens might have been one of the factors.

4.4.2 Effect of Peel Angles

The peel force can be decomposed into the vertical tensile force and the horizontal shear force. When a specimen was subjected to a peel force F at angle θ, the tensile force is equal to $F \cdot \sin\theta$ and shear force is equal to $F \cdot \cos\theta$ (Figure 4.19). Therefore, the tensile force and shear force under two different angles ($\theta 1$, $\theta 2$), can be calculated as below:

F_{T1} = F Sin (θ_1), F_{T2} = F Sin(θ_2); then $F_{T1} = F_{T2}$ (Sin (θ_1)/ Sin(θ_2)); and
F_{s1} = F Cos(θ_1), F_{s2} = F Cos(θ_2); then $F_{s1} = F_{s2}$ (Cos(θ_1)/ Cos(θ_2)),
Where F_{Ti} is vertical tensile force, and F_{si} is horizontal shear force.

If the peel resistance of an angle is given, then based on force vector analysis the tensile force and shear force for any required angles can be calculated as shown in the above equations. However, for the present study use of these equations are limited due to the following reasons:

- First, the peel resistance (force) was not constant during the present experiment. A pre-defined constant extension rate of 1.0 in./min or 25.4 mm/min is maintained in the Instron machine. This can apply variable peel forces on the specimen at different peeling time depending on the resistance offered by the adhesive.
- Second, the initial peel angle θ configured in the Instron apparatus (same shown as Figure 3.11(a)) can also vary. As the specimen starts to peel during the testing, the peel angle can increase.

An example is shown in Figure 4.20 (a) & (b) at two different time frames during testing. In figure 4.20 (a), the peel angle θ is the same as the defined initial peel angle when the test started. As peeling occurs in the specimen, the peel angle increases from θ to θ' (Figure 4.20 (b)). This is another variable that varies with experiment. Hence, a constant relationship between peel force and peel angle does not exist for the present study.

Alternatively, a standard curve of peel resistance as a function of peel angle can be developed experimentally. This can be further used to predict peel resistance under different peel angles. In order to plot the curves, peel resistance under multiple angles was examined. Samples from two industry sources were subjected to peel tests at different angles. Specifically, samples from S4 and S2 were selected based on the material availability. The sample configurations include PF/ACB and AF/ACB. Samples were subjected to the peeling force at six different peel angles from 7.5° to

45° with 7.5° increments, and at a constant rate of application of 1.0 in./min or 25.4 mm/min. All samples were standard size specimens (6 in. x 6 in. or 152 mm x 152 mm).

Figure 4.21 shows the peel resistance of **PF**/ACB samples at different peel angles. This figure shows that the peel resistance decreases as the peel angle increases. This is mainly because the effective uplift force component, or the vertical tensile force, acting on the specimen increases with the peel angle. From Figure 4.21, samples from the Sources II and IV display a similar tendency regarding peel-resistance vs. angle curve; namely, the two curves have similar trends but are offset. This resistance-versus-angle curve takes place in three distinct segments. From one and other, they are:

Segment 1: 7.5° – 15°;
Segment 2: 15°– 30°; and
Segment 3: 30° – 45°

The slope changes most significantly between 15° and 30°, indicating a rapid change in peeling force with the angle in this range. This range is thus named the **effective angle range**. Figure 4.21 indicates that peeling resistance is most sensitive to changes in peel angle over the effective angle range. Angles less than 15° and/or more than 30° would have smaller effects on the peel resistance. What is consistent with the experimental results of Phase I is that the peel resistance of the Source IV samples were always higher than those of the Source II samples at every peel angle examined. This is due to components used and application methods followed.

As mentioned in 4.3.1, the objective of the present study is to provide technical data which might be useful towards the development of a standardized peel test method. This standard protocol can then be applied to a future wind design guide of AARS. Hence, it is important to develop a generalized curve that could predict the peel resistance performance under different peel angles. In order to achieve this

objective, the peel resistance ratios, as previously described, were used as a quantitative indicator to compare the test data as documented below.

To calculate the peel resistance ratio, the peel resistance measured at a particular angle was selected as a reference to which peel resistance values from other configurations could be compared. The present study selects the peel resistance of 15° as the reference; since it falls within the effective angle range, and the failure modes (will be discussed in the Chapter 5) observed were consistence at 15° peel angle. The peel resistance ratio for any angle can be calculated by dividing the peel resistance of any angle with the peel resistance of 15°. The same procedure was followed for the results from both industrial sources. To account for the sources offset from the curves, average values were calculated for all tested peel angles. Based on this approach, a representative curve for the PF/ACB sample set was obtained (Figure 4.22).

Following the above discussion, the data of **AF**/ACB were also analyzed and presented in Figure 4.23 and Figure 4.24. Similar to PF/ACB sample set, the peel resistance decreases with increasing peel angle and Source IV samples consistently performed better than Source II samples. However, it should be noted that for **AF**/ACB samples, resistance vs. angle relationship takes place roughly in two distinct segments.

Segment 1: 7.5° – 22.5°; and

Segment 2: 22.5°– 45°.

The slope between 7.5° and 22.5° is steeper than that in the range of 22.5° to 45°. The selected reference angle 15° is still within the effect angle range; hence 15° is selected to be reference angle again.

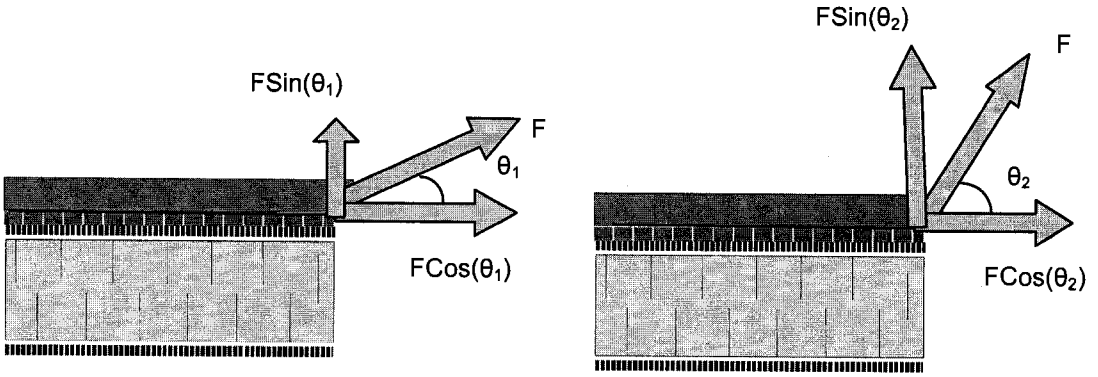

$\theta_1 < \theta_2$
$F\cos(\theta_1) > F\cos(\theta_2)$ Shear Component
$F\sin(\theta_1) < F\sin(\theta_2)$ Tensile Component

Figure 4.19 Peel force analysis at different peel angles

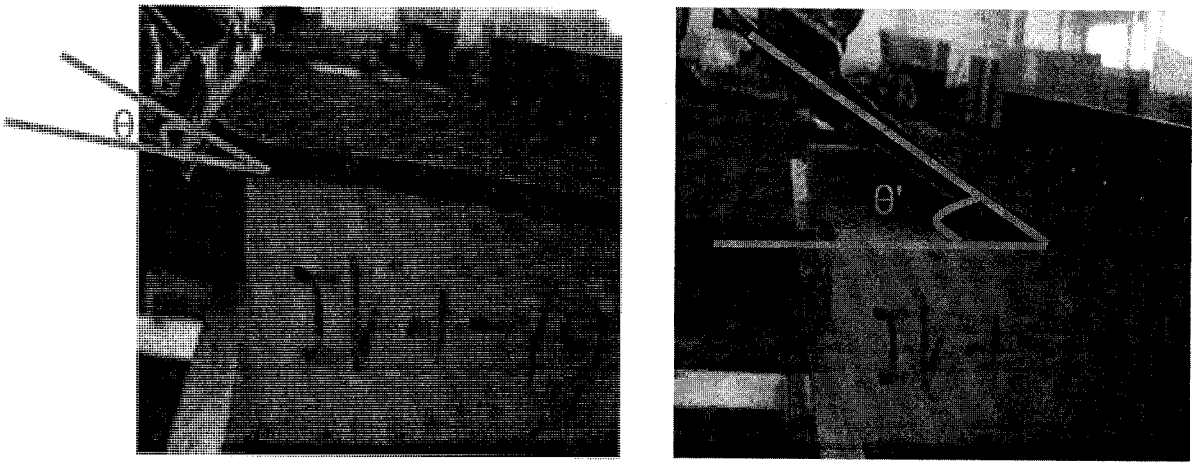

(a) Peel angle at beginning time (b) Peel angle at failure time

Figure 4.20 Photograph of peel angle at different test time

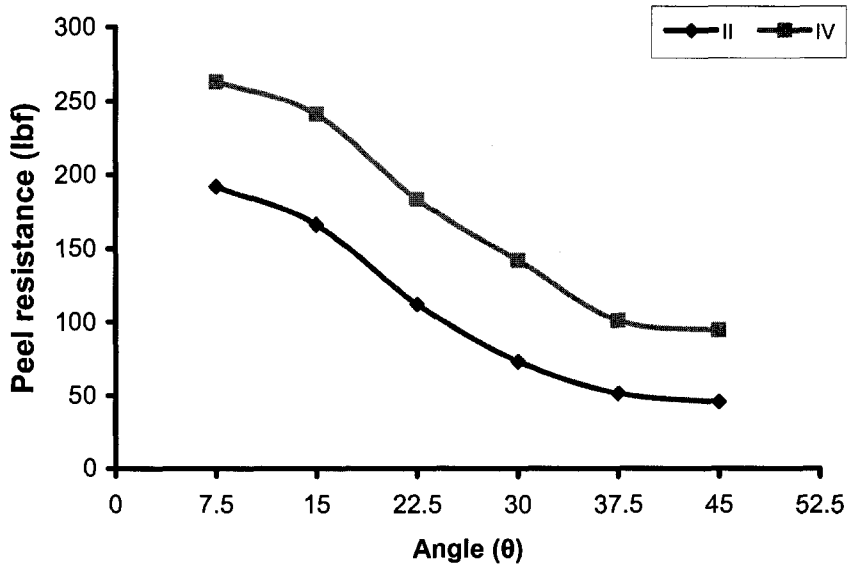

Figure 4.21 Effect of peel angles on the peel resistance of *PF/ACB* samples

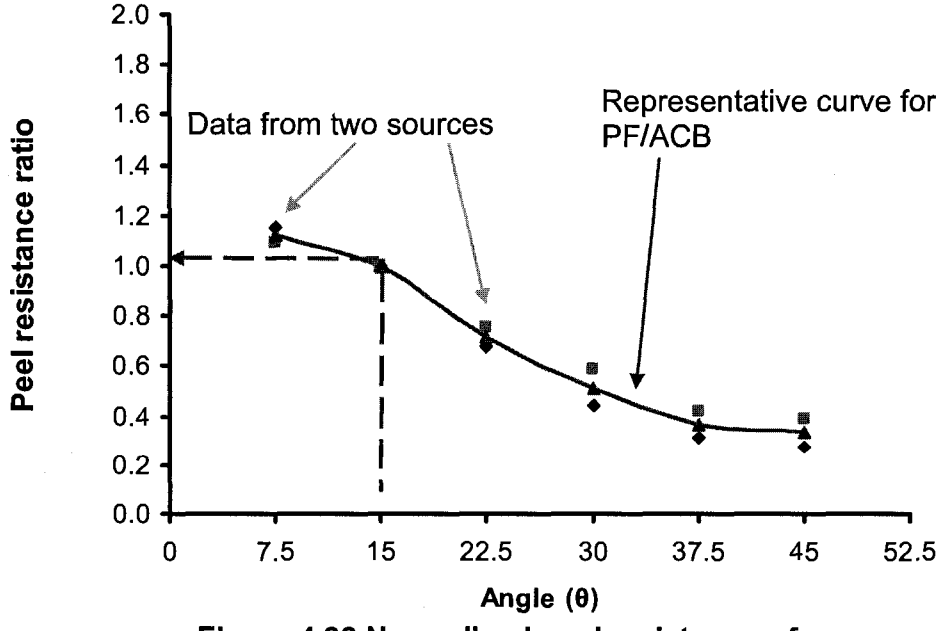

Figure 4.22 Normalized peel resistance of *PF/ACB* samples at different angles

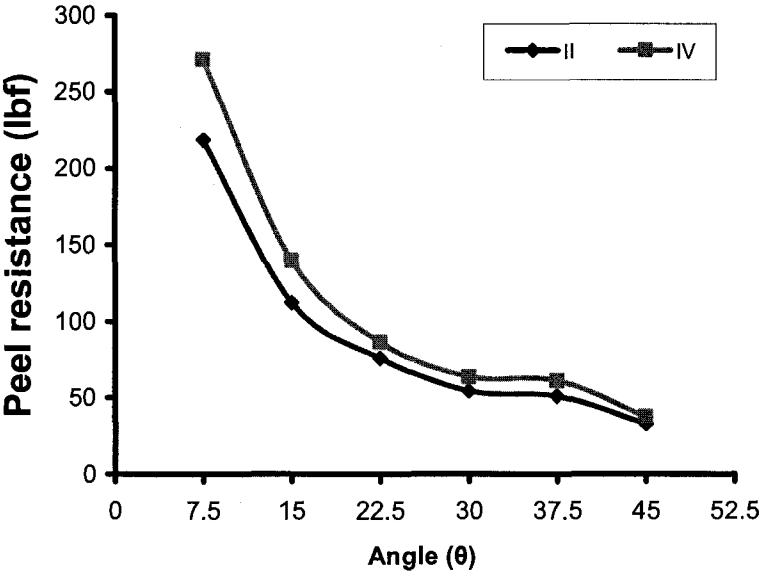

Figure 4.23 Effect of peel angles on the peel resistance of *AF/ACB* samples

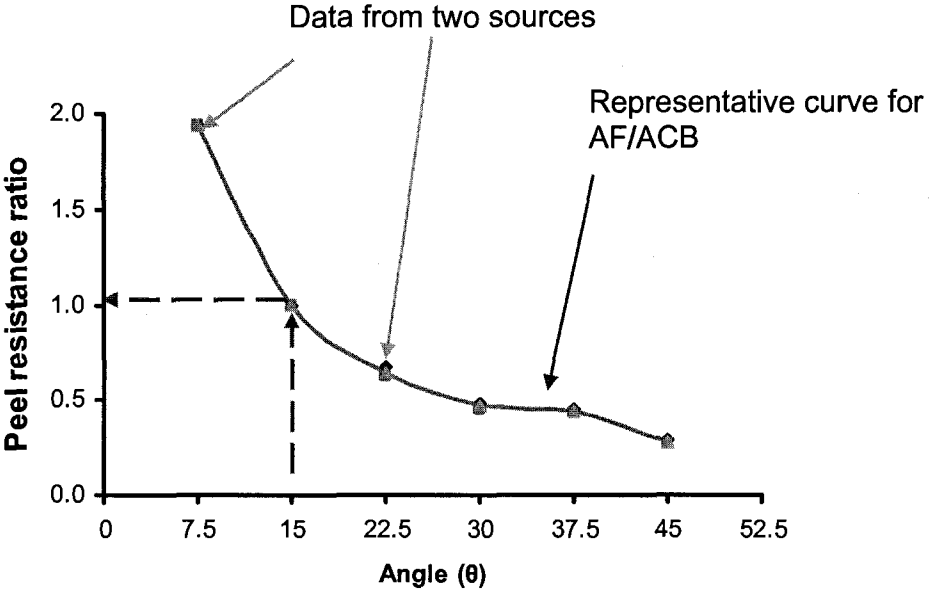

Figure 4.24 Normalized peel resistance of *AF/ACB* samples at different angles

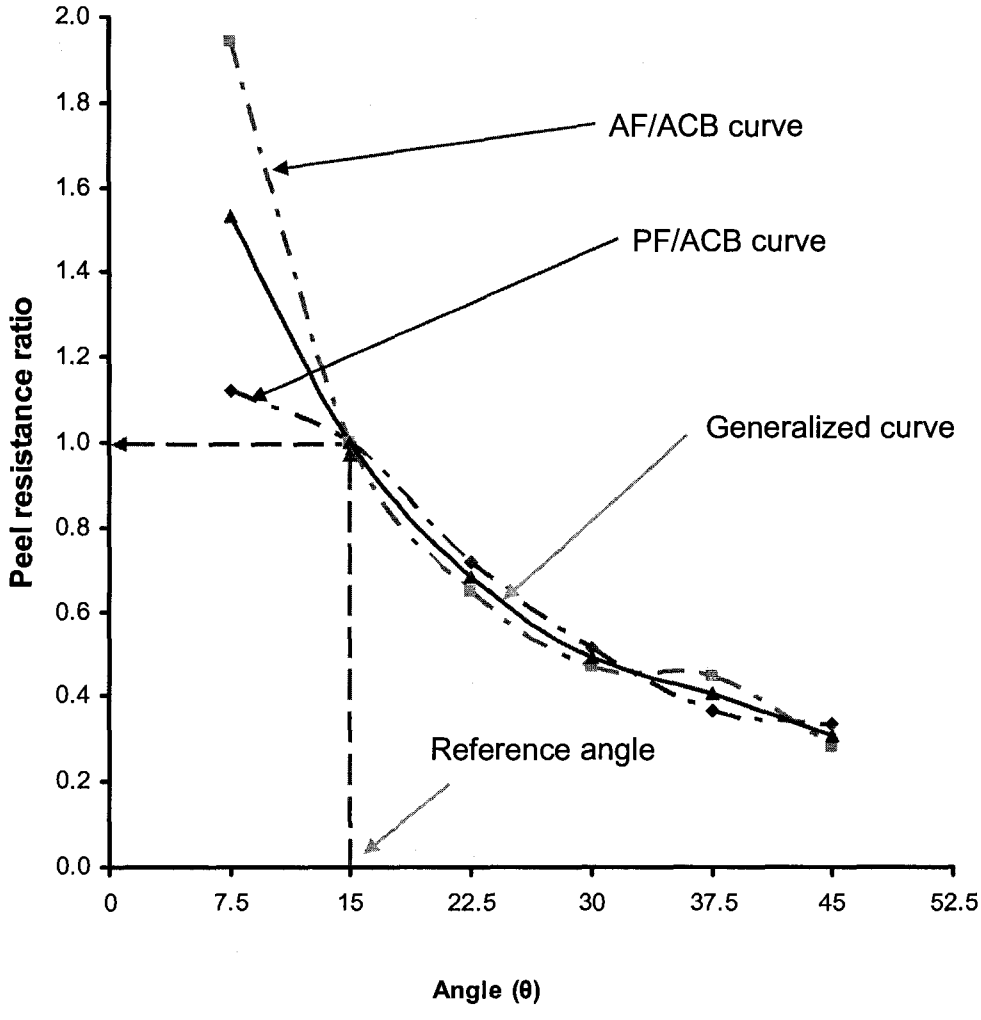

Figure 4.25 Development of a generalized angle curve for peel resistance of AARS

Using the above calculated two representative curves (Figure 4.22 and Figure 4.24) of two component sets, an attempt was made to develop a generalized understanding regarding the effect of peel angle on AARS peel resistance performance. Figure 4.25 shows such a generalized idea, accounting for the material variations. Following observations are highlighted from this figure.

- Differences between AF and PF curves are significant for angles less than the reference angle of 15°;
- Curves intersect at the reference angle of 15°;
- Peel resistance is not affected much when specimens are tested at greater than 15°;
- This generalized curve could be probably applied to calculate the peel resistance at various angles after obtaining the peel resistance at 15°; and
- Based on the above detailed analysis, the present study proposes 15° as the appropriate angle for the standard test method given in Chapter 6.

Interestingly, exceptional results were observed at the 7.5° peeling angle, where the peel resistance of AF/ACB was found to be marginally higher than that of PF/ACB (224 lbf versus 218 lbf for Source II sample; 271 lbf versus 263 lbf for Source IV sample) (Figure 4.25; Appendix 5 & 6). The reason for this discrepancy is not immediately clear, though similar variations were observed in PF/ACB and AF/ACB samples from three of four sources (Figure 4.10 in Section 4.3.2).

It is worth to validate this angle selection with different cover boards as well. Also, it is believed that the trend will remain same for variations of the rate of peeling force applied. Note that for the present study, all experiments were carried out at a constant rate of peeling force of 1.0 in./min or 25.4 mm/min.

4.4.3 Effect of Sample Size

As the final investigation of the impact of experimental parameters on AARS peel resistance, the effect of sample size was examined in Phase II. Samples of four different sizes, 4 in. x 4 in. or 102 mm x 102 mm, 6 in. x 6 in. or 152 mm x 152 mm,

8 in. x 8 in. or 203 mm x 203 mm and 10 in. x 10 in. or 254 mm x 254mm were tested at the E-P position and 15° peel angle. All samples for this experiment were assembled as the **PF/ACB** configuration and provided by two industrial sources, sources II and IV.

The experimental results are reported in Figure 4.26. The figure shows that the peel resistance increases with the sample size for both Source II and Source IV samples. This is because under the same peeling force condition, a larger size specimen is subjected to the smaller peel stress compared to the smaller size specimen. Moreover, samples from Source IV outperformed those from Source II in peel resistance at all sizes examined. This observation is consistent with the previous results.

Further analysis of Figure 4.26 indicates that the corves which represent the peel resistance versus sample linear dimension relationship contain roughly two distinct segments as follows:.

- Segment 1: 4 in.x 4 in. or 102 mm x 102 mm to 6 in. x 6 in. or 152 mm x 152 mm
- Segment 2: 6 in. x 6 in. or 152 mm x 152 mm to 10 in. x 10 in. or 254 mm x 254 mm

The slope of segment 1 is a little bit steeper than that of segment 2 for both curves. This observation suggests that the sample size has some influence on peel resistance between 4 in. or 102mm and 6 in. or 152mm, which is referred to as the **effective size range** hereafter. For samples larger than 6 in. x 6 in. or 152 mm x 152 mm, the slope is a little smaller, suggesting the sample size effects is less when the size is greater than 6 in. or 152mm.

Since 6 in. or 152mm is decided to be the standard sample size for most experiments in this study and 6 in. or 152 mm is in the effective size range for all samples examined, the peel resistance of the 6x6 in. or 152 x 152 mm was used as

the reference value for normalization of the peel resistance ratio of other samples of various sizes.

Following this procedure, the peel resistance ratio versus sample size curve for Sources II and IV samples was plotted in Figure 4.26 dotted lines. The peel resistance ratio curves in Figure 4.26 indicate that:

- Difference between Source II and Source IV curves is not significant when sample size is less than 8 in. or 203 mm.
- Difference between the two curves is evident at 10 in. x10 in. or 254 mm x 254 mm sample size, suggesting that the materials may have more profound effects on peel resistance.

As before, a generalized curve representing the averaged values from the two sample sets was created, which is shown by the solid curve in Figure 4.27. It is expected that the generalized curve can be used to calculate the peel resistance of various sample sizes if the peel resistance of a given sample size is obtained.

Together, the peel tests in this study show peel resistance ranking and peel resistant ratio of materials from various commercial sources, and consistent effect of peel positions, peel angles and sample sizes on peel resistance. Based on these peel test results, a *generalized angle curve* and a *generalized size curve* are developed for peel resistance of AARS. These curves will serve as useful tools for predicting AARS wind resistance under various stress modes. More importantly, the consistency in the peel test results suggest that the peel test experiments developed in this study are sound and can be utilized for the establishment of a standard protocol for AARS peel test. Such a standard protocol for AARS peel test is presented in Chapter 6.

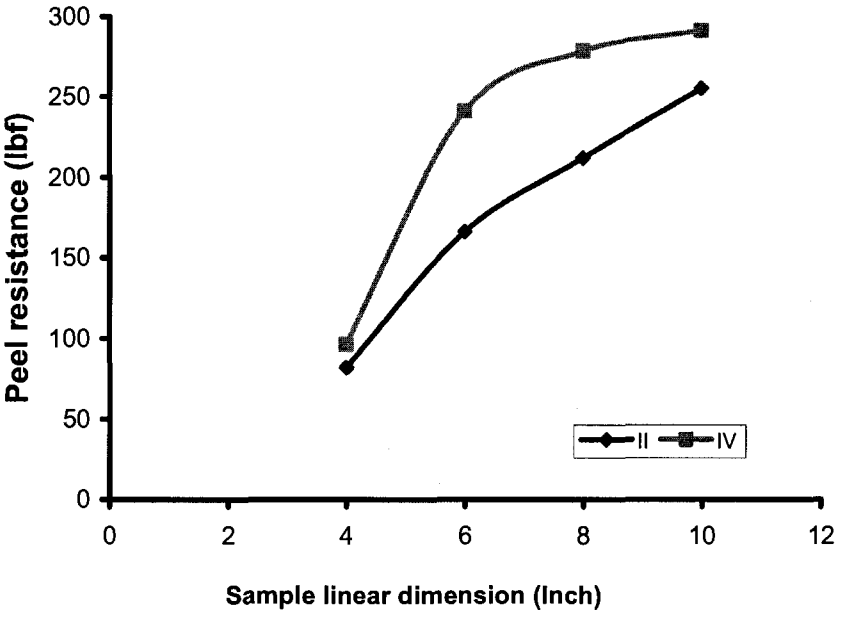

Figure 4.26 Effect of sample size on the peel resistance of PJ/ACB samples

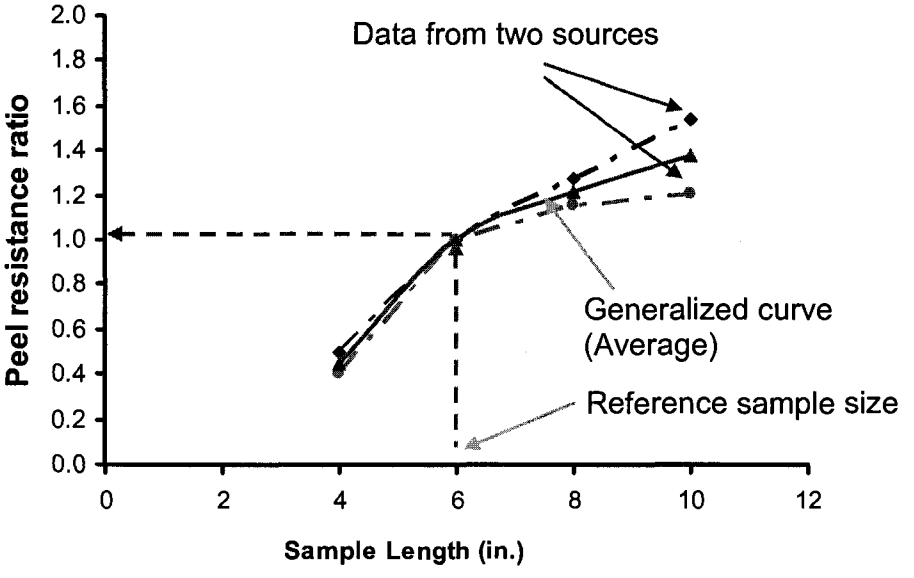

Figure 4.27 Development of a generalized sample size curve for peel resistance of AARS

Chapter 5 Failure Mode Analysis

Each type of roof systems responds differently to wind effects, resulting in various failure modes under wind induced peeling action. Chapter 4 presented the peel resistance, an overall indicator of the ultimate strength of the Adhesive Applied Roofing Systems (AARS). Similarly, the failure mode is an important indicator of the weakest link of the AARS. In the Mechanically Attached Roofing Systems (MARS), where anchorages are used to assemble the roofing system, the location with the weakest resistance against wind uplift forces for this case is often the location of anchorages themselves (Ko and Baskaran, 2007). The AARS, however, do not require any anchorages for their installation. Therefore, a comprehensive understanding of the various failure modes observed during the peel resistance investigation is important not only for the improvement of roofing design, but also for the establishment of a standard test protocol to evaluate the wind resistance of the AARS.

5.1 Failure Mode Classification and Definition

To ensure the consistency of the test results, throughout the experimental program, failure modes were observed and recorded by the same Instron operator, who was the author of this thesis. In addition, the standard criteria were used for the classification of different failure modes. This criterion was based on the percentage of the failure area of an individual failure to the total failure surface area. For example, several types of failure could occur during the peel test of a specimen but, for classification purposes, the failure mode was recorded only when the area of failure covered 1/3 or more of the total surface area of the specimen. Furthermore, each failure mode was documented with photographs as a reference for the development of a standard test procedure and all the photographs are grouped in the Appendices 1 to 6.

Depending on the components involved, failures can be classified as follows:

- Insulation failure
- Cover board failure
- Adhesive failure

Each of these components' failures is further classified based on the failure mode. Figure 5.1 classifies these various failure modes. The insulation failure can take place in the modes of delamination, tearing, and rupture, whereas the cover board failure modes are separation, splitting and brittle. The following section defines each of these failure modes with a representative photograph and an accompanying illustrative diagram.

5.1.1 Insulation Failure Modes

Facer Delamination: Figure 5.2 (a) displays a sketch and a photograph of a typical facer de-lamination failure mode. In this mode, the failure occurs at the facer layer of the insulation foam. During the experiments, it was observed that this kind of failure takes place rapidly, within a short duration, regardless of the type of insulation facers (paper facer or PF and acrylic facer or AF).

Facer Tearing: This failure refers to the tearing of the top facer from the insulation foam. Figure 5.2 (b) shows an illustration of a typical facer tearing failure mode with a representative photograph. As shown in this photo, a part of the facer was torn but most of the facer area was simply separated into two discrete layers. In general, the tearing behavior depends upon the tensile and shear strength of the facer material. The applied peel force can be considered in two components as tensile force towards the Y-axis and shear force along the X-axis. Since the peel angle increases as the specimen peels off, the Y-axis tensile force should increase during the peel test (refer to Chapter 4, section 4.4.2). Facer tearing failure typically happens when this tensile force exceeds the tensile resistance of the top insulation facer.

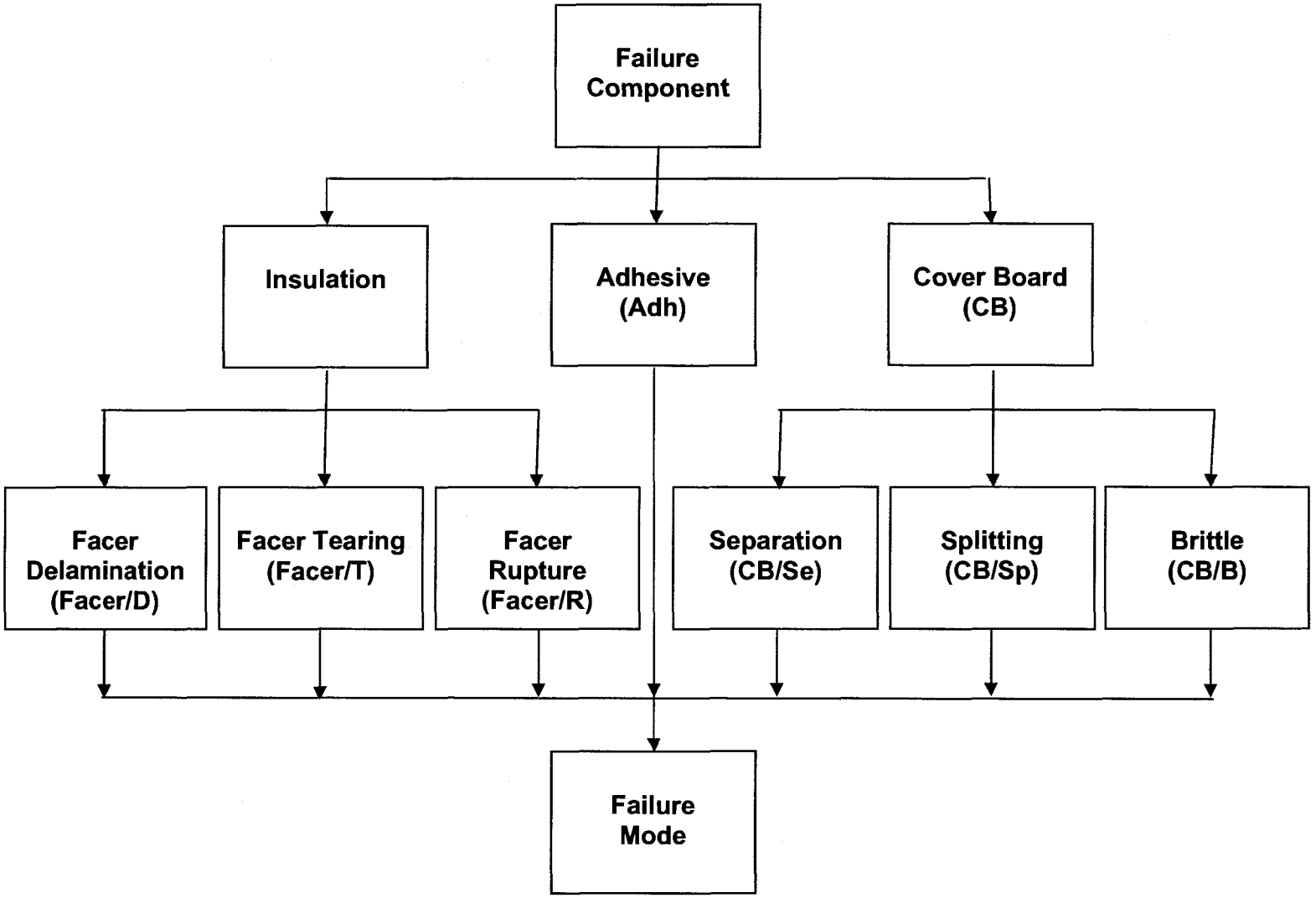

Figure 5.1 Failure mode classifications

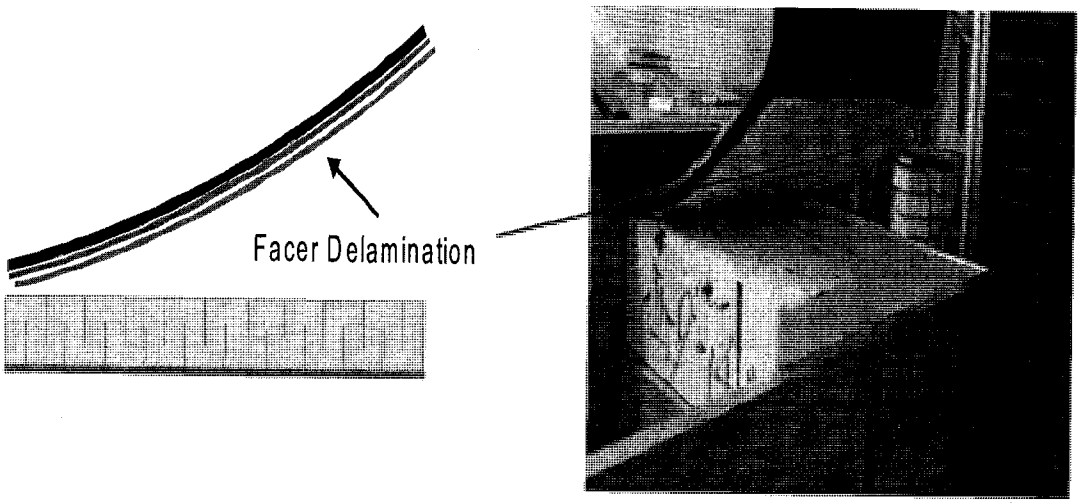

(a) Facer Delamination

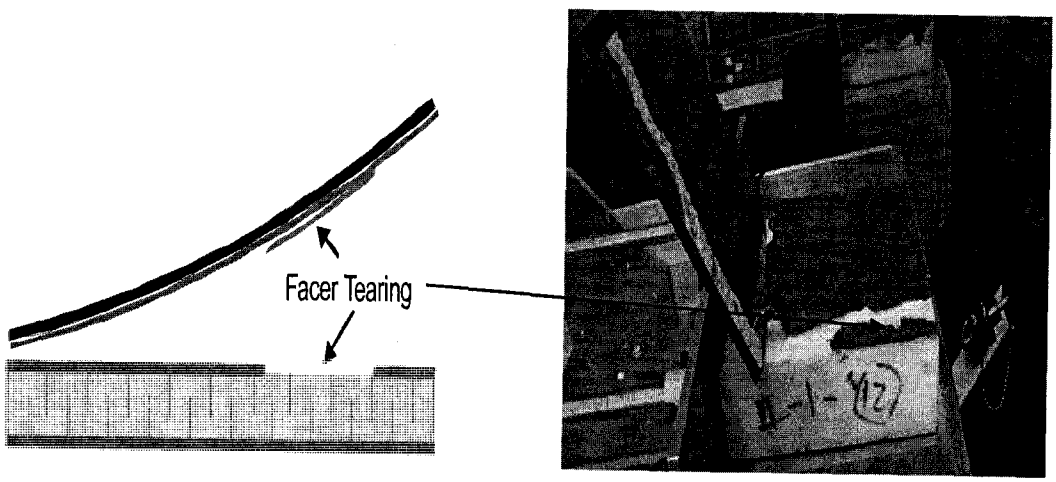

(b) Facer Tearing

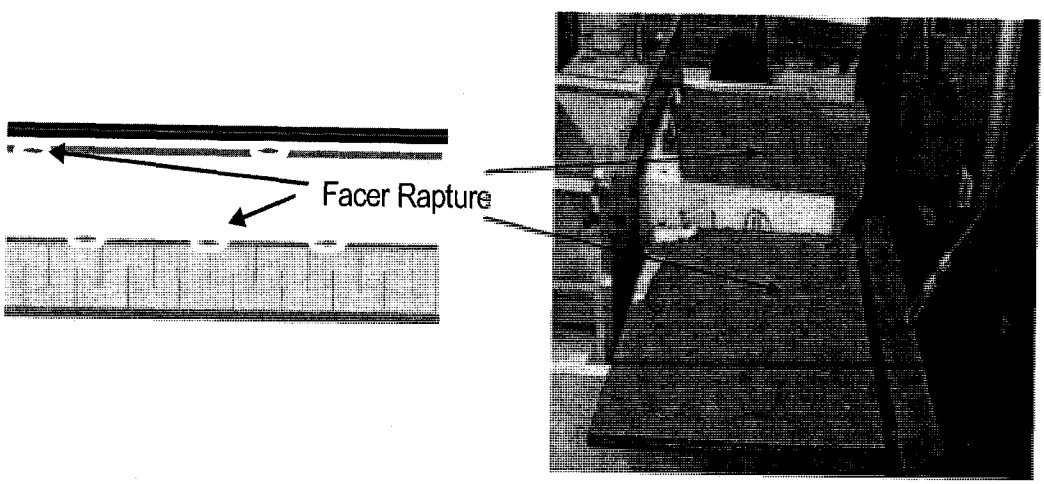

(c) Facer Rapture

Figure 5.2 Typical insulation failure mode sketch and photograph

Facer Rupture: In contrast to facer tearing failure, rupture failure results in complete separation of the entire paper surface area. This separates the top facer layer into two discrete layers without any tear damage. Figure 5.2 (c) depicts a sketch and a photograph of the typical facer rupture failure mode. Similar to facer tearing failure, facer rupture failure predominantly happens in insulation with paper facer. In the photograph of Figure 5.2 (c), a small delamination was observed at the back corner of the specimen. This was due to experimental set up. Note that a set of fasteners was used to hold the specimen in place (refer to Chapter 3, section 3.2.2) and these fasteners, in this case, penetrated into the foam, resulting in the delamination.

5.1.2 Cover Board Failure Modes

Separation: Figure 5.3 (a) displays a sketch and a photograph of a typical separation failure mode. Separation failure of a CB results in separation of cover board, with parts of CB material remaining in the adhesive layer. This failure mode normally happens in specimens with ACB (asphalt core cover board).

Splitting: Figure 5.3 (b) shows, together with a representative photograph, an illustration of the typical splitting failure mode. The splitting failure is somewhat similar to the facer rupture failure, except that the failure occurs in the cover board. Splitting failures result in complete separation of the cover board into two discrete layers. This type of failure predominantly occurs in specimen with FB (fiber cover board) configuration.

Brittle: A sketch and a representative photograph of a typical brittle failure mode are given in Figure 5.3 (c). The photograph indicates that the peeled edge (or corner) of a cover board was torn off from the specimen. This type of failure happens in both fiber cover board (FB) and asphalt core cover board (ACB). However, in the case of ACB, brittle failure mainly occurs during the experiment with corner peeling. It should be mentioned that the brittle failure process always took place within a very short duration.

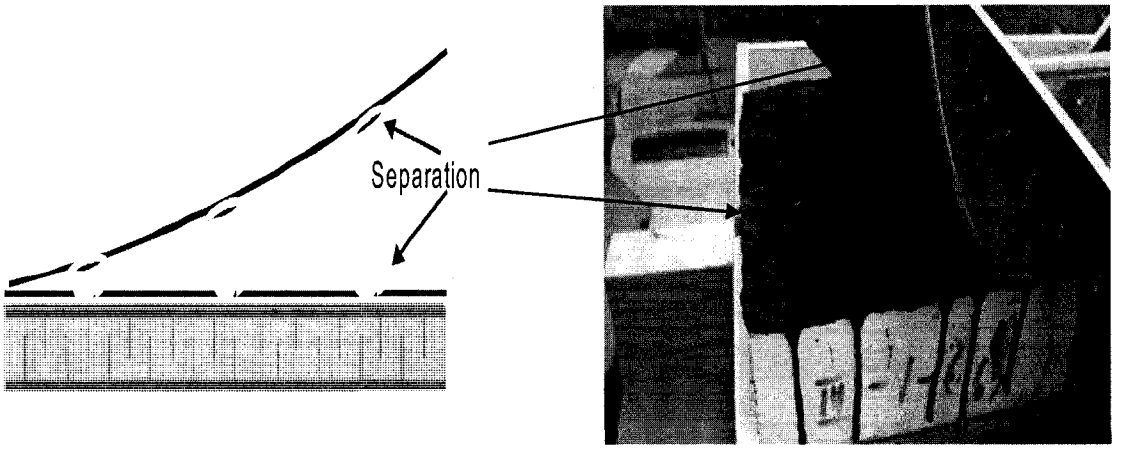

(a) Cover board separation

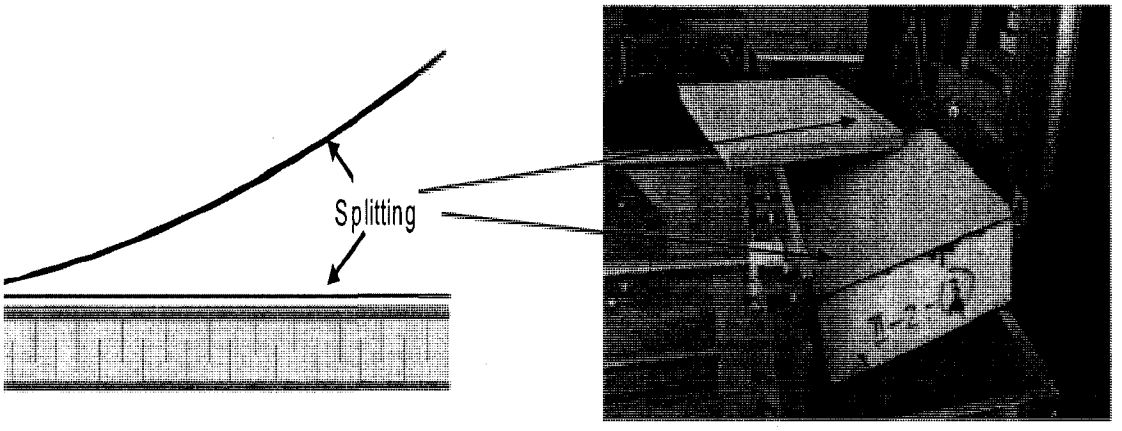

(b) Cover board splitting

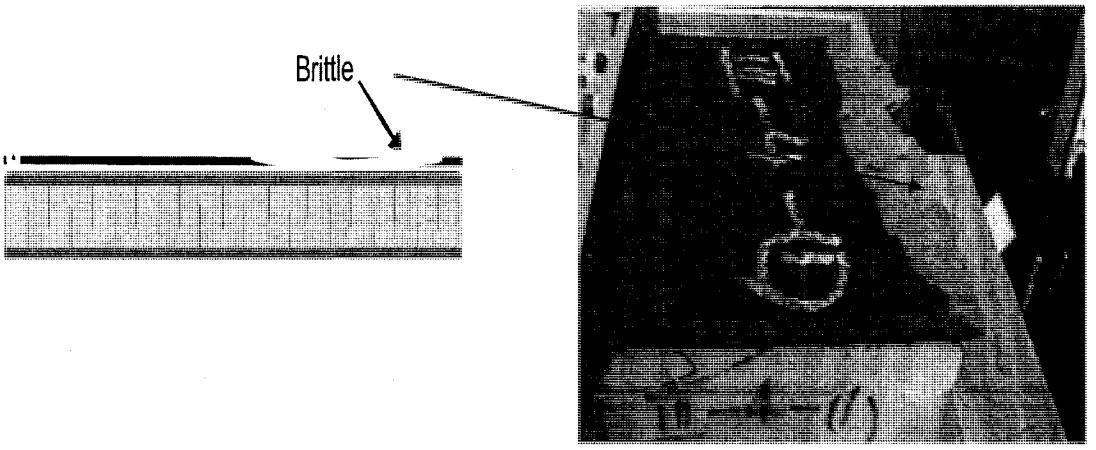

(C) Cover board brittle

Figure 5.3 Typical cover board failure mode sketch and photograph

5.1.3 Adhesive Failure

Figure 5.4 displays a sketch and a photograph of a typical adhesive failure mode. In this mode, the failure occurs between CB and the insulation top facer, resulting in a clean separation of the top cover board from the bottom insulation. Adhesive failure mainly happens in the specimens with ACB configuration and, in most cases, it occurs in combination with one of the other failure modes involved in the cover board or insulation components.

In general, each specimen failed due to one type of failure mode. However, occasionally, specimens failed due to combined failure modes. When one AF/ACB specimen was tested, a delamination failure at the facer was observed initially and followed by an adhesive failure as the peel force was increased. The photograph of Figure 5.5 shows the combined failure modes.

5.2 Failure Mode Investigation

The failure mode indicates the weakest link within the specimen. The weakest link of roofing systems varies depending on the components used. To investigate the relationship between failure mode; i.e., the weakest link, and the components, the raw experimental data were analyzed as follows:

After a specimen was tested, the failure mode of the specimen was determined based on the percentage of the failure area to the total failure surface. To illustrate this process, Table 5.1 summarizes the various failure modes of tested samples comprised of paper facer insulation and asphalt core cover board, labeled as PF/ACB. Parallel samples were provided by four different industry partners, each of which is identified here by a 'Source' number such as I-1, II-1 etc., and were subject to the peel test at the edge position (E-P) at 15° angle. The resulting failure modes are summarized similar to Table 4.2, which presents the peel resistance of each specimen. Some specimens have only one failure mode, whereas others have combined failure modes. Therefore, the weakest link for each sample can be judged

by comparing the failure modes as described in the failure mode table. Nine similar tables, compiled for all samples with different component configurations, are presented in Appendix 7.

At the end of the experiment, the **failure occurrence value** (**FOV**) for each sample was calculated. FOV is the number of failures that occurred in various modes in a sample set. In principle, the FOV of each sample set should be equal to the total number of specimens tested. As mentioned in Chapter 4, each sample contains 5 to 7 specimens, but only 5 specimens were used for failure analysis. In this scenario, following the above way of counting, each sample set has a total of 5 FOV. If a specimen fails in a combination of 2 failure modes, 0.5 FOV was assigned to each of the modes. During the present study all specimens failed in one or two failure modes, but no more than two modes.

This is further illustrated by taking the II-1 sample set as an example (Table 5.1). This set has 5 specimens. Hence, the total FOV is 5. Out of these 5 failures, 1 specimen failed in facer tearing (Facer/T), 3 specimens failed due to facer rupture (Facer/R) and 1 specimen had a mixed failure mode of adhesive failure (Adh) and facer rupture (Facer/R). Therefore, the FOV for this case is counted as:

- Facer tearing = 1
- Adhesive failure = 0.5
- Facer rupture = 3.5

Table 5.2 summarizes the Phase I FOV distribution of all failure modes of 24 sample sets from 4 different industry sources, designated as I, II, III and IV. In total, 120 FOV, 24 sample sets, 5 FOV per sample set, were considered for analysis out of 168 specimens tested. As seen in Table 5.2, the occurrence of failure modes is arranged according to the types of samples and sources. The distribution of FOV is extracted from the failure mode records in Appendix 7.

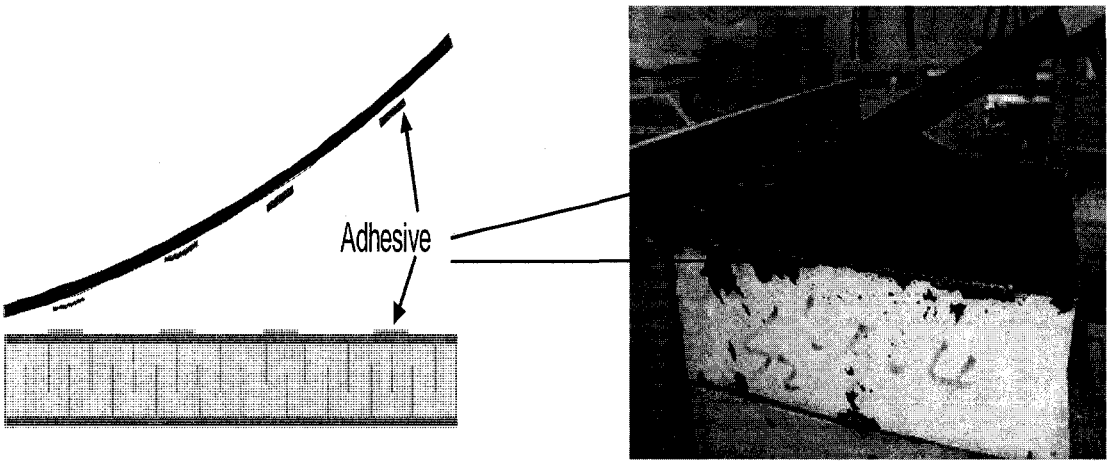

Figure 5.4 Typical adhesive failure mode sketch and photograph

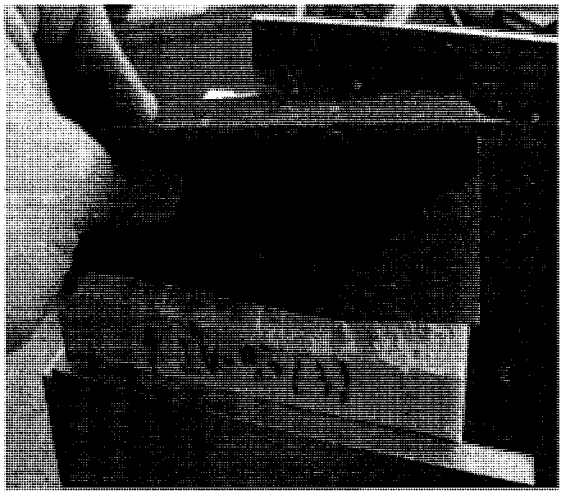

Figure 5.5 One type of combined failure mode photograph

Table 5.1 Failure mode comparison of PF-ACB-15°-E-P samples

Sample ID	I-1	II-1	III-1	IV-1
Specimen #	Failure Mode			
#1	Facer/D	Facer/R & Adh	CB/Se	Facer/D
#2	Facer/D	Facer/R	CB/Se	Facer/D & Adh
#3	Facer/D	Facer/R	CB/Se	Facer/D & Adh
#4	Facer/D	Facer/T	CB/Se	Facer/D
#5	Facer/D	Facer/R	CB/Se	Facer/D

Table 5.2 Failure occurrence value (FOV) distribution for Phase I samples

Sample ID	Failure Mode						
	Insulation			Cover Board			Adhesive
	Delamination	Tearing	Rupture	Separation	Splitting	Brittle	Adhesive
I-1 (PF/ACB-E)	5						
I-2 (PF/FB-E)						5	
I-3 (AF/ACB-E)	5						
I-4 (AF/FB-E)					1	4	
I-5 (PF/ACB-C)	3					2	
I-6 (AF/ACB-C)	4					1	
Total/Source I	**17**	**0**	**0**	**0**	**1**	**12**	**0**
II-1 (PF/ACB-E)		1	3.5				0.5
II-2 (PF/FB-E)					5		
II-3 (AF/ACB-E)	5						
II-4 (AF/FB-E)					5		
II-5 (PF/ACB-C)			2.5				2.5
II-6 (AF/ACB-C)	2.5						2.5
Total/Source II	**7.5**	**1**	**6**	**0**	**10**	**0**	**5.5**
III-1 (PF/ACB-E)				5			
III-2 (PF/FB-E)					1	4	
III-3 (AF/ACB-E)	3						2
III-4 (AF/FB-E)						5	
III-5 (PF/ACB-C)						5	
III-6 (AF/ACB-C)	1					4	
Total/Source III	**4**	**0**	**0**	**5**	**1**	**18**	**2**
IV-1 (PF/ACB-E)	4						1
IV-2 (PF/FB-E)					1	4	
IV-3 (AF/ACB-E)	2.5			0.5			2
IV-4 (AF/FB-E)						5	
IV-5 (PF/ACB-C)	0.5					4	0.5
Iv-6 (AF/ACB-C)	2.5					2	0.5
Total/Source IV	**9.5**	**0**	**0**	**0.5**	**1**	**15**	**4**
Total/All Sources	38	1	6	6	13	45	12
Total Percentage	31%	1%	5%	5%	11%	37%	10%

The percentage frequency of FOV under each failure mode represents the probability of that particular failure mode being the weakest link in the samples examined. For example, of all samples examined, the likelihood of having an insulation tearing failure is less than 1%, or only 1 case observed out of 120. The occurrence of a cover board brittle failure, however, is 37%. Of course, one can also calculate the likelihood of each failure mode occurring in samples from different sources or different configurations. This is explained hereafter.

5.2.1 Investigation of Insulation Failure Mode

In order to determine which insulation configuration (AF or PF) is more prone to failure under wind pressure, the failure modes of AF and PF were investigated. Table 5.3 summarizes the percentage of FOV for different insulation failure modes under different roofing configurations. Higher frequency is an indication of the weaker link of that material. From this table, it is clear that the performance of each configuration varies. When PF insulation and AF insulation are considered, regardless of the cover board combination, AF failed more frequently than PF. The percentage of FOV for AF is 25.5/120=21%, whereas it is 19.5/120=16% for PF. This result suggests that PF performs significantly better than AF under wind peeling pressures. The observation is supported by previous peel resistance analyses, demonstrating that AF has lower peel resistance than PF (Chapter 4, section 4.3.2).

As mentioned in section 5.1, the insulation failure can be classified into three modes: facer delamination, facer tearing, and facer rupture. This study also analyzes which of these failure modes is more likely to occur in the insulation component. The facer delamination, with a total of 38 FOV, is the most frequent failure mode when compared to the other two types; 1 FOV for the facer tearing and 6 FOV for the facer rupture. In Phase I experiments in particular, there was only one case of tearing failure in all samples examined as seen in Table 5.3. The facer delamination failures mostly occurred at the top surface of the insulation foam. This fact was probably due to physical characteristics of the foam; weak tensile strength, low thermal

conductivity, low heat capacity, low permeability, or material incompatibility. However, this interpretation needs further investigation.

In this study, the facer delamination failures which 25.5 FOV predominantly (took place in specimens with AF configuration, suggesting that the AF configuration is more prone to the facer delamination failure than the PF configuration. Indeed, all AF specimens' insulation failures were in the facer delamination mode as seen in Table 5.3, suggesting the material incompatibility between AF and the insulation foam.

5.2.2 Investigation of Cover Board (CB) Failures

In order to investigate the failure mode within the CB component, the percentage of FOV for the ACB and FB are summarized in Table 5.4. Table 5.4 is of similar format to Table 5.3. It shows that FB is more likely to fail than ACB; the frequency of FB failure is 33% (40/120), whereas the frequency of ACB failure is 20% (23.5/120). This result is consistent with the earlier results of the peel resistance of ACB and FB, as discussed in section 4.3.1. The reason for this is probably due to the lack of stiffness of FB materials, as explained in 4.3.1.

Table 5.4 also shows the detailed frequency distribution, calculated as the FOV of all failure modes in the CB component. CB failures were found to be mostly brittle failures. Further analysis shows that the brittle failure mode is related to different material configuration. Normally, brittleness and splitting are caused by material stiffness, stress concentration, insulation movement, or thermal contraction. In this study, for the specimens with FB configuration, the brittle failure may be caused by material stiffness, since all FB specimens failed with brittle or splitting mode (Table 5.5). However, for specimens with ACB configurations, all brittle failures happened with the corner peeling condition. The details are illustrated by photographs in Appendix 1 though 4, suggesting that they were caused by stress concentration.

Table 5.3 Failure occurrence value (FOV) distribution of insulation

Component		Insulation					
Type		Paper Facer (PF)			Acrylic Facer (AF)		
Failure Mode		Delamination	Tearing	Rupture	Delamination	Tearing	Rupture
Failure Occurrence Value (FOV)	Source I	8	0	0	9	0	0
	Source II	0	1	6	7.5	0	0
	Source III	0	0	0	4	0	0
	Source IV	4.5	0	0	5	0	0
	Total/Mode	12.5	1	6	25.5	0	0
	Total/Type	19.5			25.5		
	Total/Component	45					
Percentage of All Specimens		16%			21%		

Table 5.4 Failure occurrence value (FOV) distribution of cover board

Component		Cover Board					
Type		Asphalt Core Board (ACB)			Fiber Board (FB)		
Failure Mode		Separation	Splitting	Brittle	Separation	Splitting	Brittle
Failure Occurrence Value (FOV)	Source I	0	0	3	0	1	9
	Source II	0	0	0	0	10	0
	Source III	5	0	9	0	1	9
	Source IV	0.5	0	6	0	1	9
	Total/Mode	5.5	0	18	0	13	27
	Total/Type	23.5			40		
	Total/Component	63.5					
Percentage of All Specimens		20%			33%		

Table 5.5 CB failure distribution under different material configurations

Sample component	Failure Mode		
	Cover Board		
	Separation	Splitting	Brittle
PF/**ACB**	5	0	11
AF/**ACB**	0.5	0	7
PF/**FB**	0	7	13
AF/**FB**	0	6	14

Table 5.6 Failure occurrence value (FOV) distribution of adhesive

Component		Adhesive
Failure Occurrence Value (FOV)	Source I	0
	Source II	5.5
	Source III	2
	Source IV	4
	Total/Component	11.5
Percentage of All Specimens		10%

5.2.3 Investigation of Adhesive Failure

Adhesive failures represent 10% of all samples (Table 5.6). All adhesive failures occurred in combination with secondary failure modes (Appendix 7). This may be due to bonding conditions as follows. During the fabrication of specimens, many factors, such as surface flatting and adhesive thickness, can affect the specimens' bonding conditions, resulting in poor bonding at the edges. When the specimens were subjected to the peel force, an adhesive failure occurred first, because of a poorly bonded edge, followed by the secondary failure mode as the peeling proceeded.

As discussed in the section 3.3.3, for the present study, in all specimens, adhesives were applied in the full coating coverage format. This is due to the size of specimens used (i.e., 6 in. x 6 in. or 152 mm x 152 mm). However, in the field, both full coating coverage and ribbon application are common. Therefore, it is likely that the occurrence of adhesive failure in the field will be higher than the observed frequency in this study. This is because full coating adhesive applications provide stronger adhesion than ribbon format adhesive applications. The relative failure occurrence between full coating and ribbon coating is not investigated in this thesis.

5.2.4 A summary of Failure Mode Investigation

Tables 5.3, 5.4 and 5.6 represent the percentage failure mode distribution for insulation, cover board, and adhesive. Figure 5.6 provides a summary that combines these data. This figure indicates that over a half (53%) of the failures occurred in CB component and 37% in the insulation component, leaving about 10% due to adhesives. These results suggest that the CB component is the weakest link, followed by the insulation, in AARS performance under wind uplift.

Overall, CB seems to have higher probability of failing under the current peel test conditions. But the above analysis also indicates that the industrial sources of assembly were another important factor to be considered. The high frequency of FB failure was the biggest contributing factor as to why CB was the weakest link in the

samples examined in Phase I. It is reasonable to consider that if ACB materials were used for the CB component with different insulation for AARS, most failures would have occurred in the insulation layer. This means that when the wind uplift acts on AARS, the weakest link is in the insulation layer if ACB is used as cover board. However, if FB is used for the cover board, the failure is likely to occur in the cover board layer.

The above analyses also indicate that the weakest links where failures are most likely to happen are in the CB and insulation components. Figure 5.6 shows the detailed frequency distribution, calculated by percentage, of the failure modes of all samples from the Phase I testing. In summary, the delamination represents the weakest link for insulation component, and brittle failure represents the highest frequency for CB component under wind peel force.

5.3 Correlation of the Failure Mode and Peel Resistance

Although there have been some earlier studies on the failure modes of various AARS (Baskaran & Murty, 2007), little is known about the relationship between wind uplift peel resistance and the resulting failure modes. This section aims at establishing a detailed correlation analysis between the weakest link components and peel resistance of AARS.

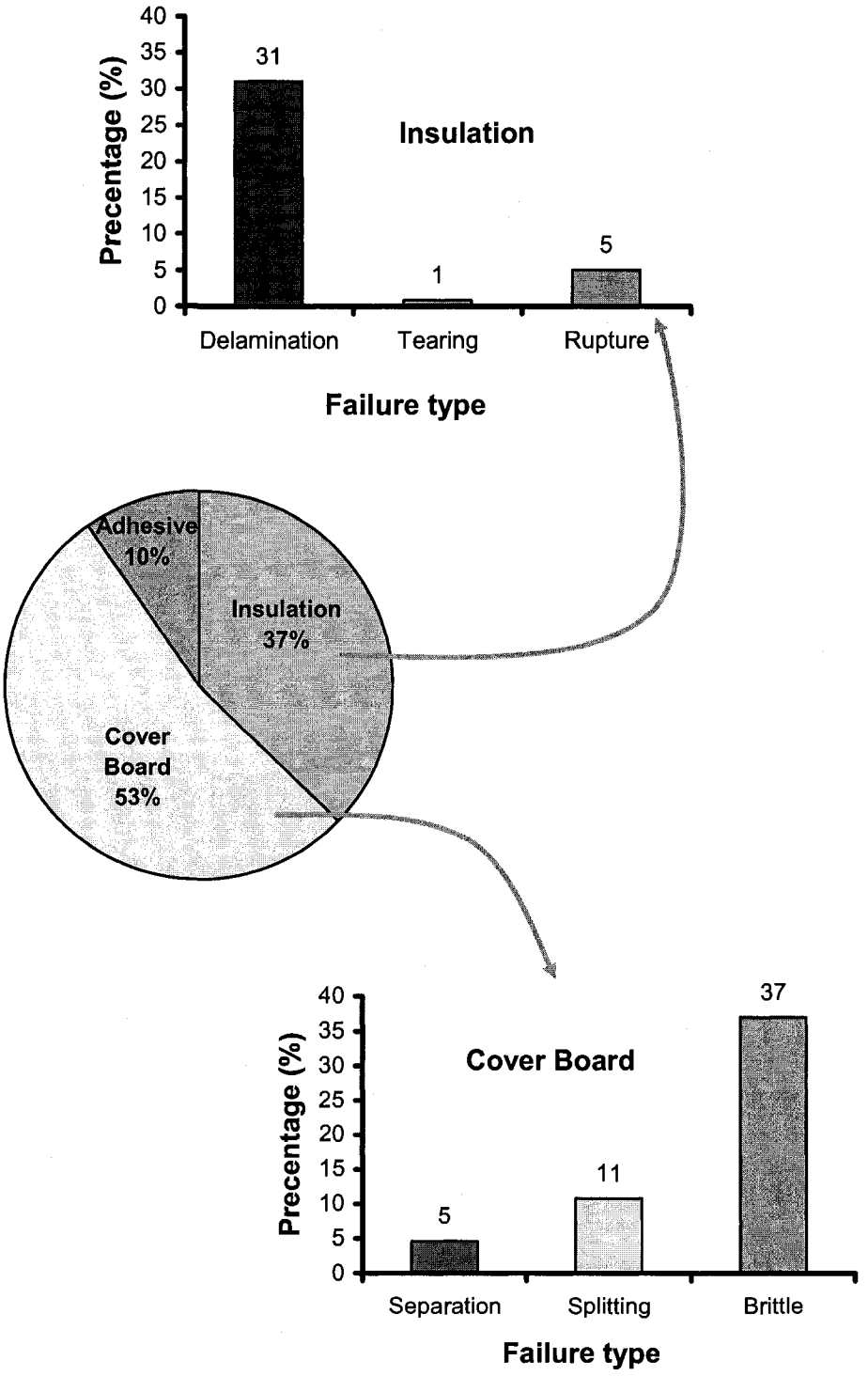

Figure 5.6 Summary of the failure mode distribution for Phase I samples

Table 5.7 summarizes the various failure modes and their corresponding mean peel resistance data. These data represent samples investigated in Phase I testing. The mean peel resistance was calculated based on data in Tables 4.2, 5.1 and Appendix 7, using the two criteria described below:

(1) If a group of samples has the same failure mode, the peel resistance value of this failure mode is the mean peel resistance value of the samples. For example, all specimens of Sample I-1 have the same failure mode as facer delamination (Facer/D) (Table 5.1). Therefore, the delamination peel resistance value is 232 lbf or 1032 N (Table 4.2).

(2) If a group of samples includes two or more failure modes, the peel resistance value for each failure mode is calculated based on the peel resistance of specimens that share the same failure mode. For instance, Sample II-1 in Table 5.1 includes the facer rupture failure (Facer/R), adhesive failure (Adh) and facer tearing failure (Facer/T). Since the facer tearing occurred only in one specimen in this group of samples, its peel resistance is equal to the specimen's tearing peel resistance, 100 lbf or 445 N (Table 4.2). In contrast, there were four cases of the facer rupture failure in this group of samples. Hence the rupture peel resistance is equal to the mean peel resistance of these four specimens, (121+99+104+89)/4 = 103 lbf or 458 N.

All the Phase I data were analyzed based on the results calculated according to the procedure mentioned above. Each failure mode peel resistance from four industry sources was calculated and ranked as shown below:

- Separation: 188 ± 19 lbf or 836 ± 84 N
- Adhesive: 166 ± 29 lbf or 738 ± 129 N
- Delamination: 155 ± 31 lbf or 690 ± 138 N
- Rupture: 125 ± 0 lbf or 556 ± 0 N
- Brittle: 117 ± 7 lbf or 520 ± 31 N
- Tearing: 100 ± 0 lbf or 445 ± 0 N
- Splitting: 83 ± 40 lbf or 369 ± 178 N

Table 5.7 Failure mode distribution at various peel resistance (lbf) of Phase I samples

Sample ID	Failure Mode						
	Insulation			Cover Board			Adhesive
	Delamination	Tear	Rupture	Separation	Splitting	Brittle	Adhesive
I-1 (PF/ACB-E)	232						
I-2 (PF/FB-E)						117	
I-3 (AF/ACB-E)	226						
I-4 (AF/FB-E)					86	129	
I-5 (PF/ACB-C)	176					140	
I-6 (AF/ACB-C)	137					89	
Total/Source I	**193**				**86**	**119**	
II-1 (PF/ACB-E)		100	103				121
II-2 (PF/FB-E)					44		
II-3 (AF/ACB-E)	85						
II-4 (AF/FB-E)					46		
II-5 (PF/ACB-C)			147				147
II-6 (AF/ACB-C)	147						147
Total/Source II	**116**	**100**	**125**		**45**		**138**
III-1 (PF/ACB-E)				202			
III-2 (PF/FB-E)					64	84	
III-3 (AF/ACB-E)	199						196
III-4 (AF/FB-E)						91	
III-5 (PF/ACB-C)						142	
III-6 (AF/ACB-C)	117					121	
Total/Source III	**158**			**202**	**64**	**109**	**196**
IV-1 (PF/ACB-E)	223						234
IV-2 (PF/FB-E)					138	97	
IV-3 (AF/ACB-E)	131			175			142
IV-4 (AF/FB-E)						101	
IV-5 (PF/ACB-C)	151					176	151
Iv-6 (AF/ACB-C)	108					117	126
Total/Source IV	**153**			**175**	**138**	**123**	**163**
Mean/All Sources	**155**	**100**	**125**	**188**	**83**	**117**	**166**
SD	**31**	**0**	**0**	**19**	**40**	**7**	**29**

The above failure mode ranking clearly shows that separation (169 to 207 lbf or 752 to 921 N) of the components in between the adhesives (137 to 195 or 609 to 867 N) has the maximum resistance against peel failure, whereas the brittle has the least resistance (124 to 110 lbf or 552 to 489 N) and higher probability (37%) to fail. It is interesting to compare these observations with that of the Figure 5.6, which in turn cross-checks this observation to verify the failure mode peel resistance ranking. The above failure mode ranking and the failure occurrence value distribution shown in Figure 5.6 are complementary to each other. Brittle failure occurs mainly in the cover board, whereas delamination occurs in the insulation. To understand this further, the same data were analyzed with respect to the components used.

It should be noted that the rupture and tearing failure modes occurred only in samples from one particular industry source, and hence were excluded from the presentation. Further experimental study is needed to validate the occurrence of these two failure modes. In the same token, peel resistance of the splitting failure mode has significant variations from one source to another, and this failure mode only occurs in FB configuration (Table 5.5), a fact which also needs confirmation.

Table 5.8 provides the analysed data identifying the weakest link of the AARS samples. The numerical procedure is similar to that of Table 5.7, which focuses on the failure mode. As discussed in Table 5.6, the adhesive was excluded from the analysis as it has a minimum contribution. Two types of insulation and two types of cover boards are included. The ranking of component configuration based on their peel resistance is as follows:

- ACB: 159 ± 28 lbf or 707 ± 125 N
- PF: 144 ± 33 lbf or 641 ± 147 N
- AF: 126 ± 28 lbf or 561 ± 125 N
- FB: 88 ± 32 lbf or 391 ± 142 N

Note that the ranking is shown from the strongest to the weakest in terms of peel resistance. It indicates that the FB is the weakest link in the AARS samples and can

cause major failures. This observation has been found from data in failure mode observation as well. The combination of paper facer insulation with ACB forms the best combination, and yields the highest peel resistance. Discussion of these data with the industrial partners confirmed that similar observations were noticed in the field. Also, as shown in Figure 1.7, the hurricane Katrina caused peel failures at the weakest links of roofing systems. This chapter presented the detailed analysis of the failure modes, ranking of those failures, and concluded by identifying the weakest links in the AARS samples.

Table 5.8 Weakest link identification at various peel resistance (lbf) of Phase I samples

Sample ID	Component at Which Failure Occurs			
	Insulation		Cover Board	
	PF	AF	ACB	FB
I-1 (PF/ACB-E)	232		232	
I-2 (PF/FB-E)	117			117
I-3 (AF/ACB-E)		226	226	
I-4 (AF/FB-E)		121		121
I-5 (PF/ACB-C)	162		162	
I-6 (AF/ACB-C)		127	127	
Total/Source I	**170**	**158**	**187**	**119**
II-1 (PF/ACB-E)	102		102	
II-2 (PF/FB-E)	44			44
II-3 (AF/ACB-E)		85	85	
II-4 (AF/FB-E)		46		46
II-5 (PF/ACB-C)	147		147	
II-6 (AF/ACB-C)		147	147	
Total/Source II	**98**	**93**	**120**	**45**
III-1 (PF/ACB-E)	202		202	
III-2 (PF/FB-E)	80			80
III-3 (AF/ACB-E)		199	199	
III-4 (AF/FB-E)		91		91
III-5 (PF/ACB-C)	142		142	
III-6 (AF/ACB-C)		120	120	
Total/Source III	**141**	**137**	**166**	**85**
IV-1 (PF/ACB-E)	223		223	
IV-2 (PF/FB-E)	105			105
IV-3 (AF/ACB-E)		140	140	
IV-4 (AF/FB-E)		101		101
IV-5 (PF/ACB-C)	171		171	
Iv-6 (AF/ACB-C)		112	112	
Total/Source IV	**166**	**118**	**161**	**103**
Mean/All Sources	**144**	**126**	**159**	**88**
SD	**33**	**28**	**28**	**32**

Chapter 6 Standard Test Method for Peel Resistance of Roofing Components Bonded using Cold Adhesives

One of the main objectives of this thesis is to draft a standard test method for peel resistance of AARS. Such a standard test method is presented in this Chapter. Experimental results obtained in this thesis and inputs received from the participating industrial partners formed basis for this standard development. The draft is written following the format requirement of the ASTM standards. The format includes the scope, test apparatus, test conditions, procedures for the preparation of specimens and reporting of the test results. It is expected that this draft will be submitted to standard development organizations such as ASTM and CSA. Then this draft will undergo consensus process. Upon completion, this standard method will serve as a regulatory guide for Canadian roofing community in testing the peel resistance of various AARS materials.

6.1 Introduction

The purpose of this test is to determine the resistance-to-peel strength of adhesives when surfaces joined by an adhesive are separated by applying a force to one of the surfaces at 15° angle. The accuracy of the results of strength tests of adhesive bonds will depend on the conditions under which the bonding process is carried out. Unless otherwise agreed upon between the manufacturer and the purchaser, the bonding conditions shall be prescribed by the manufacturer of the adhesive. In order to ensure that complete information is available to the individual conducting the tests, the manufacturer of the adhesive shall furnish numerical values and other specific information for each of the following variables:

(1) Procedure for preparation of the surfaces prior to application of the adhesive, the cleaning and drying of surfaces, and special surface treatments, which are not specifically limited by the pertinent test method.

(2) Complete mixing directions for the adhesive.

(3) Conditions for the application of the adhesive, including the rate of spread or thickness of the film, number of coats to be applied, whether to one or both of the surfaces, and the conditions of drying.

(4) Assembly conditions before the application of adhesion, including room temperature and length of time.

(5) Curing conditions, including the amount of pressure to be applied, the length of time under pressure, and the temperature of the assembly when under pressure. It should be stated whether this temperature is that of the glue line or of the atmosphere at which the assembly is to be maintained.

(6) Conditioning procedure before testing, unless a standard procedure is specified, including length of time and relative humidity.

6.2 Scope

This test method covers the determination of the resistance-to-peel strength of an adhesive bond between two rigid adherend when tested at 15° angle under specified conditions of preparation and testing.

The values stated in SI units are to be regarded as the standard. The values given in parentheses are for information only. This standard does not purport to address all of the safety concerns, if any, associated with its use. It is the responsibility of the user of this standard to establish appropriate safety and health practices and determine the applicability of regulatory limitations prior to use.

6.3 Referenced Documents

ASTM standards include:

- D 907 "Terminology of adhesives";
- D 3167 – 03a "Standard test method for floating roller peel resistance of adhesives";
- D 6862 – 04 "Standard test method for 90 degree peel resistance of adhesives"; and
- D 1876 – 01 "Standard test method for peel resistance of adhesives (T-peel test)"

ISO Standard includes:

- ISO 4578 "Adhesives – Determination of peel resistance of high=strength adhesive bonds – floating-roller method"

European Standards include:

- DIN EN 12316 – 2 "Flexible sheets for waterproofing – determination of peel resistance of joints Part 2: Plastic and rubber sheets for roof waterproofing"; and
- BS EN 12316-2:2000 "Flexible sheets for waterproofing – determination of peel resistance of joints Part 2: Plastic and rubber sheets for roof waterproofing".

6.4 Terminology

Many of the definitions used in this test method are defined in ASTM D 907 – 06 "Standard terminology of adhesives".

6.5 Summary of Test Method

This test method consists of testing bonded adherends, where two adherend are rigid, by peeling of the top rigid adherend from bottom rigid adherend at a specified angle of peel using the test machine, test fixture, gripper and angle controller.

6.6 Significance and Use

This test method is useful for acceptance and quality control testing. Adherends, application procedure, and sample conditioning shall be as agreed upon by the manufacturer and the user of the adherends and the adhesive.

6.7 Apparatus

6.7.1 Testing Machine

The testing machine shall have a load weighing system conforming to the requirements of Practice E 4. It shall have the capability of constant rate of extension (CRE) with a crosshead speed of 25 mm/min or 1.0 in./min. The testing machine shall have an adequate pen or computer response to record the force-time curve. Self-aligning grips shall be used to hold the top rigid adherend. The breaking load shall fall between 15% and 85% of the full scale load range. The grips need to engage the top rigid adherent firmly and, when load is applied, the direction of the applied force needs to be through the center line of the grip assembly. The proposed machine for this standard test method is Instron machine 5566 (Figure 6.1 (a)).

6.7.2 Test Fixer

The fixer is a steel plate functioning to hold the specimen stably during the peel test. The fixer's size is 406mm x 356mm x 102 mm or 16 in. x 14 in. x 4 in. (length x width x height).The fixer is mounted on a supporting table (Figure 6.1 (b)).

6.7.3 Grippers

The grippers are a link connecting the specimen to the test machine. The main part of the grippers consists of two pieces of parallel steel plates (Figure 6.1 (c)). The length of these steel plates is 203mm or 8in.. That firmly grips the top rigid adherend. The gripper is then connected to the testing machine by a steel wire, through the center line of the specimen assembly. The steel wire diameter is 3mm or 1/8 in. In order to balance the thickness of top rigid adherend, springs need to be installed into gripper to minimize slipping during the test.

6.7.4 Angle controller

The angle controller serves to control the peel angel during peel tests (Figure 6.1 (d)). The angle controller has two parts, a pulley and a steel holder. The length of the holder can be adjusted by sliding the inside steel bar along the outside tube. The inside steel bar is scaled by 6mm or 1/4 in. increment for fine-tuning the peel angle. The peel angle 15 degree is determined by adjusting the roller height by sliding the inside steel bar into the holder. During the testing, the angle controller mounted on the bottom of the machine, the steel wire of the gripper goes though the pulley of the angle controller, and connects to the machine's upper jaw. The pulley is used to keep the steel wire moving freely during the peel test with minimum friction.

6.8 Specimen preparation

- Cut the bottom rigid material into a 152 mm x 152 mm or 6 in. x 6 in. square size specimen, then the top rigid layer is cut into pieces that are 13 mm or 0.5 in. longer than the bottom rigid layer on one edge so that a 13 mm or 0.5 in. overhang is available for gripping during the peel test;
- These two rigid layers are bond together by applying adhesives; and
- A minimum of seven specimens per aging condition. Typical sample aging conditions call for testing of panels after 28 days assembly.

6.9 Test Method

- Insert the test specimen into the peel test fixer as shown in Fig. 6.2, with the unbonded end of the top rigid adherend gripped with the test gripper, then the steel wire of gripper gripped in the test machine jaw through the angle control. Peel the specimen at a constant crosshead speed of 25.4 mm/min. or 1.0 in./min. Other crosshead speeds may be used as required by a particular test specification or at a speed agreed upon by the manufacturer;
- During the resistance-to-peel test, make an autographic recording of load versus time history (peel resistance versus peeled time); and
- Record the load until the top rigid adherend tear off from the bottom rigid adherend or as agreed to by the adhesive manufacturer and the end user. Record the failure mode for each specimen based on pre-defined criteria.

6.10 Calculation

- Determine from the autographic curve of peeling, the mean resistance-to-peel strength in kilonewtons or pounds-force of the specimen required to separate the adherends. The mean value may be calculated as the average of load readings of five tested specimens, which have the smallest standard deviations;
- A minimum value of X kilonewtons or pounds-force as is should be obtained as the peel resistance of the sample.

6.11 Report

Report the following information:

- Complete identification of the adhesive tested including type, source, etc;

- Compete description of the test specimen, including material name, dimensions and construction of the test specimen, conditions used for cutting individual test specimens, number of individual test specimens;
- Description of bonding process, including method of application of adhesive, glue-line thickness assembly methods, curing time, temperature and relative humidity;
- Method of recording load and determining average load;
- Average, maximum, and minimum resistance-to-peel load values for each individual specimen;
- Mean resistance-to-peel strength in kilonewtons or pounds-force for each combination of materials and constructions under test; and
- Description type of failure mode for each individual specimen, the failure mode is pre-defined by test operator or manufacturers.

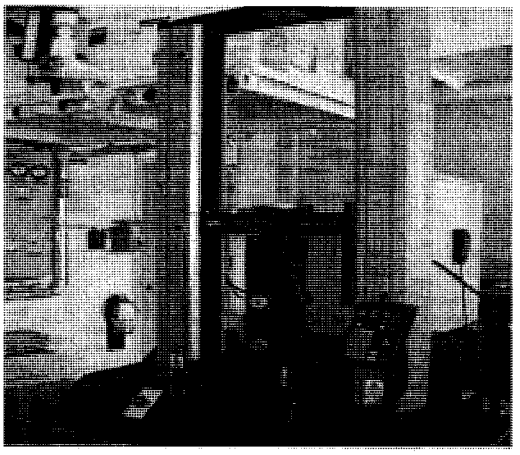

(a) Instron Machine

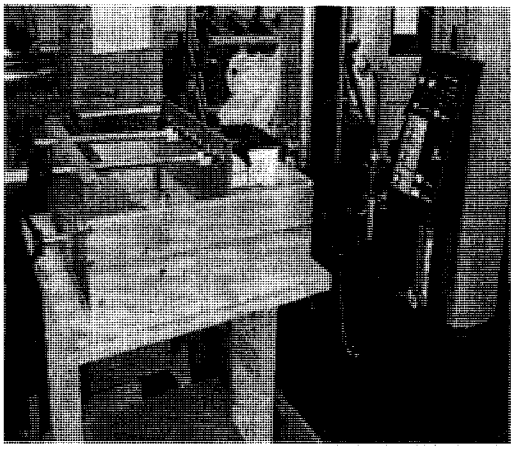

(b) Fixer to mount the test specimen

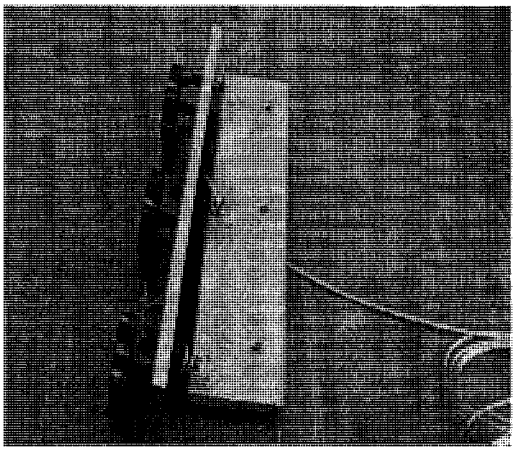

(c) Gripper

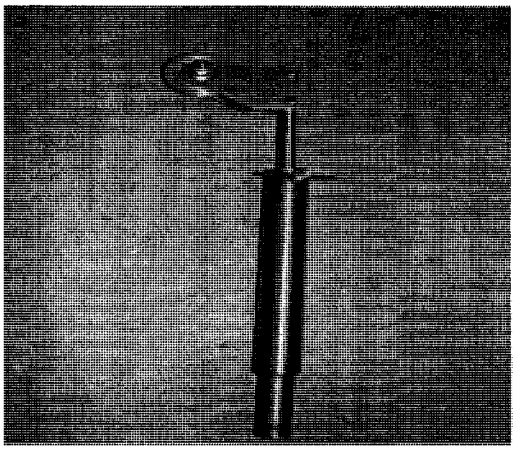

(d) Angle controller

Figure 6.1 Test apparatus

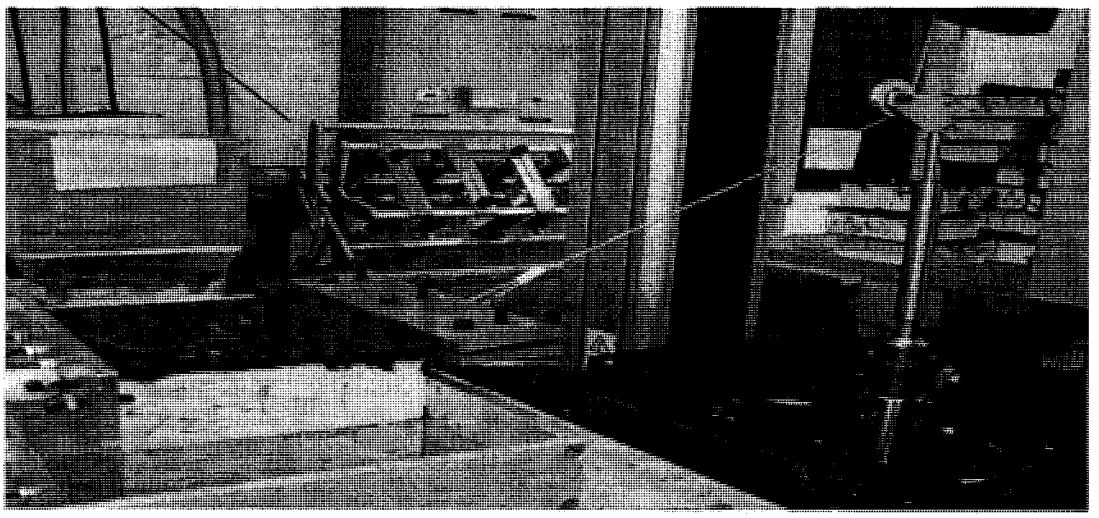

Figure 6.2 Peel test set up

Chapter 7 Conclusions and Recommendations

7.1 Conclusions

Many standard testing methods are used today for the evaluation of wind-induced peeling of roofing assemblies. However, after careful review of 5 different standards commonly practiced in North American and Europe, it is concluded that none of these existing standards are appropriate for the evaluation of peel resistance between two rigid adhesive membrane systems. Since the Adhesive Applied Roof Systems (AARS) are exclusively assemblies of rigid layers, a standard for evaluating their wind peel performance is still lacking. In this study, a series of peel tests was carried out to evaluate the peel resistance of various rigid adhesive membrane systems used in AARS. These peel tests provided both quantitative (peel resistance) and qualitative (failure mode) measurements of AARS performance under simulated peel loads. The experimental setups reported in this study comprised the central components of a standard peel-test protocol for the AARS. Such a standard would facilitate more effective building design criteria, which in turn would help to minimize the wind-induced peel failures in AARS.

These peel tests simulate the wind's peeling effect on the roofing insulation and cover board assemblies by taking various peel angles, peel positions and specimen sizes as physical parameters. This study collected extensive peel resistance data by using specimens from four major industry sources. The resulting test data can be used as a practical criterion for AARS design purposes.

The following concluding remarks can be drawn as an outcome of this study:

First of all, the results of this study provide an important insight into the suitability of components used in AARS. Through analysis of peel resistance ratios of various components, it is concluded that:

- Asphalt core cover board performs better than fiber cover board under all peel test conditions;
- Paper facer insulation out-performs arcylic facer insulation, if AARS use asphalt core cover board configurations; and
- Insulation has no significant influence on the peel resistance, if AARS use fiber cover board.

Second, these peel test results have revealed the common failure modes that normally occur in AARS. Seven major failure modes were identified in the three failure components.

- At the insulation, three failure modes, namely facer delamination, facer tearing, and facer rapture failure, can occur;
- At the cover board, three failure modes, namely splitting, brittle and separation failure, can develop; and
- Adhesive failure can take place as a different failure mode from any of above.

Thirdly, the analysis of the frequency of various failure modes is identified to determine the weakest link in AARS.

- In general, the insulation layer represents the weakest link, if Asphalt core cover board is used as cover board. Otherwise, if fiber cover board is used in the cover board layer, the failure is likely to take place in the cover board.
- Within the insulation and cover board, the insulation foam position is the weakest link for insulation component; and the cover board brittle represents the most frequent failure mode for cover board component.

Fourthly, AARS performance under wind peel resistance was ranked based on the failure mode and material performance.

- The rank by the frequency of various failure modes is:
  Separation > Adhesive > Delamination > Brittle

- The rank by material performance (wind peel resistance from high to low) is: Asphalt core cover board > Paper facer insulaiton > Arcylic facer insulation > Fiber cover board

Finally, the following conclusions can be drawn from the investigation of the effects of peel angle, peel position and sample size on the peel resistance:

- Peel force at E-Position is higher than the force at C-Position
- The peel resistance decreases as the peel angle increases; and
- The peel resistance increases as the sample size increases.

Hence, based on above conclusions, this study proposes the following guidelines for the development of a standard peel-test protocol;

- The proposal for testing position: E-P;
- The proposal for testing angle: 15°;
- The proposal for specimen size: 6 x 6 in. or 152 x 152mm

7.2 Recommendations for Future Research

Proof-of-principle applications of the peel tests developed in this study have generated relatively consistent results from a variety of small-scale samples. However, several issues associated with this protocol await future improvement before this protocol can be used in field applications.

First, the experiments carried out in the present study mainly concern the wind peeling action, which is assumed to be static. The natural wind, however, generates dynamic loading on the roofing systems. A previous study indicates that static uplift test tends to overestimate the wind uplift resistance of AARS due to the fact that it does not simulate real wind loading behavior (Baskaran et al,, 2007). Further

research should explore the effects of dynamic loading on the peel resistance of AARS and develop a relationship between the static and dynamic peel resistance.

Second, the conclusions in this study are based on peel testing results from samples provided by four industrial sources. The configurations of sample components only involve two types of insulation and two types of cover board. The generalized curve describing the relationship of peel resistance and peel angle is based on samples configured as Arcylic Facer Insulation/Asphalt Core Cover Board and Paper Facer Insulation /Asphalt Core Cover Board, and the generalized peel resistance versus sample size curve is based on samples configured as Paper Facer Insulation/Asphalt Core Cover Board only. Hence, in the further research, samples from different sources should be considered so as the types of insulation and cover board components. In particular, the effects of peel angle and sample size on AARS samples configured with FB cover board should be examined to improve the accuracy of the two aforementioned generalized curves.

Thirdly, it needs to be ascertained that results from the small-scale samples are amenable to the full-size situation in the field applications. The full-coating adhesion protocol is used in the present study, whereas full-scale AARS are normally adhered with ribbon format bonding. Future study should examine the peel resistance of full scale assemblies and develop a correlation between results from full size and small scale test results.

Finally, some of the failure modes were observed less than 5 times in the present study. It is unclear how accurately these events represent the real occurrence of these failure modes. Future studies should address this issue by examining more specimens.

Appendix

Legend

Abbreviations			Detail
Sample Compoment / Configuration	Insulation	**PF**	Paper Facer Insulation
		AF	Acrylic Facer Insulation
	Cover Board (CB)	**ACB**	Asphalt Core Cover Board
		FB	Fiber Cover Board
Failure Component / Failure Modes	Insulation	**Facer/T**	Insulation Facer Tearing
		Facer/D	Insulation Facer Delamination
		Facer/T	Insulation Facer Rupture
	Cover Board (CB)	**CB/Se**	Cover Board Separation
		CB/Sp	Cover Board Splitting
		CB/B	Cover Board Brittle
	Adhesive	**Adh**	Adhesive Failure
Peel Position	Edge	**E**	Edge Position
	Corner	**C**	Corner Position

Appendix 1

Peel Resistance Data from Source I

(Phase I)

Table 1. Peel Resistance (lbf) for 15 Degree Peel test at the Edge Position

Test ID	I-1		I-3		I-2		I-4	
Specimen ID	PF/ACB	Failure Mode	AF/ACB	Failure Mode	PF/FB	Failure Mode	AF/FB	Failure Mode
#1	243	Facer/D	257	Facer/D	116	CB/B	86	CB/Sp
#2	216	Facer/D	267	Facer/D	105	CB/B	125	CB/B
#3	259	Facer/D	302	Facer/D	125	CB/B	116	CB/B
#4	228	Facer/D	139	Facer/D	107	CB/B	130	CB/B
#5	215	Facer/D	168	Facer/D	130	CB/B	147	CB/B
Mean Load	232		226		117		121	
Standard Deviation	19		70		11		23	

Table 2. Peel Resistance (lbf) for 15 Degree Peel test at the Corner Position

Test ID	I-5		I-6	
Specimen ID	PF/ACB	Failure Mode	AF/ACB	Failure Mode
#1	137	Facer/D	163	Facer/D
#2	124	CB/B	89	CB/B
#3	156	CB/B	140	Facer/D
#4	194	Facer/D	137	Facer/D
#5	197	Facer/D	108	Facer/D
Mean Load	162		127	
Standard Deviation	33		29	

Sample #1: PF-ACB-15°-E (I-1)

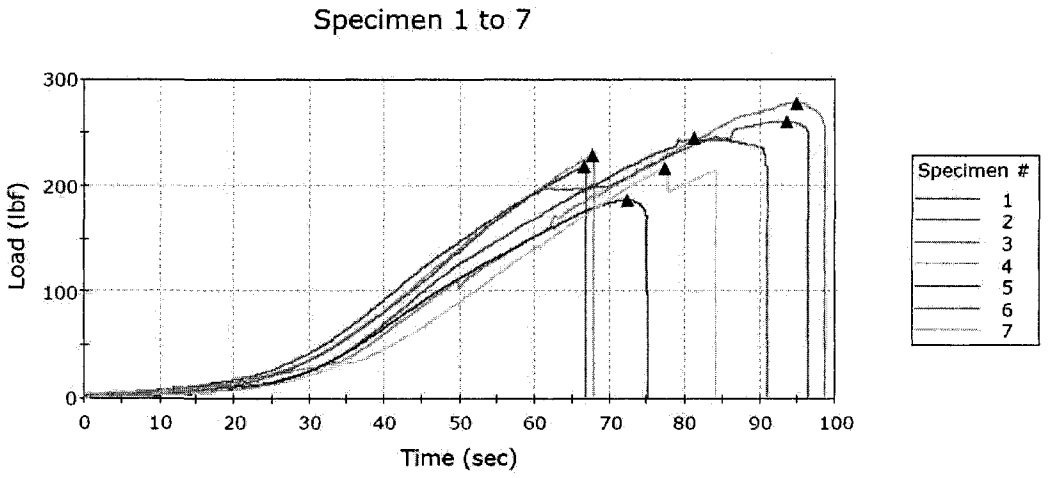

	Maximum Load (lbf)	Time at Maximum Load (sec)	Load at First Peak (lbf)	Time at First Peak (sec)	Average Load at Average Value (All Peaks) (lbf)
1	243	81	243	81	243
2	216	67	216	67	216
X 3	277	95	277	95	277
4	228	68	228	68	228
X 5	185	72	185	72	185
6	259	94	259	94	259
7	215	77	215	77	214
Maximum	259	94	259	94	259
Mean	232	77	232	77	232
Minimum	215	67	215	67	214

	Maximum Load (lbf)	Time at Maximum Load (sec)	Load at First Peak (lbf)	Time at First Peak (sec)	Average Load at Average Value (All Peaks) (lbf)
Standard Deviation	19	11	19	11	19
Mean + 1 SD	251	88	251	88	251
Mean - 1 SD	213	66	213	66	213

X: data excluded

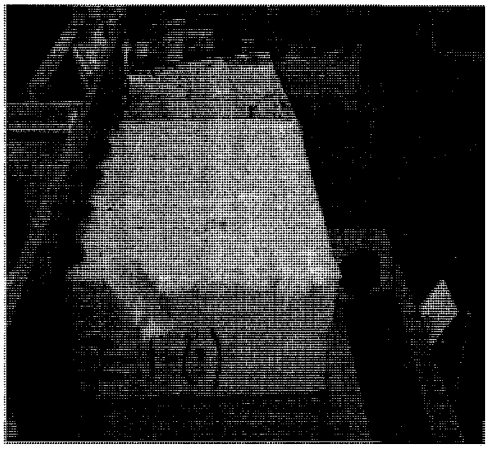

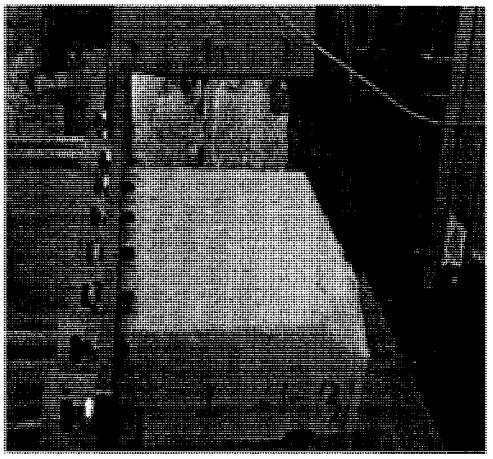

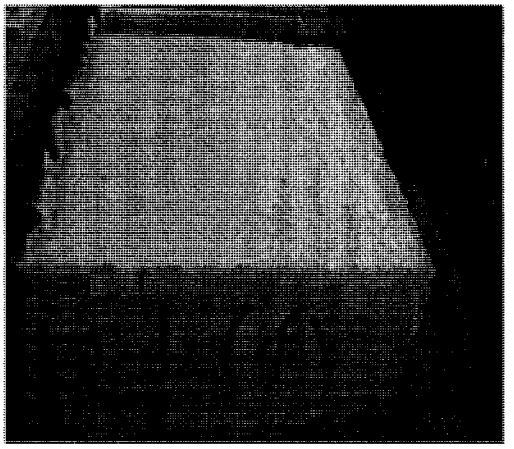

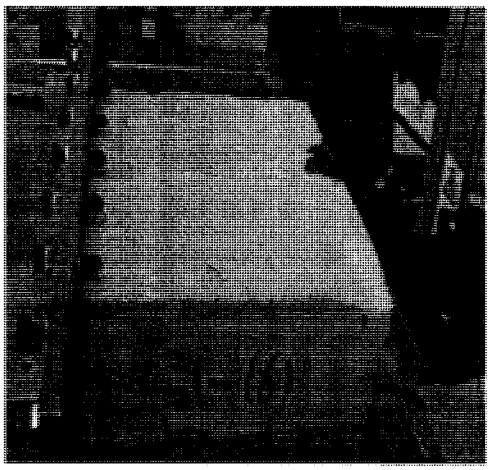

Sample #2: PF-FB-15°-E (I-2)

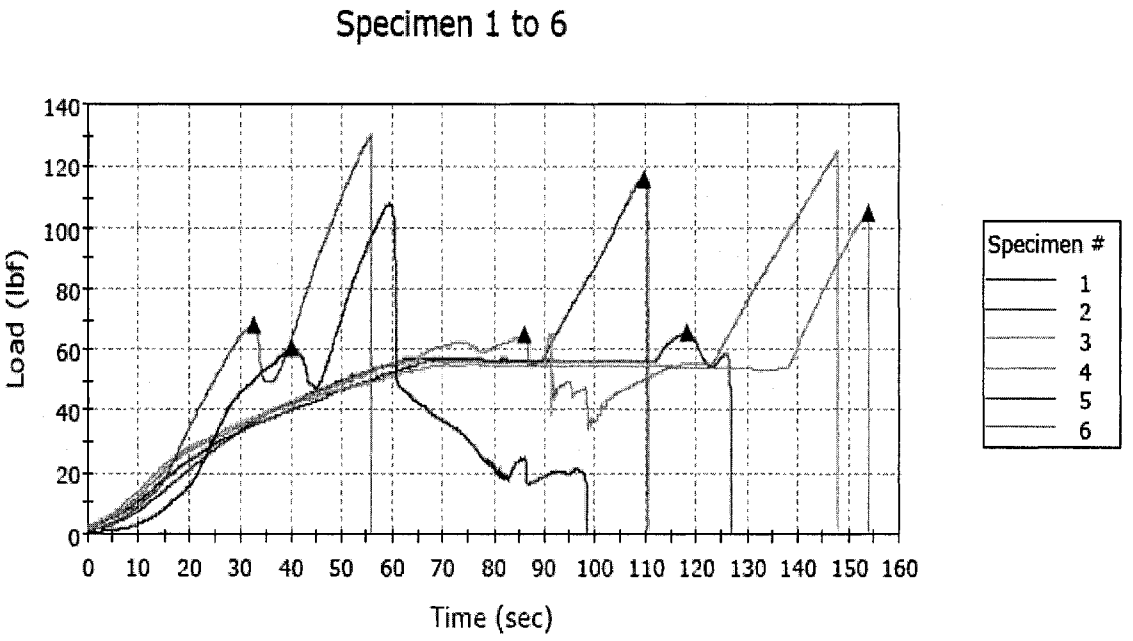

	Maximum Load (lbf)	Time at Maximum Load (sec)	Load at First Peak (lbf)	Time at First Peak (sec)	Average Load at Average Value (All Peaks) (lbf)
1	116	110	116	110	116
X 2	66	118	66	118	66
3	105	154	105	154	105
4	125	148	65	86	68
5	107	59	61	40	84
6	130	56	68	33	-----
Maximum	130	154	116	154	116
Mean	117	105	83	85	93
Minimum	105	56	61	33	68
Standard Deviation	11	47	25	50	21
Mean + 1 SD	128	152	108	135	114
Mean - 1 SD	106	59	57	34	72

X: data excluded

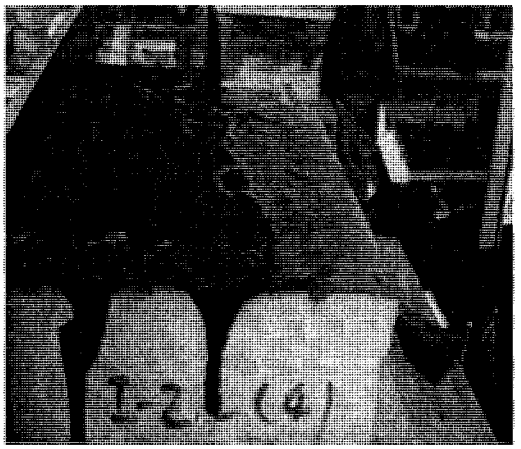

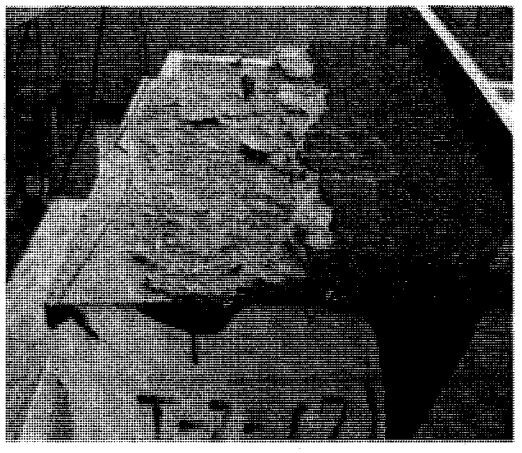

Sample #3: AF-ACB-15°-E (I-3)

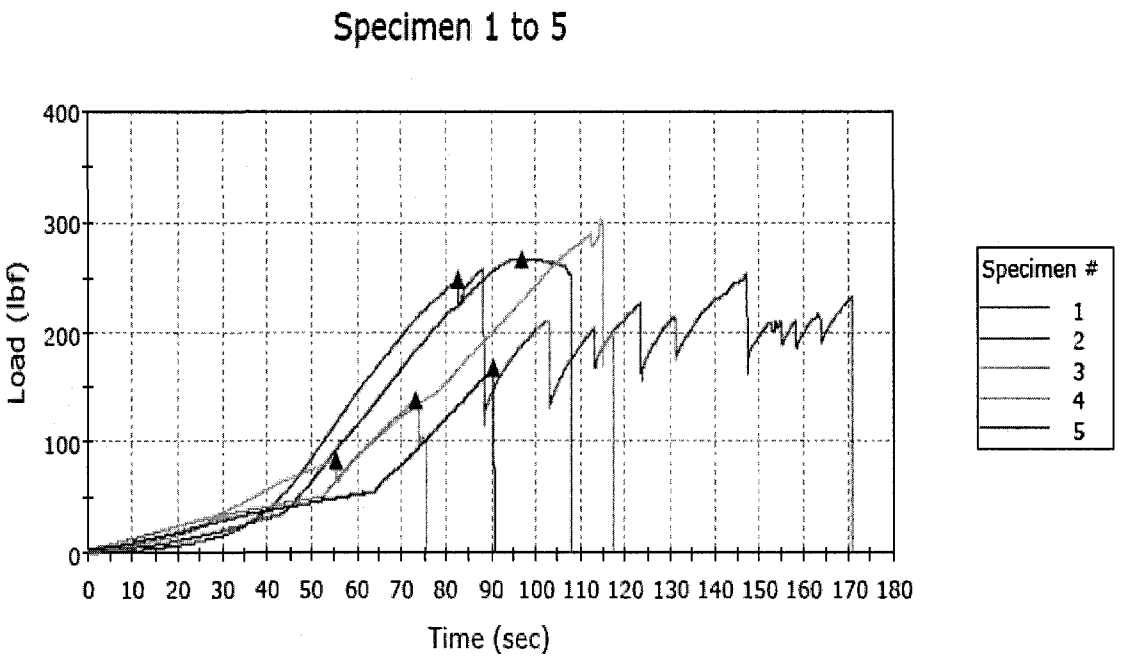

	Maximum Load (lbf)	Time at Maximum Load (sec)	Load at First Peak (lbf)	Time at First Peak (sec)	Average Load at Average Value (All Peaks) (lbf)
1	257	88	247	83	225
2	267	97	267	97	267
3	302	115	84	56	193
4	139	73	139	73	139
5	168	91	168	91	168
Maximum	302	115	267	97	267
Mean	226	93	181	80	198
Minimum	139	73	84	56	139
Standard Deviation	70	15	76	16	50
Mean + 1 SD	296	108	257	96	248
Mean - 1 SD	157	78	105	64	148

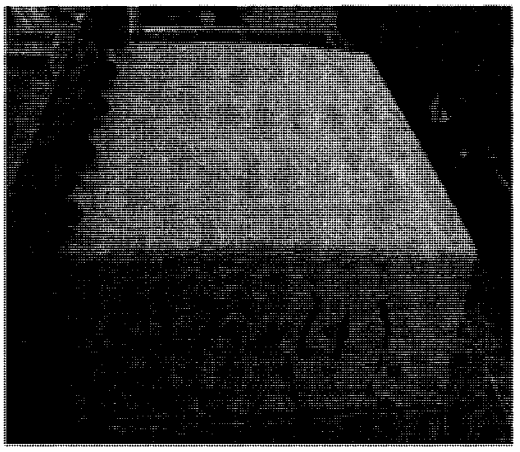

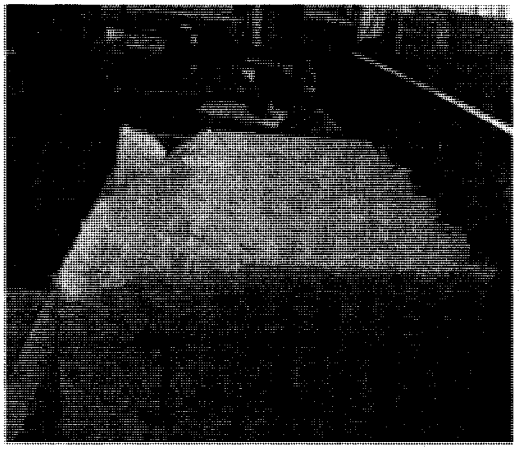

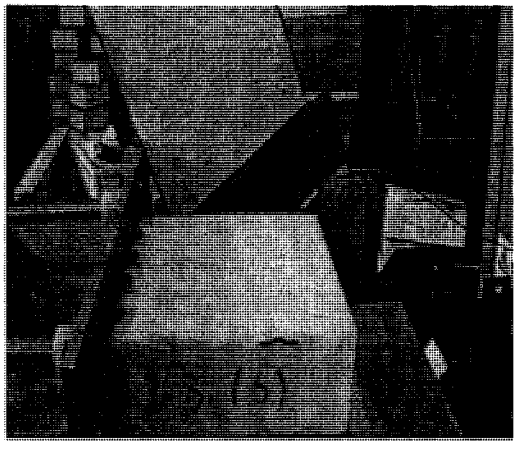

Sample #4: AF-FB-15°-E (I-4)

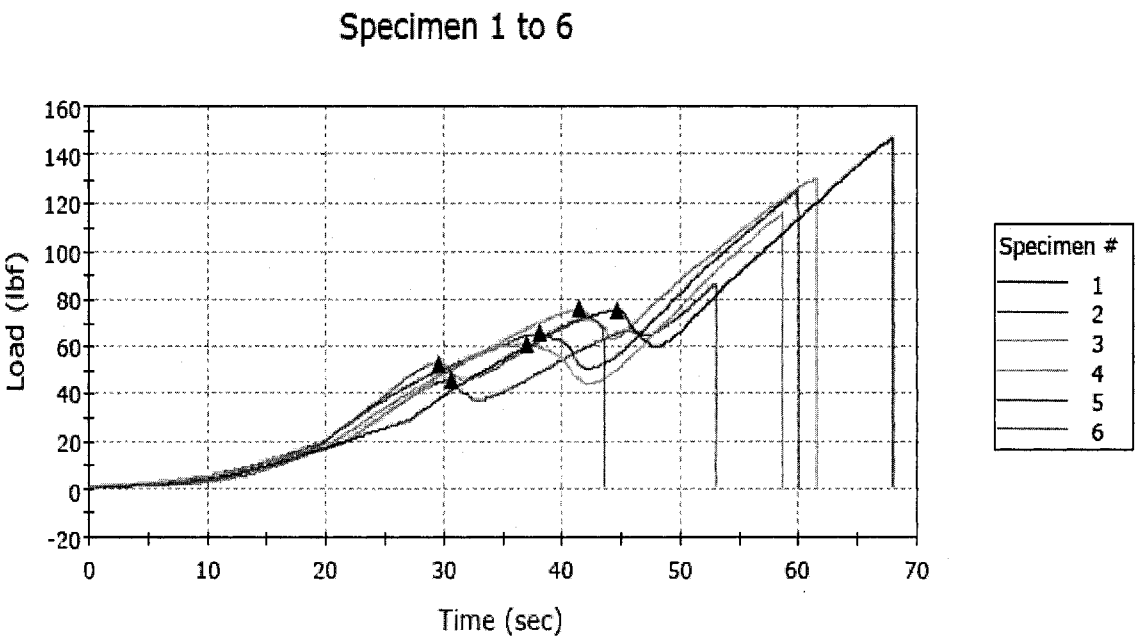

	Maximum Load (lbf)	Time at Maximum Load (sec)	Load at First Peak (lbf)	Time at First Peak (sec)	Average Load at Average Value (All Peaks) (lbf)
1	86	53	46	31	66
2	125	60	65	38	125
3	116	59	61	37	88
4	130	62	76	42	103
5	147	68	75	45	75
X 6	71	42	53	30	62
Maximum	147	68	76	45	125
Mean	121	60	65	38	92
Minimum	86	53	46	31	66

	Maximum Load (lbf)	Time at Maximum Load (sec)	Load at First Peak (lbf)	Time at First Peak (sec)	Average Load at Average Value (All Peaks) (lbf)
Standard Deviation	23	5	12	5	23
Mean + 1 SD	143	66	77	44	115
Mean - 1 SD	98	55	53	33	68

X: data excluded

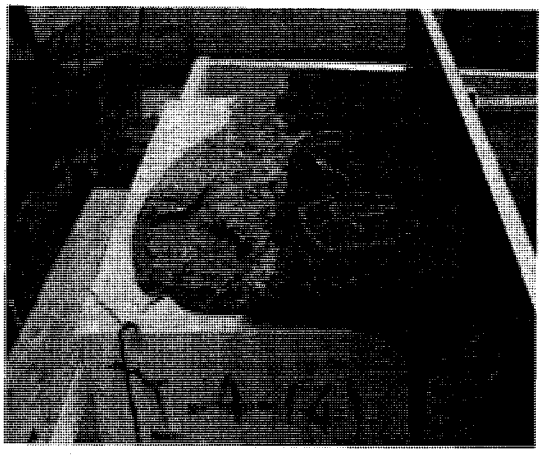

Sample #5: PF-ACB-15°-C (I-5)

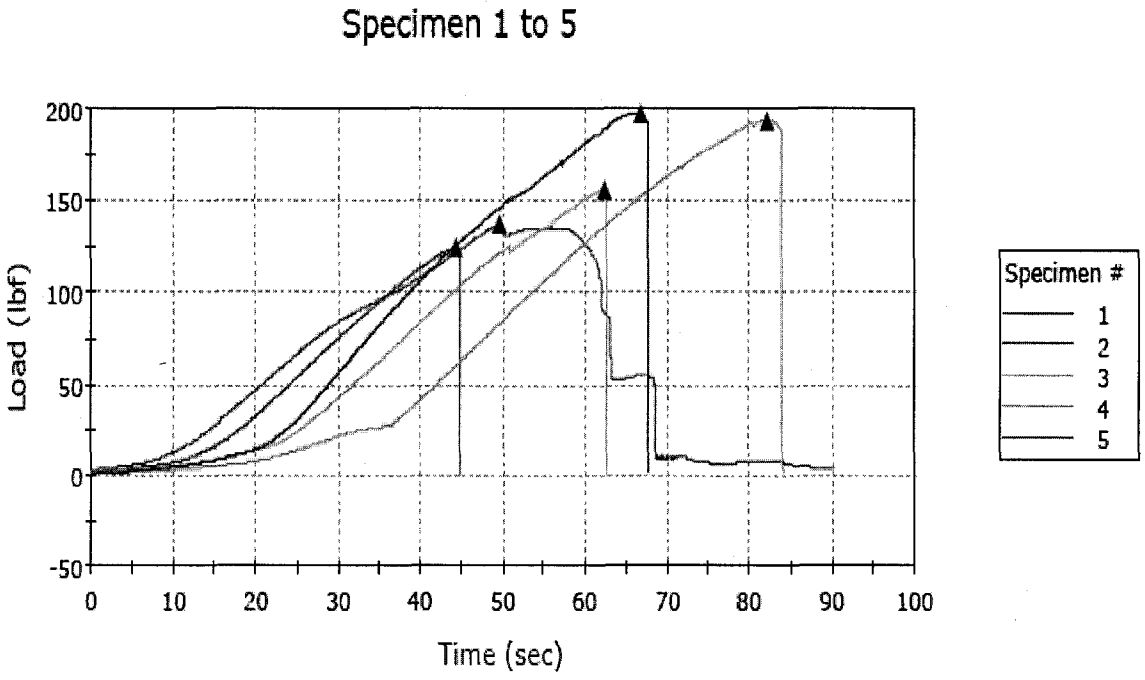

	Maximum Load (lbf)	Time at Maximum Load (sec)	Load at First Peak (lbf)	Time at First Peak (sec)	Average Load at Average Value (All Peaks) (lbf)
1	137	50	137	50	137
2	124	44	124	44	124
3	156	62	156	62	156
4	194	82	194	82	194
5	197	67	197	67	197
Maximum	197	82	197	82	197
Mean	162	61	162	61	162
Minimum	124	44	124	44	124
Standard Deviation	33	15	33	15	33
Mean + 1 SD	195	76	195	76	195
Mean - 1 SD	128	46	128	46	128

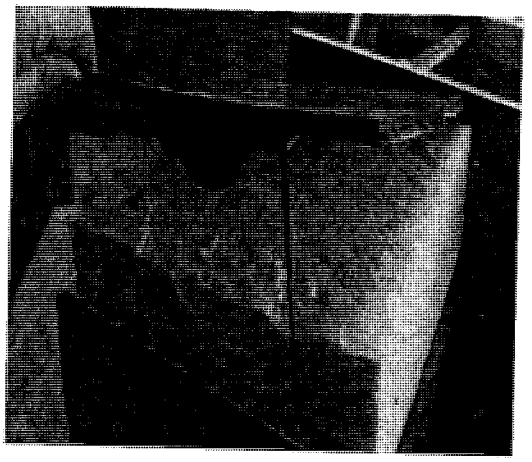

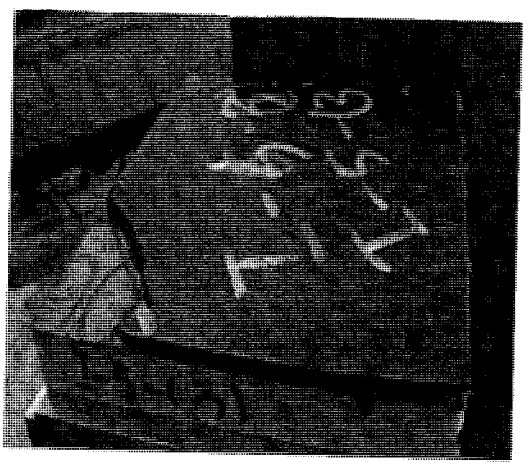

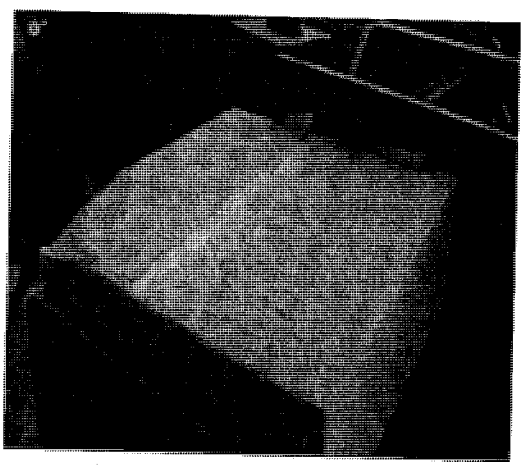

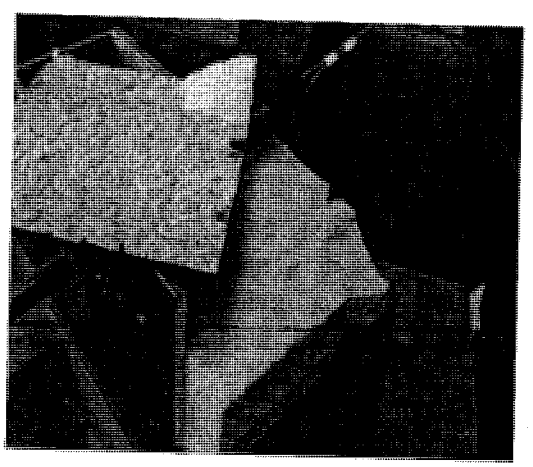

Sample #6: AF-ACB-15°-C (I-6)

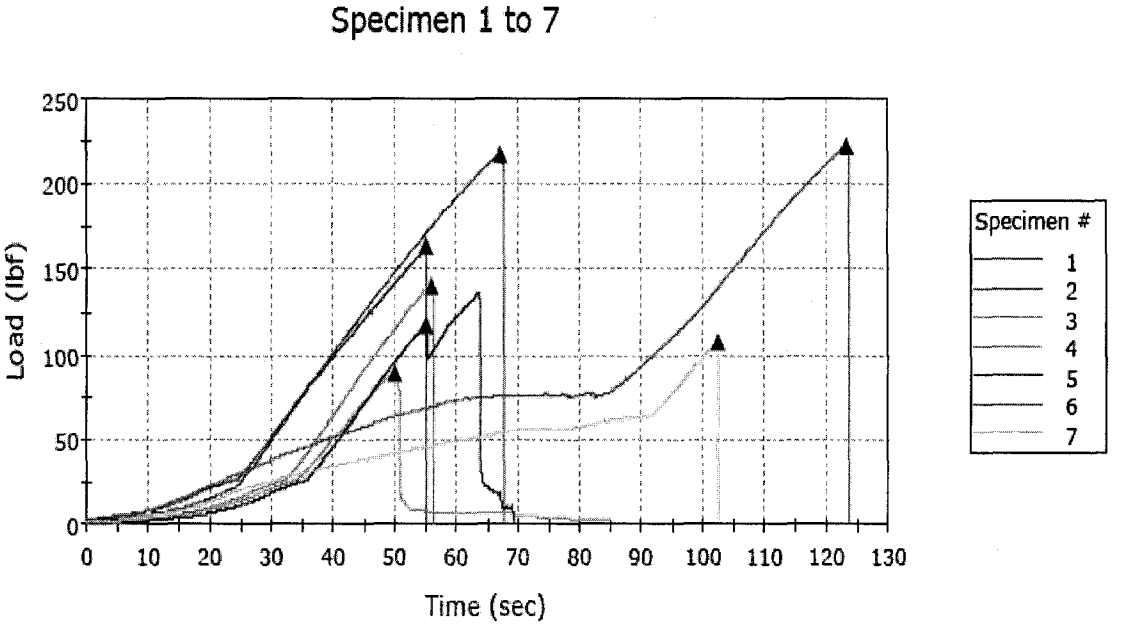

	Maximum Load (lbf)	Time at Maximum Load (sec)	Load at First Peak (lbf)	Time at First Peak (sec)	Average Load at Average Value (All Peaks) (lbf)
X 1	217	67	217	67	217
2	163	55	163	55	163
3	89	50	89	50	89
4	140	56	140	56	-----
5	137	64	118	55	127
X 6	223	123	223	123	223
7	108	102	108	102	108
Maximum	163	102	163	102	163
Mean	127	66	124	64	122
Minimum	89	50	89	50	89
Standard Deviation	29	21	29	22	32
Mean + 1 SD	156	87	152	86	154

	Maximum Load (lbf)	Time at Maximum Load (sec)	Load at First Peak (lbf)	Time at First Peak (sec)	Average Load at Average Value (All Peaks) (lbf)
Mean - 1 SD	98	44	95	42	90

X: data excluded

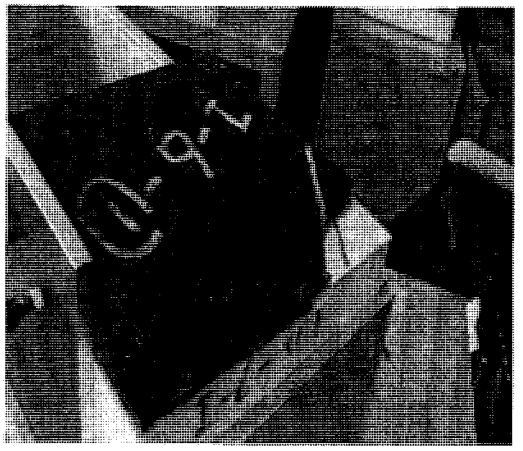

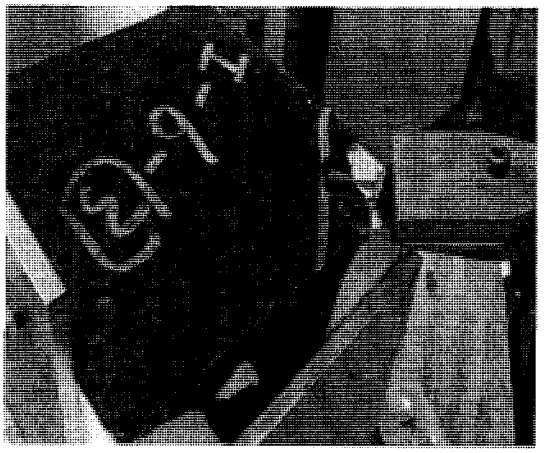

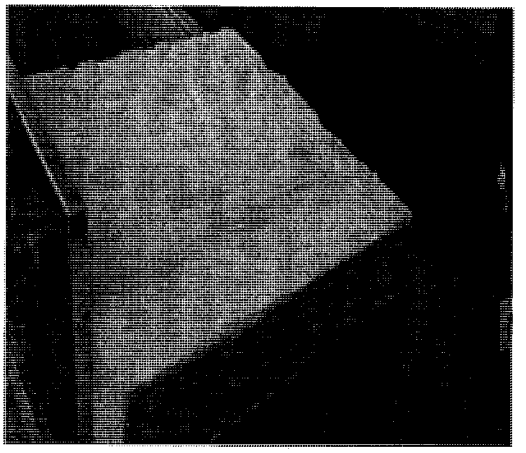

Appendix 2

Peel Resistance Data from Source II

(Phase I)

Table 1. Peel Resistance (lbf) for 15 Degree Peel test at the Edge Position

Test ID	II-1		II-3		II-2		II-4	
Specimen ID	PF/ACB	Failure Mode	AF/ACB	Failure Mode	PF/FB	Failure Mode	AF/FB	Failure Mode
#1	121	Facer/R & Adh	79	Facer/D	46	CB/Sp	51	CB/Sp
#2	99	Facer/R	122	Facer/D	43	CB/Sp	43	CB/Sp
#3	104	Facer/R	70	Facer/D	44	CB/Sp	45	CB/Sp
#4	100	Facer/T	72	Facer/D	43	CB/Sp	50	CB/Sp
#5	89	Facer/R	83	Facer/D	44	CB/Sp	42	CB/Sp
Ave. Load	102		85		44		46	
Standard Deviation	12		21		1		4	

Table 2. Peel Resistance (lbf) for 15 Degree Peel test at the Corner Position

Test ID	II-5		II-6	
Specimen ID	PF/ACB	Failure Mode	AF/ACB	Failure Mode
#1	140	Facer/R & Adh	165	Facer/D & Adh
#2	160	Facer/R & Adh	150	Facer/D & Adh
#3	125	Facer/R & Adh	134	Facer/D & Adh
#4	140	Facer/R & Adh	128	Facer/D & Adh
#5	169	Facer/R & Adh	159	Facer/D & Adh
Ave. Load	147		147	
Standard Deviation	17		16	

Sample #1: PF-ACB-15°-E (II-1)

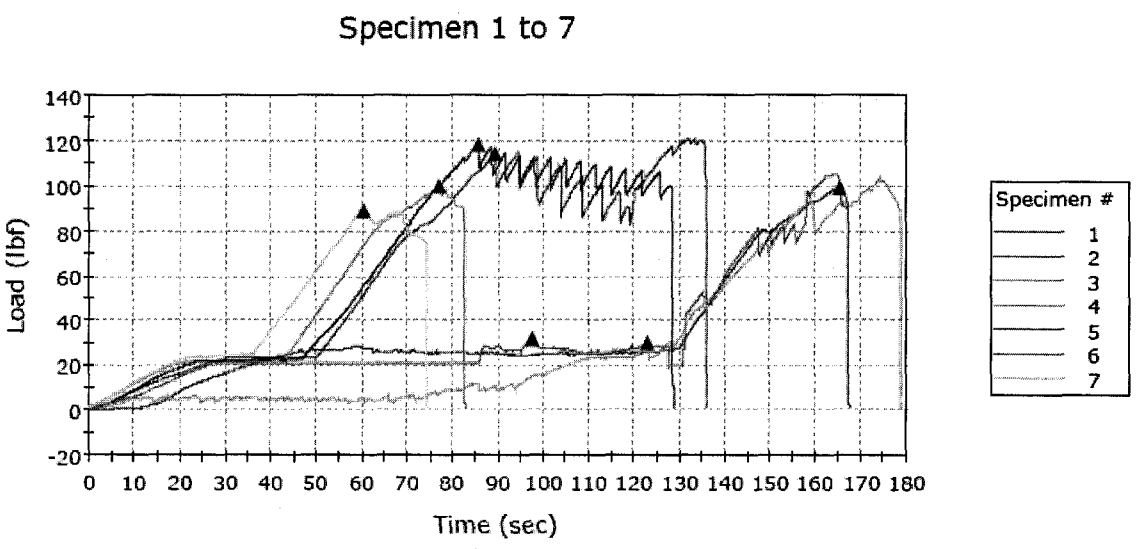

	Maximum Load (lbf)	Time at Maximum Load (sec)	Load at First Peak (lbf)	Time at First Peak (sec)	Average Load at Average Value (All Peaks) (lbf)
1	121	132	114	90	107

	Maximum Load (lbf)	Time at Maximum Load (sec)	Load at First Peak (lbf)	Time at First Peak (sec)	Average Load at Average Value (All Peaks) (lbf)
2	99	165	99	165	99
3	104	174	30	123	76
4	100	77	100	77	100
X 5	118	86	118	86	111
X 6	105	165	32	98	74
7	89	61	89	61	88
Maximum	121	174	114	165	107
Minimum	89	61	30	61	76
Mean	102	122	86	103	94
Standard Deviation	12	51	33	42	12
Mean + 1 SD	114	173	119	145	106
Mean - 1 SD	91	71	53	62	82

X: data excluded

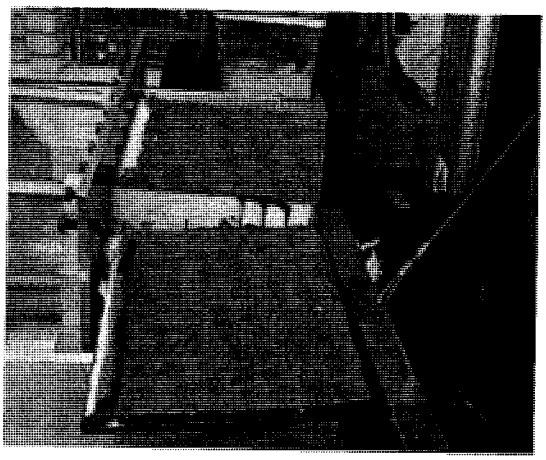

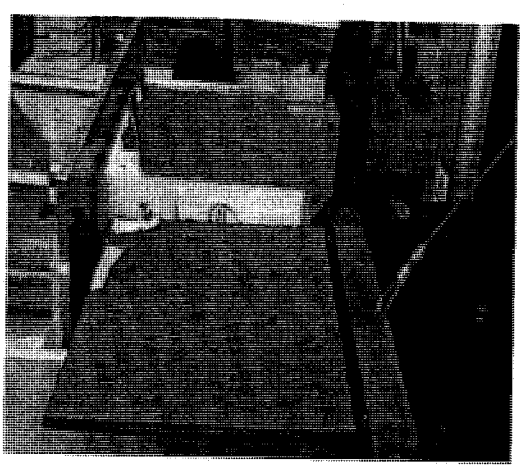

Sample #2: PF-FB-15°-E (II-2)

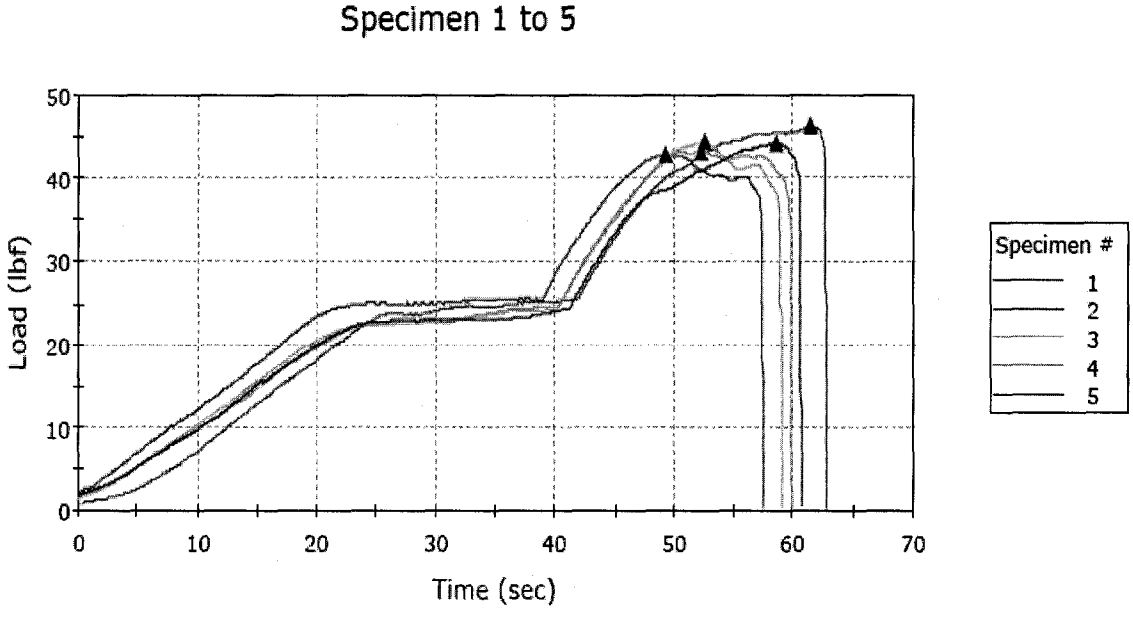

	Maximum Load (lbf)	Time at Maximum Load (sec)	Load at First Peak (lbf)	Time at First Peak (sec)	Average Load at Average Value (All Peaks) (lbf)
1	46	62	46	62	46
2	43	49	43	49	43
3	44	53	44	53	44
4	43	52	43	52	43
5	44	59	44	59	44
Maximum	46	62	46	62	46
Minimum	43	49	43	49	43
Mean	44	55	44	55	44
Standard Deviation	1	5	1	5	1
Mean + 1 SD	46	60	46	60	46
Mean - 1 SD	43	50	43	50	43

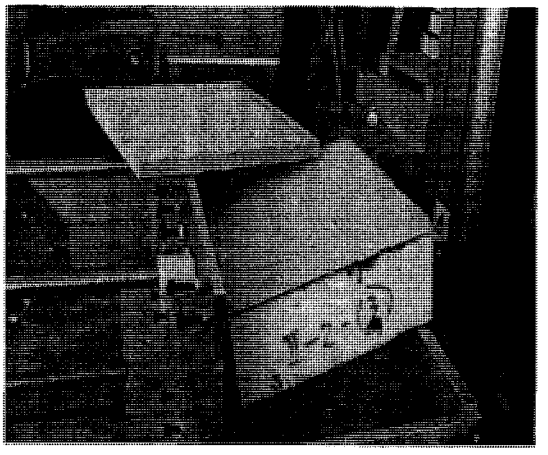

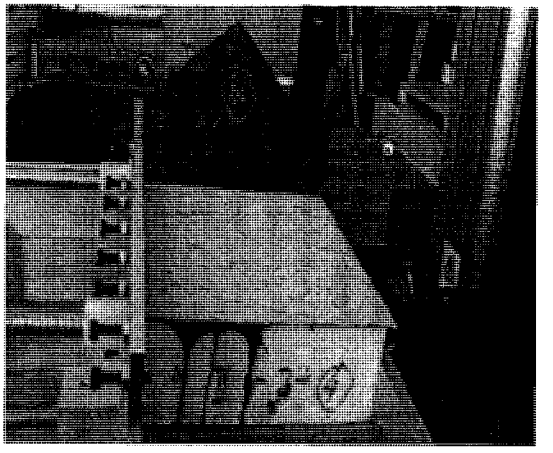

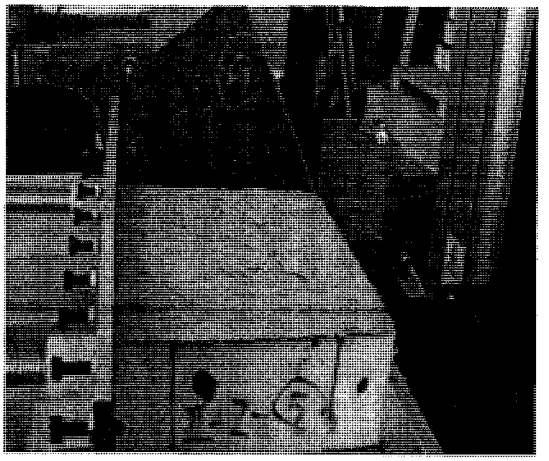

Sample #3: AF-ACB-15°-E (II-3)

Specimen 1 to 6

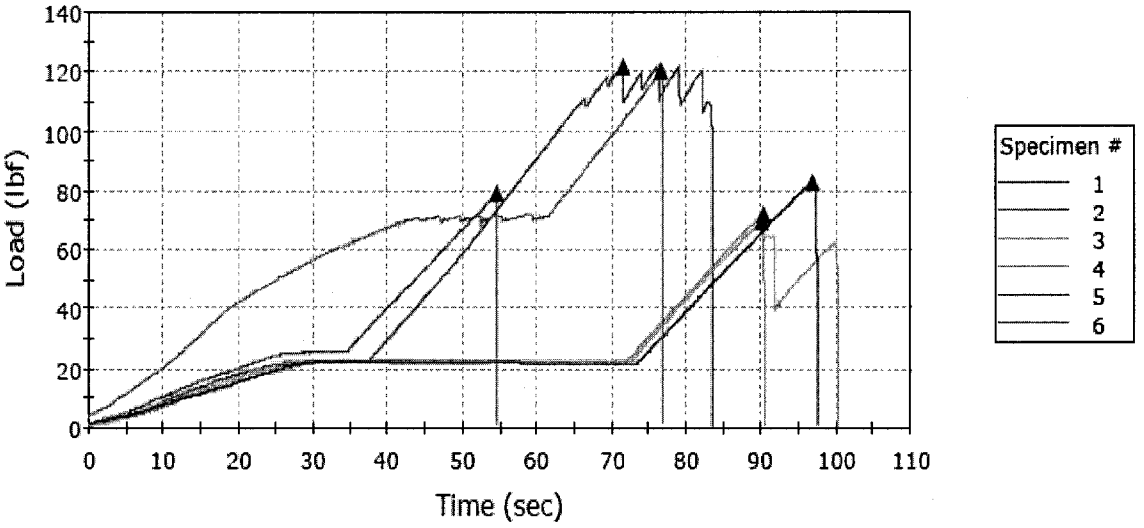

	Maximum Load (lbf)	Time at Maximum Load (sec)	Load at First Peak (lbf)	Time at First Peak (sec)	Average Load at Average Value (All Peaks) (lbf)
1	79	55	79	55	79
2	122	71	122	71	121
3	70	90	70	90	70
4	72	90	72	90	72
5	83	97	83	97	83
X 6	120	77	120	77	120
Maximum	122	97	122	97	121
Minimum	70	55	70	55	70
Mean	85	81	85	81	85
Standard Deviation	21	17	21	17	21
Mean + 1 SD	106	98	106	98	106

	Maximum Load (lbf)	Time at Maximum Load (sec)	Load at First Peak (lbf)	Time at First Peak (sec)	Average Load at Average Value (All Peaks) (lbf)
Mean - 1 SD	64	63	64	63	64

X: data excluded

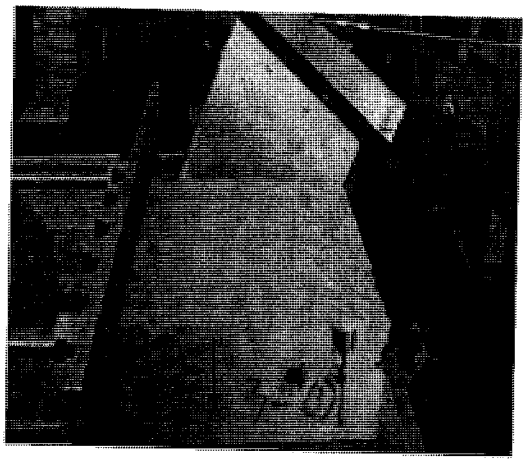

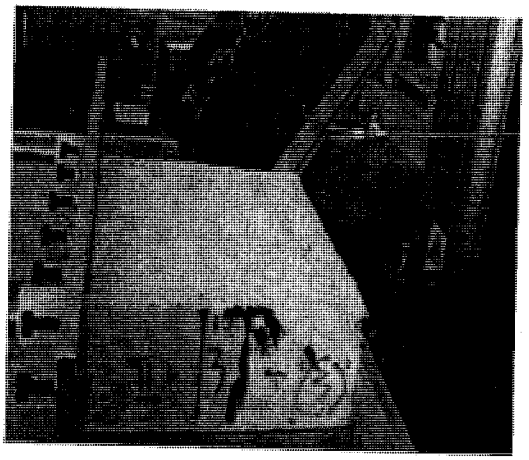

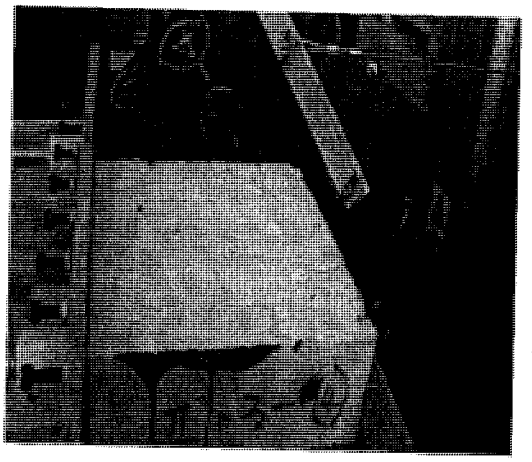

Sample #4: AF-FB-15°-E (II-4)

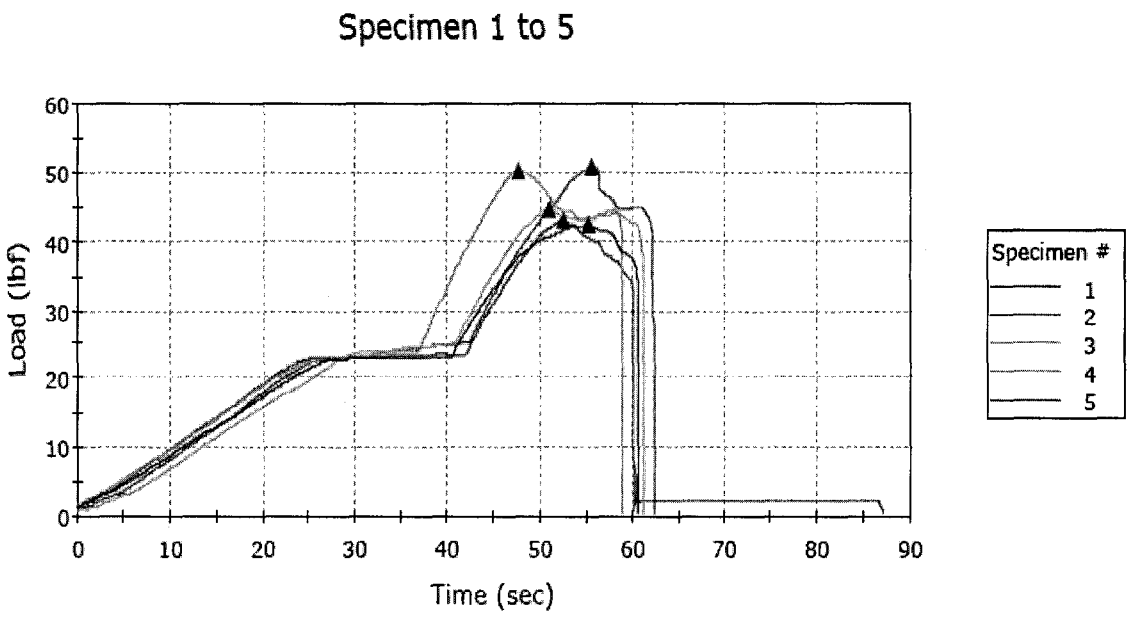

	Maximum Load (lbf)	Time at Maximum Load (sec)	Load at First Peak (lbf)	Time at First Peak (sec)	Average Load at Average Value (All Peaks) (lbf)
1	51	56	51	56	51
2	43	53	43	53	43
3	45	51	45	51	45
4	50	48	50	48	50
5	42	55	42	55	42
Maximum	51	56	51	56	51
Minimum	42	48	42	48	42
Mean	46	52	46	52	46
Standard Deviation	4	3	4	3	4
Mean + 1 SD	50	56	50	56	50
Mean - 1 SD	42	49	42	49	42

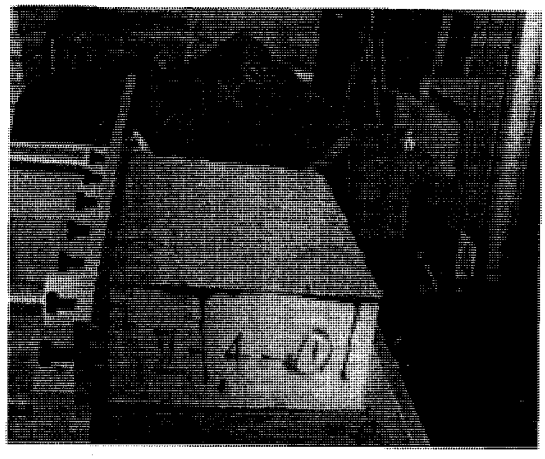

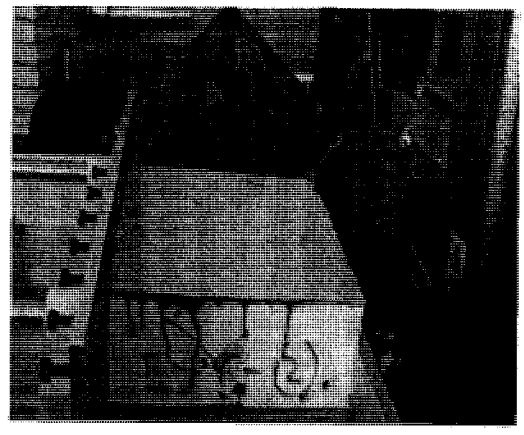

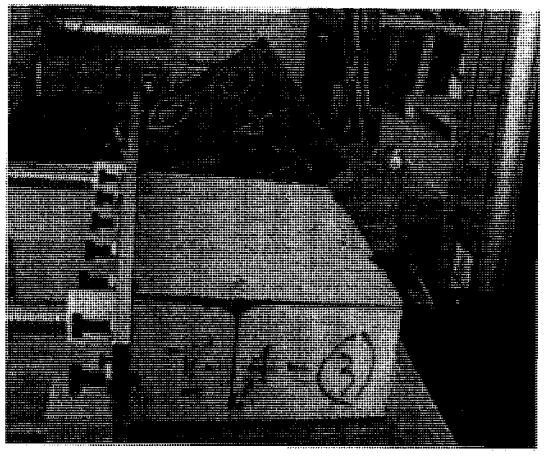

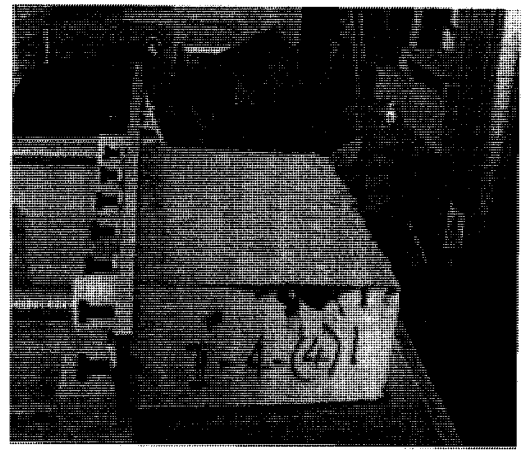

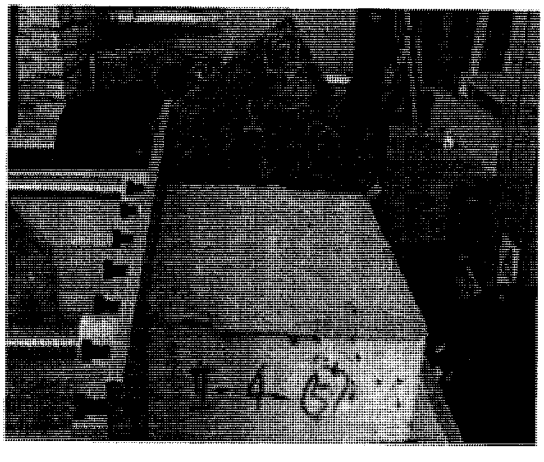

Sample #5: PF-ACB-15°-C (II-5)

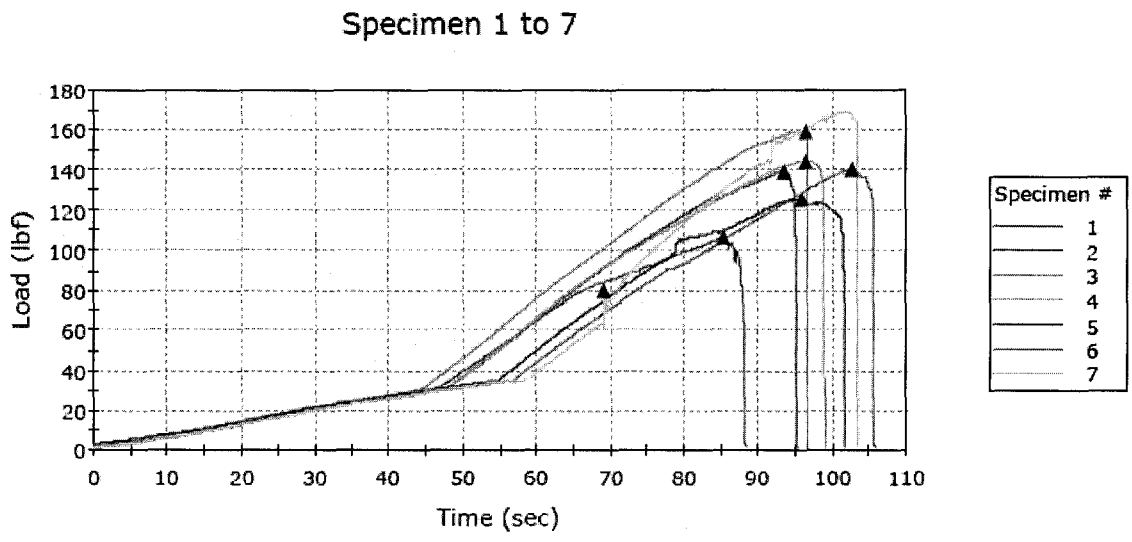

	Maximum Load (lbf)	Time at Maximum Load (sec)	Load at First Peak (lbf)	Time at First Peak (sec)	Average Load at Average Value (All Peaks) (lbf)
X 1	106	85	106	85	106
2	140	94	140	94	140
X 3	144	96	144	96	144
4	160	96	160	96	160
5	125	96	125	96	125
6	140	103	140	103	140
7	169	102	80	69	125
Maximum	169	103	160	103	160
Mean	147	98	129	92	138
Minimum	125	94	80	69	125
Standard Deviation	17	4	30	13	14
Mean + 1 SD	164	102	159	105	152
Mean - 1 SD	129	94	99	79	124

X: data excluded

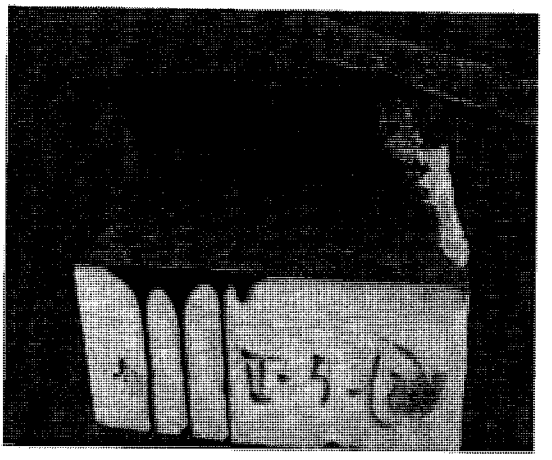

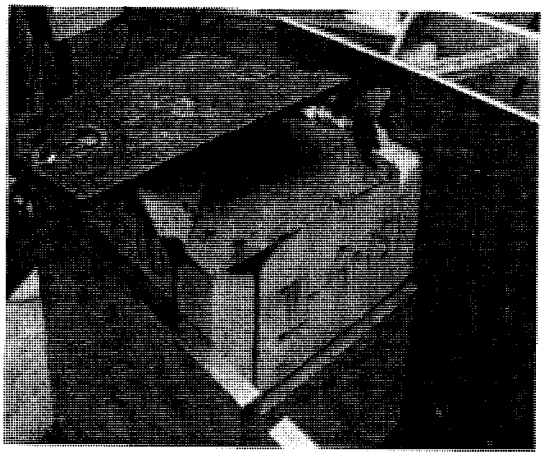

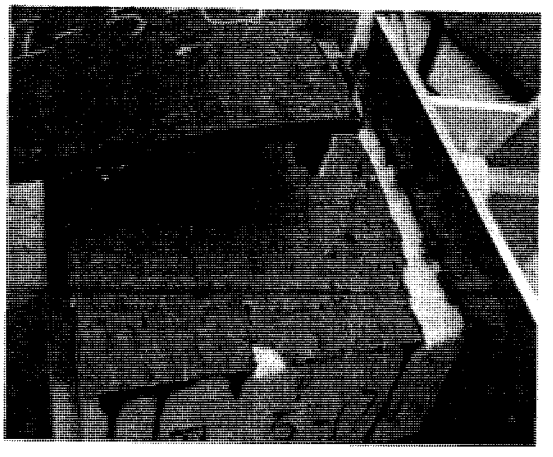

Sample #6: AF-ACB-15°-C (II-6)

Specimen 1 to 5

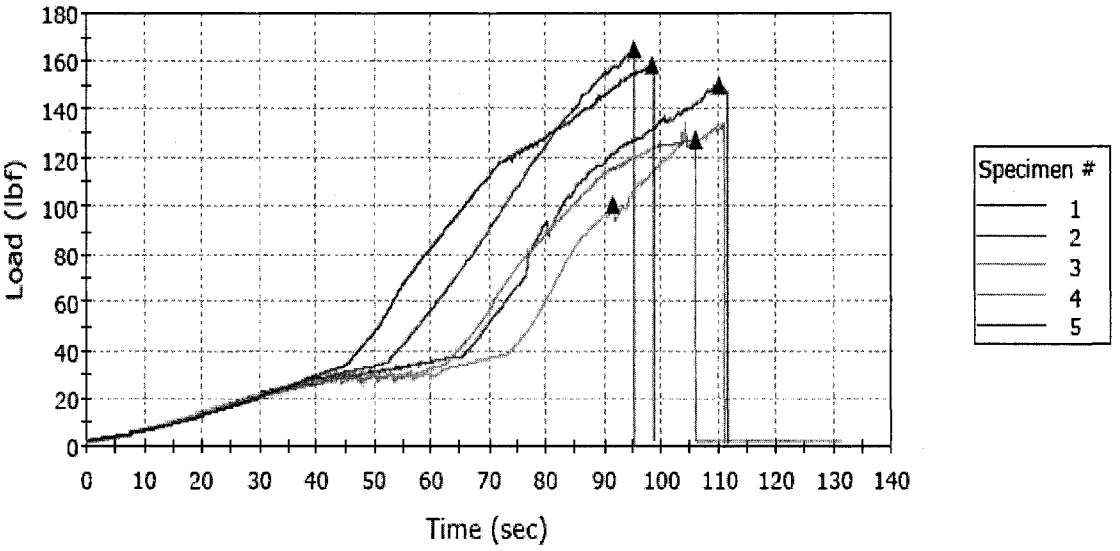

	Maximum Load (lbf)	Time at Maximum Load (sec)	Load at First Peak (lbf)	Time at First Peak (sec)	Average Load at Average Value (All Peaks) (lbf)
1	165	95	165	95	-----
2	150	110	150	110	150
3	134	104	100	92	123
4	128	106	128	106	128
5	159	98	159	98	159
Maximum	165	110	165	110	159
Mean	147	103	140	100	140
Minimum	128	95	100	92	123
Standard Deviation	16	6	26	8	17
Mean + 1 SD	163	109	167	108	157
Mean - 1 SD	131	97	114	93	123

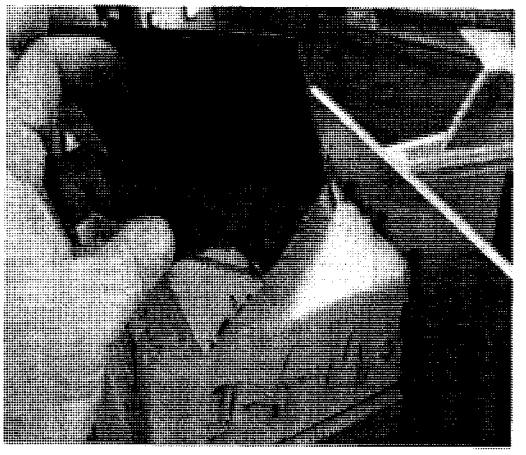

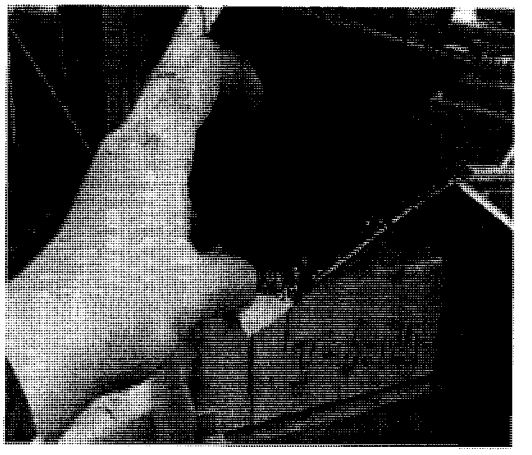

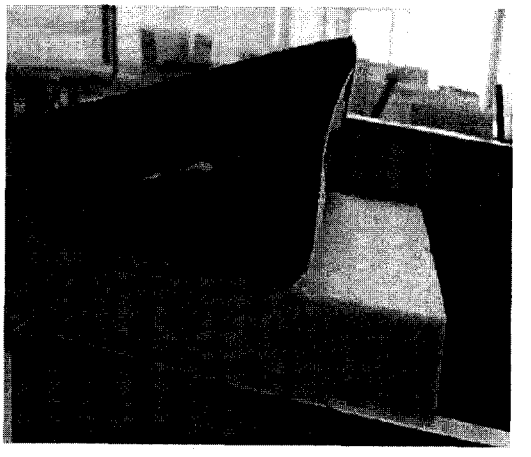

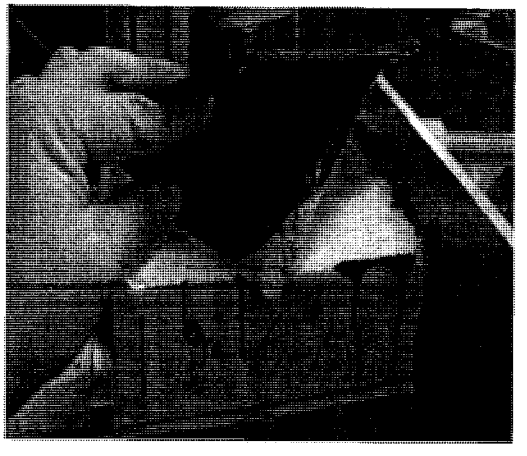

Appendix 3

Peel Resistance Data from Source III

(Phase I)

Table 1. Peel Resistance (lbf) for 15 Degree Peel test at the Edge Position

Test ID	III-1		III-3		III-2		III-4	
Specimen ID	PF/ACB	Failure Mode	AF/ACB	Failure Mode	PF/FB	Failure Mode	AF/FB	Failure Mode
#1	196	CB/Se	217	Facer/D & Adh	78	CB/B	95	CB/B
#2	185	CB/Se	150	Facer/D & Adh	80	CB/B	69	CB/B
#3	209	CB/Se	187	Facer/D & Adh	88	CB/B	101	CB/B
#4	227	CB/Se	229	Facer/D & Adh	89	CB/B	98	CB/B
#5	190	CB/Se	211	Facer/D	64	CB/Sp	91	CB/B
Ave. Load	202		199		80		91	
Standard Deviation	17		31		10		13	

Table 2. Peel Resistance (lbf) for 15 Degree Peel test at the Corner Position

Test ID	III-5		III-6	
Specimen ID	PF/ACB	Failure Mode	AF/ACB	Failure Mode
#1	148	CB/B	117	Facer/D
#2	149	CB/B	100	CB/B
#3	133	CB/B	162	CB/B
#4	146	CB/B	108	CB/B
#5	133	CB/B	116	CB/B
Ave. Load	142		120	
Standard Deviation	8		24	

Sample #1: PF-ACB-15°-E (III-1)

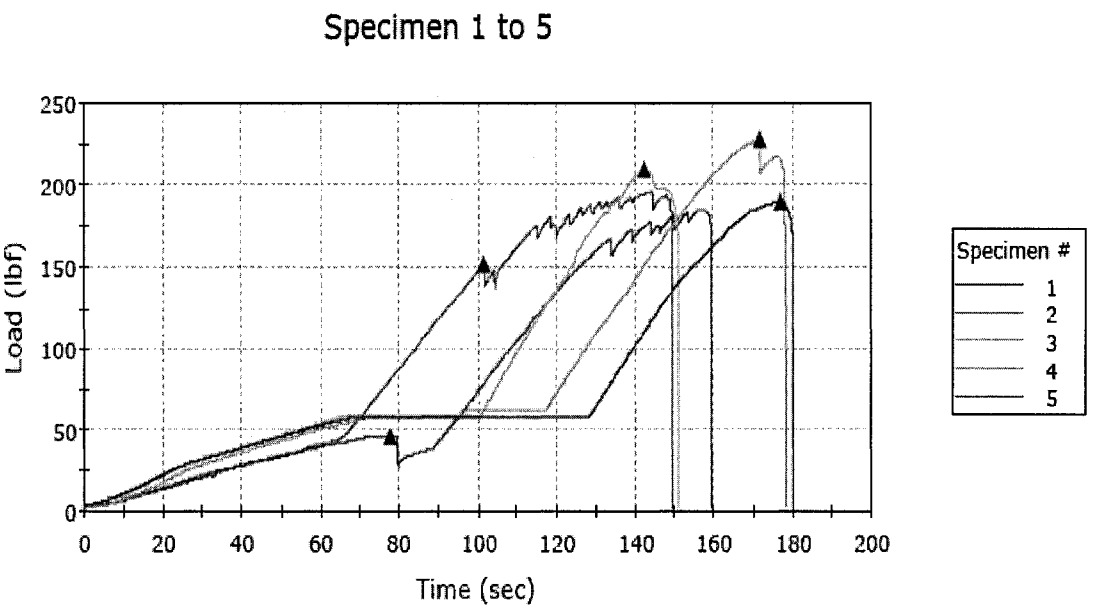

	Maximum Load (lbf)	Time at Maximum Load (sec)	Load at First Peak (lbf)	Time at First Peak (sec)	Average Load at Average Value (All Peaks) (lbf)
1	196	144	152	102	176
2	185	157	46	78	178
3	209	142	209	142	209
4	227	172	227	172	227
5	190	177	190	177	190
Maximum	227	177	227	177	227
Mean	202	158	165	134	196
Minimum	185	142	46	78	176
Standard Deviation	17	16	72	43	22
Mean + 1 SD	219	174	237	178	218
Mean - 1 SD	184	143	93	91	175

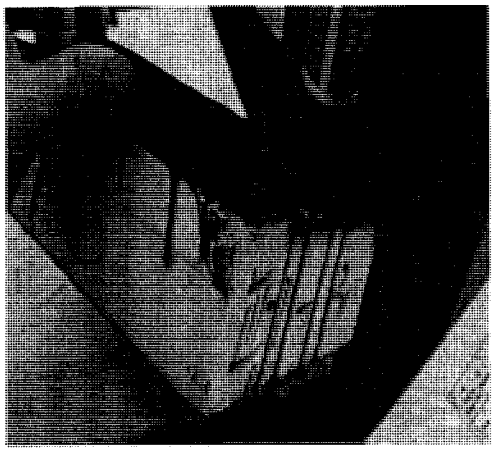

Sample #2: PF-FB-15°-E (III-2)

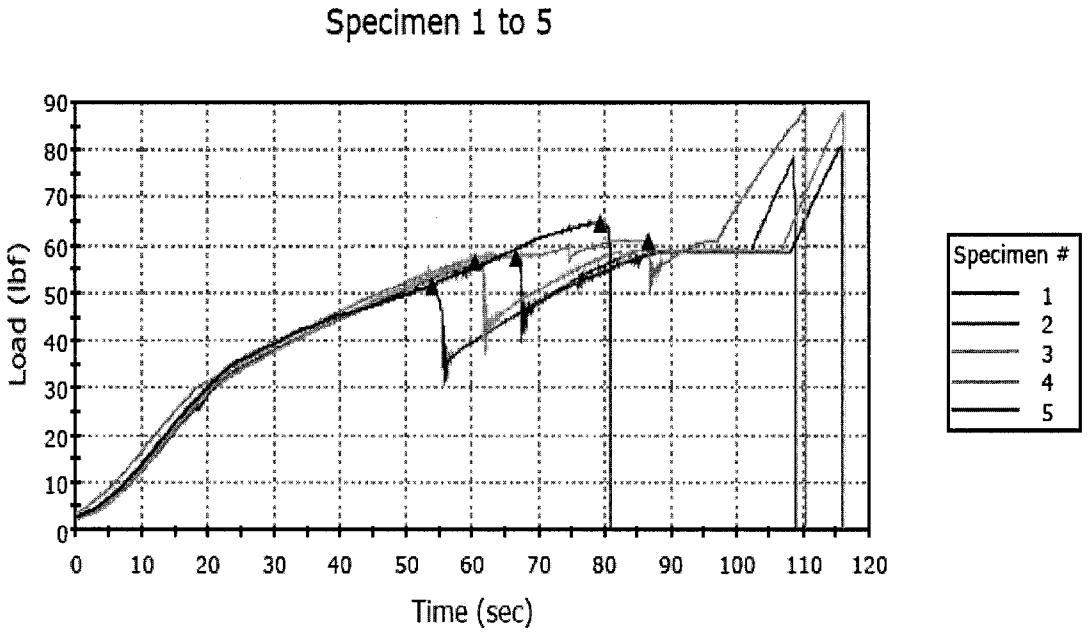

	Maximum Load (lbf)	Time at Maximum Load (sec)	Load at First Peak (lbf)	Time at First Peak (sec)	Average Load at Average Value (All Peaks) (lbf)
1	78	109	58	67	59
2	80	116	51	54	50
3	88	116	57	61	59
4	89	111	61	87	59
5	64	79	64	79	64
Maximum	89	116	64	87	64
Mean	80	106	58	69	58
Minimum	64	79	51	54	50
Standard Deviation	10	15	5	13	5
Mean + 1 SD	90	122	63	83	63
Mean - 1 SD	70	91	53	56	53

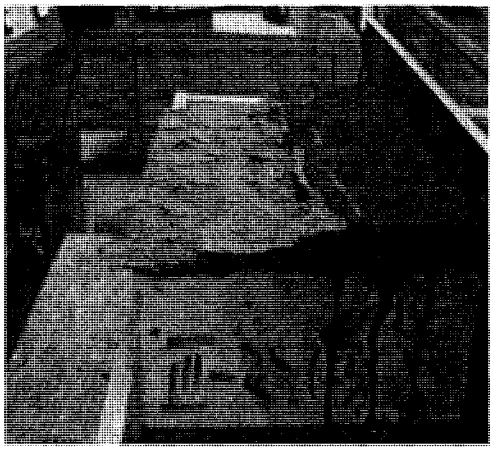

Sample #3: AF-ACB-15°-E (III-3)

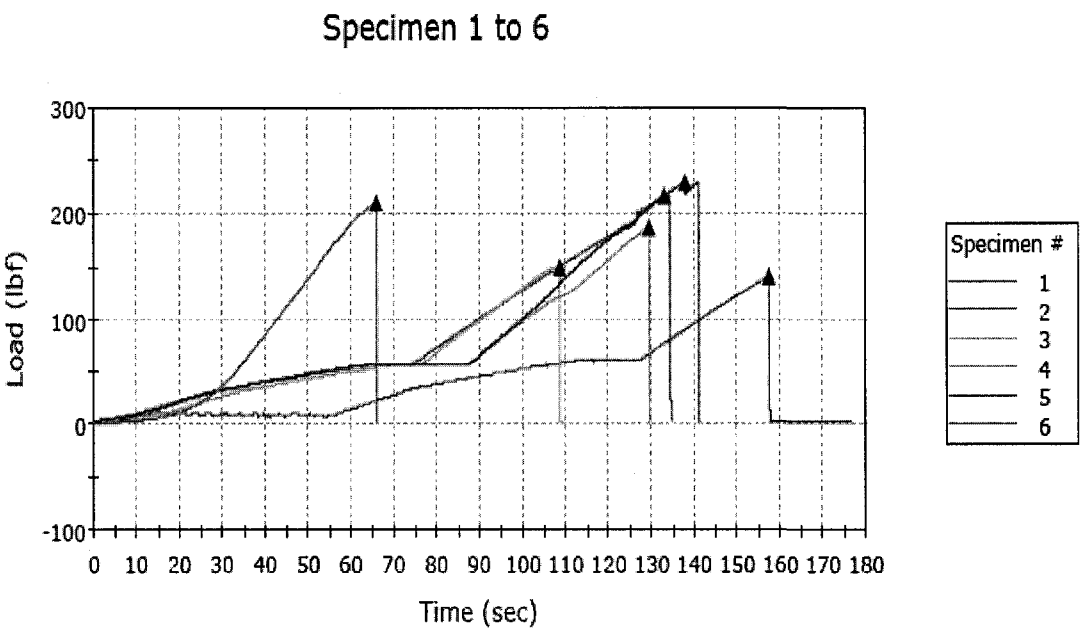

	Maximum Load (lbf)	Time at Maximum Load (sec)	Load at First Peak (lbf)	Time at First Peak (sec)	Average Load at Average Value (All Peaks) (lbf)
X 1	141	158	141	158	141
2	217	133	217	133	217
3	150	109	150	109	150
4	187	129	187	129	187
5	229	138	229	138	229
6	211	66	211	66	-----
Maximum	229	138	229	138	229
Mean	199	115	199	115	196
Minimum	150	66	150	66	150
Standard Deviation	31	30	31	30	35
Mean + 1 SD	230	145	230	145	231
Mean - 1 SD	167	85	167	85	160

X: data excluded

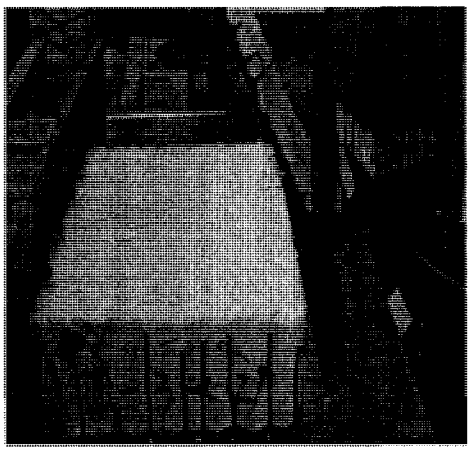

Sample #4: AF-FB-15°-E (III-4)

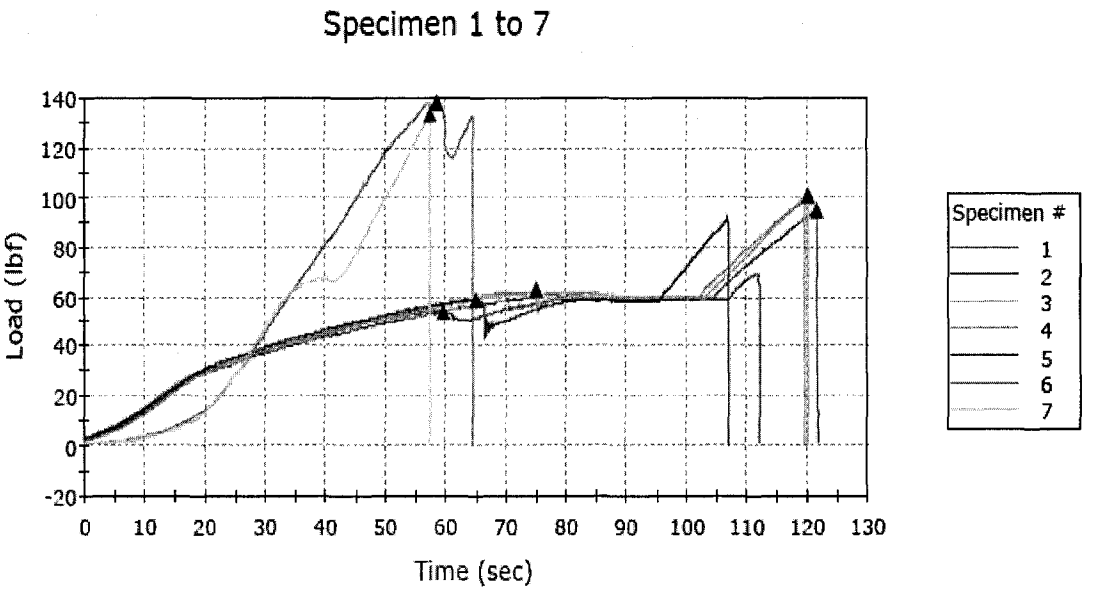

	Maximum Load (lbf)	Time at Maximum Load (sec)	Load at First Peak (lbf)	Time at First Peak (sec)	Average Load at Average Value (All Peaks) (lbf)
1	95	122	95	122	95
2	69	112	54	60	69
3	101	120	101	120	101
4	98	120	63	75	63
5	91	107	59	65	61
X 6	138	59	138	59	135
X 7	134	57	134	57	134
Maximum	101	122	101	122	101
Mean	91	116	74	88	77
Minimum	69	107	54	60	61
Standard Deviation	13	6	22	30	19
Mean + 1 SD	103	122	96	119	96

	Maximum Load (lbf)	Time at Maximum Load (sec)	Load at First Peak (lbf)	Time at First Peak (sec)	Average Load at Average Value (All Peaks) (lbf)
Standard Deviation	23	5	12	5	23
Mean + 1 SD	143	66	77	44	115
Mean - 1 SD	98	55	53	33	68

X: data excluded

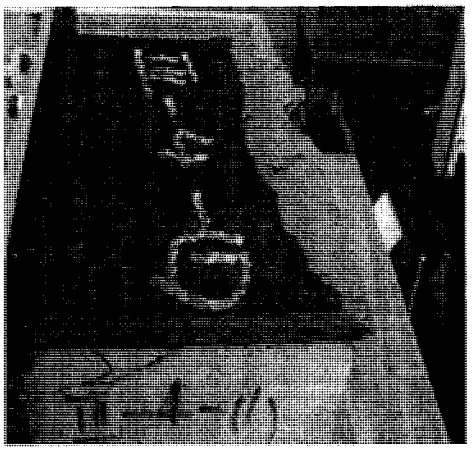

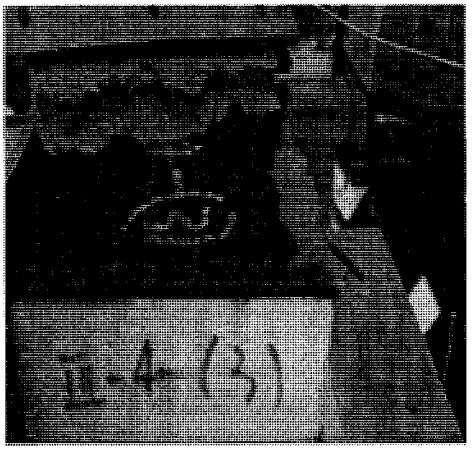

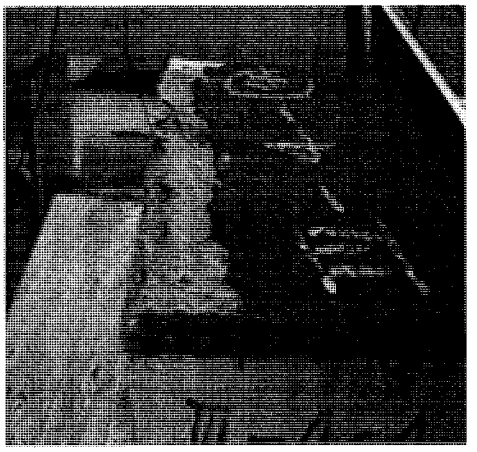

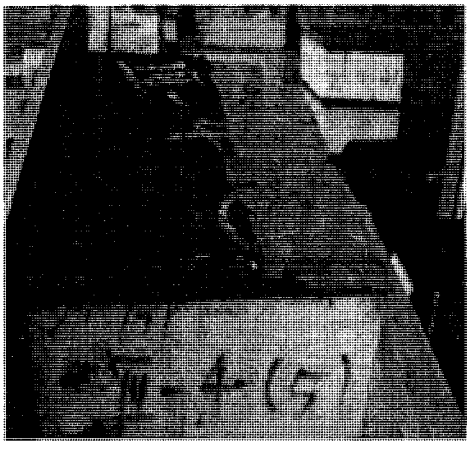

Sample #5: PF-ACB-15°-C (III-5)

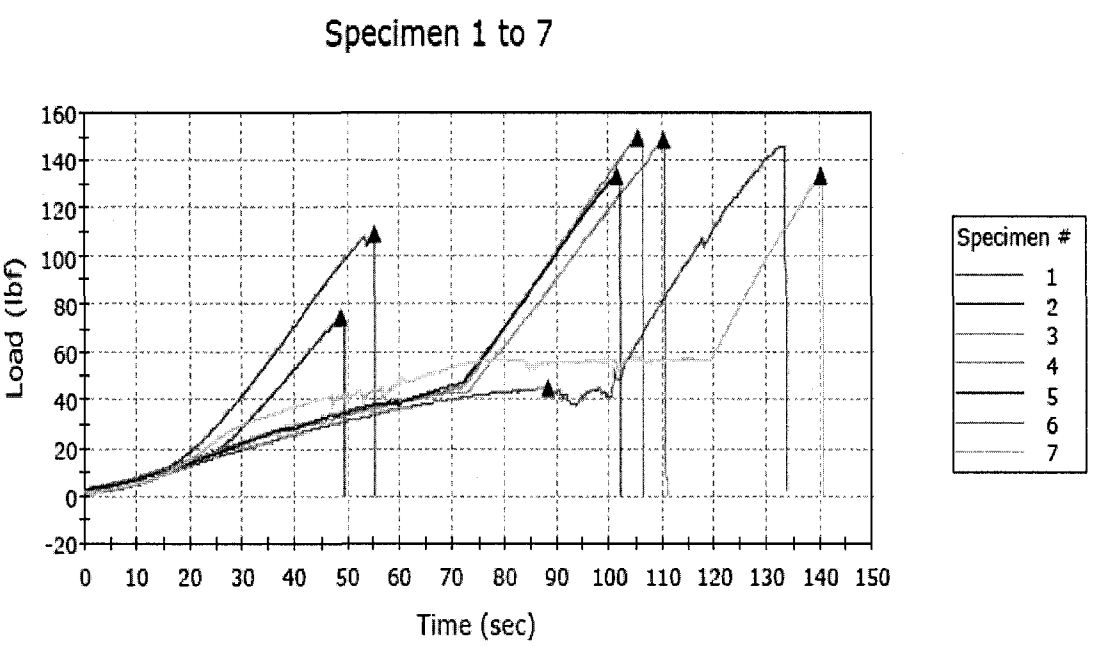

	Maximum Load (lbf)	Time at Maximum Load (sec)	Load at First Peak (lbf)	Time at First Peak (sec)	Average Load at Average Value (All Peaks) (lbf)
X 1	109	55	109	55	109
X 2	75	49	75	49	75
3	148	110	148	110	148
4	149	106	149	106	149
5	133	102	133	102	133
6	146	133	45	89	45
7	133	140	133	140	133
Maximum	149	140	149	140	149
Mean	142	118	122	109	122
Minimum	133	102	45	89	45
Standard Deviation	8	17	44	19	44
Mean + 1 SD	150	136	165	129	165
Mean - 1 SD	134	101	78	90	78

X: data excluded

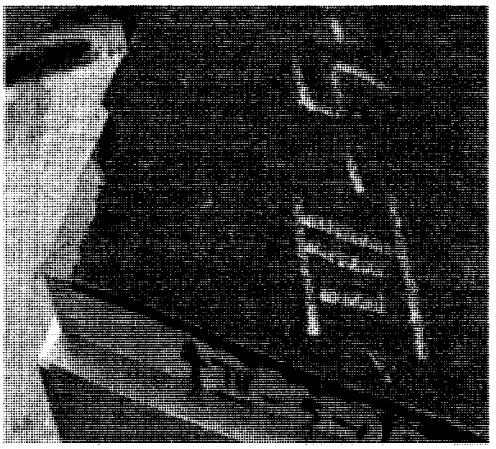

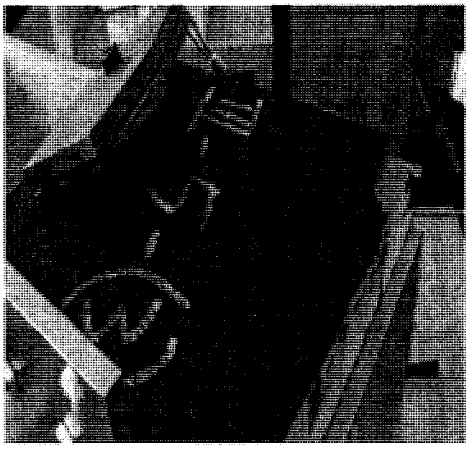

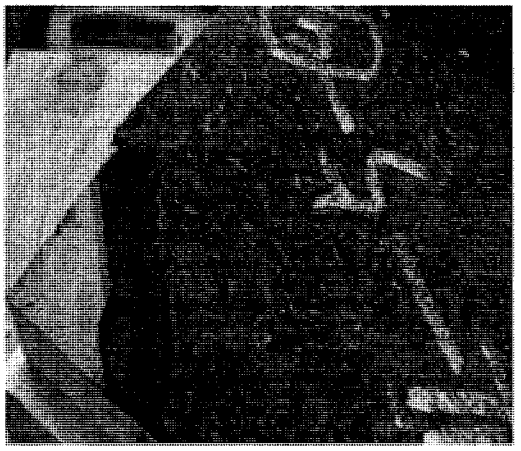

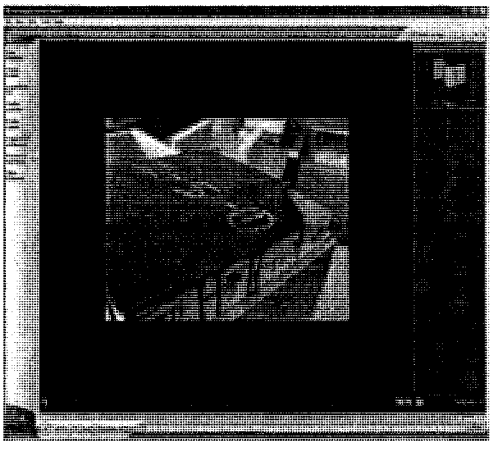

Sample #6: AF-ACB-15°-C (III-6)

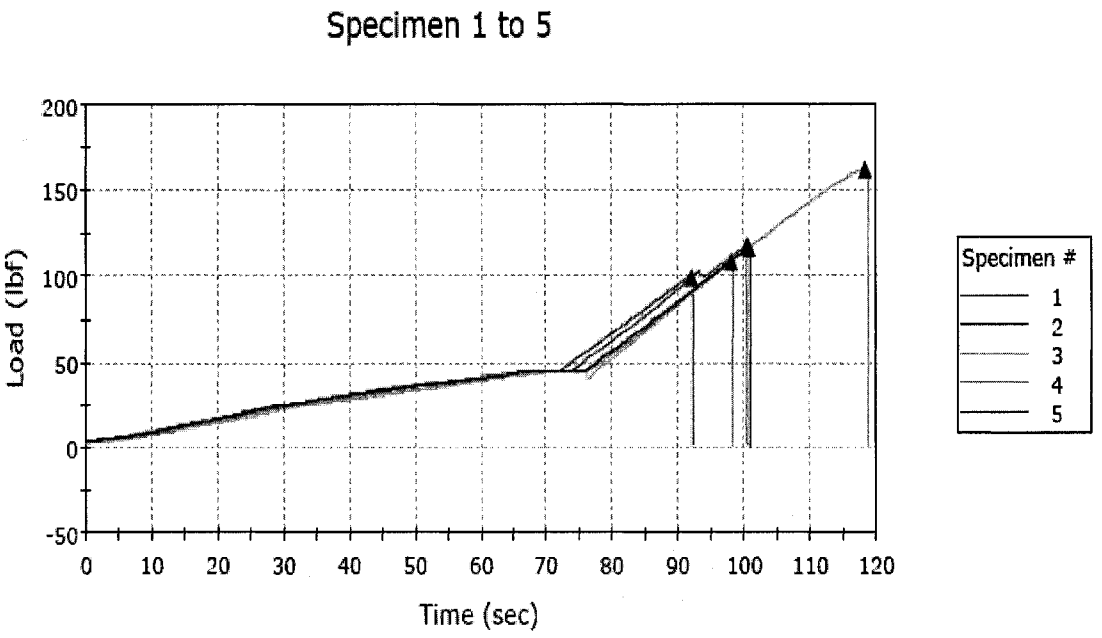

	Maximum Load (lbf)	Time at Maximum Load (sec)	Load at First Peak (lbf)	Time at First Peak (sec)	Average Load at Average Value (All Peaks) (lbf)
1	117	100	117	100	117
2	100	92	100	92	-----
3	162	118	162	118	162
4	108	98	108	98	108
5	116	101	116	101	-----
Maximum	162	118	162	118	162
Mean	120	102	120	102	129
Minimum	100	92	100	92	108
Standard Deviation	24	10	24	10	29
Mean + 1 SD	145	112	145	112	158
Mean - 1 SD	96	92	96	92	100

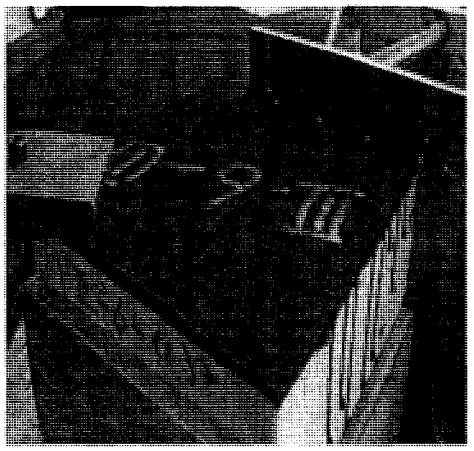

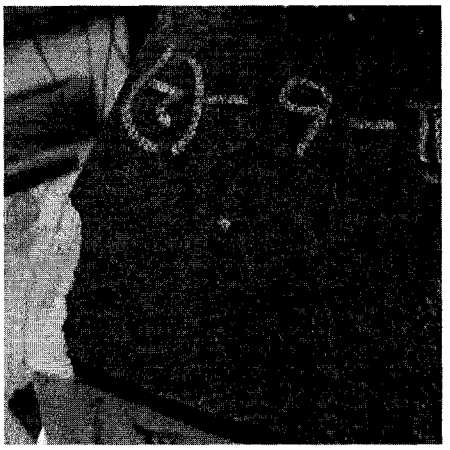

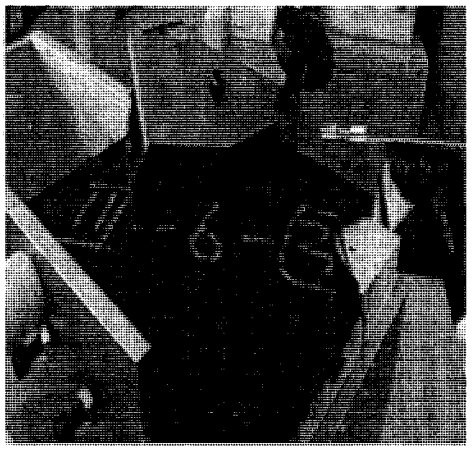

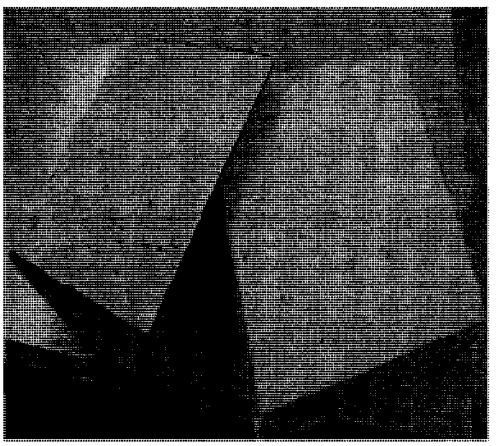

Appendix 4

Peel Resistance Data from Source IV

(Phase I)

Table 1. Peel Resistance (lbf) for 15 Degree Peel test at the Edge Position

Test ID	IV-1		IV-3		IV-2		IV-4	
Specimen ID	**PF/ACB**	**Failure Mode**	**AF/ACB**	**Failure Mode**	**PF/FB**	**Failure Mode**	**AF/FB**	**Failure Mode**
#1	192	Facer/D	132	Facer/D & Adh	105	CB/B	106	CB/B
#2	210	Facer/D & Adh	142	Facer/D & Adh	94	CB/B	104	CB/B
#3	258	Facer/D & Adh	175	CB/Se & Adh	138	CB/Sp	105	CB/B
#4	197	Facer/D	118	Facer/D & Adh	90	CB/B	98	CB/B
#5	258	Facer/D	131	Facer/D	97	CB/B	91	CB/B
Ave. Load	223		140		105		101	
Standard Deviation	33		22		20		6	

Table 2. Peel Resistance (lbf) for 15 Degree Peel test at the Corner Position

Test ID	IV-5		IV-6	
Specimen ID	**PF/ACB**	**Failure Mode**	**AF/ACB**	**Failure Mode**
#1	173	CB/B	111	CB/B
#2	151	Facer/D & Adh	126	Facer/D & Adh
#3	169	CB/B	124	CB/B
#4	173	CB/B	113	Facer/D
#5	190	CB/B	86	Facer/D
Ave. Load	171		112	
Standard Deviation	14		16	

Sample #1: PF-ACB-15°-E (IV-1)

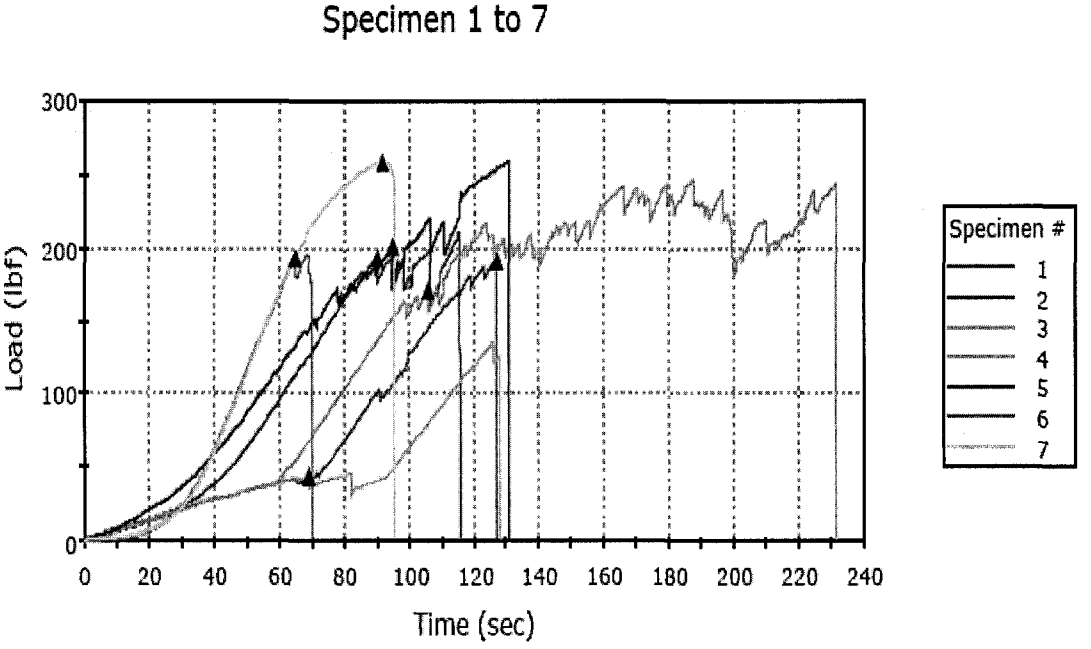

	Maximum Load (lbf)	Time at Maximum Load (sec)	Load at First Peak (lbf)	Time at First Peak (sec)	Average Load at Average Value (All Peaks) (lbf)
1	192	127	192	127	192
2	210	116	193	90	193
X 3	135	126	44	69	75
X 4	247	188	172	106	226
5	258	131	201	95	213
6	197	69	193	65	195
7	258	92	258	92	258
Maximum	258	131	258	127	258
Mean	223	107	207	94	210
Minimum	192	69	192	65	192
Standard Deviation	33	26	29	22	28
Mean + 1 SD	256	133	236	116	238

	Maximum Load (lbf)	Time at Maximum Load (sec)	Load at First Peak (lbf)	Time at First Peak (sec)	Average Load at Average Value (All Peaks) (lbf)
Mean - 1 SD	190	81	179	72	182

X: data excluded

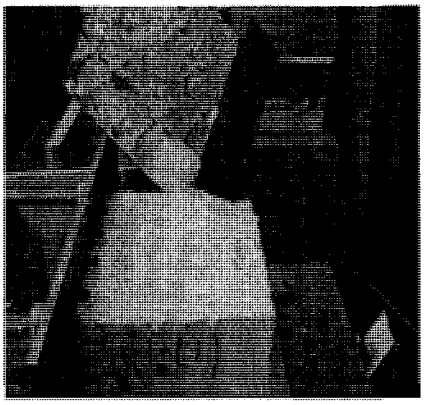

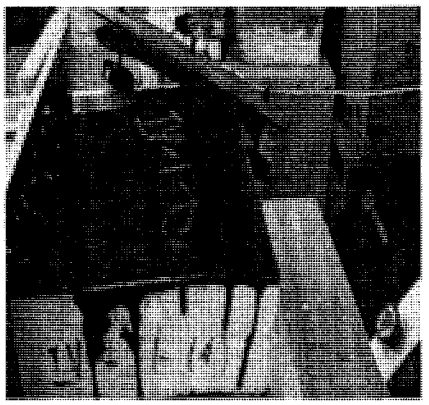

Sample #2: PF-FB-15°-E (IV-2)

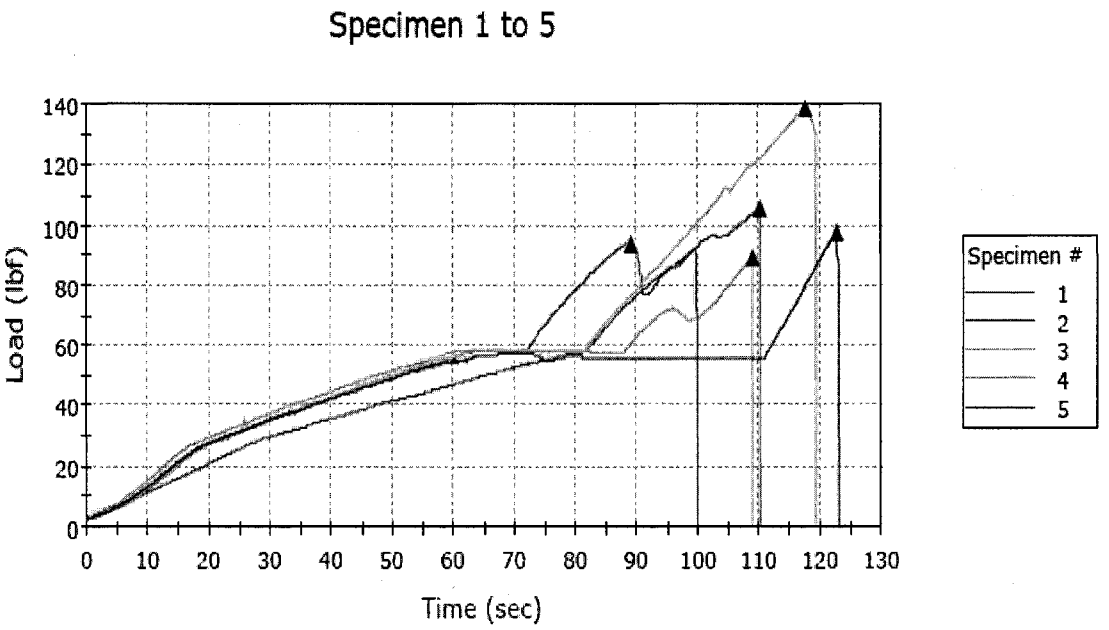

	Maximum Load (lbf)	Time at Maximum Load (sec)	Load at First Peak (lbf)	Time at First Peak (sec)	Average Load at Average Value (All Peaks) (lbf)
1	105	110	105	110	-----
2	94	89	94	89	93
3	138	118	138	118	138
4	90	109	90	109	90
5	97	123	97	123	97
Maximum	138	123	138	123	138
Mean	105	110	105	110	105
Minimum	90	89	90	89	90
Standard Deviation	20	13	20	13	23
Mean + 1 SD	124	123	124	123	127
Mean - 1 SD	85	97	85	97	82

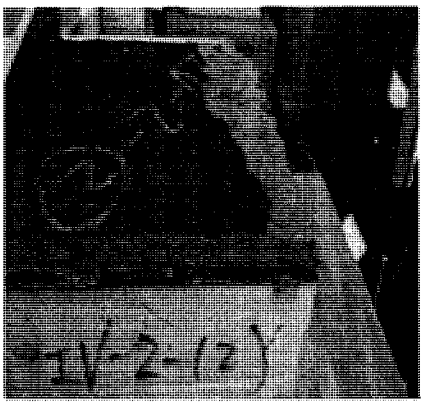

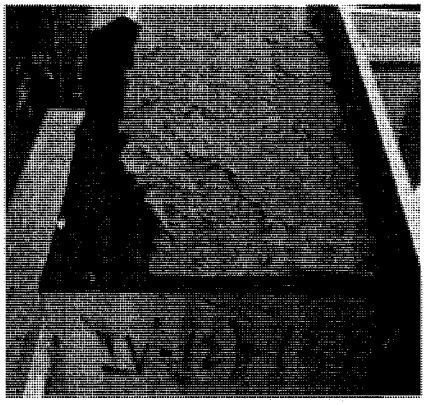

Sample #3: AF-ACB-15°-E (IV-3)

Specimen 1 to 7

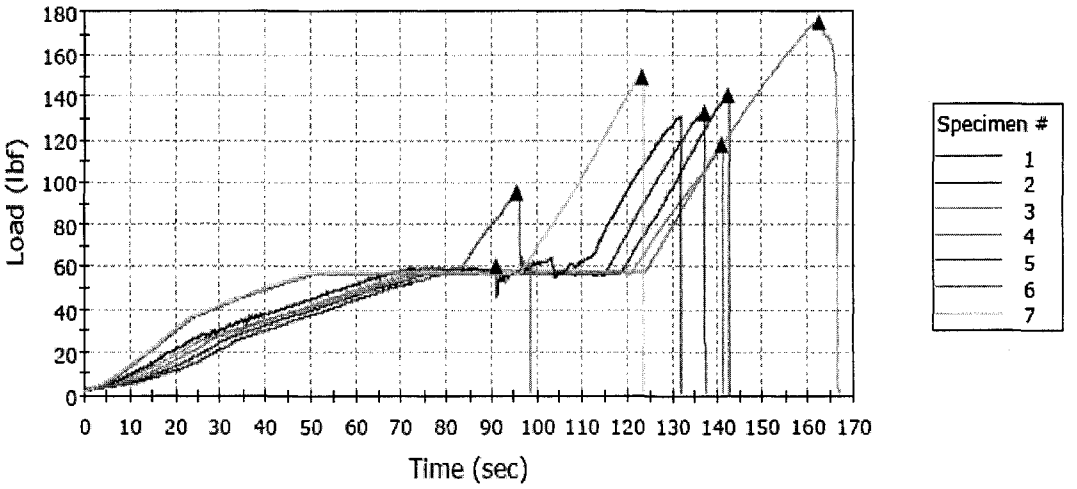

	Maximum Load (lbf)	Time at Maximum Load (sec)	Load at First Peak (lbf)	Time at First Peak (sec)	Average Load at Average Value (All Peaks) (lbf)
1	132	137	132	137	132
2	142	143	142	143	-----
3	175	162	175	162	175
4	118	141	118	141	118
5	131	132	60	91	85
X 6	95	96	95	96	95
X 7	150	123	150	123	150
Maximum	175	162	175	162	175

	Maximum Load (lbf)	Time at Maximum Load (sec)	Load at First Peak (lbf)	Time at First Peak (sec)	Average Load at Average Value (All Peaks) (lbf)
Mean	140	143	125	135	128
Minimum	118	132	60	91	85
Standard Deviation	22	12	42	26	37
Mean + 1 SD	161	155	168	161	165
Mean - 1 SD	118	131	83	108	90

X: data excluded

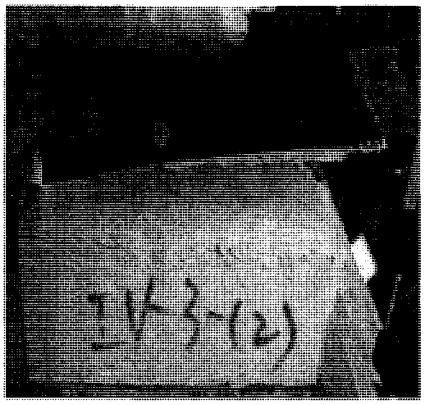

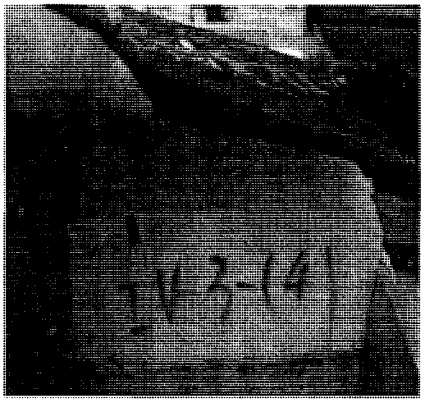

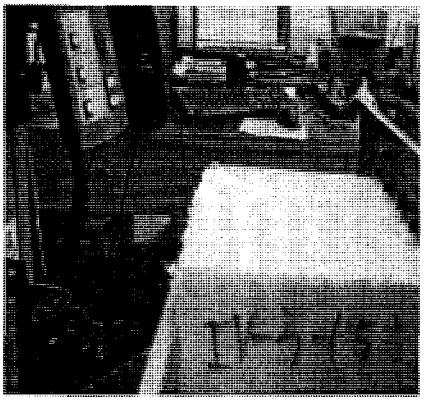

Sample #4: AF-FB-15°-E (IV-4)

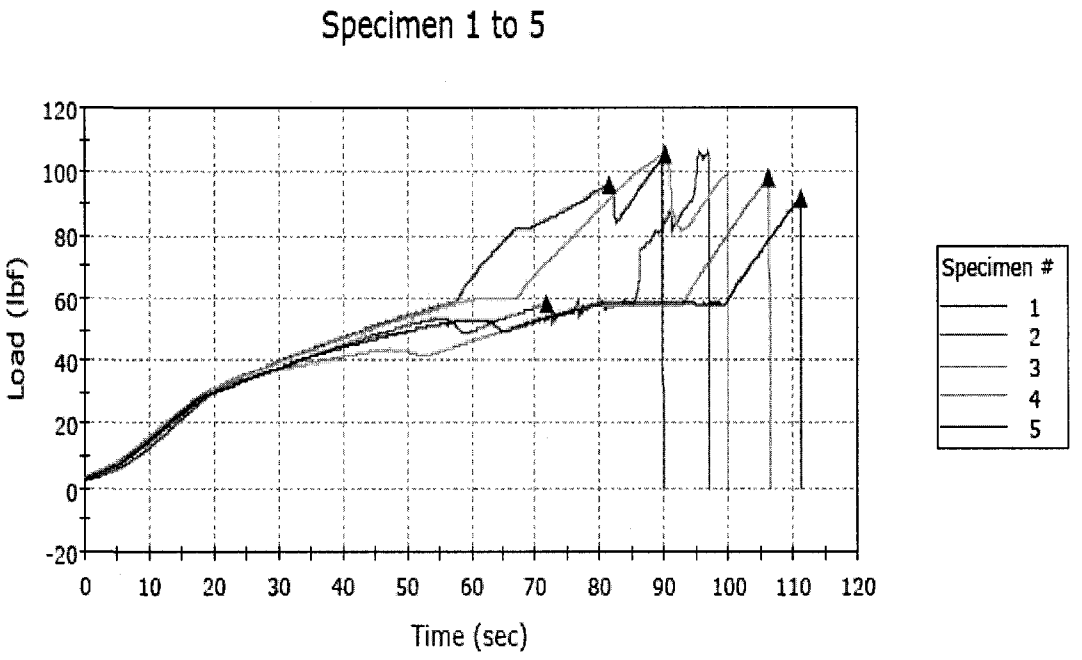

	Maximum Load (lbf)	Time at Maximum Load (sec)	Load at First Peak (lbf)	Time at First Peak (sec)	Average Load at Average Value (All Peaks) (lbf)
1	106	95	58	72	84
2	104	90	96	82	96
3	105	90	105	90	102
4	98	106	98	106	98
5	91	111	91	111	-----
Maximum	106	111	105	111	102
Mean	101	99	90	92	95
Minimum	91	90	58	72	84
Standard Deviation	6	10	18	17	8
Mean + 1 SD	107	108	108	109	103
Mean - 1 SD	95	89	71	76	87

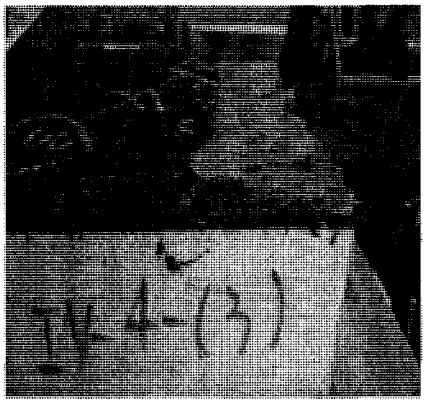

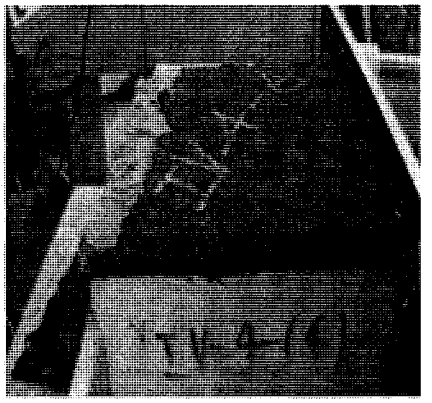

Sample #5: PF-ACB-15°-C (IV-5)

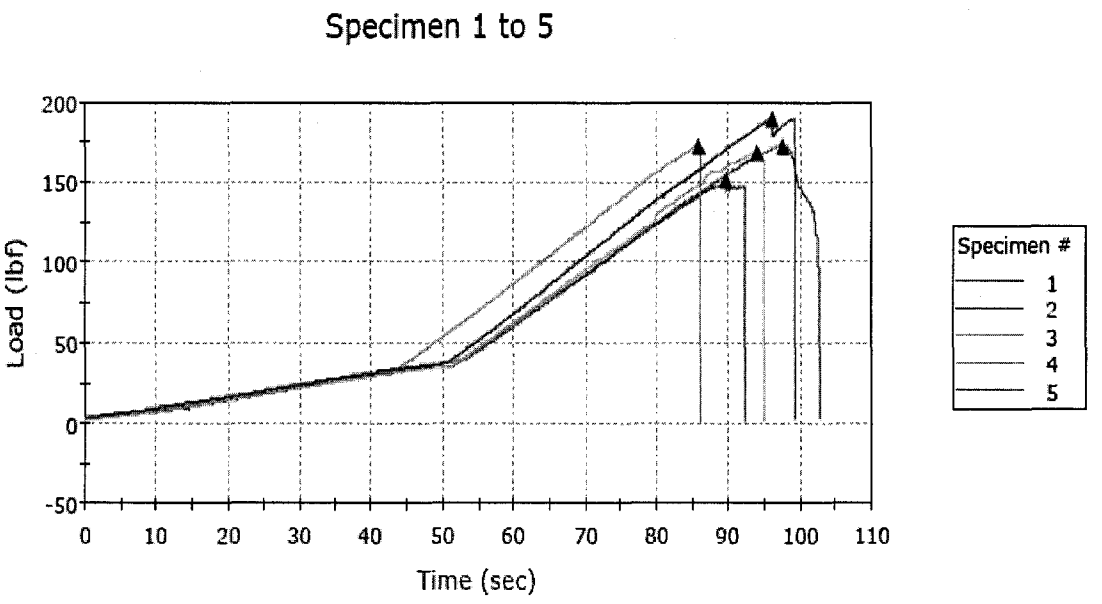

	Maximum Load (lbf)	Time at Maximum Load (sec)	Load at First Peak (lbf)	Time at First Peak (sec)	Average Load at Average Value (All Peaks) (lbf)
1	173	98	173	98	173
2	151	90	151	90	151
3	169	94	169	94	169
4	173	86	173	86	173
5	190	96	190	96	190
Maximum	190	98	190	98	190
Mean	171	93	171	93	171
Minimum	151	86	151	86	151
Standard Deviation	14	5	14	5	14
Mean + 1 SD	185	98	185	98	185
Mean - 1 SD	157	88	157	88	157

Sample #6: AF-ACB-15°-C (IV-6)

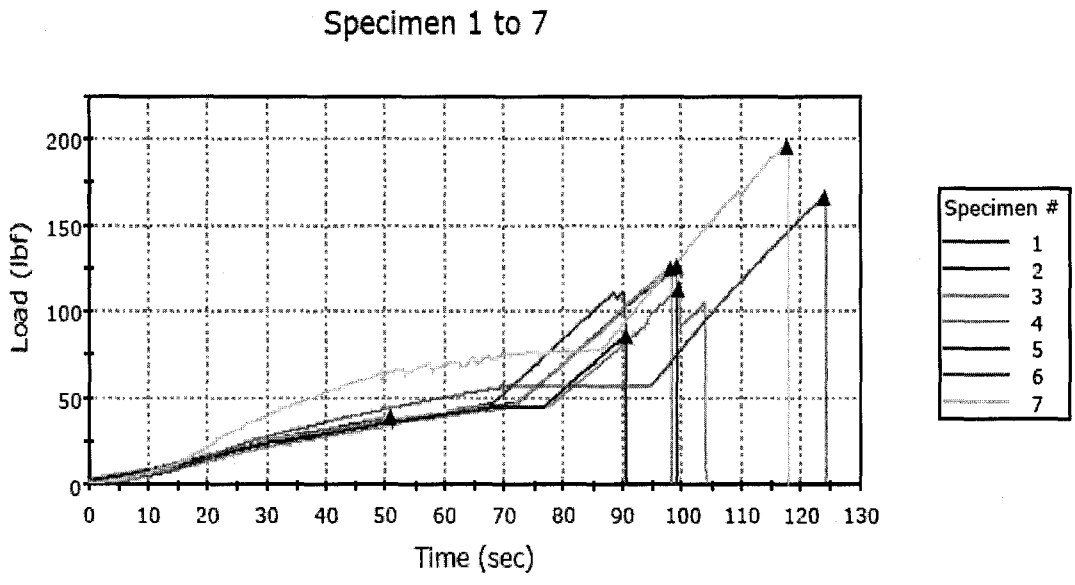

	Maximum Load (lbf)	Time at Maximum Load (sec)	Load at First Peak (lbf)	Time at First Peak (sec)	Average Load at Average Value (All Peaks) (lbf)
1	111	90	38	51	111
2	126	99	126	99	126
3	124	98	124	98	124
4	113	100	113	100	109
5	86	91	86	91	86
X 6	166	124	166	124	166
X 7	195	118	195	118	195
Maximum	126	100	126	100	126
Mean	112	95	98	88	111

	Maximum Load (lbf)	Time at Maximum Load (sec)	Load at First Peak (lbf)	Time at First Peak (sec)	Average Load at Average Value (All Peaks) (lbf)
Minimum	86	90	38	51	86
Standard Deviation	16	5	37	21	16
Mean + 1 SD	128	100	134	108	127
Mean - 1 SD	96	91	61	67	95

X: data excluded

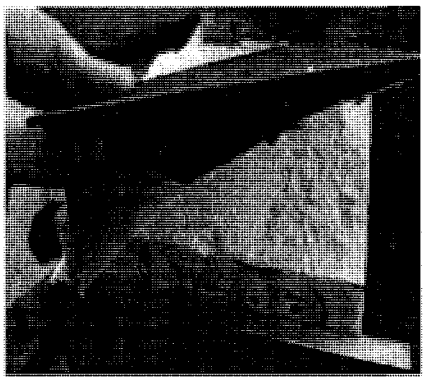

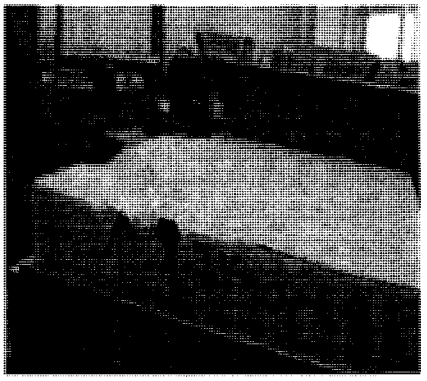

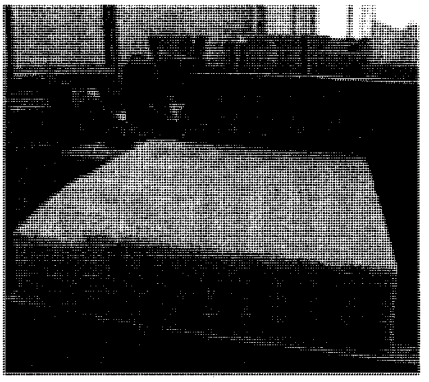

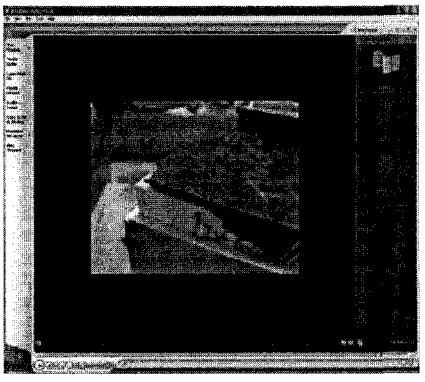

Appendix 5

Peel Resistance Data from Source II

(Phase II)

Table 1. Peel Resistance (lbf) of PF/ACB Samples for Different Angle Peel test at the Edge Position

Test Anger (°)	7.5		15		22.5		30		37.5		45	
Specimen PF/ACB ID	Peel Resistance	Failure Mode	Peel Resistance	Failure Mode	Peel Resistance	Failure Mode	Peel Resistance	Failure Mode	Peel Resistance	Failure Mode	Peel Resistance	Failure Mode
#1	212	Facer/D &Adh	157	Adh	98	Adh	72	Facer/D &Adh	55	Adh	53	Facer/D &Adh
#2	207	Facer/D &Adh	190	Adh	151	Adh	78	Adh	51	Adh	39	Facer/D &Adh
#3	170	Adh	149	Adh	139	Facer/D &Adh	73	Adh	55	Adh	68	Adh
#4	196	Adh	175	Adh	89	Adh	80	Adh	38	Adh	36	Adh
#5	174	Adh	160	Adh	85	Facer/D &Adh	63	Adh	59	Adh	33	Adh
Mean Load	**192**		**166**		**113**		**73**		**52**		**46**	
Standard Deviation	19		16		30		6		8		15	

Table 2. Peel Resistance (lbf) of AF/ACB Samples for Different Angle Peel test at the Edge Position

Test Anger (°)	7.5		15		22.5		30		37.5		45	
Specimen AF/ACB ID	Peel Resistance	Failure Mode	Peel Resistance	Failure Mode	Peel Resistance	Failure Mode	Peel Resistance	Failure Mode	Peel Resistance	Failure Mode	Peel Resistance	Failure Mode
#1	241	Adh.	123	Facer/D	56	Facer/D &Adh	56	Adh	51	Adh	27	Facer/D &Adh
#2	181	Facer/D &Adh	100	Adh	98	Adh	48	Facer/D &Adh	47	Facer/D &Adh	44	Adh
#3	195	Adh	87	Facer/D &Adh	80	Facer/D &Adh	59	Adh	56	Adh	25	Adh
#4	233	Facer/D &Adh	125	Adh	59	Facer/D &Adh	57	Facer/D	43	Facer/D &Adh	44	Adh
#5	242	Adh	127	Facer/D &Adh	87	Facer/D &Adh	52	Adh	58	Adh	24	Facer/D &Adh
Mean Load	**218**		**112**		**76**		**54**		**51**		**33**	
Standard Deviation	29		18		18		4		6		10	

Table 3. Peel Resistance (lbf) of PF/ACB Samples for Different Sample Size Peel test at the Edge Position

Sample Size	4x4		6x6		8x8		10x10	
Specimen PF/ACB ID	Peel Resistance	Failure Mode	Peel Resistance	Failure Mode	Peel Resistance	Failure Mode	Peel Resistance	Failure Mode
#1	83	Adh	157	Adh	197	Adh	260	Adh
#2	79	Adh	190	Adh	212	Adh	236	Adh
#3	79	Adh	149	Adh	190	Facer/D &Adh	274	Adh
#4	92	Facer/R	175	Adh	232	Facer/D &Adh	267	Adh
#5	77	Facer/D &Adh	160	Adh	230	Facer/D &Adh	239	Adh
Ave. Load	**82**		166		**212**		**255**	
Standard Deviation	6		16		19		17	

Sample #1: PF-ACB-7.5°-E (S2'-2)

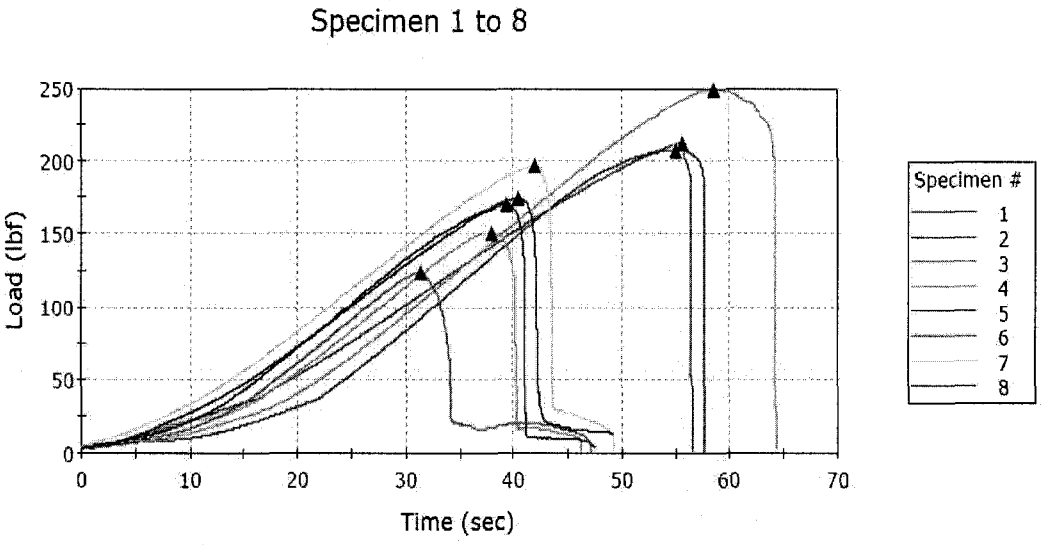

	Maximum Load (lbf)	Time at Maximum Load (sec)	Load at First Peak (lbf)	Time at First Peak (sec)	Average Load at Average Value (All Peaks) (lbf)
1	212	56	212	56	212
2	207	55	207	55	207
X 3	249	59	249	59	249
X 4	151	38	151	38	151
5	170	39	170	39	170
X 6	124	31	124	31	124
7	196	42	196	42	196
8	174	40	174	40	174
Maximum	212	56	212	56	212
Mean	192	46	192	46	192
Minimum	170	39	170	39	170
Standard Deviation	19	8	19	8	19
Mean + 1 SD	211	55	211	55	211
Mean - 1 SD	173	38	173	38	173

X: data excluded

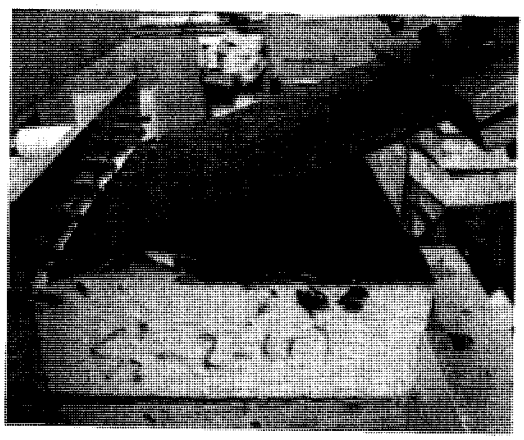

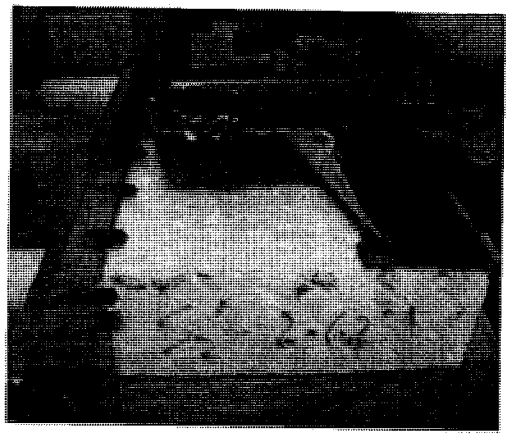

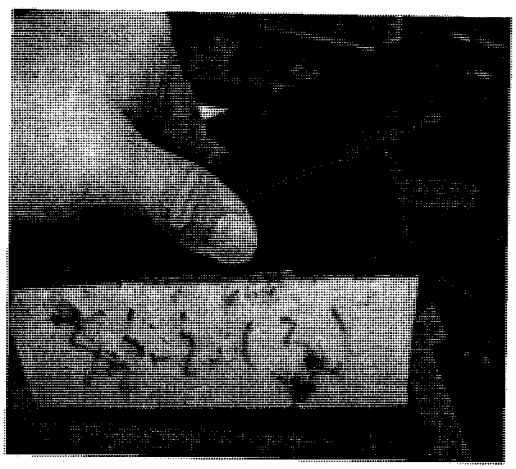

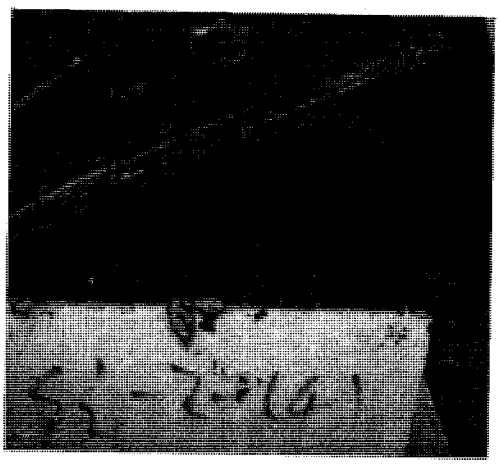

Sample #2: PF-ACB-15°-E (S2'-1)

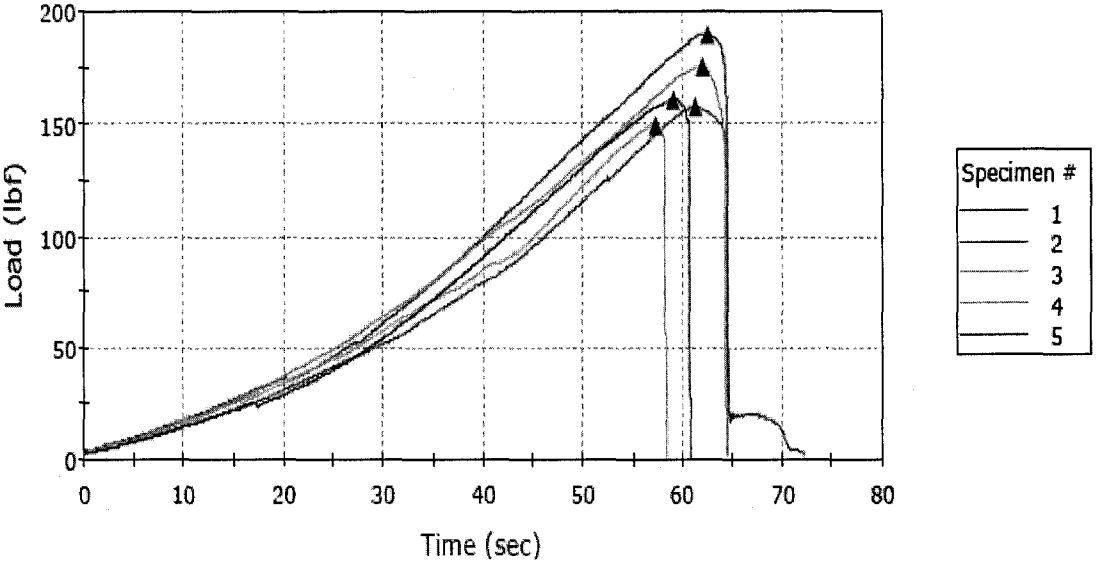

	Maximum Load (lbf)	Time at Maximum Load (sec)	Load at First Peak (lbf)	Time at First Peak (sec)	Average Load at Average Value (All Peaks) (lbf)
1	157	61	157	61	157
2	190	63	190	63	190
3	149	57	149	57	149
4	175	62	175	62	175
5	160	59	160	59	160
Maximum	190	63	190	63	190
Mean	166	60	166	60	166
Minimum	149	57	149	57	149
Standard Deviation	16	2	16	2	16
Mean + 1 SD	182	63	182	63	182
Mean - 1 SD	150	58	150	58	150

Sample #3: PF-ACB-22.5°-E (S2'-3)

Specimen 1 to 7

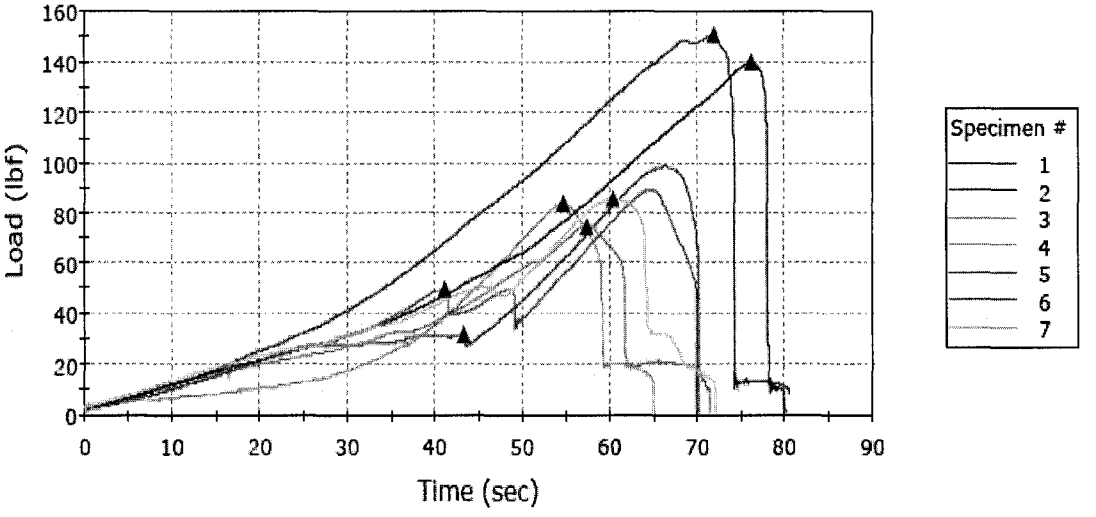

	Maximum Load (lbf)	Time at Maximum Load (sec)	Load at First Peak (lbf)	Time at First Peak (sec)	Average Load at Average Value (All Peaks) (lbf)
1	98	66	32	43	65
2	151	72	151	72	151
X 3	84	55	84	55	84
X 4	75	58	75	58	75
5	139	76	139	76	139
6	89	65	50	41	63
7	85	60	85	60	85
Maximum	151	76	151	76	151
Mean	113	68	91	59	101
Minimum	85	60	32	41	63
Standard Deviation	30	6	53	16	42

	Maximum Load (lbf)	Time at Maximum Load (sec)	Load at First Peak (lbf)	Time at First Peak (sec)	Average Load at Average Value (All Peaks) (lbf)
Mean + 1 SD	143	74	144	75	143
Mean - 1 SD	82	62	38	43	59

X: data excluded

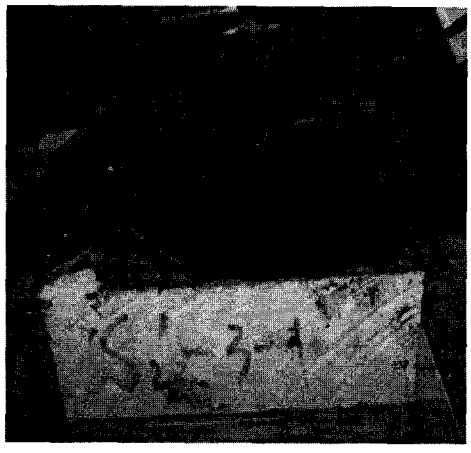

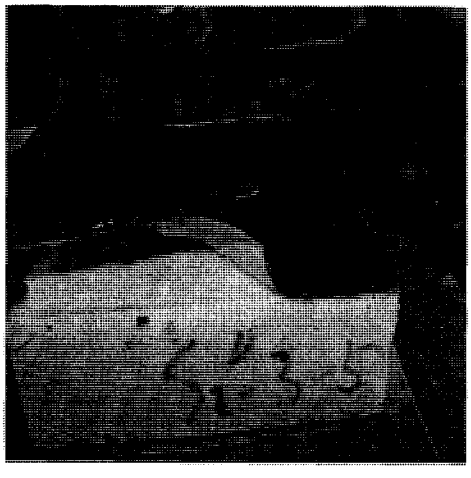

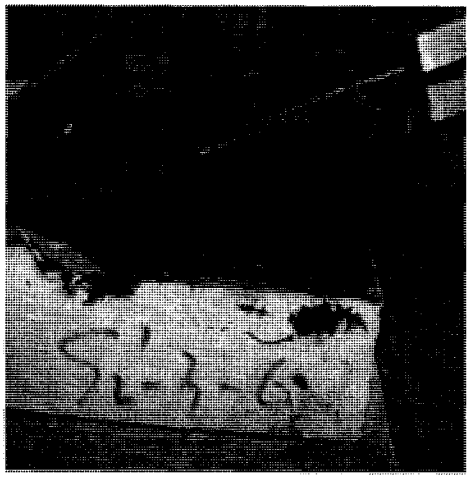

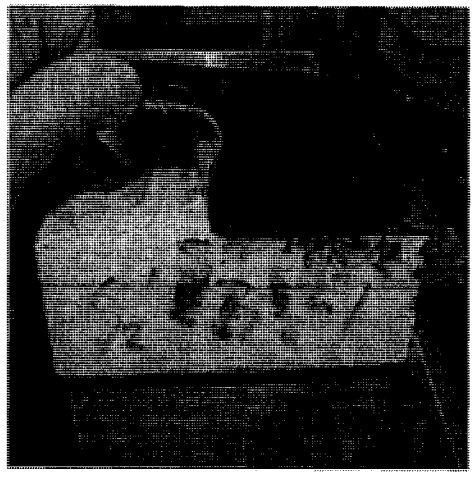

Sample #4: PF-ACB-30°-E (S2'-4)

Specimen 1 to 6

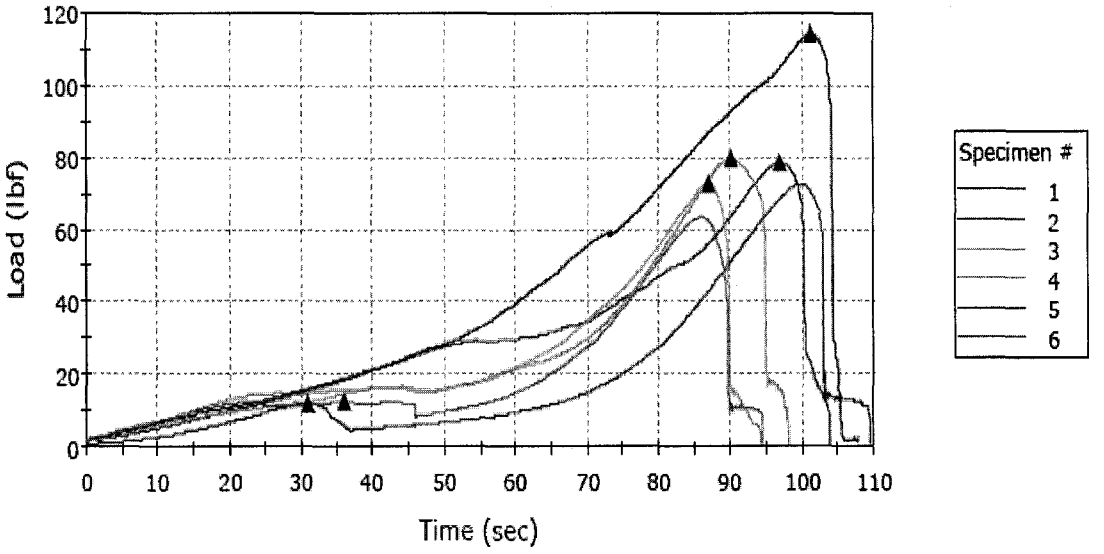

	Maximum Load (lbf)	Time at Maximum Load (sec)	Load at First Peak (lbf)	Time at First Peak (sec)	Average Load at Average Value (All Peaks) (lbf)
1	72	100	12	31	42
2	78	97	78	97	78
3	73	87	73	87	-----
4	80	90	80	90	80
X 5	114	101	114	101	114
6	63	86	13	36	38
Maximum	80	100	80	97	80
Mean	73	92	51	68	60
Minimum	63	86	12	31	38
Standard Deviation	6	6	36	32	23
Mean + 1 SD	80	98	87	100	82
Mean - 1 SD	67	86	16	36	37

X: data excluded

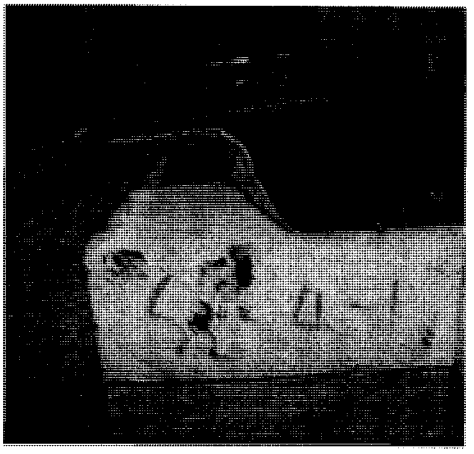

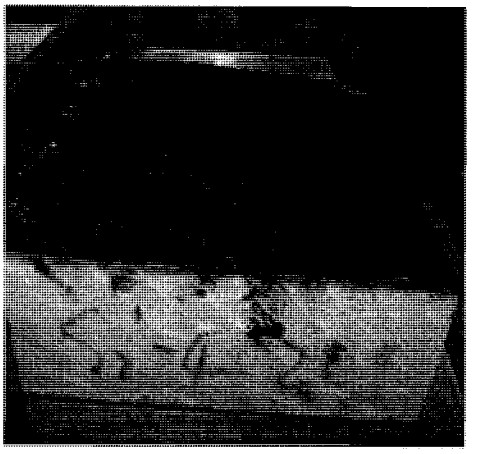

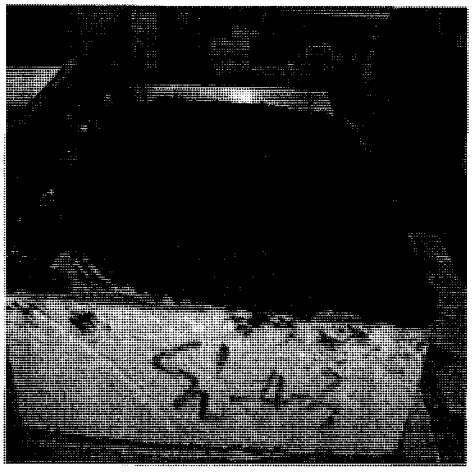

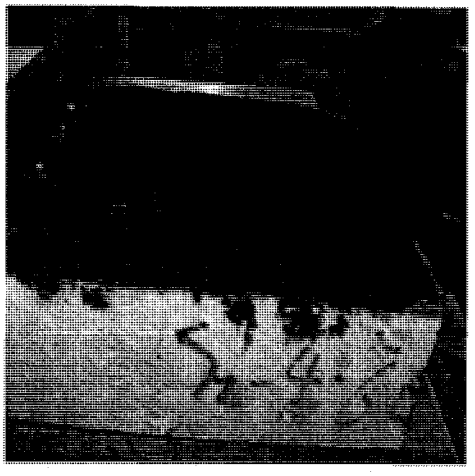

Sample #5: PF-ACB-37.5°-E (S2'-5)

Specimen 1 to 7

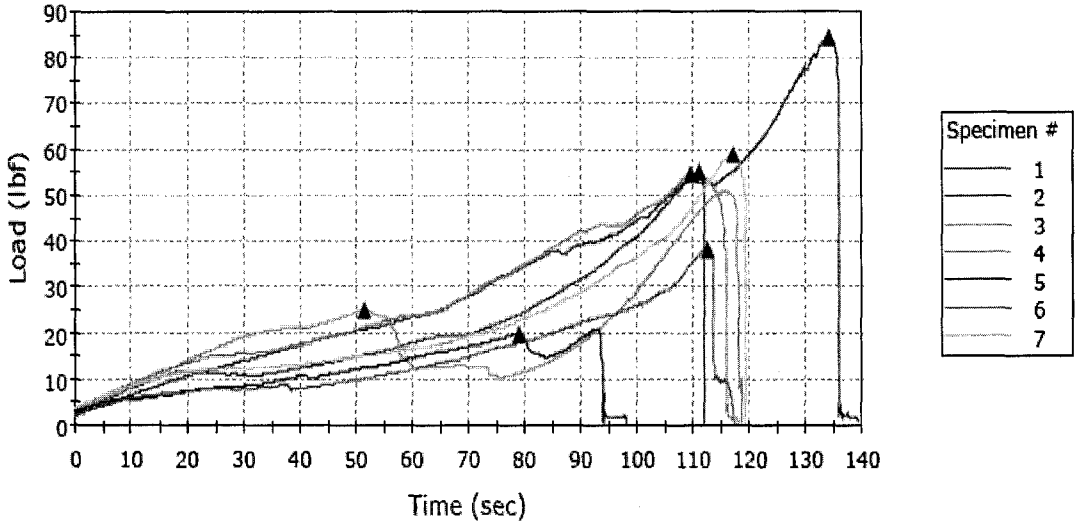

	Maximum Load (lbf)	Time at Maximum Load (sec)	Load at First Peak (lbf)	Time at First Peak (sec)	Average Load at Average Value (All Peaks) (lbf)
1	55	111	55	111	55
X 2	84	134	84	134	84
3	51	116	25	52	38
4	55	110	55	110	55
X 5	21	93	20	79	20
6	38	113	38	113	38
7	59	117	59	117	59
Maximum	59	117	59	117	59
Mean	52	113	46	100	49
Minimum	38	110	25	52	38
Standard Deviation	8	3	14	27	10
Mean + 1 SD	59	117	61	128	59
Mean - 1 SD	44	110	32	73	39

X: data excluded

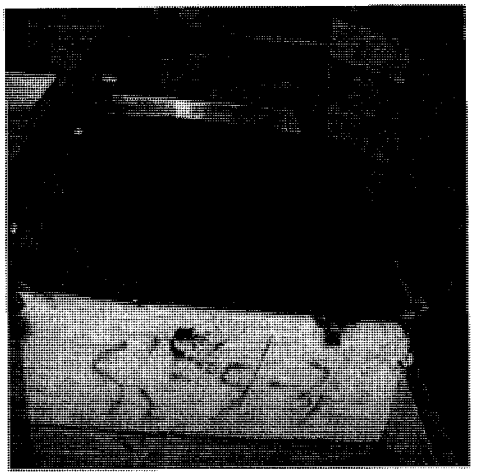

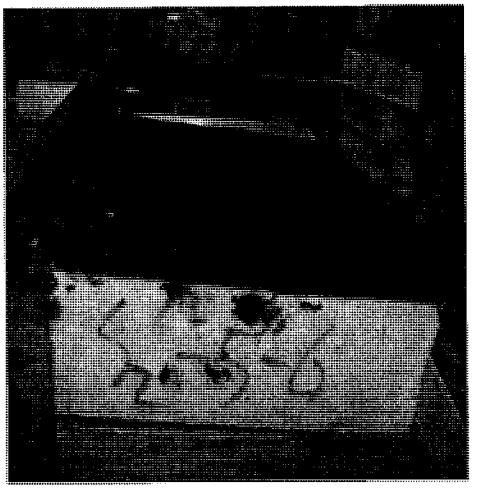

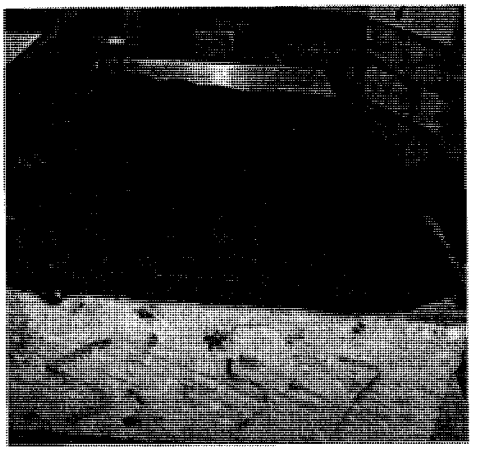

Sample #6: PF-ACB-45°-E (S2'-6)

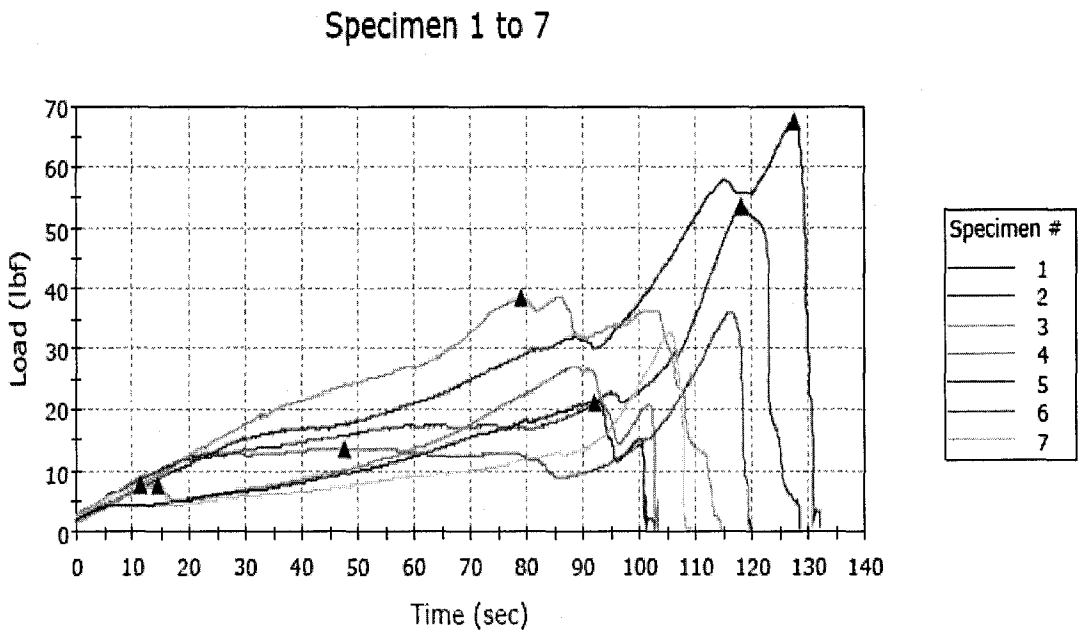

	Maximum Load (lbf)	Time at Maximum Load (sec)	Load at First Peak (lbf)	Time at First Peak (sec)	Average Load at Average Value (All Peaks) (lbf)
1	53	118	53	118	53
2	68	128	68	128	68
3	39	86	38	79	38
X 4	27	89	8	15	17
X 5	21	92	21	92	21
6	36	116	14	48	14
7	33	106	8	12	33
Maximum	68	128	68	128	68
Mean	46	111	36	77	41
Minimum	33	86	8	12	14
Standard Deviation	15	16	26	49	21
Mean + 1 SD	60	127	62	125	62
Mean - 1 SD	31	95	11	28	21

X: data excluded

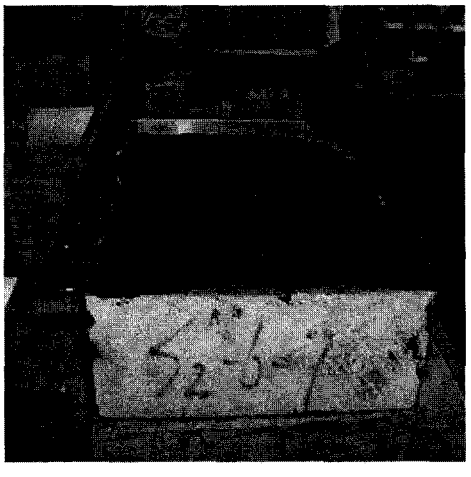

Sample #7: AF-ACB-7.5°-E (S2-2)

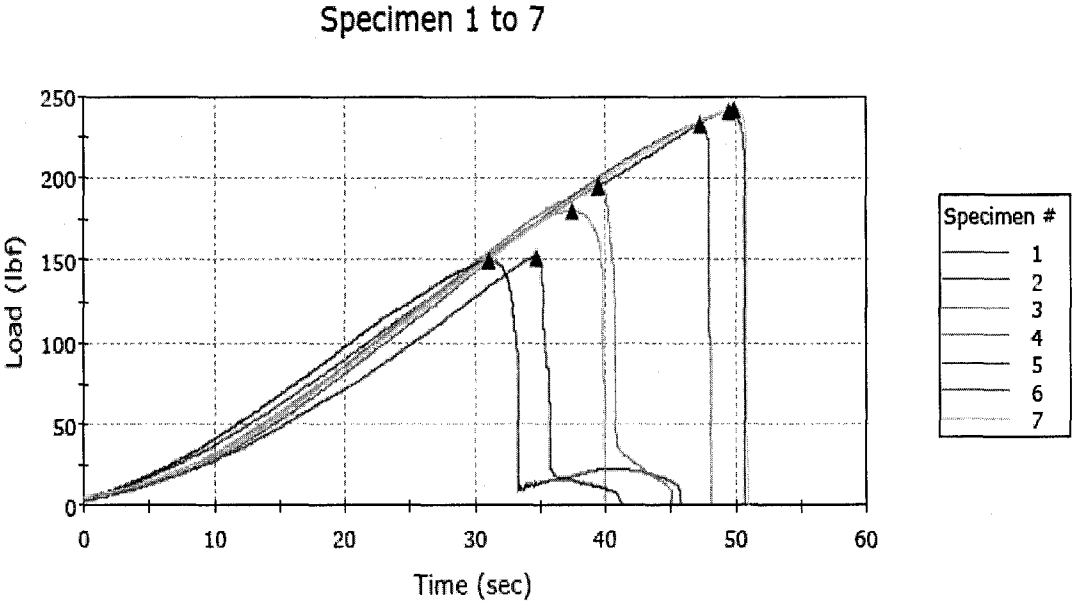

	Maximum Load (lbf)	Time at Maximum Load (sec)	Load at First Peak (lbf)	Time at First Peak (sec)	Average Load at Average Value (All Peaks) (lbf)
1	241	50	241	50	241
X 2	152	35	152	35	152
3	181	38	181	38	181
4	195	40	195	40	195
X 5	150	31	150	31	150
6	233	47	233	47	233
7	242	50	242	50	242
Maximum	242	50	242	50	242
Mean	218	45	218	45	218
Minimum	181	38	181	38	181
Standard Deviation	29	6	29	6	29
Mean + 1 SD	247	51	247	51	247
Mean - 1 SD	190	39	190	39	190

X: data excluded

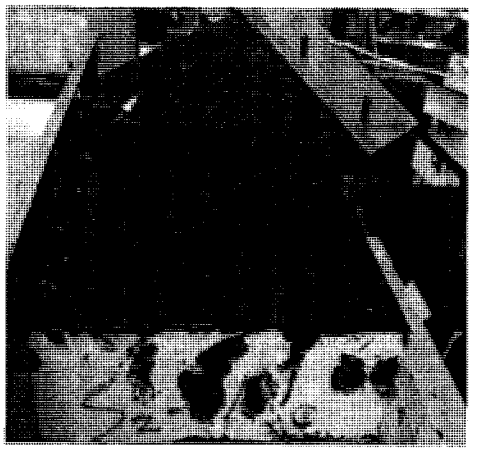

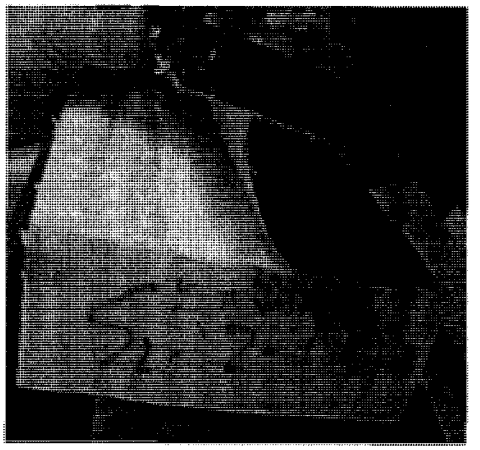

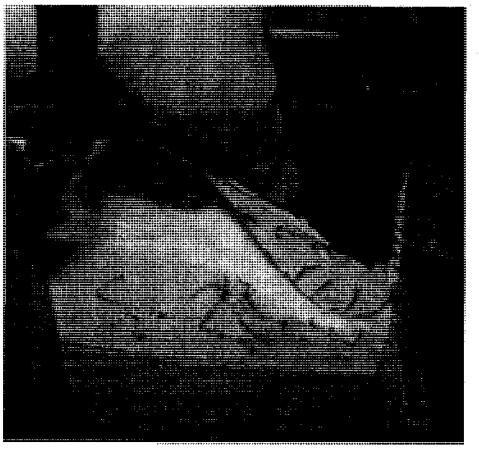

Sample #8: AF-ACB-15°-E (S2-1)

Specimen 1 to 7

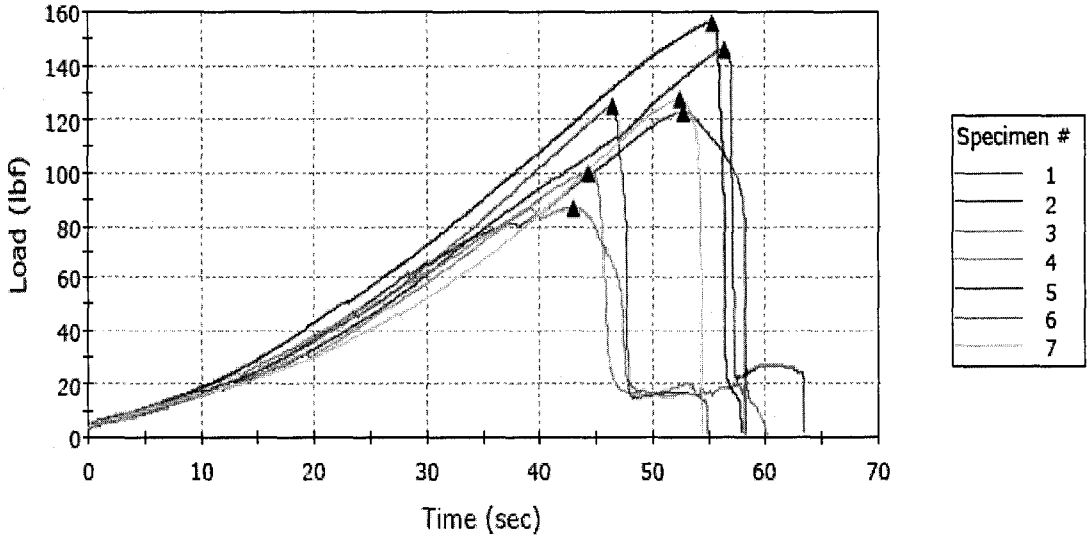

	Maximum Load (lbf)	Time at Maximum Load (sec)	Load at First Peak (lbf)	Time at First Peak (sec)	Average Load at Average Value (All Peaks) (lbf)
1	123	53	123	53	123
X 2	146	56	146	56	146
3	100	44	100	44	100
4	87	43	87	43	-----
X 5	156	55	156	55	156
6	125	47	125	47	125
7	127	52	127	52	127
Maximum	127	53	127	53	127
Mean	112	48	112	48	119
Minimum	87	43	87	43	100
Standard Deviation	18	5	18	5	13
Mean + 1 SD	130	52	130	52	131
Mean - 1 SD	94	43	94	43	106

X: data excluded

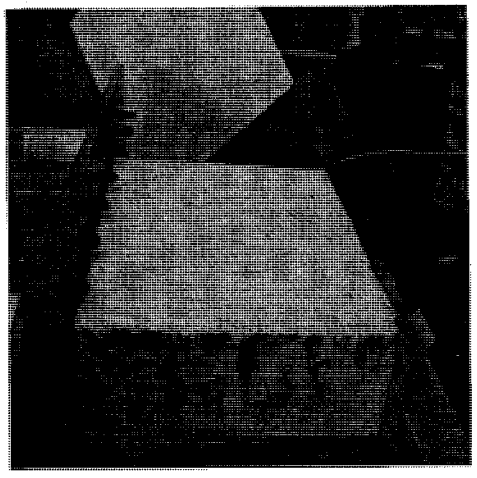

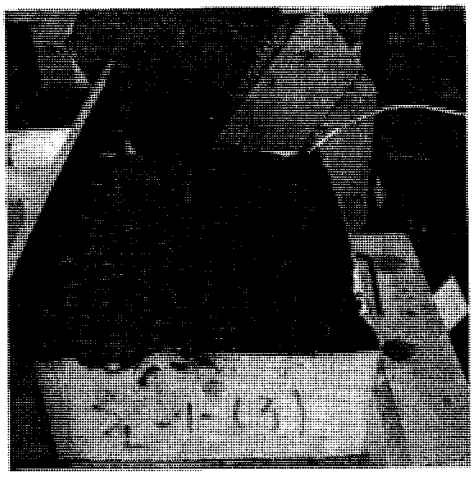

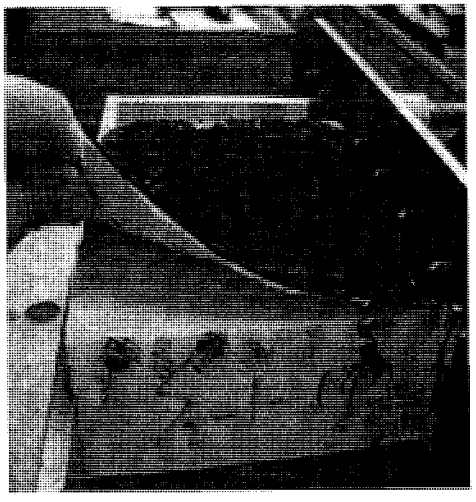

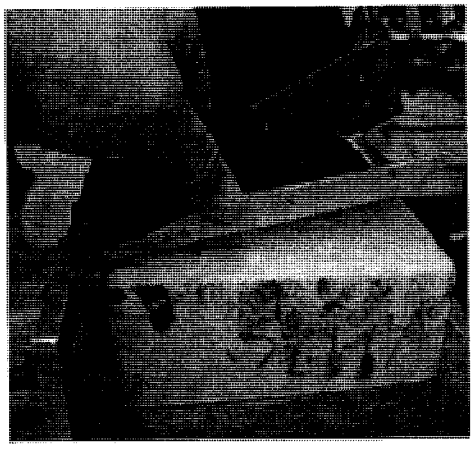

Sample #9: AF-ACB-22.5°-E (S2-3)

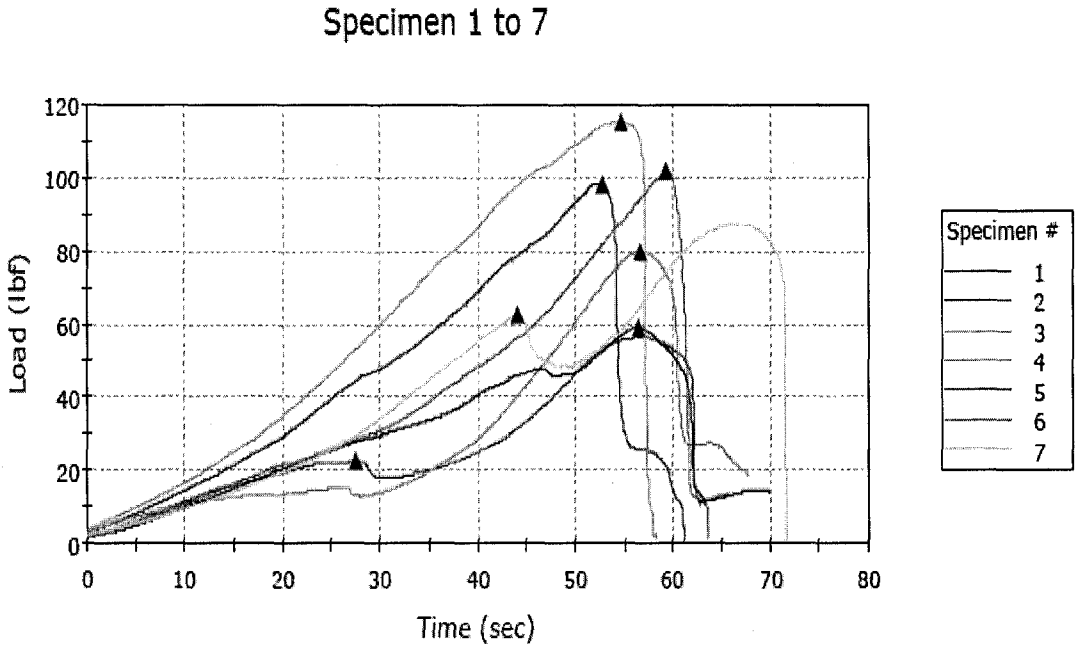

	Maximum Load (lbf)	Time at Maximum Load (sec)	Load at First Peak (lbf)	Time at First Peak (sec)	Average Load at Average Value (All Peaks) (lbf)
1	56	57	23	28	39
2	98	53	98	53	98
X 3	115	55	115	55	115
4	80	57	80	57	80
5	59	56	59	56	59
X 6	101	59	101	59	101
7	87	67	63	44	75
Maximum	98	67	98	57	98
Mean	76	58	64	48	70
Minimum	56	53	23	28	39
Standard Deviation	18	5	28	12	22
Mean + 1 SD	94	63	93	60	93
Mean - 1 SD	58	53	36	35	48

X: data excluded

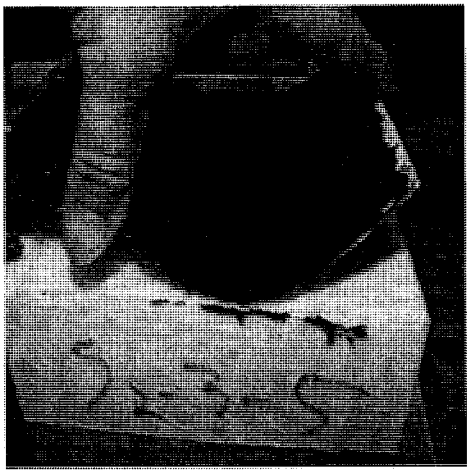

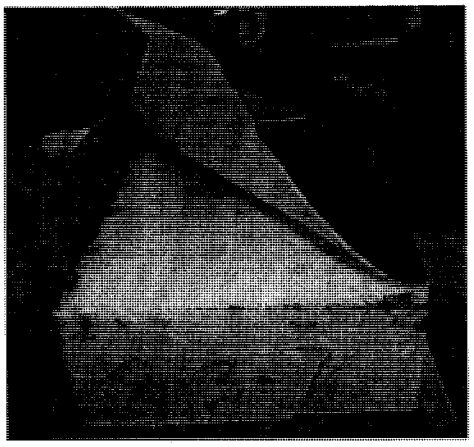

Sample #10: AF-ACB-30º-E (S2-4)

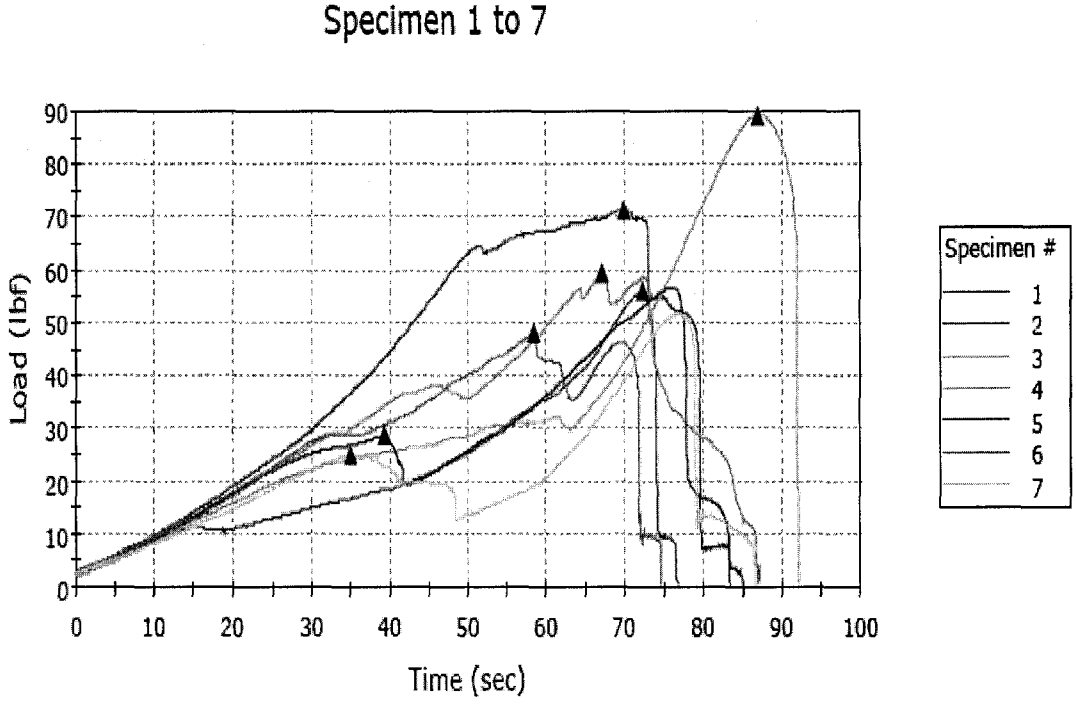

	Maximum Load (lbf)	Time at Maximum Load (sec)	Load at First Peak (lbf)	Time at First Peak (sec)	Average Load at Average Value (All Peaks) (lbf)
1	56	72	56	72	56
X 2	71	70	71	70	71
X 3	89	87	89	87	89
4	59	67	59	67	59
5	57	76	29	40	43
6	48	58	48	58	47
7	52	77	25	35	38
Maximum	59	77	59	72	59
Mean	54	70	43	54	49
Minimum	48	58	25	35	38
Standard Deviation	4	8	16	17	9
Mean + 1 SD	59	78	59	71	57
Mean - 1 SD	50	63	27	38	40

X: data excluded

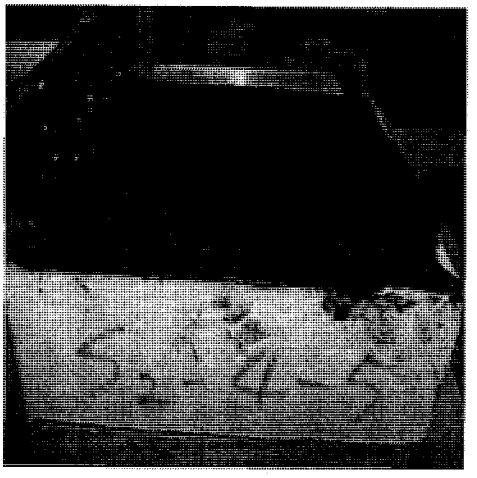

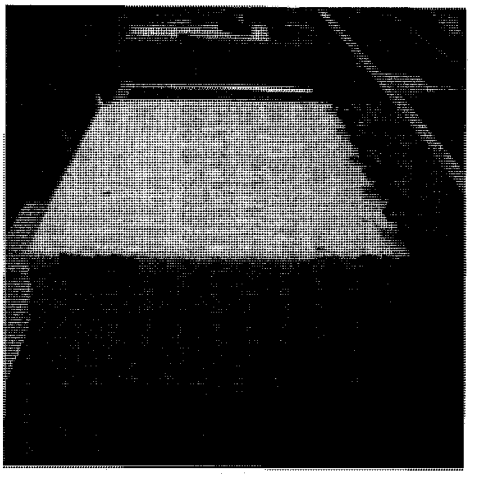

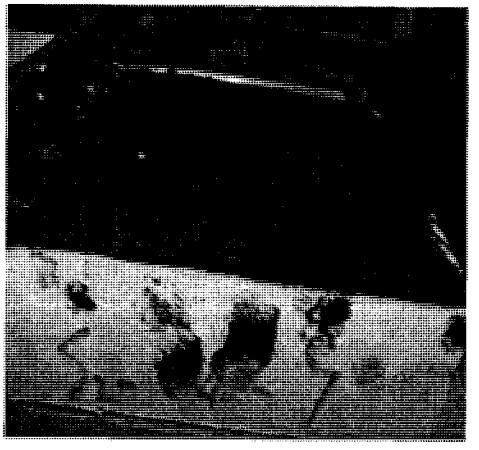

Sample #11: AF-ACB-37.5°-E (S2-5)

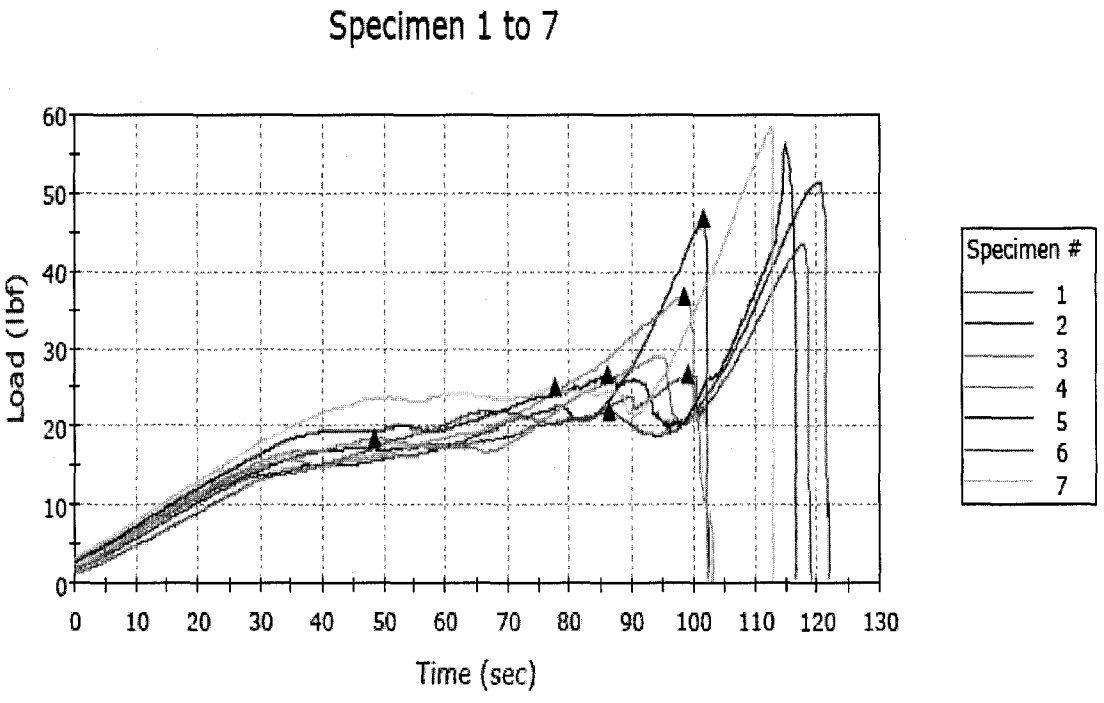

	Maximum Load (lbf)	Time at Maximum Load (sec)	Load at First Peak (lbf)	Time at First Peak (sec)	Average Load at Average Value (All Peaks) (lbf)
1	51	121	22	87	37
2	47	102	47	102	-----
X 3	37	99	37	99	37
X 4	29	95	18	48	24
5	56	115	27	86	27
6	43	118	27	99	35
7	58	113	25	78	42
Maximum	58	121	47	102	42
Mean	51	113	29	90	35
Minimum	43	102	22	78	27
Standard Deviation	6	7	10	10	6
Mean + 1 SD	57	121	39	100	41
Mean - 1 SD	45	106	19	80	29

X: data excluded

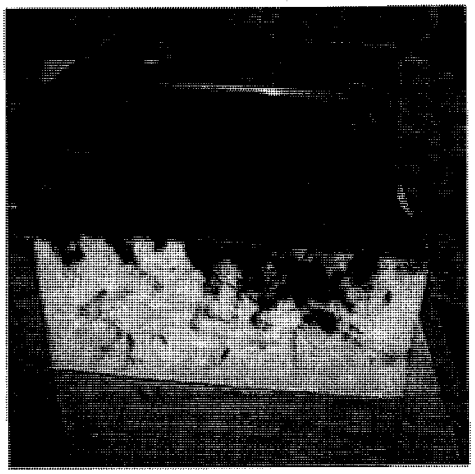

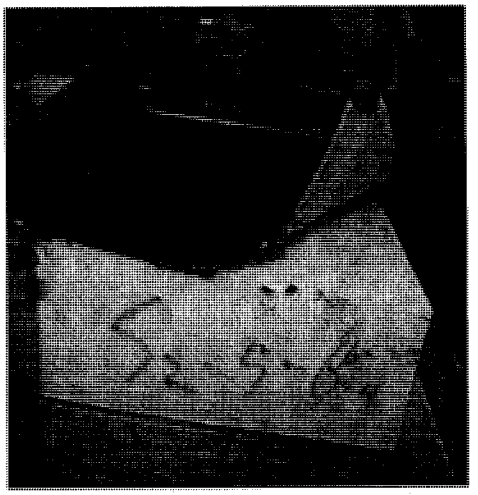

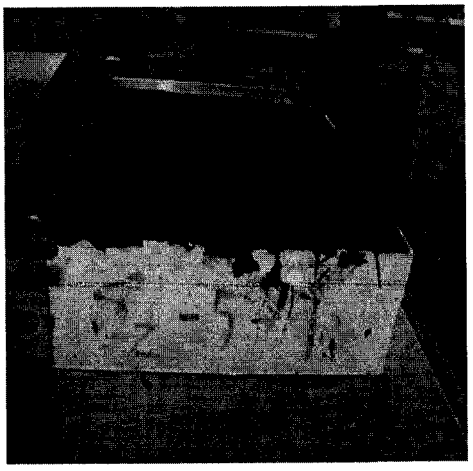

Sample #12: AF-ACB-45°-E (S2-6)

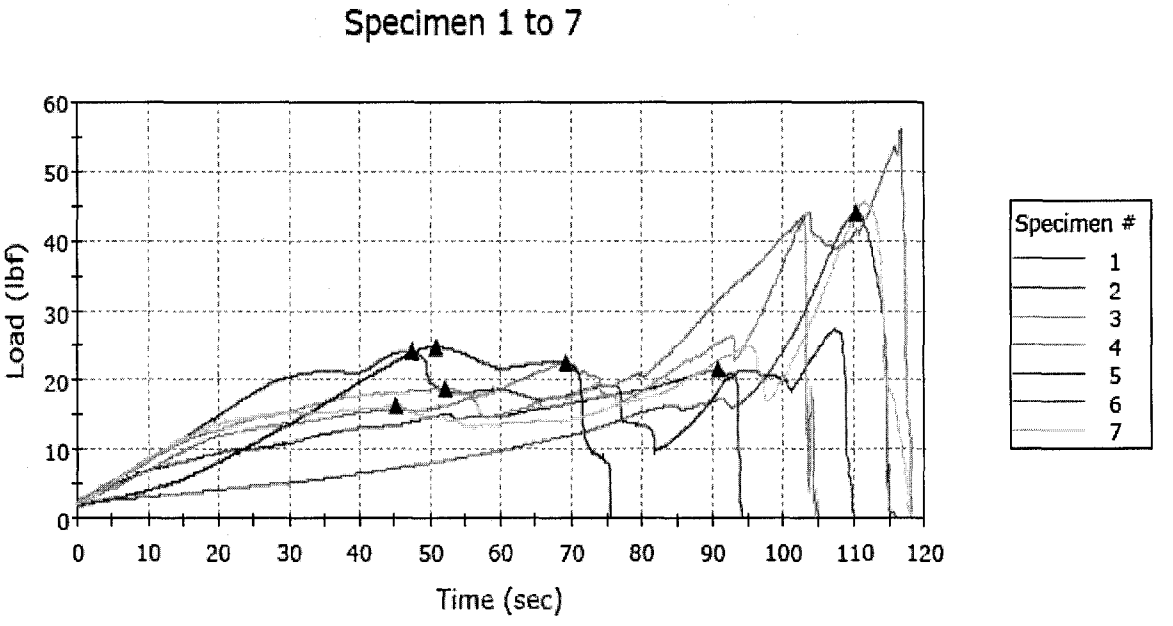

	Maximum Load (lbf)	Time at Maximum Load (sec)	Load at First Peak (lbf)	Time at First Peak (sec)	Average Load at Average Value (All Peaks) (lbf)
1	27	108	22	91	22
2	24	48	24	48	22
3	44	103	19	52	27
X 4	56	117	23	69	33
5	25	51	25	51	25
6	44	110	44	110	44
X 7	45	112	16	45	29
Maximum	44	110	44	110	44
Mean	33	84	27	70	28
Minimum	24	48	19	48	22
Standard Deviation	10	32	10	28	9
Mean + 1 SD	43	116	37	99	37

	Maximum Load (lbf)	Time at Maximum Load (sec)	Load at First Peak (lbf)	Time at First Peak (sec)	Average Load at Average Value (All Peaks) (lbf)
Mean - 1 SD	23	52	17	42	18

X: data excluded

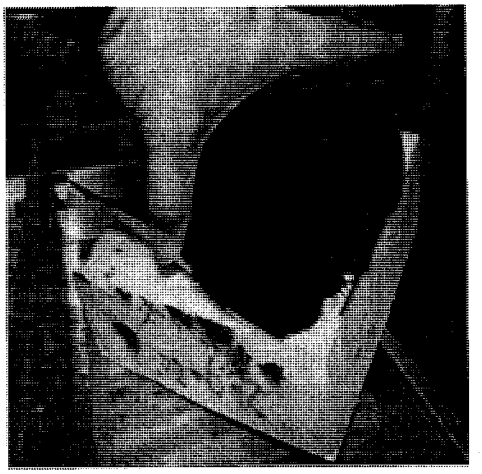

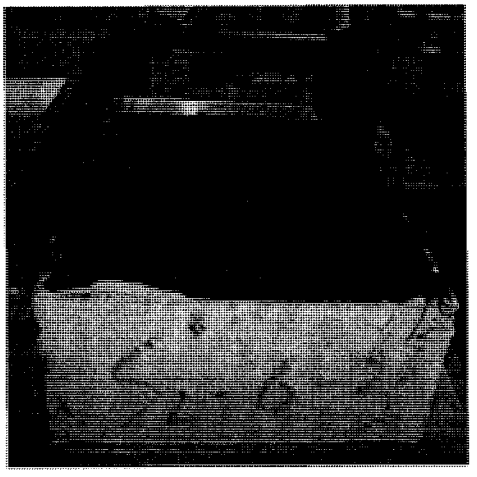

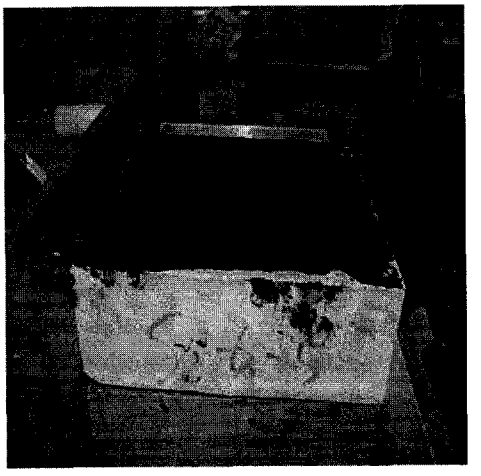

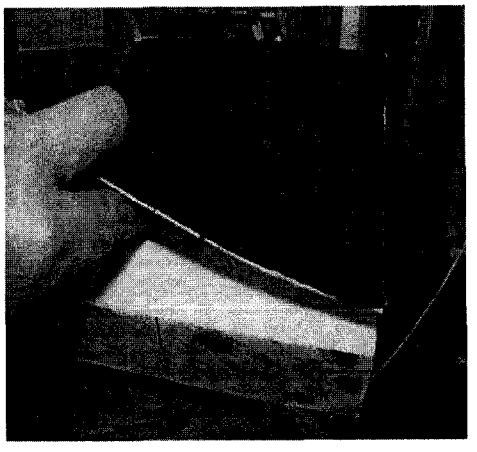

Sample #13: PF-ACB-4x4-E (S2'-4x4)

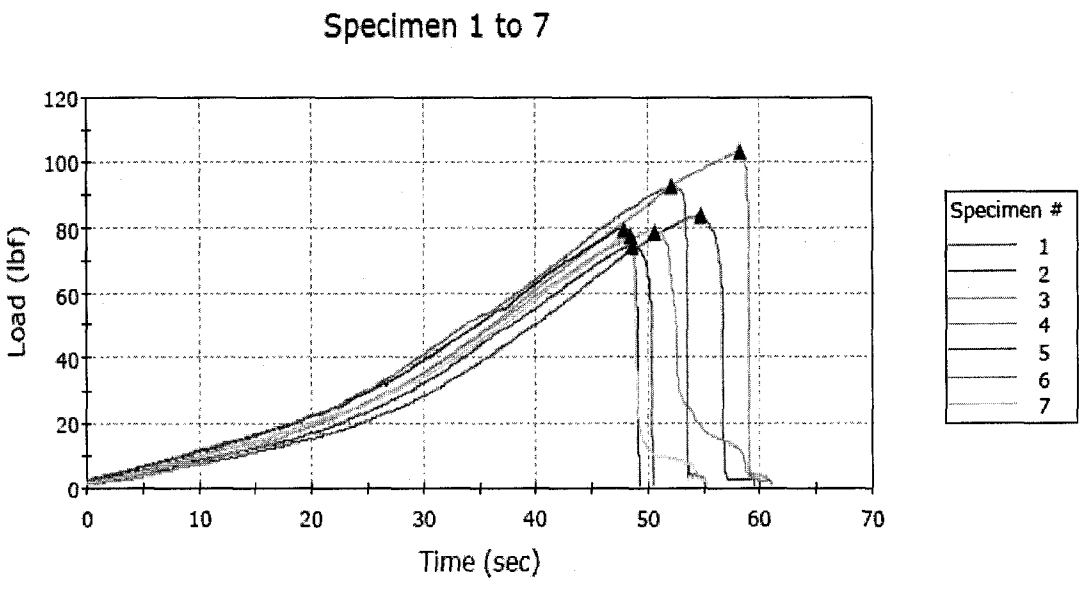

	Maximum Load (lbf)	Time at Maximum Load (sec)	Load at First Peak (lbf)	Time at First Peak (sec)	Average Load at Average Value (All Peaks) (lbf)
1	83	55	83	55	83
X 2	74	49	74	49	74
3	79	51	79	51	-----
X 4	103	58	103	58	103
5	79	48	79	48	79
6	92	52	92	52	92
7	77	49	77	49	77
Maximum	92	55	92	55	92

	Maximum Load (lbf)	Time at Maximum Load (sec)	Load at First Peak (lbf)	Time at First Peak (sec)	Average Load at Average Value (All Peaks) (lbf)
Mean	82	51	82	51	83
Minimum	77	48	77	48	77
Standard Deviation	6	3	6	3	7
Mean + 1 SD	88	54	88	54	90
Mean - 1 SD	76	48	76	48	76

X: data excluded

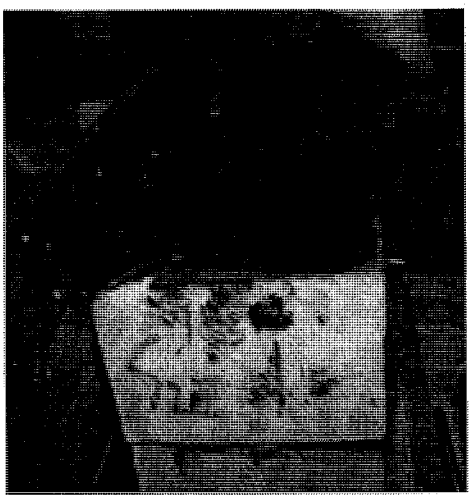

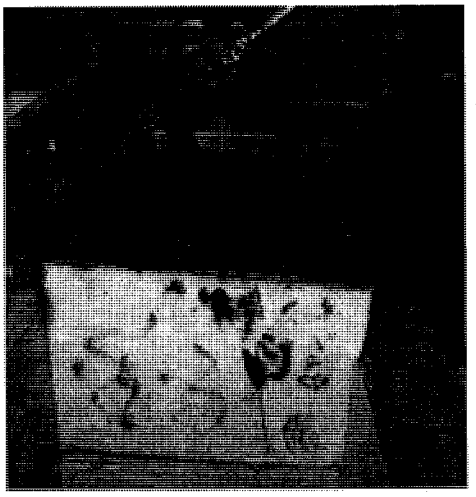

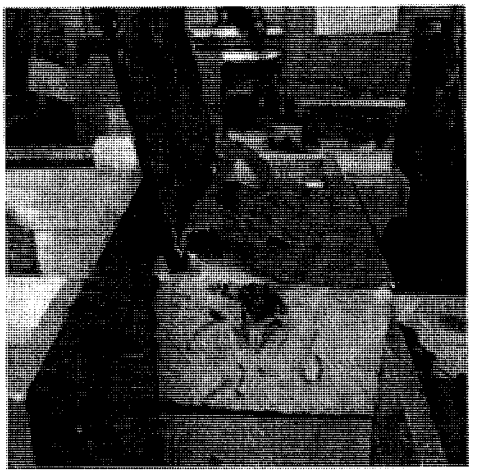

Sample #14: PF-ACB-8x8-E (S2'-8x8)

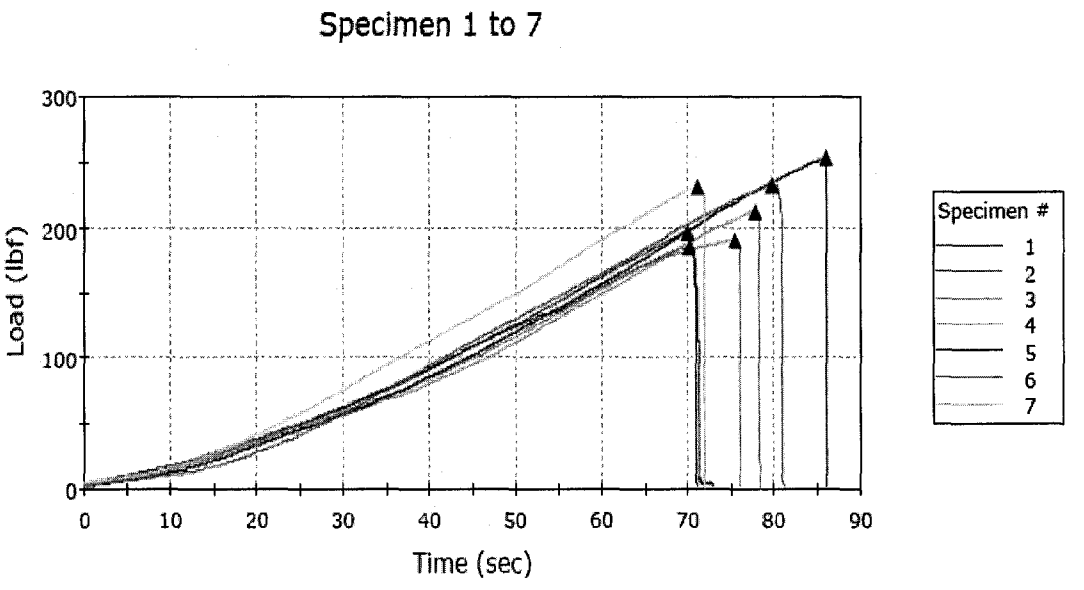

	Maximum Load (lbf)	Time at Maximum Load (sec)	Load at First Peak (lbf)	Time at First Peak (sec)	Average Load at Average Value (All Peaks) (lbf)
1	197	70	197	70	-----
X 2	185	70	185	70	185
3	212	78	212	78	212
4	190	75	190	75	190
X 5	253	86	253	86	253
6	232	80	232	80	232
7	230	71	230	71	230
Maximum	232	80	232	80	232

	Maximum Load (lbf)	Time at Maximum Load (sec)	Load at First Peak (lbf)	Time at First Peak (sec)	Average Load at Average Value (All Peaks) (lbf)
Mean	212	75	212	75	216
Minimum	190	70	190	70	190
Standard Deviation	19	4	19	4	20
Mean + 1 SD	231	79	231	79	236
Mean - 1 SD	193	71	193	71	197

X: data excluded

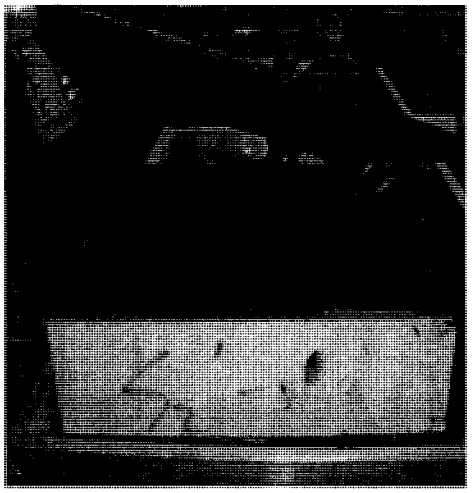

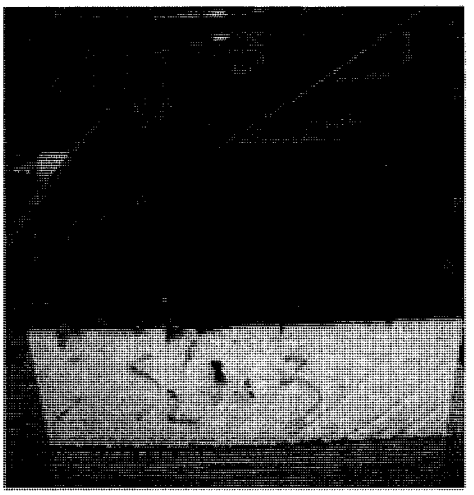

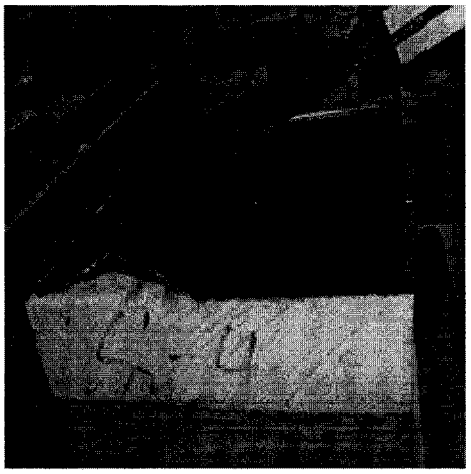

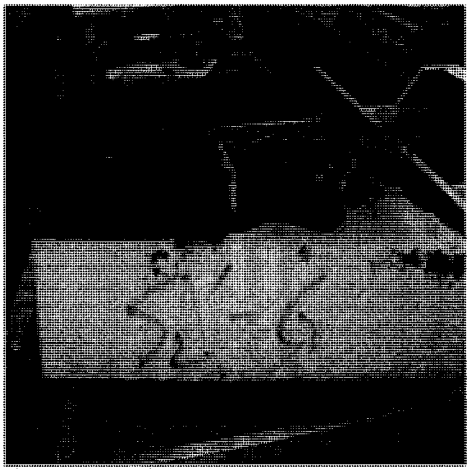

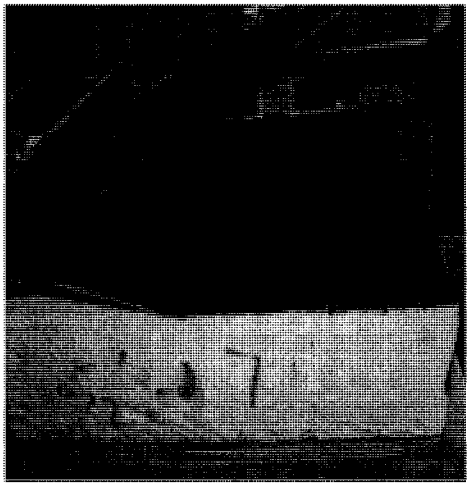

Sample #15: PF-ACB-10x10-E (S2'-10x10)

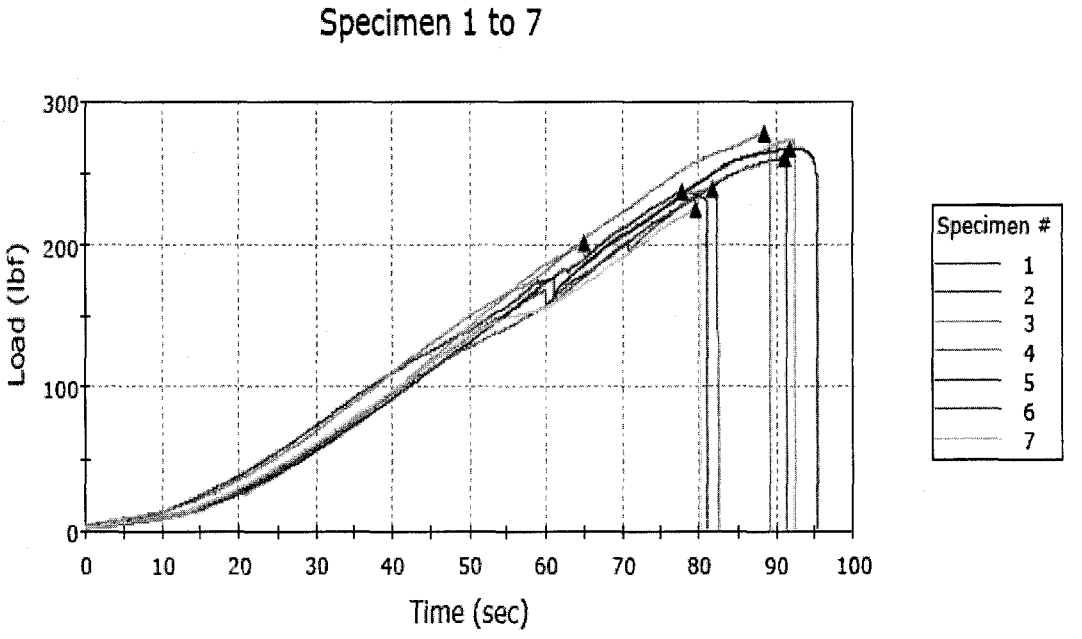

	Maximum Load (lbf)	Time at Maximum Load (sec)	Load at First Peak (lbf)	Time at First Peak (sec)	Average Load at Average Value (All Peaks) (lbf)
1	260	91	260	91	260
2	236	78	236	78	236
3	274	92	201	65	237
X 4	278	89	278	89	278
5	267	92	267	92	267
6	239	82	239	82	239
X 7	225	80	225	80	225
Maximum	274	92	267	92	267
Mean	255	87	241	82	248

	Maximum Load (lbf)	Time at Maximum Load (sec)	Load at First Peak (lbf)	Time at First Peak (sec)	Average Load at Average Value (All Peaks) (lbf)
Minimum	236	78	201	65	236
Standard Deviation	17	7	26	11	15
Mean + 1 SD	272	94	267	92	263
Mean - 1 SD	239	80	215	71	234

X: data excluded

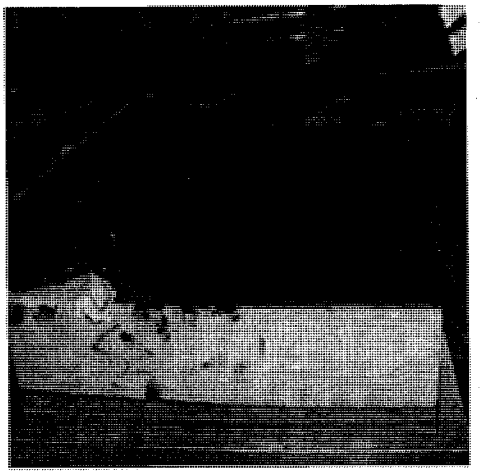

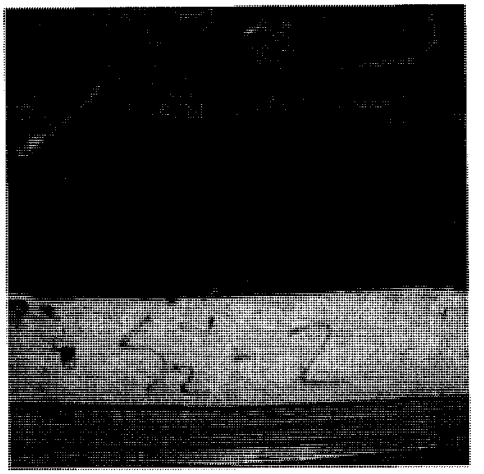

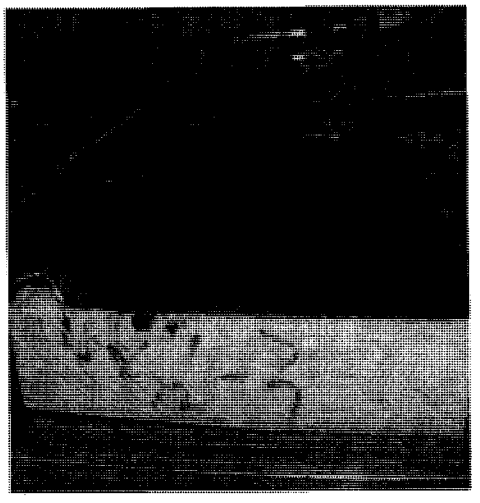

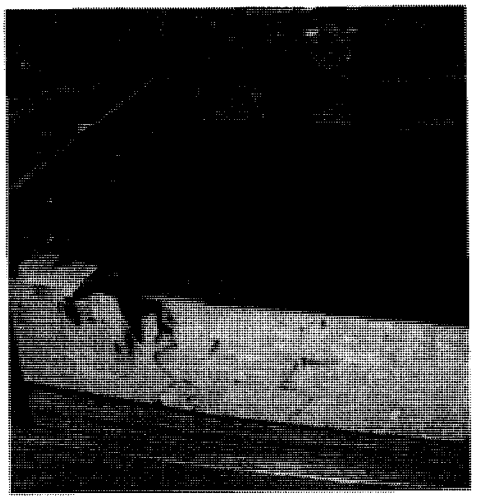

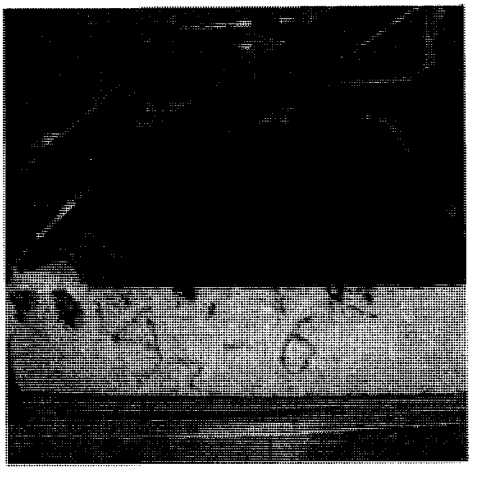

Appendix 6

Peel Resistance Data from Source IV

(Phase II)

Table 1. Peel Resistance (lbf) of PF/ACB Samples for Different Angle Peel test at the Edge Position

Test Anger (°)	7.5		15		22.5		30		37.5		45	
Specimen PF/ACB ID	Peel Resistance	Failure Mode	Peel Resistanc	Failure Mode	Peel Resistanc	Failure Mode	Peel Resistanc	Failure Mode	Peel Resistanc	Failure Mode	Peel Resistanc	Failure Mode
#1	263	Facer/D	251	Facer/D	205	CB/B	131	Facer/R	94	Adh	93	Facer/R
#2	254	Adh	249	Facer/D	176	Facer/R	133	Facer/R	110	Facer/R	85	Adhesive
#3	275	Facer/D	220	Facer/D	160	Adh	161	Adh	93	Adh	100	Facer/(D & R)
#4	273	Adh	268	Adh	209	Adh	160	Facer/R	98	Facer/R	102	Adh
#5	251	Adh	218	Adh	166	Adh	126	Facer/R	110	Adh	92	Facer/R
Mean Load	263		241		183		142		101		94	
Standard Deviation	11		22		22		17		8		7	

Table 2. Peel Resistance (lbf) of AF/ACB Samples for Different Angle Peel test at the Edge Position

Test Anger (°)	7.5		15		22.5		30		37.5		45	
Specimen AF/ACB ID	Peel Resistance	Failure Mode	Peel Resistance	Failure Mode	Peel Resistance	Failure Mode	Peel Resistance	Failure Mode	Peel Resistance	Failure Mode	Peel Resistance	Failure Mode
#1	344	Facer/D	136	Facer/D	67	Facer/D	60	Facer/D	67	Facer/D	39	Facer/D
#2	282	Facer/D	145	Facer/D	75	Facer/D	66	Facer/D	64	Facer/D	37	Facer/D
#3	314	CB/B	105	Facer/D	99	Facer/D	65	Facer/D	50	Facer/D	43	Facer/D
#4	216	CB/B	127	CB/B	81	Facer/D	72	Facer/D	69	Facer/D	35	Facer/D
#5	200	Facer/D	111	Facer/D	111	Facer/D	56	Facer/D	56	Facer/D	33	Facer/D
Mean Load	**271**		**125**		**87**		**64**		**61**		**37**	
Standard Deviation	62		17		18		6		8		4	

Table 3. Peel Resistance (lbf) of PF/ACB Samples for Different Sample Size Peel test at the Edge Position

Sample Size	4x4		6x6		8x8		10x10	
Specimen PF/ACB ID	Peel Resistance	Failure Mode	Peel Resistance	Failure Mode	Peel Resistance	Failure Mode	Peel Resistance	Failure Mode
#1	98	Adh.	251	Facer/D	263	CB/B	272	CB/B
#2	102	Adh.	249	Facer/D	252	Facer/D	310	CB/B
#3	90	CB/B	220	Facer/D	287	Facer/D	320	CB/B
#4	97	Adh.	268	Adh.	296	Facer/D	273	CB/B
#5	96	CB/B	218	Adh.	295	CB/B	282	CB/B
Ave. Load	97		241		278		291	
Standard Deviation	5		22		20		22	

Sample #1: PF-ACB-7.5°-E (S4'-1)

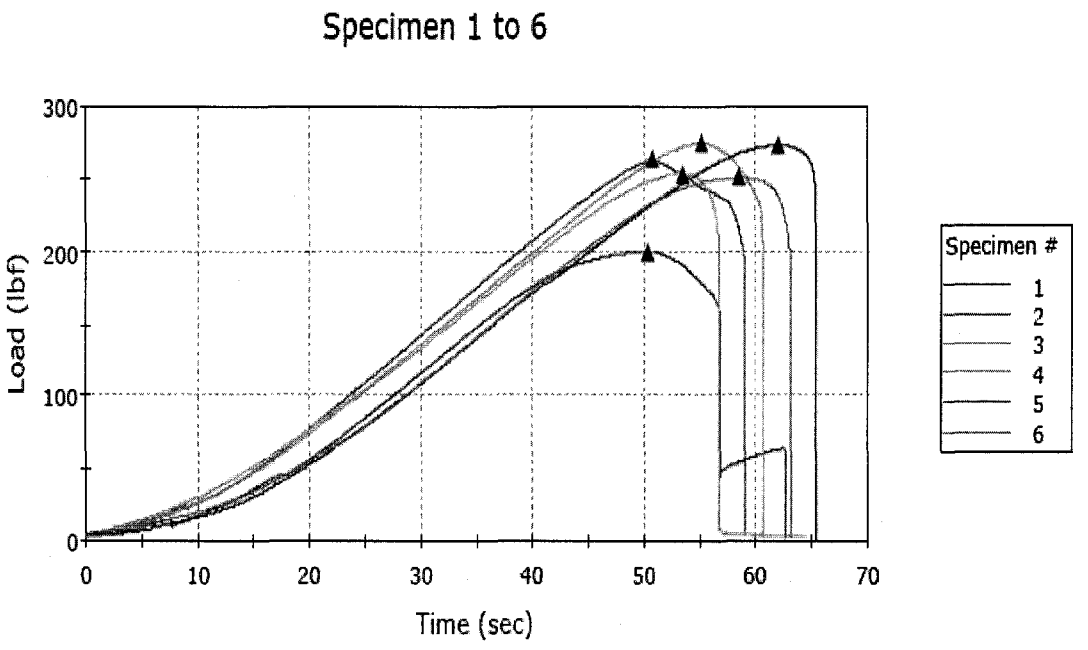

	Maximum Load (lbf)	Time at Maximum Load (sec)	Load at First Peak (lbf)	Time at First Peak (sec)	Average Load at Average Value (All Peaks) (lbf)
1	263	51	263	51	263
X 2	200	50	200	50	200
3	254	54	254	54	254
4	275	55	275	55	275
5	273	62	273	62	273
6	251	59	251	59	251
Maximum	275	62	275	62	275
Mean	263	56	263	56	263
Minimum	251	51	251	51	251
Standard Deviation	11	4	11	4	11
Mean + 1 SD	274	60	274	60	274
Mean - 1 SD	252	52	252	52	252

X: data excluded

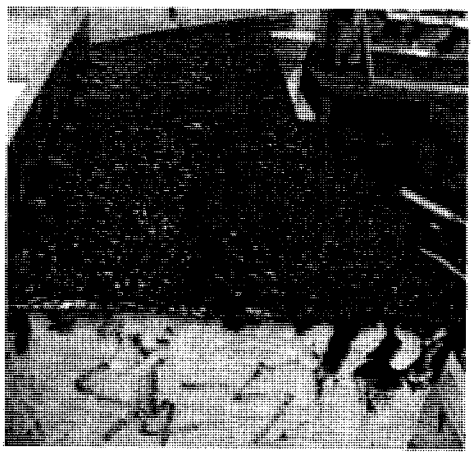

Sample #2: PF-ACB-15°-E (S4'-2)

Specimen 1 to 6

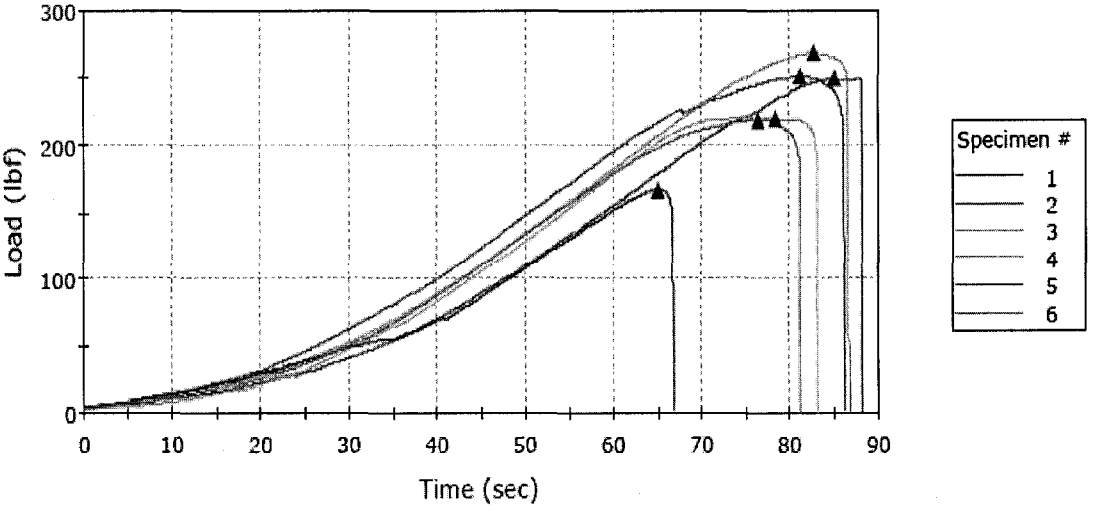

	Maximum Load (lbf)	Time at Maximum Load (sec)	Load at First Peak (lbf)	Time at First Peak (sec)	Average Load at Average Value (All Peaks) (lbf)
1	251	81	251	81	251
2	249	85	249	85	249
3	220	78	220	78	220
4	268	83	268	83	268
X 5	167	65	167	65	167
6	218	77	218	77	218
Maximum	268	85	268	85	268
Mean	241	81	241	81	241
Minimum	218	77	218	77	218
Standard Deviation	22	3	22	3	22
Mean + 1 SD	263	84	263	84	263
Mean - 1 SD	220	77	220	77	220

X: data excluded

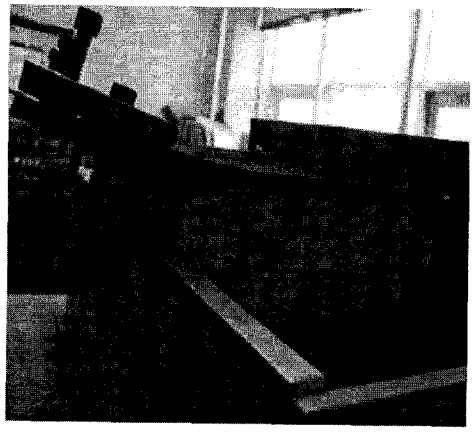

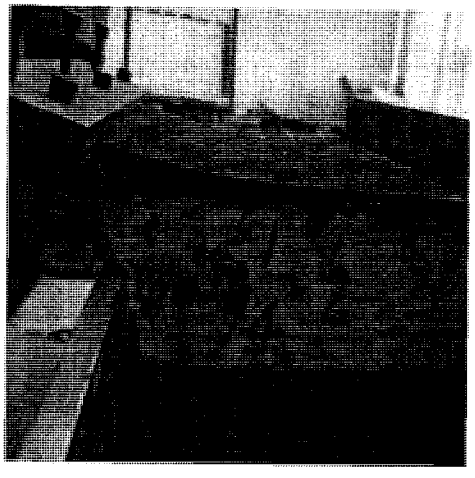

Sample #3: PF-ACB-22.5°-E (S4'-3)

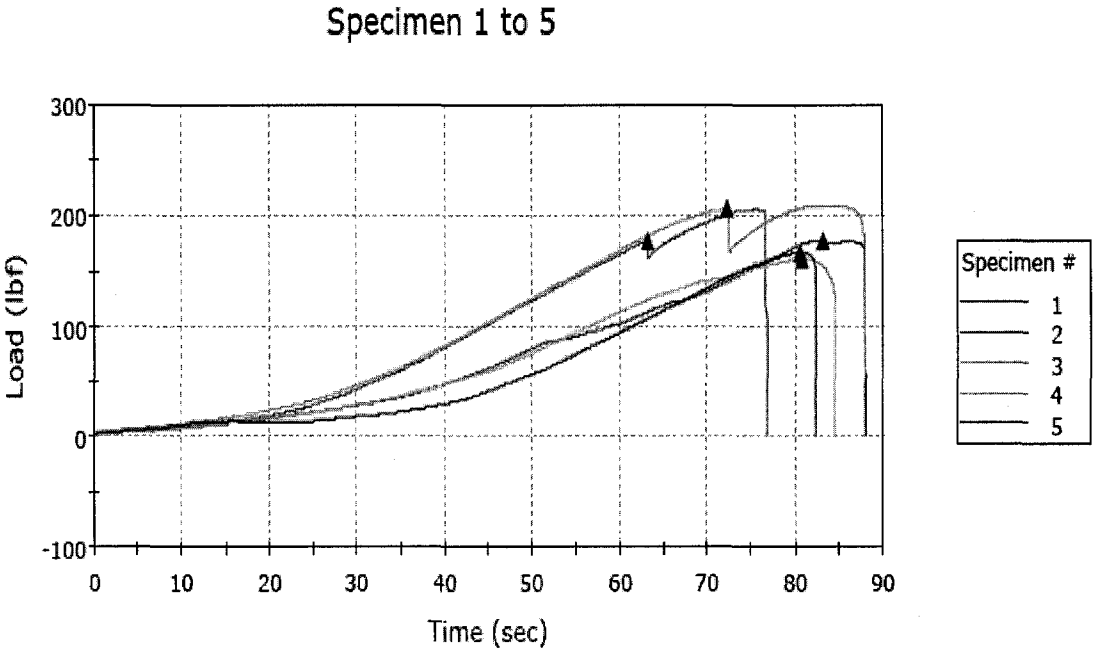

	Maximum Load (lbf)	Time at Maximum Load (sec)	Load at First Peak (lbf)	Time at First Peak (sec)	Average Load at Average Value (All Peaks) (lbf)
1	205	76	177	63	191
2	176	83	176	83	176
3	160	81	160	81	160
4	209	83	205	72	207
5	166	81	166	81	166
Maximum	209	83	205	83	207
Mean	183	81	177	76	180
Minimum	160	76	160	63	160
Standard Deviation	22	3	17	8	19
Mean + 1 SD	206	84	194	84	199
Mean - 1 SD	161	78	159	68	161

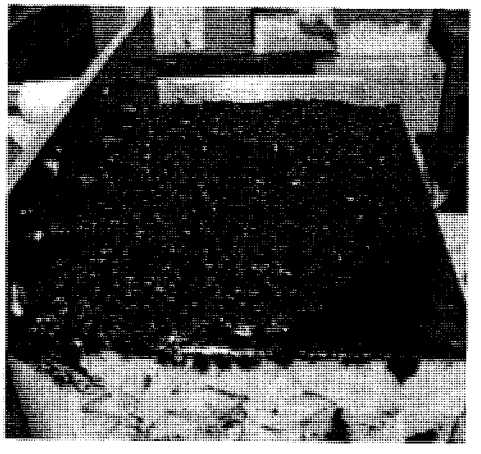

Sample #4: PF-ACB-30°-E (S4'-4)

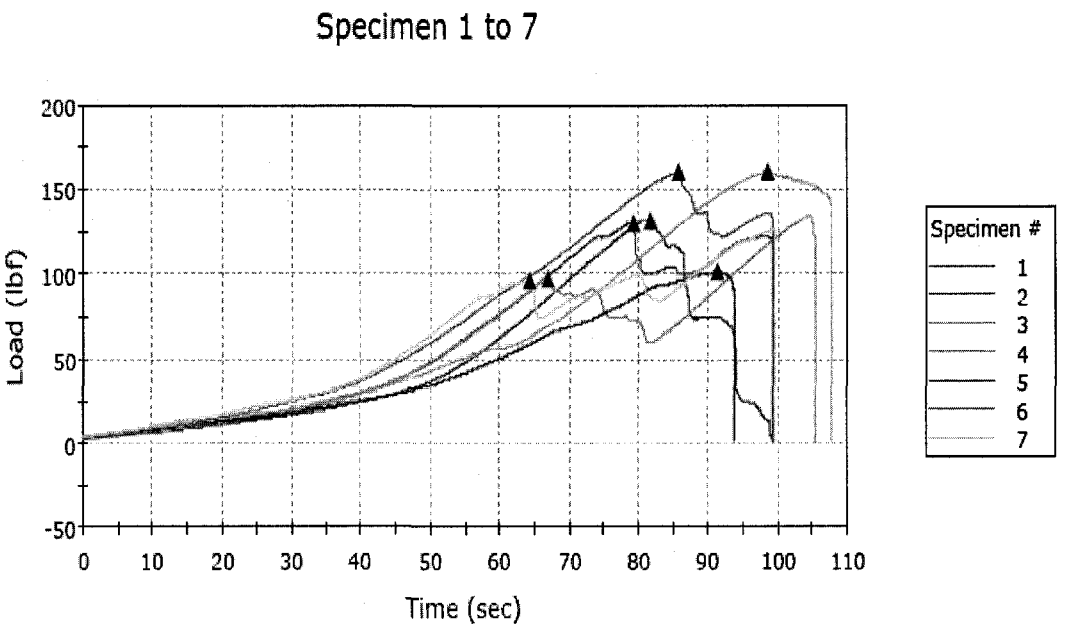

	Maximum Load (lbf)	Time at Maximum Load (sec)	Load at First Peak (lbf)	Time at First Peak (sec)	Average Load at Average Value (All Peaks) (lbf)
1	131	79	131	79	131
2	133	82	133	82	133
3	161	99	161	99	-----
X 4	135	105	99	67	117
X 5	101	92	101	92	101
6	160	86	160	86	148
7	126	99	96	64	108
Maximum	161	99	161	99	148
Mean	142	89	136	82	130
Minimum	126	79	96	64	108
Standard Deviation	17	9	26	12	17
Mean + 1 SD	159	98	163	94	146
Mean - 1 SD	125	79	110	70	113

X: data excluded

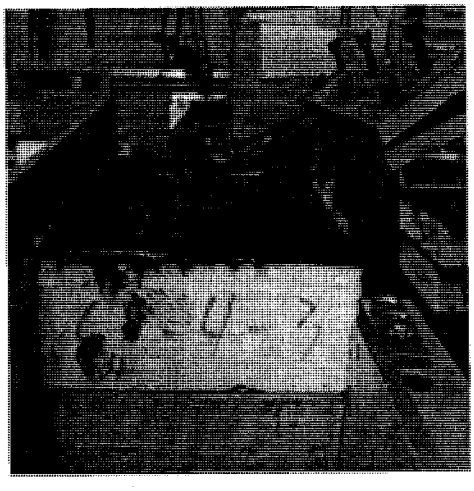

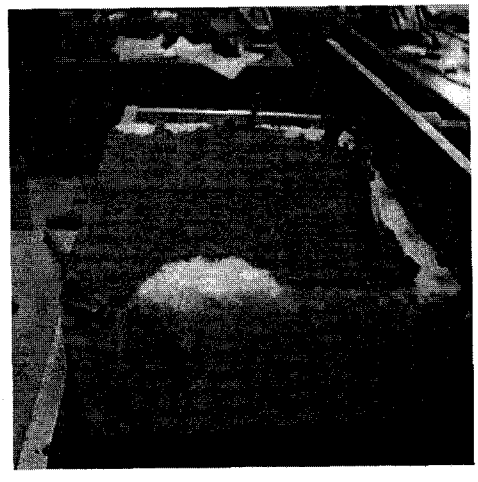

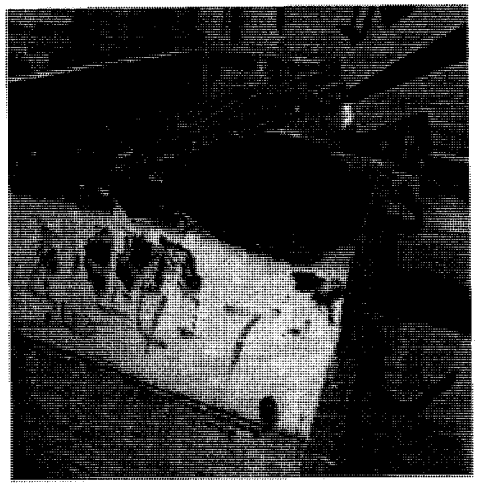

Sample #5: PF-ACB-37.5°-E (S4'-5)

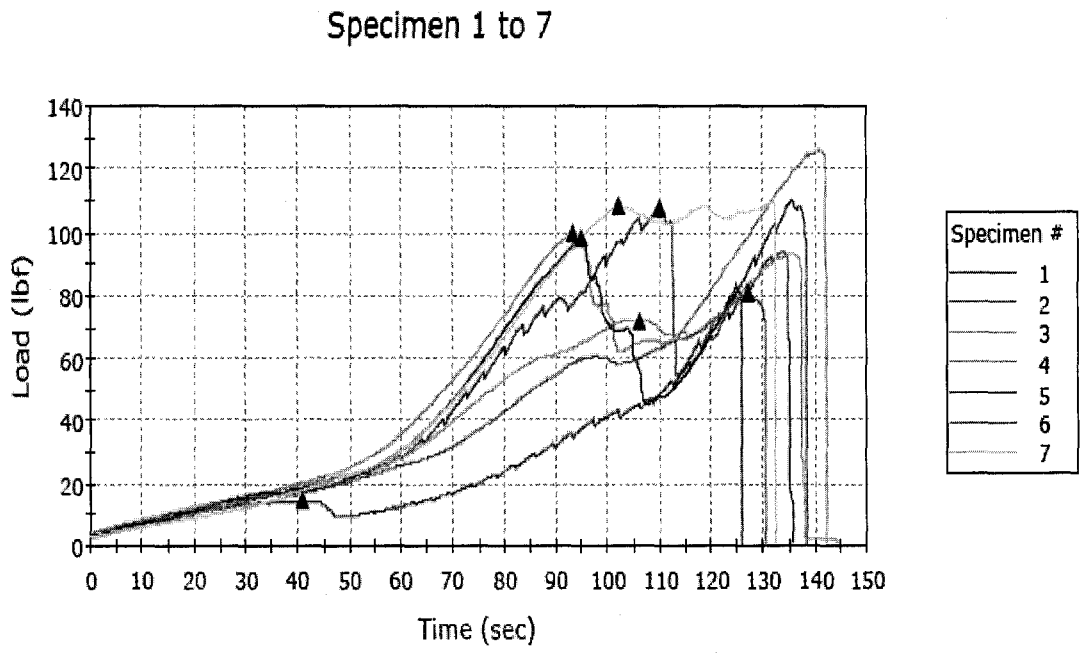

	Maximum Load (lbf)	Time at Maximum Load (sec)	Load at First Peak (lbf)	Time at First Peak (sec)	Average Load at Average Value (All Peaks) (lbf)
1	94	134	14	41	54
2	110	136	107	110	109
3	93	136	72	106	83
X 4	126	141	100	93	113
5	98	95	98	95	98
X 6	80	127	80	127	80
7	110	132	109	102	109
Maximum	110	136	109	110	109
Mean	101	126	80	91	90
Minimum	93	95	14	41	54
Standard Deviation	8	18	40	28	23
Mean + 1 SD	109	144	120	119	113
Mean - 1 SD	93	109	41	62	67

X: data excluded

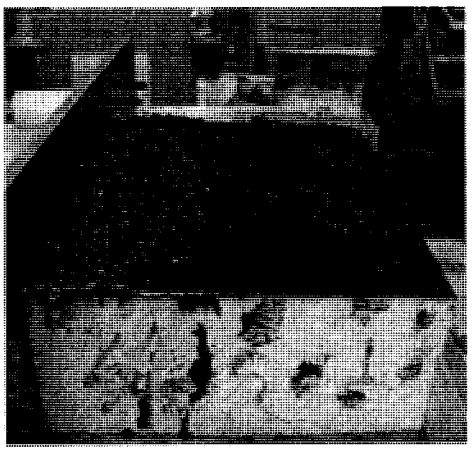

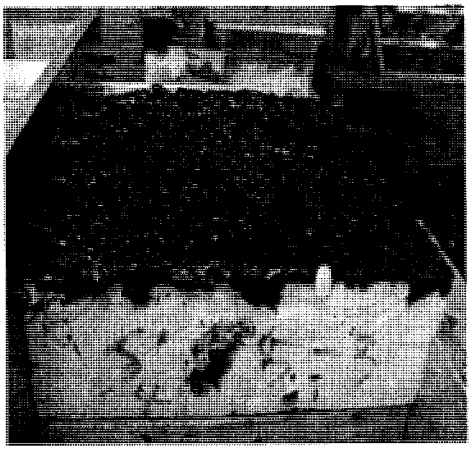

Sample #6: PF-ACB-45°-E (S4'-6)

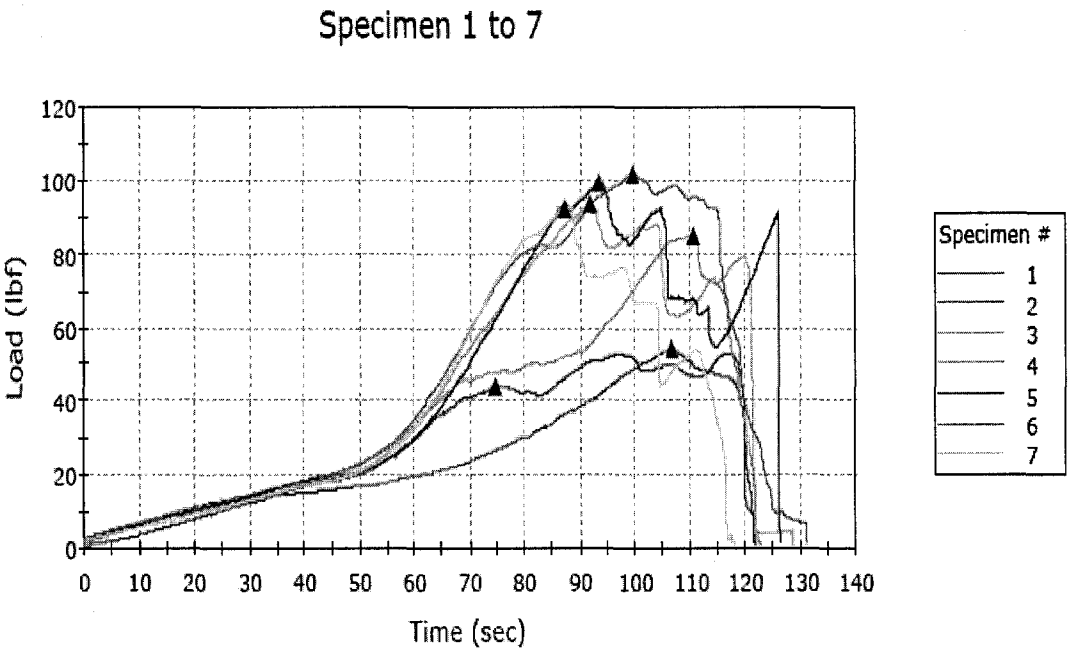

	Maximum Load (lbf)	Time at Maximum Load (sec)	Load at First Peak (lbf)	Time at First Peak (sec)	Average Load at Average Value (All Peaks) (lbf)
X 1	54	107	54	107	54
X 2	53	117	44	75	50
3	93	92	93	92	87
4	85	111	85	111	85
5	100	94	100	94	96
6	102	100	102	100	102
7	92	88	92	88	92
Maximum	102	111	102	111	102
Mean	94	97	94	97	92
Minimum	85	88	85	88	85
Standard Deviation	7	9	7	9	7
Mean + 1 SD	101	106	101	106	99
Mean - 1 SD	88	88	88	88	86

X: data excluded

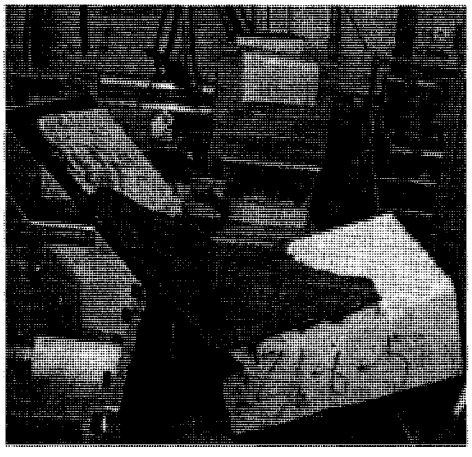

Sample #7: AF-ACB-7.5°-E (S4-1)

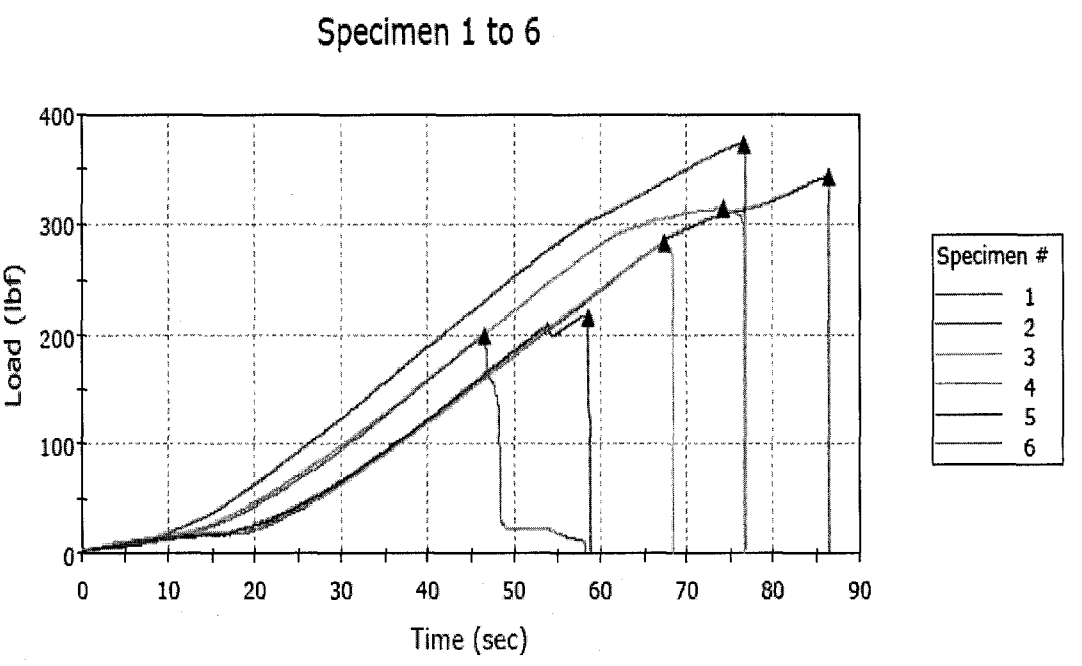

	Maximum Load (lbf)	Time at Maximum Load (sec)	Load at First Peak (lbf)	Time at First Peak (sec)	Average Load at Average Value (All Peaks) (lbf)
X 1	373	77	373	77	-----
2	344	86	344	86	344
3	282	68	282	68	282
4	314	74	314	74	314
5	216	59	216	59	216
6	200	47	200	47	200
Maximum	344	86	344	86	344
Mean	271	67	271	67	271
Minimum	200	47	200	47	200

	Maximum Load (lbf)	Time at Maximum Load (sec)	Load at First Peak (lbf)	Time at First Peak (sec)	Average Load at Average Value (All Peaks) (lbf)
Standard Deviation	62	15	62	15	62
Mean + 1 SD	333	82	333	82	333
Mean - 1 SD	209	52	209	52	209

X: data excluded

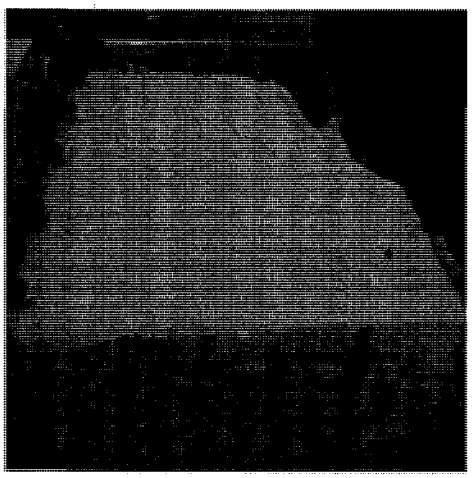

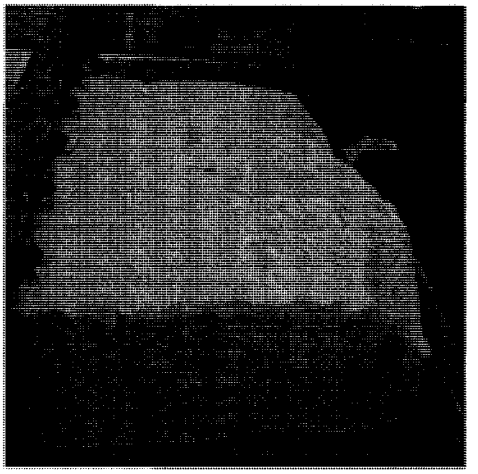

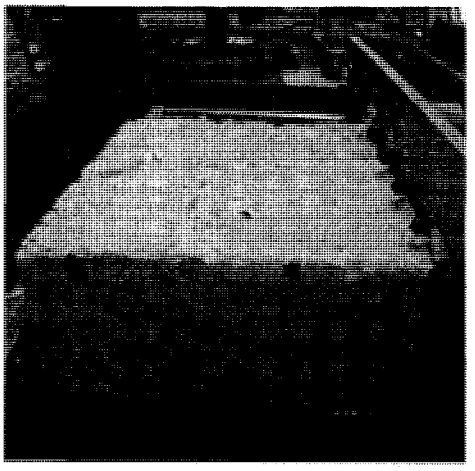

Sample #8: AF-ACB-15°-E (S4-2)

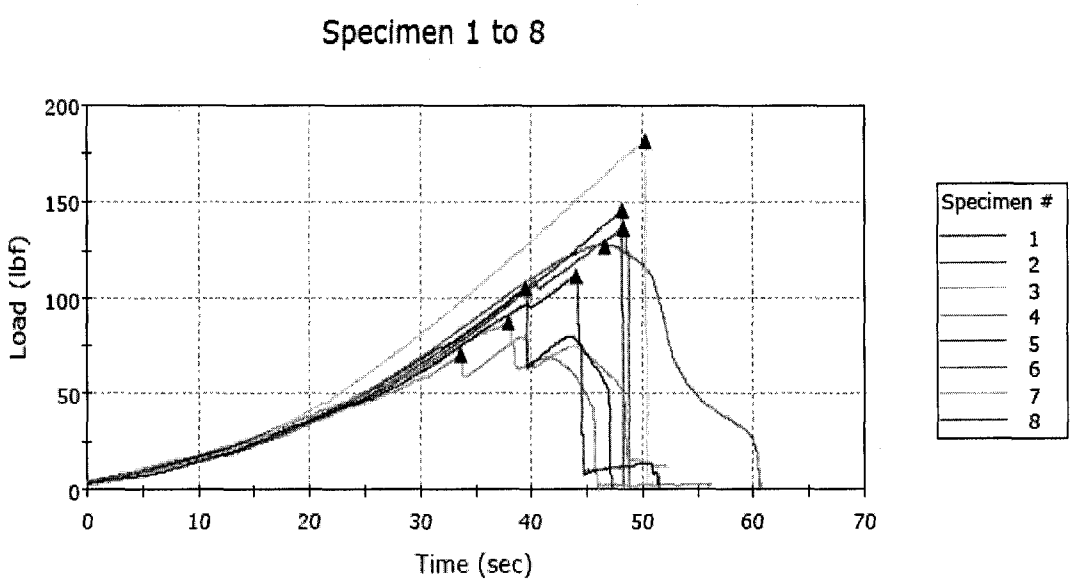

	Maximum Load (lbf)	Time at Maximum Load (sec)	Load at First Peak (lbf)	Time at First Peak (sec)	Average Load at Average Value (All Peaks) (lbf)
1	136	48	136	48	136
2	145	48	145	48	145
X 3	80	39	70	34	75
X 4	86	38	86	38	86
5	105	40	105	40	105
6	127	47	127	47	127
X 7	181	50	181	50	181
8	111	44	111	44	111
Maximum	145	48	145	48	145
Mean	125	45	125	45	125
Minimum	105	40	105	40	105
Standard Deviation	17	4	17	4	17
Mean + 1 SD	142	49	142	49	142

	Maximum Load (lbf)	Time at Maximum Load (sec)	Load at First Peak (lbf)	Time at First Peak (sec)	Average Load at Average Value (All Peaks) (lbf)
Mean - 1 SD	108	42	108	42	108

X: data excluded

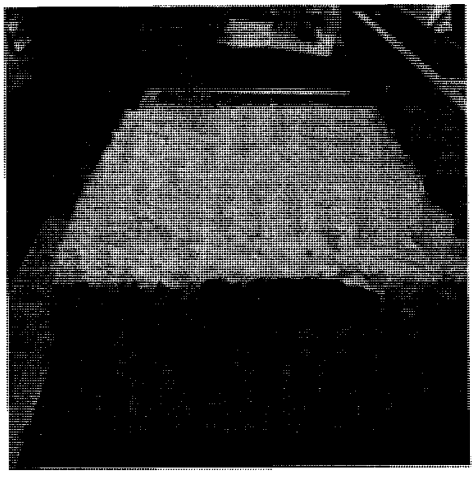

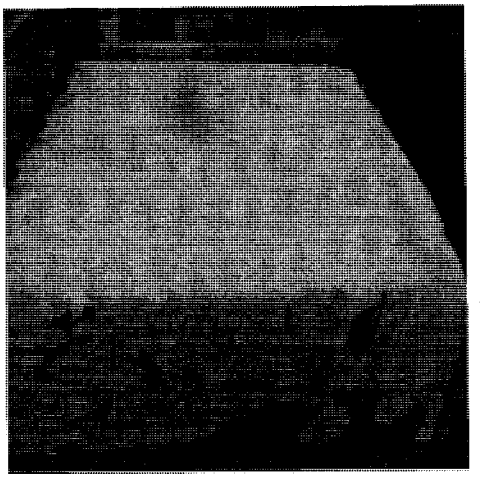

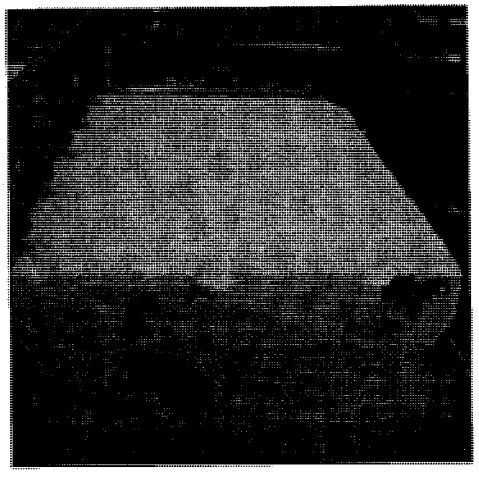

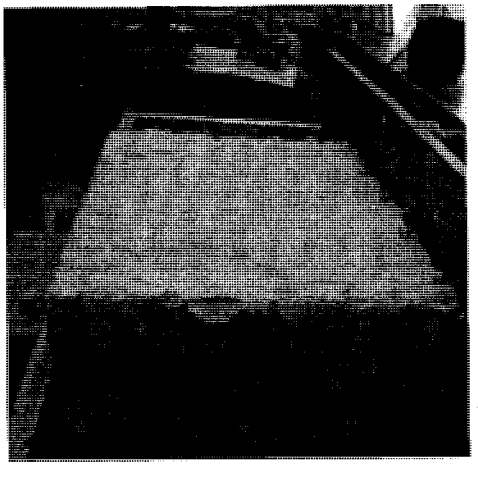

Sample #9: AF-ACB-22.5°-E (S4-3

Specimen 1 to 6

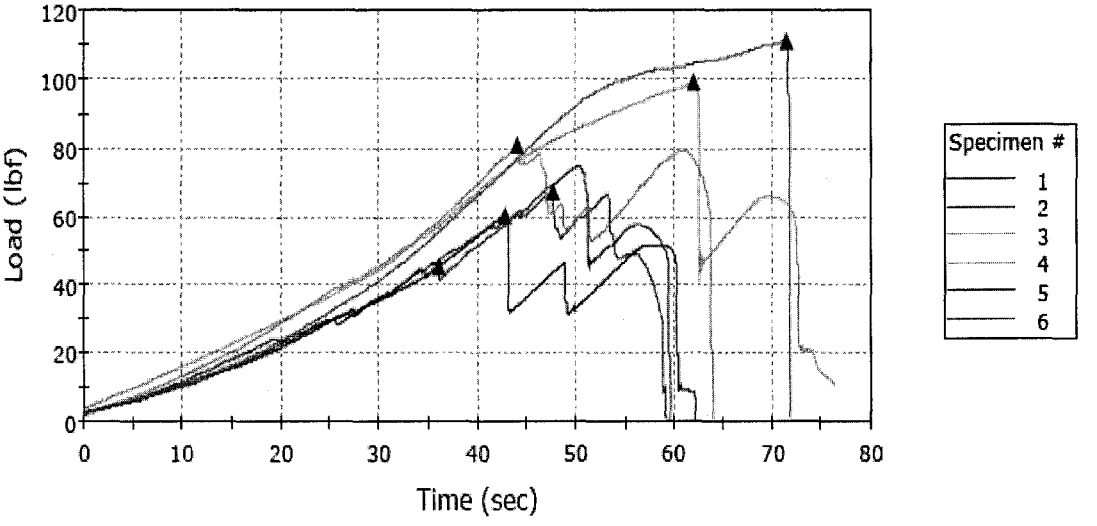

	Maximum Load (lbf)	Time at Maximum Load (sec)	Load at First Peak (lbf)	Time at First Peak (sec)	Average Load at Average Value (All Peaks) (lbf)
1	67	48	67	48	67
2	75	50	45	36	60
3	99	62	99	62	99
4	81	44	81	44	81
X 5	61	43	61	43	61
6	111	71	111	71	111
Maximum	111	71	111	71	111
Mean	87	55	81	52	84
Minimum	67	44	45	36	60

	Maximum Load (lbf)	Time at Maximum Load (sec)	Load at First Peak (lbf)	Time at First Peak (sec)	Average Load at Average Value (All Peaks) (lbf)
Standard Deviation	18.08345	11.30450	26.00218	14.24097	21.45706
Mean + 1 SD	105	66	107	66	105
Mean - 1 SD	69	44	55	38	62

X: data excluded

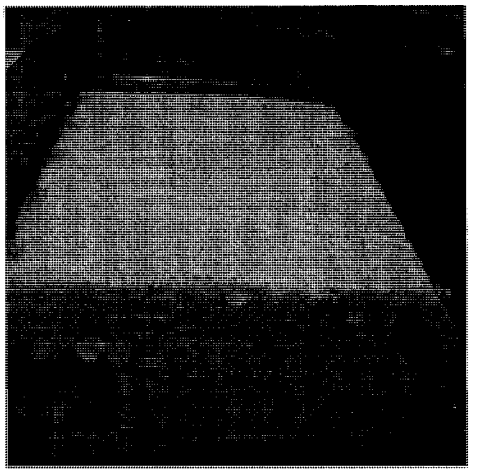

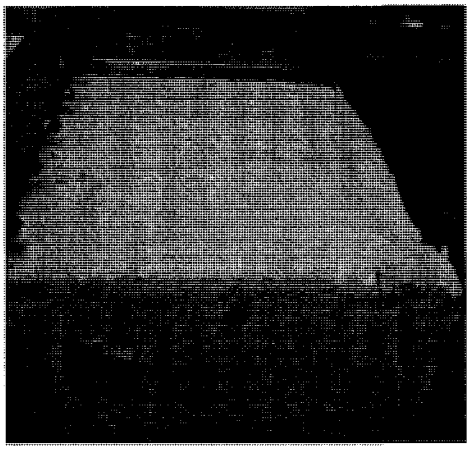

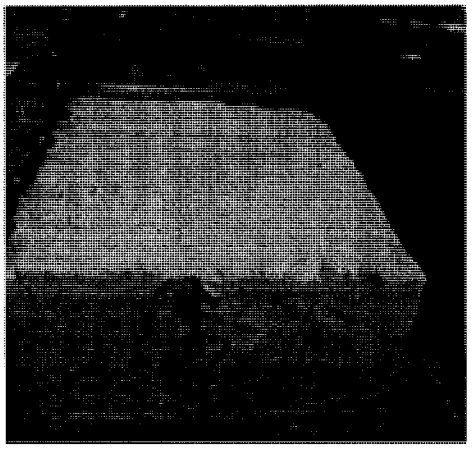

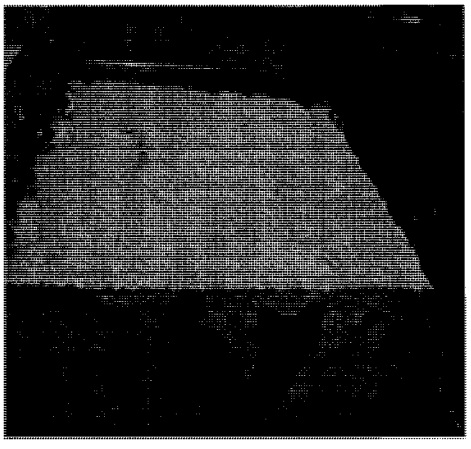

Sample #10: AF-ACB-30°-E (S4-4)

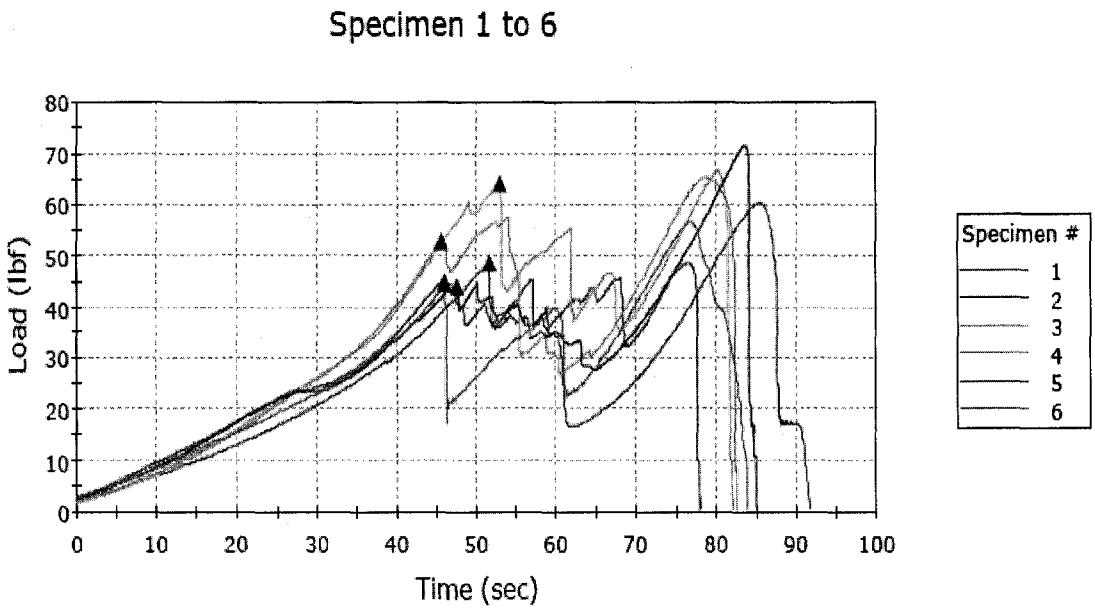

	Maximum Load (lbf)	Time at Maximum Load (sec)	Load at First Peak (lbf)	Time at First Peak (sec)	Average Load at Average Value (All Peaks) (lbf)
1	60	86	49	52	-----
X 2	49	76	45	46	43
3	66	80	64	53	55
4	65	79	53	46	55
5	72	84	44	48	44
6	56	77	44	46	42
Maximum	72	86	64	53	55
Mean	64	81	51	49	49
Minimum	56	77	44	46	42
Standard Deviation	5.82430	3.56738	8.35284	3.31557	7.05886
Mean + 1 SD	70	85	59	52	56

	Maximum Load (lbf)	Time at Maximum Load (sec)	Load at First Peak (lbf)	Time at First Peak (sec)	Average Load at Average Value (All Peaks) (lbf)
Mean - 1 SD	58	77	42	45	42

X: data excluded

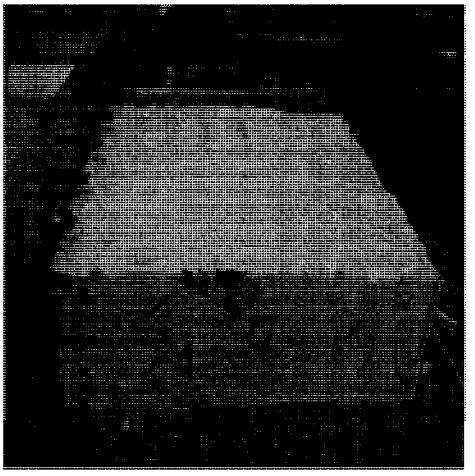

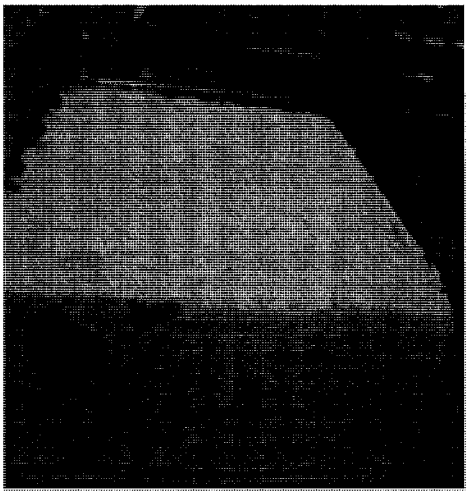

Sample #11: AF-ACB-37.5°-E (S4-5)

Specimen 1 to 7

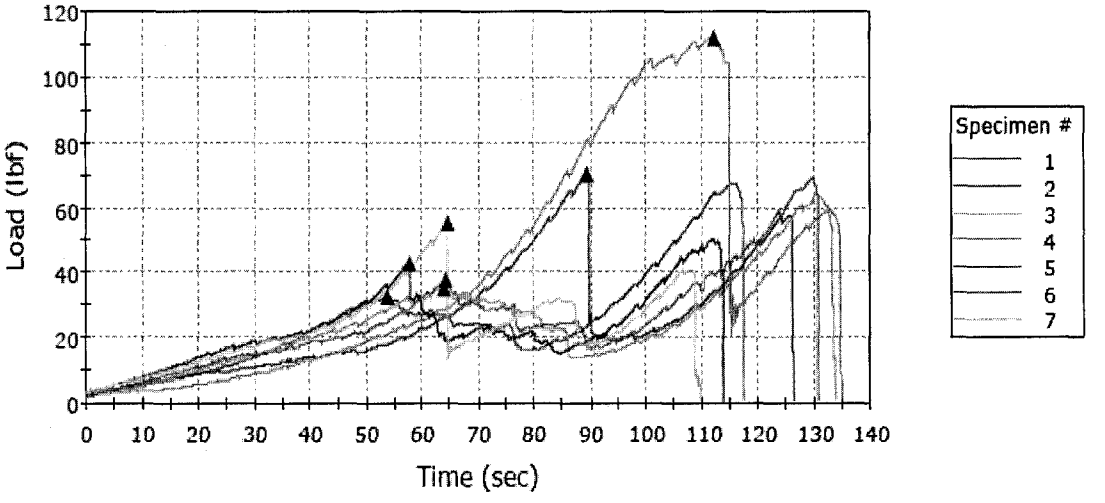

	Maximum Load (lbf)	Time at Maximum Load (sec)	Load at First Peak (lbf)	Time at First Peak (sec)	Average Load at Average Value (All Peaks) (lbf)
1	67	116	33	54	33
X 2	70	89	70	89	-----
3	64	131	35	64	35
X 4	112	112	112	112	112
5	50	112	43	58	29
6	69	130	38	64	38
7	56	65	56	65	35
Maximum	69	131	56	65	38
Mean	61	111	41	61	34
Minimum	50	65	33	54	29
Standard Deviation	8.05874	27.04780	9.07003	4.86374	3.15811

	Maximum Load (lbf)	Time at Maximum Load (sec)	Load at First Peak (lbf)	Time at First Peak (sec)	Average Load at Average Value (All Peaks) (lbf)
Mean + 1 SD	69	138	50	66	37
Mean - 1 SD	53	84	32	56	31

X: data excluded

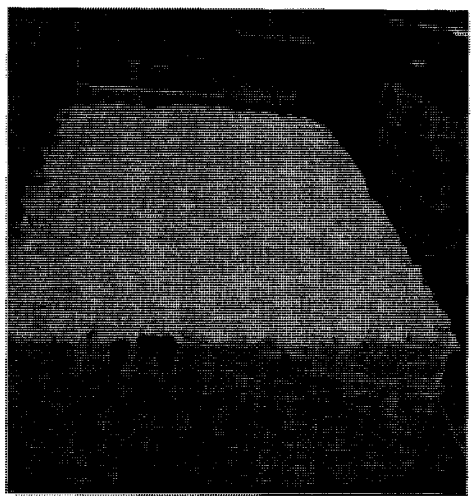

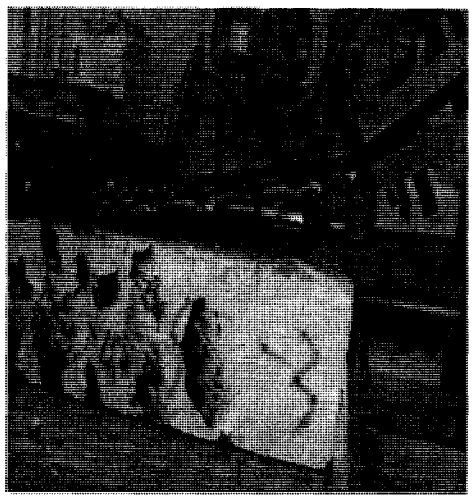

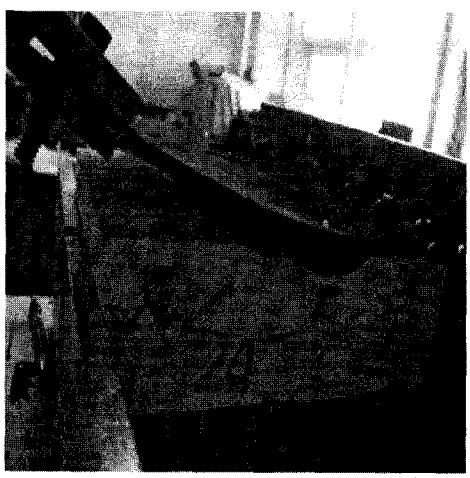

Sample #12: AF-ACB-45°-E (S4-6)

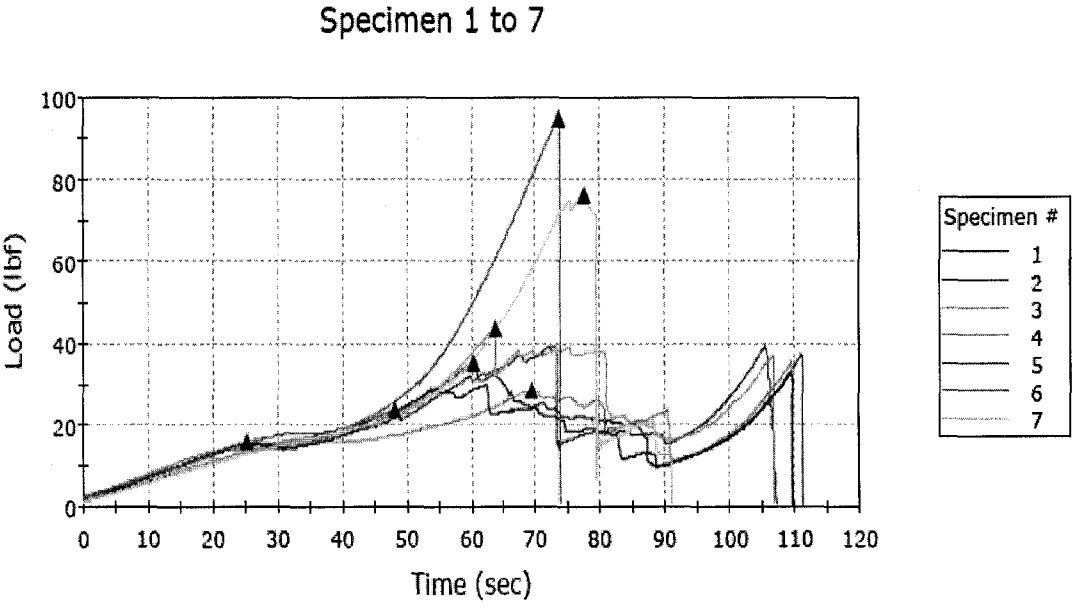

	Maximum Load (lbf)	Time at Maximum Load (sec)	Load at First Peak (lbf)	Time at First Peak (sec)	Average Load at Average Value (All Peaks) (lbf)
1	39	73	23	48	23
2	37	111	35	61	35
3	43	64	43	64	41
4	35	109	28	69	29
5	33	110	15	25	24
X 6	95	74	95	74	95
X 7	76	78	76	78	76
Maximum	43	111	43	69	41
Mean	37	93	29	53	31
Minimum	33	64	15	25	23
Standard Deviation	4.14605	23.04337	10.75572	17.48151	7.59797

	Maximum Load (lbf)	Time at Maximum Load (sec)	Load at First Peak (lbf)	Time at First Peak (sec)	Average Load at Average Value (All Peaks) (lbf)
Mean + 1 SD	42	116	40	71	38
Mean - 1 SD	33	70	18	36	23

X: data excluded

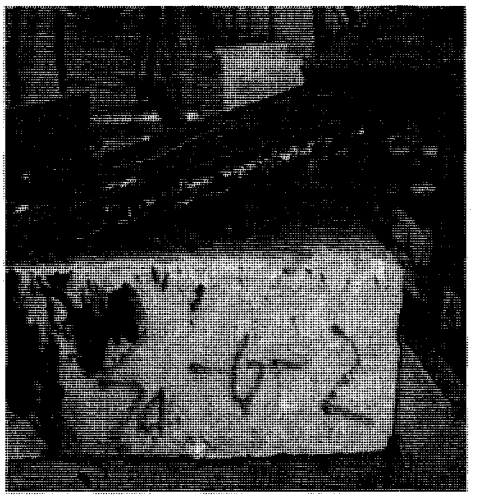

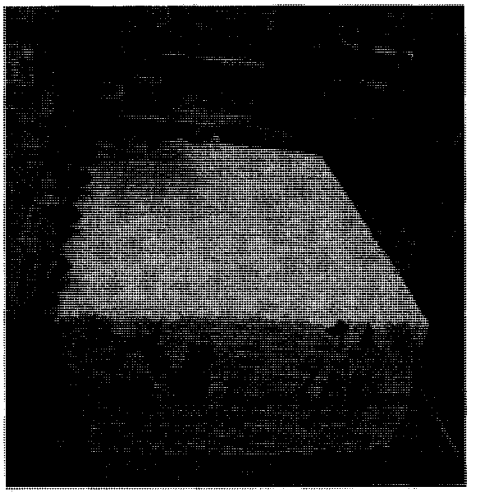

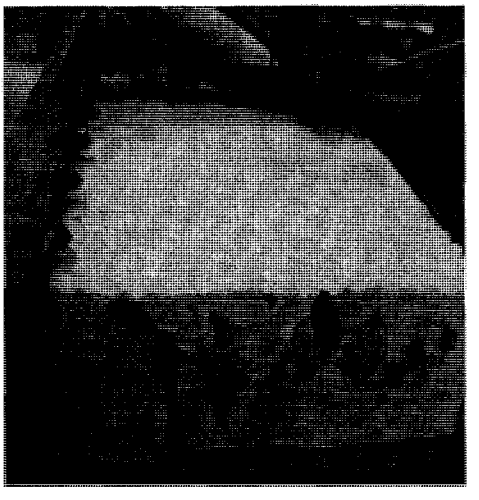

Sample #13: PF-ACB-4x4-E (S4'-4x4)

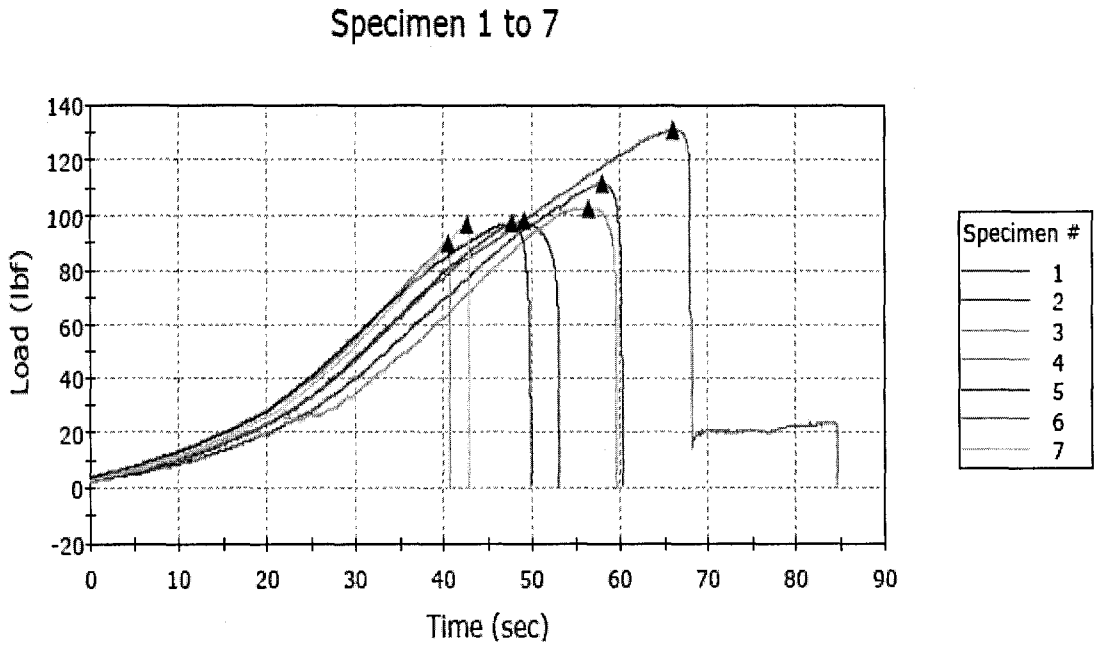

	Maximum Load (lbf)	Time at Maximum Load (sec)	Load at First Peak (lbf)	Time at First Peak (sec)	Average Load at Average Value (All Peaks) (lbf)
X 1	111	58	111	58	111
2	98	49	98	49	98
3	102	56	102	56	102
4	90	41	90	41	-----
5	97	48	97	48	97
X 6	131	66	131	66	131
7	96	43	96	43	96
Maximum	102	56	102	56	102
Mean	97	47	97	47	98

	Maximum Load (lbf)	Time at Maximum Load (sec)	Load at First Peak (lbf)	Time at First Peak (sec)	Average Load at Average Value (All Peaks) (lbf)
Minimum	90	41	90	41	96
Standard Deviation	4.53222	6.18652	4.53222	6.18652	2.77229
Mean + 1 SD	101	54	101	54	101
Mean - 1 SD	92	41	92	41	96

X: data excluded

Sample #14: PF-ACB-8x8-E (S4'-8x8)

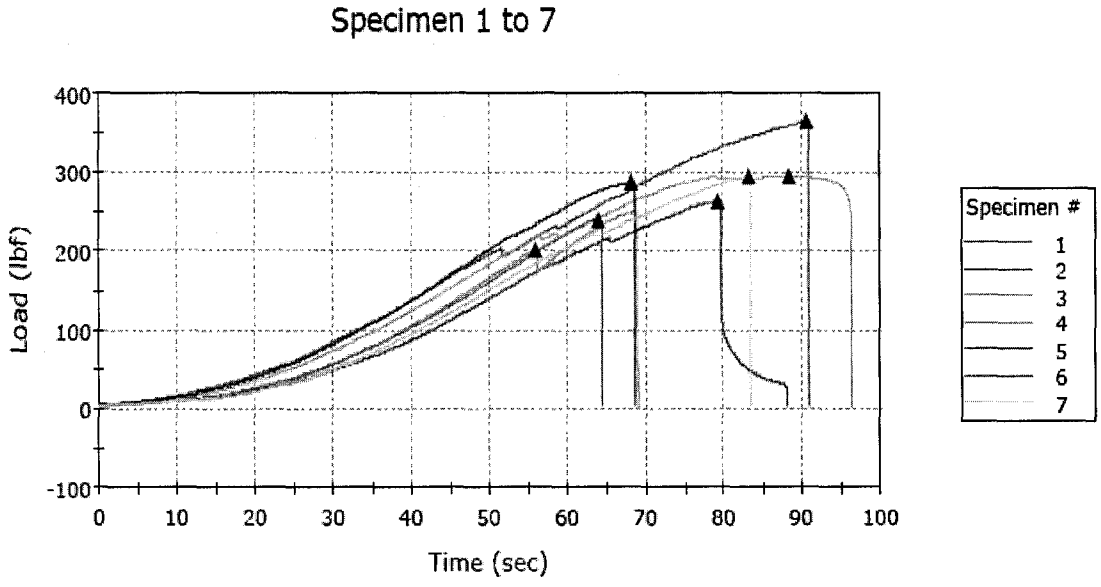

	Maximum Load (lbf)	Time at Maximum Load (sec)	Load at First Peak (lbf)	Time at First Peak (sec)	Average Load at Average Value (All Peaks) (lbf)
X 1	365	91	365	91	365
2	263	79	263	79	263
3	296	88	296	88	296
4	252	69	202	56	227
5	287	68	287	68	287
X 6	241	64	241	64	-----
7	295	83	295	83	-----
Maximum	296	88	296	88	296
Mean	278	78	268	75	268
Minimum	252	68	202	56	227
Standard Deviation	20	9	40	13	31
Mean + 1 SD	298	87	308	88	299

	Maximum Load (lbf)	Time at Maximum Load (sec)	Load at First Peak (lbf)	Time at First Peak (sec)	Average Load at Average Value (All Peaks) (lbf)
Mean - 1 SD	258	69	229	62	237

X: data excluded

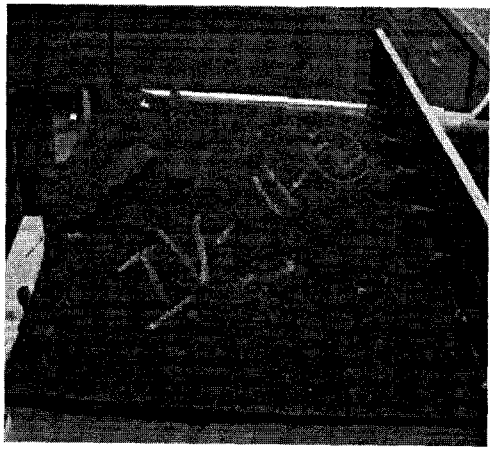

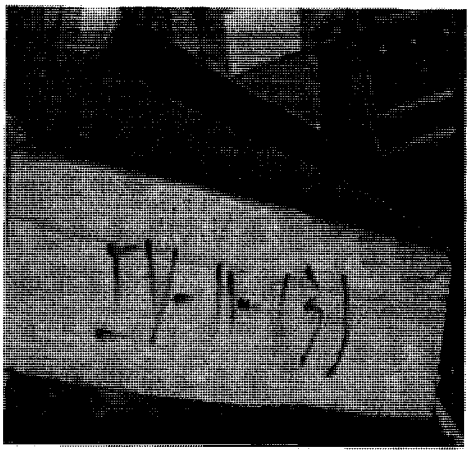

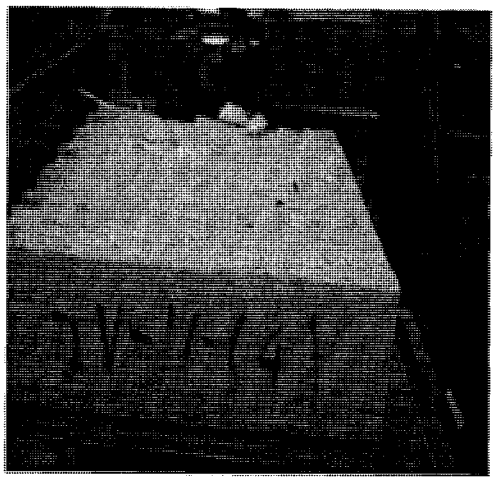

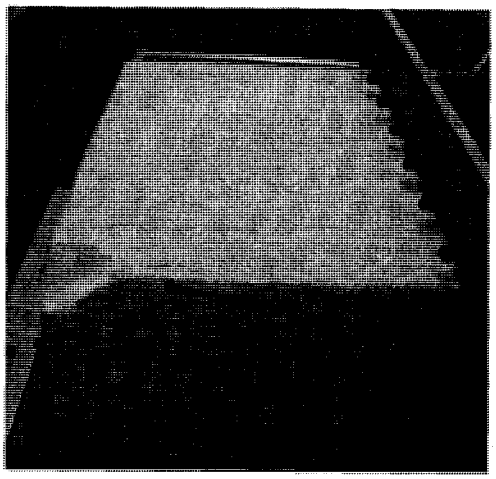

Sample #15: PF-ACB-10x10-E (S4'-10x10)

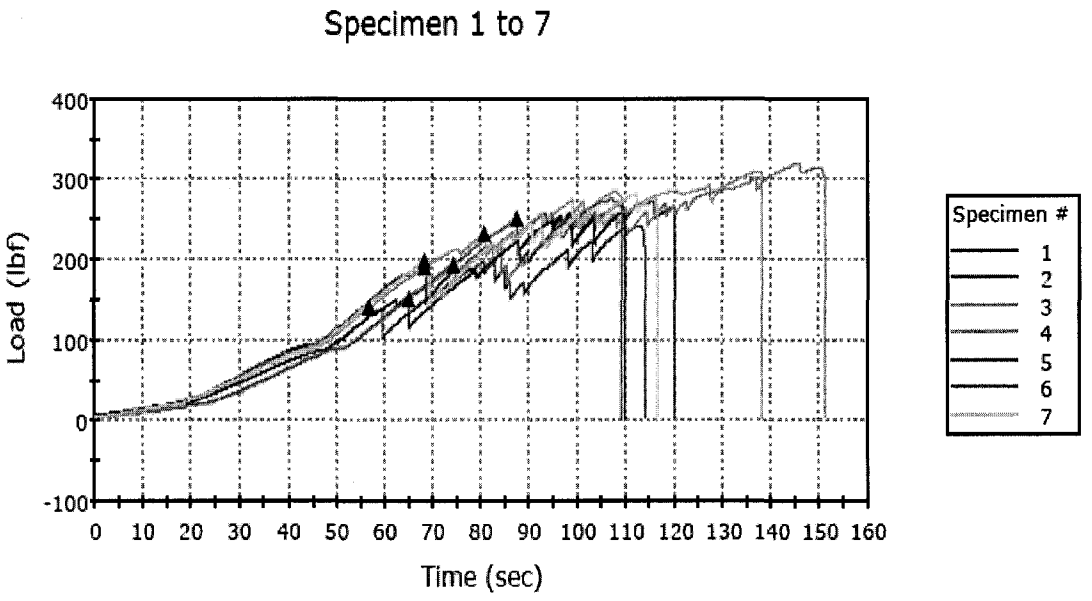

	Maximum Load (lbf)	Time at Maximum Load (sec)	Load at First Peak (lbf)	Time at First Peak (sec)	Average Load at Average Value (All Peaks) (lbf)
X 1	241	113	140	57	196
2	272	116	190	68	252
3	310	138	232	81	277
4	320	146	192	74	251
X 5	257	109	151	65	228
6	273	107	250	87	244
7	282	112	200	68	247
Maximum	320	146	250	87	277
Mean	291	124	213	76	254
Minimum	272	107	190	68	244
Standard Deviation	21.97763	17.01570	26.73787	8.28824	13.15668
Mean + 1 SD	313	141	239	84	267

	Maximum Load (lbf)	Time at Maximum Load (sec)	Load at First Peak (lbf)	Time at First Peak (sec)	Average Load at Average Value (All Peaks) (lbf)
Mean - 1 SD	269	107	186	68	241

X: data excluded

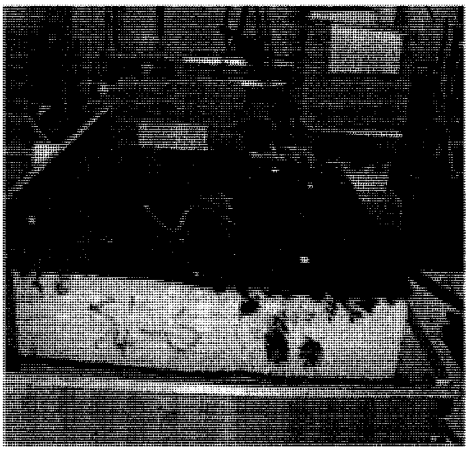

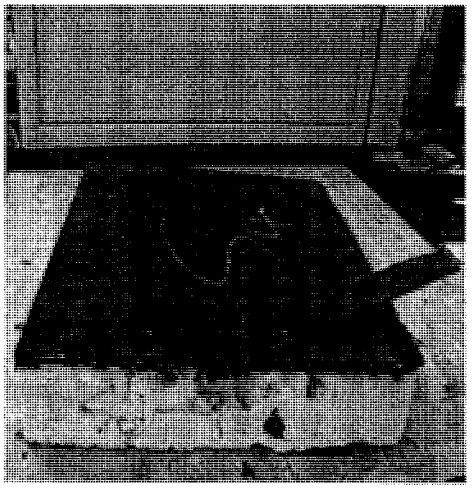

Appendix 7

Source I – IV Data Comparison

(Phase I & II)

Table 1. Peel resistance (lbf) comparison of **PF/ACB** samples for 15 degree peel test at the **Edge Position**

Source ID	I-1		II-1		III-1		IV-1	
Specimen #	**PF/ACB**	**Failure Mode**	**PF/ACB**	**Failure Mode**	**PF/ACB**	**Failure Mode**	**PF/ACB**	**Failure Mode**
#1	243	Facer/D	121	Facer/R & Adh	196	CB/Se	192	Facer/D
#2	216	Facer/D	99	Facer/R	185	CB/Se	210	Facer/D & Adh
#3	259	Facer/D	104	Facer/R	209	CB/Se	258	Facer/D & Adh
#4	228	Facer/D	100	Facer/T	227	CB/Se	197	Facer/D
#5	215	Facer/D	89	Facer/R	190	CB/Se	258	Facer/D
Mean Load	232		102		202		223	
Standard Deviation	19		12		17		33	

Table 2. Peel resistance (lbf) comparison of **PF/FB** samples for 15 degree peel test at the **Edge Position**

Source ID	I-2		II-2		III-2		IV-2	
Specimen #	**PF/FB**	**Failure Mode**	**PF/FB**	**Failure Mode**	**PF/FB**	**Failure Mode**	**PF/FB**	**Failure Mode**
#1	116	CB/B	46	CB/Sp	78	CB/B	105	CB/B
#2	105	CB/B	43	CB/Sp	80	CB/B	94	CB/B
#3	125	CB/B	44	CB/Sp	88	CB/B	138	CB/Sp
#4	107	CB/B	43	CB/Sp	89	CB/B	90	CB/B
#5	130	CB/B	44	CB/Sp	64	CB/Sp	97	CB/B
Mean Load	117		44		80		105	
Standard Deviation	11		1		10		20	

Table 3. Peel resistance (lbf) comparison of **AF/ACB** samples for 15 degree peel test at the **Edge Position**

Source ID	I-3		II-3		III-3		IV-3	
Specimen #	**AF/ACB**	**Failure Mode**	**AF/ACB**	**Failure Mode**	**AF/ACB**	**Failure Mode**	**AF/ACB**	**Failure Mode**
#1	257	Facer/D	79	Facer/D	217	Facer/D & Adh	132	Facer/D & Adh
#2	267	Facer/D	122	Facer/D	150	Facer/D & Adh	142	Facer/D & Adh
#3	302	Facer/D	70	Facer/D	187	Facer/D & Adh	175	CB/Se & Adh
#4	139	Facer/D	72	Facer/D	229	Facer/D & Adh	118	Facer/D & Adh
#5	168	Facer/D	83	Facer/D	211	Facer/D	131	Facer/D
Mean Load	226		85		199		140	
Standard Deviation	70		21		31		22	

Table 4. Peel resistance (lbf) comparison of **AF/FB** samples for 15 degree peel test at the **Edge Position**

Source ID	I-4		II-4		III-4		IV-4	
Specimen #	**AF/FB**	**Failure Mode**	**AF/FB**	**Failure Mode**	**AF/FB**	**Failure Mode**	**AF/FB**	**Failure Mode**
#1	86	CB/Sp	51	CB/Sp	95	CB/B	106	CB/B
#2	125	CB/B	43	CB/Sp	69	CB/B	104	CB/B
#3	116	CB/B	45	CB/Sp	101	CB/B	105	CB/B
#4	130	CB/B	50	CB/Sp	98	CB/B	98	CB/B
#5	147	CB/B	42	CB/Sp	91	CB/B	91	CB/B
Mean Load	121		46		91		101	
Standard Deviation	23		4		13		6	

Table 5. Peel resistance (lbf) comparison of **PF/FB** samples for 15 degree peel test at the **Corner Position**

Source ID	I-5		II-5		III-5		IV-5	
Specimen #	**PF/ACB**	**Failure Mode**	**PF/ACB**	**Failure Mode**	**PF/ACB**	**Failure Mode**	**PF/ACB**	**Failure Mode**
#1	137	Facer/D	140	Facer/R & Adh	148	CB/B	173	CB/B
#2	124	CB/B	160	Facer/R & Adh	149	CB/B	151	Facer/D & Adh
#3	156	CB/B	125	Facer/R & Adh	133	CB/B	169	CB/B
#4	194	Facer/D	140	Facer/R & Adh	146	CB/B	173	CB/B
#5	197	Facer/D	169	Facer/R & Adh	133	CB/B	190	CB/B
Mean Load	162		147		142		171	
Standard Deviation	33		18		8		14	

Table 6. Peel resistance (lbf) comparison of **AF/FB** samples for 15 degree peel test at the **Corner Position**

Source ID	I-6		II-6		III-6		
Specimen #	**AF/ACB**	**Failure Mode**	**AF/ACB**	**Failure Mode**	**AF/ACB**	**Failure Mode**	**AF/ACB**
#1	163	Facer/D	165	Facer/D & Adh	117	Facer/D	111
#2	89	CB/B	150	Facer/D & Adh	100	CB/B	126
#3	140	Facer/D	134	Facer/D & Adh	162	CB/B	124
#4	137	Facer/D	128	Facer/D & Adh	108	CB/B	113
#5	108	Facer/D	159	Facer/D & Adh	116	CB/B	86
Mean Load	127		147		120		112
Standard Deviation	29		16		24		16

Table 7. Peel resistance (lbf) comparison of **PF/ACB** samples under **different degree** peel test at the Edge Position

Specimens (PF/ACB) ID	Angle	Source ID	
		II	IV
S'-1	7.5	192	263
S'-2	15	166	241
S'-3	22.5	113	183
S'-4	30	73	142
S'-5	37.5	52	101
S'-6	45	46	94

Table 8. Peel resistance (lbf) comparison of **AF/ACB** samples under **different degree** peel test at the Edge Position

Specimens (AF/ACB) ID	Angle	Source ID	
		II	IV
S-1	7.5	218	231
S-2	15	112	140
S-3	22.5	76	87
S-4	30	54	64
S-5	37.5	51	61
S-6	45	33	37

Table 9. Peel resistance (lbf) comparison of **different size** of **PF/ACB** samples for 15 degree peel test at the Edge Position

Sample Size (in. x in.)	Source ID	
	II	IV
4 x 4	82	97
6 x 6	166	241
8 x 8	212	278
10 x 10	255	291

Appendix 8 Calculating the Student t-Test and p Value

A student ***t*-test** is a statistical analysis used to calculate the significance of observed differences between the means of two samples. The student *t*-test begins with a null hypothesis that there are no significant differences between the means of two normally distributed data sets; each characterized by its mean, standard deviation and number of data points.

When the two sample sizes (that is, the n or number of participants of each sample) are equal, the equation below is used for calculating the t-value (www.wikipedia.org).

$$t = \frac{\overline{X}_1 - \overline{X}_2}{s_{\overline{X}_1 - \overline{X}_2}} \text{ where } s_{\overline{X}_1 - \overline{X}_2} = \sqrt{\frac{s_1^2 + s_2^2}{n}}$$

In this equation, X is the mean of sample one (denoted as "1") or sample two (denoted as "2"); s is the standard deviation (SD); n is the number of participants, or specimens in this thesis, in each sample). The denominator is the standard error of the difference between the two means. In this test, the degree of freedom (f) = 2n-2.

For example, in Chapter 4.2.3 of this thesis, two independent sample sets, each contains five measured values of peel resistance, and their means and standard deviations are shown below:

Specimen ID	**Sample set 1 (lbf)**	**Sample set 2 (lbf)**
#1	192	251
#2	210	249
#3	258	220
#4	197	268
#5	258	218
Mean Value (X)	223	241
Standard Deviation (s)	33	22

Where X_1 = 223 lbf, X_2 = 241 lbf;

S_1 = 33 lbf, S_2 = 22 lbf,;

n = 5; and

f = 2n –2 =2x5-2 = 8

Following above equation, the calculated t = 1.015.

Once the *t* value and *f* are determined, a *p* value can be found from the Student's *t*-distribution Table, which is available from the most common statistical analysis tools (online such as www.graphpad.com/quickcalcs/ttest2.cfm or books). In the example above, the *p* value is equal to 0.33. Practically, the *p* value of Student's t-test can be readily calculated with any statistical software or data spreadsheet such as Microsoft Excel.

The *p* value is the probability that, under the null hypothesis of equal means, the absolute value of *t* could be that large or larger just by chance (Press et al, 1992, P. 616). In a statistical sense, the *p*-value is the probability of obtaining a result at least as extreme as a given data point, assuming the data point was the result of chance alone. The fact that *p*-values are based on this assumption is crucial to their correct interpretation. In a plain language, the *p* value is the probability of the null hypothesis, that there are no significant differences between the means of the two samples, being true. Generally, one rejects the null hypothesis if the *p*-value is samller than the significance level (usually the 0.05 level) and concludes that there are significant differences between the means of the two samples tested. Otherwise, if the *p*-value is greater than 0.05, then the null hypothesis is accepted and a conclusion can be drawn that there are no significant differences between the means of the two samples tested.

References

Style Guides and Standards:

A Guide for the Wind Design of Adhesive Applied Roofing Systems (AARS), Internal Report-IRC-NRC, version #2, June, 2007 (in Press)

American Society for Testing and Materials (2001), "Standard Test Method for Peel Resistance of Adhesives (T-Peel test)", ASTM D 1876-01, USA

American Society for Testing and Materials (2002), "Standard Specification for Faced Rigid Cellular Polyisocyanurate Thermal Insulation Board", ASTM C1289-02, USA

American Society for Testing and Materials (2003), "Standard Test Method for Floating Roller Peel Resistance of Adhesives", ASTM d 3167-03a, USA

American Society for Testing and Materials (2004), "Standard Test Method for 90 Degree Peel Resistance of Adhesives", ASTM D 6862-04, USA

American Society for Testing and Materials (2006), "Standard Terminology of Adhesives", ASTM D 907 – 06, USA

European Standards, "Flexible Sheets for Waterproofing-Determination of Peel Resistance of Joints Part2: Plastic and Rubber Sheets for Roof Waterproofing", BA EN 12316-2:2000 and DIN EN 12361-2 Standard

Instron Student Training Manual: Instron Training Center Bluehill2 Operator's Training Course. M18-14340-EN, Revision 1

The International Organization for Standardization, "Adhesive-determination of Peel Resistance of High-Strength Adhesive Bonds-Floating-Roller Method", ISO standard 4578

The International Organization for Standardization, "Adhesives – Designation of Main Failure Patterns", ISO 10365

The International Organization for Standardization, "Adhesives – Guide to the Selection of Standard Laboratory Ageing Conditions for Testing Bonded Joints", ISO 9142

The International Organization for Standardization, "Adhesives – Peel Test for a Flexible-Bonded-to-Rigid Test Specimen Assembly – Part 2: 180 Degree Peel", ISO standard 8510-2:2006

The International Organization for Standardization, "Adhesives – T-Peel Test for Flexible-to-Flexible Bonded Assemblies", ISO standard 11339:2003

The International Organization for Standardization, "Plastics – Standard Atmospheres for Conditioning and Testing", ISO standard 291: 2005

Books and Articles:

Baker, Max., (1980), "Roofs", Multi-Publications Ltd., Montreal, Condren, S.J.

Baskaran, A. and Kashef, A. (1995), "Application of Numerical Models for the Dynamic Evaluation of Roofing System – State of the Art Review", IRC Report #690, National Research Council Canada, Ottawa, Canada

Baskaran, A. and Lei, W. (1997), "New Facility for Dynamic Wind Performance Evaluation of Roofing Systems", Proceedings of the Fourth International Symposium on Roofing Technology, (Gaithersburg, MD., USA, September 17, 1997), pp. 168 -179.

Baskaran, A., Desjarlais, A., Roodvoets and D., "Hurricane Katrina Wind Investigation Report, Powder Springs, Georgia: Roofing Industry Committee on Weather Issues", Inc. pp. 183, August 01, 2007 (NRCC-50024)

Baskaran, A., Murty, B. and Tanaka, H. (2007), "Pilot Study on Wind Uplift Resistance of Adhesive Applied Low Slope Roofing", Journal of ASTM international

Borujerdi, J. (2004) "Numerical Evaluation of Low Slope Roofs for wind Uplift," M.A.S thesis, University of Ottawa, Ottawa, Canada

Burch, D. M. (1991). "An analysis of moisture accumulation in a wood frame wall subjected to winter climate", National Institute of standards and Technology: Gaithersburg, MD. (NISTIR 4674)

Burnett, E.F.P. & Howson, C. (1987) "Performance Testing of Fully Adhered, Polymer -modified Bituminous Roofing Membranes", ASTM Technical Publication 959, R.A.Critchell,ed., ASTM, Philadelphia, pp.100-109.

C. W. Griffen, "Manual of Built-up Roof Systems", (New York: McGraw-Hill, 1982)

Canada Mortgage and Housing Corporation (CMHC), Canada. 1987, "Builders Series Series Moisture Problems", CMHC publication NHA 6010, Ottawa, Canada.

Canadian Standard Association (2004), CSA 123.21-04, Standard Test Method for the Dynamic Wind Uplift Resistance of Mechanically Attached Membrane-Roofing Systems. CSA, Toronto

Current. J., Murty, B., Wu, J., Baskaran, A. and Tanaka H., 2008 "Wind Uplift Resistance Data for Adhesive Applied Roofing Systems", Research Report, National Research Council of Canada; pp 1-236.

F. J. Dechow and K. A. Epstein, " Laboratory and Field Investigations of Moisture Absorption and Its Effect on Thermal Performance of Various Insulations, " ASTM Symposium on Thermal Transmission measurements of Insulation, Philadelphia, September 1997.

Huelman H. P. & Cheple M., "Hygrothermal Performance of Basement Foundation Systems",

Ko, S.K.P. and Baskaran, A., "SIGDERS Wind Uplift Resistance Data on Mechanically Attached Single Ply Roofing Systems – Effect of Membrane Widths. Part II, Research Report, Institute for Research in Construction, National Research Council Canada, 229, pp. 105, May 01, 2007

Molleti, S. (2006), "Performance Evaluation of Mechanically", PhD. Thesis, University of Ottawa, Ottawa, Canada

Press, William H.; Saul A. Teukolsky, William T. Vetterling, Brian P. Flannery (1992). "Numerical Recipes in C: The Art of Scientific Computing". Cambridge University Press, P616

Tanaka, H., Ghariani, S., Baskaran, B.A., and Savage. M.G. "Wind Pressure Measurements on Flat Roofs Using Scaled Models," 2, 10th International Conference on Wind Engineering into the 21st Century (Copenhagen, Denmark, June 21, 1999), pp. 1195-1202, 1999

Thomas E. Phalea. Jr. "Design and Analysis of Single-Ply Roof Systems", 1993

Uematsu Y. and Isyumov N. (1999), "Review Wind Pressure Acting on Low-Rise Buildings", Journal of Wind Engineering and Industrial Aerodynamics, 82:1 – 25

Web Sites:

www.astm.org

www.everlastingroofing.com

www.graphpad.com/quickcalcs/ttest2.cfm

www.innov.com

www.ISO.org

www.randpc.com

www.roofers.org.uk

www.rooftopocs.com

www.somay.com

www.waynesroofing.com

www.wikipedia.org